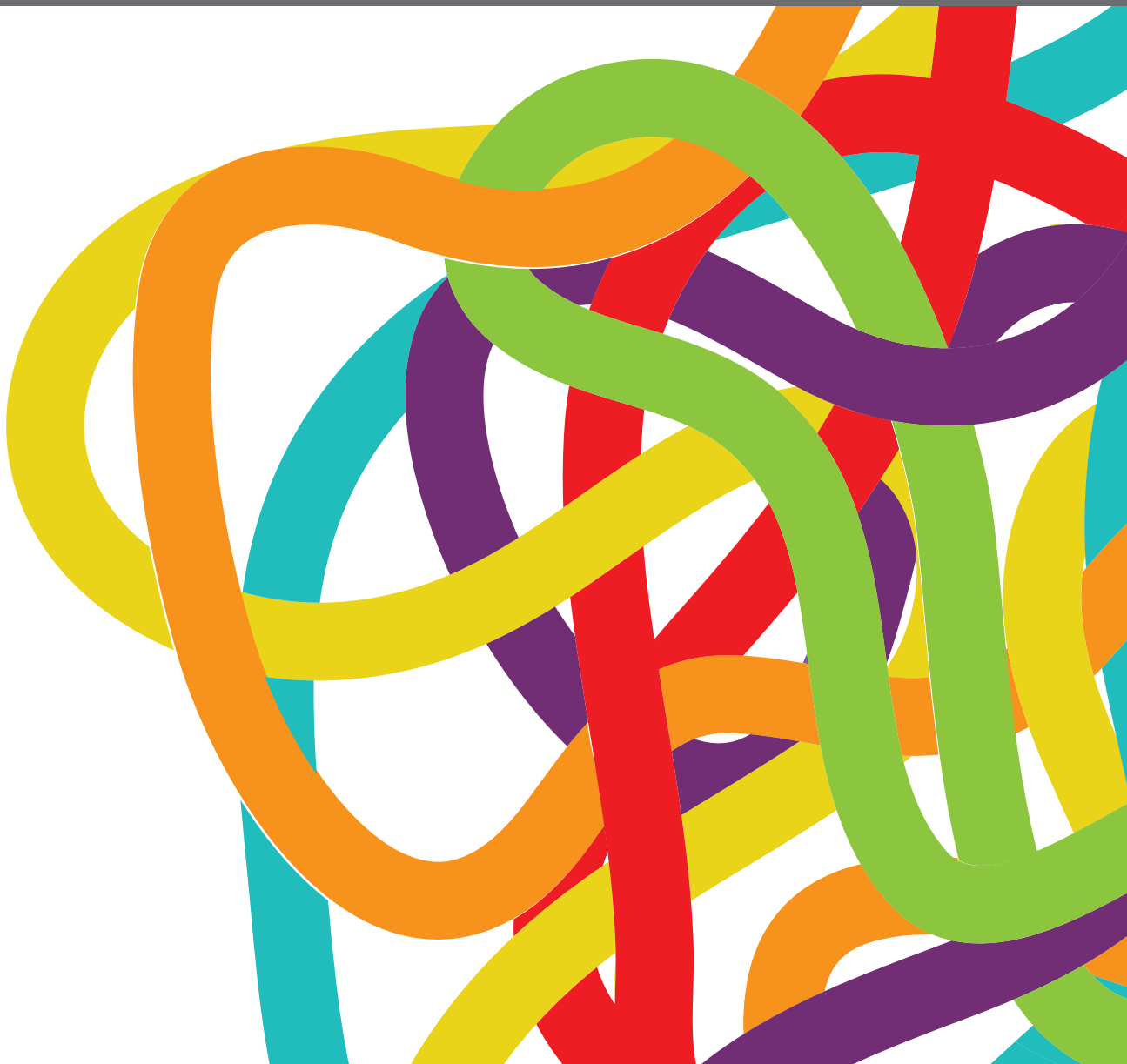


INSIGHTS IN RADIATION ONCOLOGY: 2021/2022

EDITED BY: Timothy James Kinsella
PUBLISHED IN: Frontiers in Oncology





frontiers

Frontiers eBook Copyright Statement

The copyright in the text of individual articles in this eBook is the property of their respective authors or their respective institutions or funders. The copyright in graphics and images within each article may be subject to copyright of other parties. In both cases this is subject to a license granted to Frontiers.

The compilation of articles constituting this eBook is the property of Frontiers.

Each article within this eBook, and the eBook itself, are published under the most recent version of the Creative Commons CC-BY licence.

The version current at the date of publication of this eBook is CC-BY 4.0. If the CC-BY licence is updated, the licence granted by Frontiers is automatically updated to the new version.

When exercising any right under the CC-BY licence, Frontiers must be attributed as the original publisher of the article or eBook, as applicable.

Authors have the responsibility of ensuring that any graphics or other materials which are the property of others may be included in the CC-BY licence, but this should be checked before relying on the CC-BY licence to reproduce those materials. Any copyright notices relating to those materials must be complied with.

Copyright and source acknowledgement notices may not be removed and must be displayed in any copy, derivative work or partial copy which includes the elements in question.

All copyright, and all rights therein, are protected by national and international copyright laws. The above represents a summary only. For further information please read Frontiers' Conditions for Website Use and Copyright Statement, and the applicable CC-BY licence.

ISSN 1664-8714

ISBN 978-2-88976-639-0

DOI 10.3389/978-2-88976-639-0

About Frontiers

Frontiers is more than just an open-access publisher of scholarly articles: it is a pioneering approach to the world of academia, radically improving the way scholarly research is managed. The grand vision of Frontiers is a world where all people have an equal opportunity to seek, share and generate knowledge. Frontiers provides immediate and permanent online open access to all its publications, but this alone is not enough to realize our grand goals.

Frontiers Journal Series

The Frontiers Journal Series is a multi-tier and interdisciplinary set of open-access, online journals, promising a paradigm shift from the current review, selection and dissemination processes in academic publishing. All Frontiers journals are driven by researchers for researchers; therefore, they constitute a service to the scholarly community. At the same time, the Frontiers Journal Series operates on a revolutionary invention, the tiered publishing system, initially addressing specific communities of scholars, and gradually climbing up to broader public understanding, thus serving the interests of the lay society, too.

Dedication to Quality

Each Frontiers article is a landmark of the highest quality, thanks to genuinely collaborative interactions between authors and review editors, who include some of the world's best academicians. Research must be certified by peers before entering a stream of knowledge that may eventually reach the public - and shape society; therefore, Frontiers only applies the most rigorous and unbiased reviews.

Frontiers revolutionizes research publishing by freely delivering the most outstanding research, evaluated with no bias from both the academic and social point of view. By applying the most advanced information technologies, Frontiers is catapulting scholarly publishing into a new generation.

What are Frontiers Research Topics?

Frontiers Research Topics are very popular trademarks of the Frontiers Journals Series: they are collections of at least ten articles, all centered on a particular subject. With their unique mix of varied contributions from Original Research to Review Articles, Frontiers Research Topics unify the most influential researchers, the latest key findings and historical advances in a hot research area! Find out more on how to host your own Frontiers Research Topic or contribute to one as an author by contacting the Frontiers Editorial Office: frontiersin.org/about/contact

INSIGHTS IN RADIATION ONCOLOGY: 2021/2022

Topic Editor:

Timothy James Kinsella, Brown University, United States

Citation: Kinsella, T. J., ed. (2022). Insights in Radiation Oncology: 2021/2022. Lausanne: Frontiers Media SA. doi: 10.3389/978-2-88976-639-0

Table of Contents

- 05 Efficacy of Stereotactic Body Radiotherapy in Patients With Hepatocellular Carcinoma Not Suitable for Transarterial Chemoembolization (HERACLES: HEpatocellular Carcinoma Stereotactic RAdiotherapy CLinical Efficacy Study)**
Thomas B. Brunner, Dominik Bettinger, Michael Schultheiss, Lars Maruschke, Lukas Sturm, Nico Bartl, Ivana Koundurdjieva, Simon Kirste, Hannes P. Neeff, Christian Goetz, Nils Henrik Nicolay, Gabriele Ihorst, Fabian Bamberg, Robert Thimme, Anca-Ligia Grosu and Eleni Gkika
- 16 Salvage Radiotherapy for Macroscopic Local Recurrence Following Radical Prostatectomy**
Hind Zaine, Benjamin Vandendorpe, Benoit Bataille, Thomas Lacornerie, Jennifer Wallet, Xavier Mirabel, Eric Lartigau and David Pasquier
- 24 Studies of Intra-Fraction Prostate Motion During Stereotactic Irradiation in First Irradiation and Re-Irradiation**
Alexandre Taillez, Andre-Michel Bimbai, Thomas Lacornerie, Marie-Cecile Le Deley, Eric F. Lartigau and David Pasquier
- 33 Use of a Biodegradable, Contrast-Filled Rectal Spacer Balloon in Intensity-Modulated Radiotherapy for Intermediate-Risk Prostate Cancer Patients: Dosimetric Gains in the BioPro-RCMI-1505 Study**
Igor Latorzeff, Eric Bruguière, Emilie Bogart, Marie-Cécile Le Deley, Eric Lartigau, Delphine Marre and David Pasquier
- 43 A Real-World, Multicenter, Observational Retrospective Study of Durvalumab After Concomitant or Sequential Chemoradiation for Unresectable Stage III Non-Small Cell Lung Cancer**
Alessio Bruni, Vieri Scotti, Paolo Borghetti, Stefano Vagge, Salvatore Cozzi, Elisa D'Angelo, Niccolò Giaj Levra, Alessandra Fozza, Maria Taraborrelli, Gaia Piperno, Valentina Vanoni, Matteo Sepulcri, Marco Trovò, Valerio Nardone, Elisabetta Lattanzi, Said Bou Selman, Federica Bertolini, Davide Franceschini, Francesco Agustoni, Barbara Alicja Jereczek-Fossa, Stefano Maria Magrini, Lorenzo Livi, Frank Lohr and Andrea Riccardo Filippi
- 50 Comparative Analyses of Two Established Scores to Assess the Stability of Spinal Bone Metastases Before and After Palliative Radiotherapy**
Tilman Bostel, Sati Akbaba, Daniel Wollschläger, Tristan Klodt, Laura Oebel, Arnulf Mayer, Sophia Drabke, Tanja Sprave, Jürgen Debus, Robert Förster, Harald Rief, Alexander Rühle, Anca-Ligia Grosu, Heinz Schmidberger and Nils H. Nicolay
- 59 Clinical Studies on Ultrafractionated Chemoradiation: A Systematic Review**
Erica Scirocco, Francesco Cellini, Alice Zamagni, Gabriella Macchia, Francesco Deodato, Savino Cilla, Lidia Strigari, Milly Buwenge, Stefania Rizzo, Silvia Cammelli and Alessio Giuseppe Morganti

- 70** ***Clinical Evaluation of the Inverse Planning System Utilized in Gamma Knife Lightning***
Taoran Cui, Ke Nie, Jiahua Zhu, Shabbar Danish, Joseph Weiner, Anupama Chundury, Nisha Ohri, Yin Zhang, Irina Vergalasova, Ning Yue and Xiao Wang
- 79** ***The Impact of Optic Nerve Movement on Intracranial Radiation Treatment***
Kun Qing, Ke Nie, Bo Liu, Xue Feng, James R. Stone, Taoran Cui, Yin Zhang, Jiahua Zhu, Quan Chen, Xiao Wang, Li Zhao, Shreel Parikh, John P. Mugler III, Sung Kim, Joseph Weiner, Ning Yue and Anupama Chundury
- 87** ***Please Place Your Seat in the Full Upright Position: A Technical Framework for Landing Upright Radiation Therapy in the 21st Century***
Sarah Hegarty, Nicholas Hardcastle, James Korte, Tomas Kron, Sarah Everitt, Sulman Rahim, Fiona Hegi-Johnson and Rick Franich
- 94** ***Clinical Evaluation of an Auto-Segmentation Tool for Spine SBRT Treatment***
Yingxuan Chen, Yevgeniy Vinogradskiy, Yan Yu, Wenying Shi and Haisong Liu
- 101** ***Radiation Oncology: Future Vision for Quality Assurance and Data Management in Clinical Trials and Translational Science***
Linda Ding, Carla Bradford, I-Lin Kuo, Yankhua Fan, Kenneth Ulin, Abdulnasser Khalifeh, Suhong Yu, Fenghong Liu, Jonathan Saleeby, Harry Bushe, Koren Smith, Camelia Bianciu, Salvatore LaRosa, Fred Prior, Joel Saltz, Ashish Sharma, Mark Smyczynski, Maryann Bishop-Jodoin, Fran Laurie, Matthew Iandoli, Janaki Moni, M. Giulia Cicchetti and Thomas J. FitzGerald



Efficacy of Stereotactic Body Radiotherapy in Patients With Hepatocellular Carcinoma Not Suitable for Transarterial Chemoembolization (HERACLES: HEpatocellular Carcinoma Stereotactic RAdiotherapy CLinical Efficacy Study)

OPEN ACCESS

Edited by:

Alessio G. Morganti,
University of Bologna, Italy

Reviewed by:

Ciro Franzese,
Humanitas University, Italy
Alessandra Arcelli,
University of Bologna, Italy

*Correspondence:

Eleni Gkika
eleni.gkika@uniklinik-freiburg.de

Specialty section:

This article was submitted to
Radiation Oncology,
a section of the journal
Frontiers in Oncology

Received: 13 January 2021

Accepted: 22 February 2021

Published: 19 March 2021

Citation:

Brunner TB, Bettinger D, Schultheiss M, Maruschke L, Sturm L, Bartl N, Koundurdjieva I, Kirste S, Neeff HP, Goetz C, Nicolay NH, Ihorst G, Bamberg F, Thimme R, Grosu A-L and Gkika E (2021) Efficacy of Stereotactic Body Radiotherapy in Patients With Hepatocellular Carcinoma Not Suitable for Transarterial Chemoembolization (HERACLES: HEpatocellular Carcinoma Stereotactic RAdiotherapy CLinical Efficacy Study). *Front. Oncol.* 11:653141. doi: 10.3389/fonc.2021.653141

Thomas B. Brunner¹, Dominik Bettinger^{2,3}, Michael Schultheiss³, Lars Maruschke⁴, Lukas Sturm³, Nico Bartl⁵, Ivana Koundurdjieva⁵, Simon Kirste⁵, Hannes P. Neeff⁶, Christian Goetz⁷, Nils Henrik Nicolay^{5,8,9}, Gabriele Ihorst¹⁰, Fabian Bamberg^{4,9}, Robert Thimme^{3,9}, Anca-Ligia Grosu^{5,8,9} and Eleni Gkika^{5,8,9*}

¹ Department of Radiation Oncology, University Medical Center Magdeburg, Magdeburg, Germany,

² Berta-Ottenstein-Programme, University of Freiburg, Freiburg, Germany, ³ Department of Medicine II, Medical Center-University of Freiburg, Freiburg, Germany, ⁴ Department of Radiology, University Medical Center Freiburg, Freiburg, Germany, ⁵ Department of Radiation Oncology, Medical Center - University of Freiburg, Freiburg, Germany, ⁶ Department of General and Visceral Surgery, University Medical Center Freiburg, Freiburg, Germany, ⁷ Department of Nuclear Medicine, University Medical Center Freiburg, Freiburg, Germany, ⁸ German Cancer Consortium (DKTK) Partner Site Freiburg, German Cancer Research Center (DKFZ), Heidelberg, Germany, ⁹ Faculty of Medicine, University of Freiburg, Freiburg, Germany, ¹⁰ Clinical Trials Unit Freiburg, Faculty of Medicine, University of Freiburg, Freiburg, Germany

The aim of this prospective observational trial was to evaluate the efficacy, toxicity and quality of life after stereotactic body radiation therapy (SBRT) in patients with hepatocellular carcinoma (HCC) and to assess the results of this treatment in comparison to trans-arterial chemoembolization (TACE). Patients with HCC, treated with TACE or SBRT, over a period of 12 months, enrolled in the study. The primary endpoint was feasibility; secondary endpoints were toxicity, quality of life (QOL), local progression (LP) and overall survival (OS). Between 06/2016 and 06/2017, 19 patients received TACE and 20 SBRT, 2 of whom were excluded due to progression. The median follow-up was 31 months. The QOL remained stable before and after treatment and was comparable in both treatment groups. Five patients developed grade ≥ 3 toxicities in the TACE group and 3 in the SBRT group. The cumulative incidence of LP after 1-, 2- and 3-years was 6, 6, 6% in the SBRT group and 28, 39, and 65% in the TACE group ($p = 0.02$). The 1- and 2- years OS rates were 84% and 47% in the TACE group and 44% and 39% in the SBRT group ($p = 0.20$). In conclusion, SBRT is a well-tolerated local treatment with a high local control rates and can be safely delivered, while preserving the QOL of HCC patients.

Keywords: hepatocellular carcinoma, radiotherapy, stereotactic body radiation therapy, Transarterial Chemoembolization, hepatocellular carcinoma

INTRODUCTION

The incidence and mortality of hepatocellular carcinoma (HCC) is rising worldwide due to the rise of viral hepatitis and non-alcoholic steatohepatitis (NASH) (1). The overall 5-year survival rate is 5% with more than 70% of the patients presenting with advanced disease precluding curative treatment such as liver transplantation, resection, or local ablative treatments such as radiofrequency ablation (RFA) or microwave ablation (2). According to the current Barcelona Clinic Liver Cancer (BCLC) classification for patients who are not eligible for resection or liver transplantation, treatment options include local non-surgical methods such as RFA, trans-arterial chemoembolization (TACE), and systemic therapy (3). Unfortunately, in about 15–20% of the patients who would benefit from local therapy, none of those treatments can be offered, due to the respective limitations and contraindications, such as decompensated cirrhosis, tumor extension, severely reduced portal flow, renal insufficiency (3). For these patients, SBRT could be offered as an alternative local ablative therapy with high rates of local control (4), while maintaining a good quality of life (5, 6). To date, there are no published prospective randomized trials comparing SBRT with TACE in locally advanced HCC, as these trials are ongoing (NCT02470533, NCT03326375, NCT03338647, NCT03338647). The aim of this study was to assess the feasibility of SBRT in everyday clinical practice, in patients with HCC, prior to a randomized trial.

METHODS AND MATERIALS

This is a prospective, two-arm, non-randomized, study analyzing the role of SBRT and TACE in patients with HCC. The primary objective of this trial was to investigate the feasibility of SBRT in everyday clinical practice, prior to a randomized trial. Secondary endpoints were: toxicity according to the NCI-CTCAE v4.0 for adverse events, health related quality of life (QOL), incidence of local progression (LP) (according to mRECIST), overall survival (OS) and progression free survival (PFS). The active recruitment time was 12 months. This study was registered at the German Clinical Trials Register (DRKS 00008566) and was approved by the local ethics committee (374/15).

Treatment

Patients received either TACE or SBRT according to the decision of the institutional HCC tumor board, taking into account the standard treatment algorithm (3). TACE was offered in patients with localized disease and/or with contraindications for resection, transplantation or RFA. For patients where TACE or systemic treatment were not deemed suitable either due to exclusion criteria (**Supplementary Table 1**) or for any other reason such as patient preference, SBRT was offered as an alternative.

TACE

The procedure involved gaining percutaneous trans-arterial access by the Seldinger technique to the hepatic artery with an arterial sheath, usually by puncturing the common femoral

artery in the right groin and passing a catheter guided by a wire through the abdominal aorta, through the celiac trunk and common hepatic artery, and finally into the branch of the proper hepatic artery supplying the tumor. Afterwards a selective angiogram of the celiac trunk and in specific situations additionally of the superior mesenteric artery was performed in order to identify the branches of the hepatic artery supplying the tumor(s). This was done to maximize the amount of the chemotherapeutic dose that is directed to the tumor and minimize the amount of the chemotherapeutic agent that could damage the normal liver tissue. When a tumor supplying blood vessel was selected, alternating aliquots of the chemotherapy (epirubicin or mitomycin (doses of max. 100 mg) and of embolic particles, or particles containing the chemotherapy agent, were injected through the catheter. The total chemotherapy dose was given into a single vessel, or divided among several vessels supplying the tumor/s. Patients were discharged from hospital several hours after the end of the procedure or on the following day. Re-staging CT scans were performed in accordance to clinical practice 12 weeks after TACE if complete embolization was achieved. In case of incomplete treatment and therefore tumor persistence TACE was repeated in a 4 week interval.

SBRT

Patients underwent a 4D and multiphase CT (arterial phase and/or delayed phase and venous phase), using a custom immobilization (e.g., vacuum cushion immobilization, patient positioning boards, knee cushions, and abdominal compression).

The primary tumor(s) and any tumor vascular thrombus, if present, were included into the gross tumor volume (GTV). For all patients, image guided radiotherapy (IGRT) using cone beam CT (CBCT) for every fraction were mandatory and if necessary for IGRT, fiducial marker implantation was performed prior to planning CT.

Treatment was delivered in 3, 5, 8, or 12 fractions. A total dose of 45 Gy in 3 fractions, 50 Gy in 5 fractions, 60 Gy in 8 fractions or of 66 Gy in 12 fractions, aiming to achieve a biological effective dose (BED) of close to 100 Gy ($\alpha/\beta = 10$ Gy). The number of fractions was chosen based on the volume of normal tissues irradiated, considering the dose constraints for organs at risk such as stomach, duodenum, small and large bowel and liver. Dose prescription was chosen so that 95% of the PTV received at least the nominal fraction dose, and 99% of the PTV received a minimum of 90% of the nominal dose (according to ICRU 83). The dose maximum within the PTV was 110–120% of the prescribed dose. Sub-volumes close to critical OARs were allowed to receive a lower dose to avoid toxicities, using a simultaneous integrated protection (SIP) (7).

Response Evaluation

Treatment response was evaluated using the international criteria proposed in the Reviewed Response Evaluation Criteria in Solid Tumors (mRECIST) Guideline version 1.1 (8) from a panel of an experienced radiologist and radiation oncologist. For patients treated with TACE, tumors requiring multiple embolization procedures because of residual disease were not counted as failures. Response assessments including response of

tumor thrombosis, physical examination and blood tests (such as complete blood counts and biochemical analysis including liver function) were repeated every 3 months.

Quality of Life Assessment

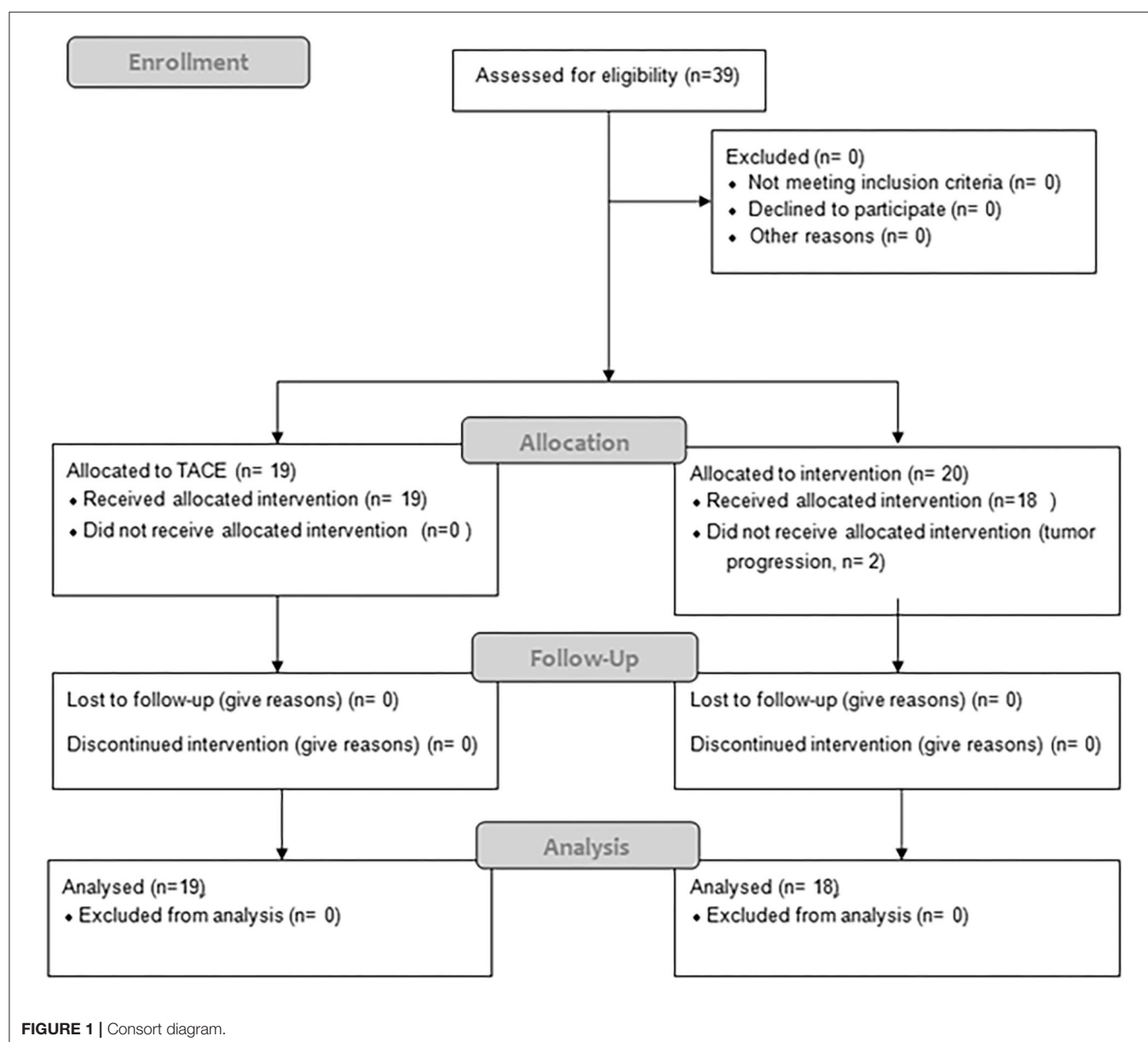
Patients treated with SBRT filled in the EORTC QLQ-C30 and QLQ C29 at the first treatment, 4 weeks after the last treatment and at the second follow up (3 months later). For the patients treated with TACE the QLQ assessment was before and after the treatment.

Statistical Methods

All analyses were based on the assigned treatment arm for all eligible patients for whom treatment was started. Continuous variables are reported as median with the corresponding

range (minimum and maximum), and categorical variables are presented as absolute and relative frequencies unless stated otherwise. Baseline group comparisons were conducted with Fisher's exact test or the Chi-square test (binary variables) or Wilcoxon's two-sample test (continuous variables) as a normal distribution was questionable for the respective variables.

OS was calculated as time from start of treatment until death from any cause, with censoring at the date last seen alive. PFS was calculated as time from start of treatment until death or documentation of progression. PFS times were censored at the date patients were last seen alive without documentation of disease progression. PFS times were censored in case that observation of death was more than 3 months after the last documented response assessment, in line with FDA recommendations (FDA Guidance for Industry, Clinical Trial



Endpoints for the Approval of Cancer Drugs and Biologics, May 2007). OS and PFS were estimated by the Kaplan-Meier method. The comparison of the two arms using log-rank tests was regarded as descriptive information. The Cox proportional hazards regression model was used for further analyses of possible prognostic factors for OS and PFS. The small number of patients did not allow complex multivariate modeling with variable selection using forward selection. Therefore, variables considered in a multivariate model were selected according to (i) large baseline differences between SBRT and TACE patients, (ii) relevant univariate impact on OS or PFS. A forward variable selection approach was then applied. Locally controlled survival (LCS) was defined as time to local progression or death, with censoring in the same manner as described for PFS. Analyses were performed with the Kaplan-Meier method and the log-rank test. The components of this combined endpoint LCS were analyzed separately under consideration of competing events. Thus, local progression (LP) was estimated as cumulative incidence rates taking into account that death without prior documentation of local disease progression is a competing event that prevents the observation of local progression.

Estimation of the effects of possible prognostic factors for LP was done with the Fine and Gray regression model. Results are presented as sub-distribution hazard ratios with 95% confidence intervals. Analyses were performed with SAS V9.4 (SAS Institute Inc., Cary, NC, USA).

RESULTS

Patient Characteristics

Between 06/2016 and 06/2017, 19 patients received TACE and 20 patients were planned for SBRT; however SBRT was halted in two patients due to progression (**Figure 1**), resulting in 18 evaluable patients. In general patients treated with SBRT were older (76 vs. 69, $p = 0.36$), had larger tumors (median 42 vs. 32 cm, $p = 0.08$) and higher BCLC stages ($p = 0.0013$). Additionally 3 patients (17%) had a metastatic disease (lung $n = 2$, adrenal $n = 1$), and a 6 patients (37%) a portal vein thrombosis (PVT), all in the SBRT arm. Seven patients (37%) in the TACE arm had HCC-directed therapy prior to enrolment and 11 (61%) in the SBRT arm (most of them had > 1 treatment modalities). The median time between diagnosis and treatment was 1 month (range: 0–28) in the TACE group and 3.5 months (range: 1–98) in the SBRT group. Ten patients (53%) in the TACE group received further treatments and 8 patients (44%) in the SBRT group. Patient and treatment characteristics are shown in **Table 1**.

Quality of Life

Patients in the SBRT group had a worse, but not statistically significant, QOL at baseline compared to the TACE group (**Supplementary Figure 1**, **Supplementary Tables 2A–C**). After treatment there was a slight, but not statistically significant, improvement in the QOL between baseline and 1st follow up in the SBRT group (**Supplementary Table 2**) and there was

TABLE 1 | Patient and treatment characteristics.

	TACE	SBRT	<i>p</i> -value*
A. PATIENT CHARACTERISTICS			
Age			0.36
median (range)	69 (45–92)	76 (58–85)	
Gender	18 (95%)	13 (72%)	0.09
Male			
Female	1 (5.3%)	5 (28%)	
Etiology of liver disease			0.74
HBV	2 (11%)	4 (22%)	
HCV	5 (23%)	5 (28%)	
Alcohol induced	2 (11%)	6 (33%)	
NASH	2 (11%)	1 (6%)	
n.a.	8 (42%)	2 (11%)	
Treatments before study inclusion†			0.19**
Resection	0 (0%)	4 (22%)	
RFA	2 (11%)	0 (0%)	
TACE	7 (26%)	11 (61%)	
SBRT	0 (0%)	1 (6%)	
Sorafenib, regorafenib	0 (0%)	0 (0%)	
SIRT	0 (0%)	2 (11%)	
No prior treatments	12 (63%)	7 (39%)	
Further treatments after study inclusion†			0.6
Resection	1 (5%)	0 (0%)	
Transplantation	1 (5%)	0 (0%)	
TACE	6 (32%)	2 (11%)	
SBRT	2 (11%)	3 (17%)	
Sorafenib, regorafenib	2 (11%)	5 (28%)	
SIRT	0 (0%)	1 (6%)	
No further treatments	9 (47%)	10 (56%)	
BCLC			0.0013
A	7 (37%)	2 (11%)	
B	12 (63%)	7 (40%)	
C	0 (0%)	9 (50%)	
D	0 (0%)	0 (0%)	
Metastatic disease	0 (0%)	3 (17%)	0.10
Child pugh score baseline			0.40***
A	17 (90%)	14 (78%)	
5	15	8	
6	2	6	
B	2 (10%)	4 (22%)	
7	1	2	
8	1	2	
ALBI grade			0.51
1	9 (47%)	11 (61%)	
2	10 (53%)	7 (40%)	
3	0 (0%)	0 (0%)	
Maximal tumor diameter (median, range), mm	32 (10–78)	42 (21–210)	0.08
Portal vein thrombosis (PVT)	0 (0%)	6 (37%)	0.01

(Continued)

TABLE 1 | Continued

TACE	
B. TREATMENT CHARACTERISTICS	
cTACE	8 (42%)
Drug-eluting beads TACE	11 (58%)
Total number of TACE sessions	
One TACE	6 (32%)
Two TACE	7 (37%)
Three TACE	2 (11%)
Five TACE	1 (5%)
Six TACE	1 (5%)
SBRT	
Total prescribed dose, median (IQR)	55 (49–60) Gy
BED ₁₀ , median (IQR)	100 (75–139) Gy
Dose per fraction, median (IQR)	7.2 (5–15.9) Gy
Nr of fractions, median (IQR)	5 (3–12)

cTACE, conventional transarterial chemoembolization; BED, biological effective dose; NASH, non-alcoholic steatohepatitis; BCLC, Barcelona Clinic Liver Cancer; TACE, trans-arterial chemoembolization; PVT, portal vein thrombosis; SBRT, stereotactic body radiation therapy; cTACE, conventional transarterial chemoembolization; *Fisher's exact test (binary variables) or Wilcoxon's two-sample test (continuous variables); **yes vs. no prior treatment; ***A vs. B; n.a., not available.

[†]some patients received multiple treatments.

no difference between the pre- and post-TACE quality QOL (Supplementary Table 2).

Toxicity

Toxicities were moderate in both groups. Three (17%) patients developed grade ≥ 3 toxicities in the SBRT group, two patients developed grade 3 hepatic failure with grade 3 bilirubin increase in the SBRT group and one patient developed a grade 5 fistula. In the TACE group, 5 (26%) patients developed grade ≥ 3 toxicities. One patient developed a grade 3 bilirubin increase, grade 4 aspartat aminotransferase (AST) and alanine aminotransferase (ALT) increase grade 3 pain and grade 5 hepatic failure. One patient developed grade 4 bilirubin increase, grade 3 AST increase, grade 3 ascites and grade 3 hepatic failure. One patient developed a grade 4 ALT increase, a grade 3 AST increase, a grade 3 pancreatitis and a grade 5 liver abscess. Another patient developed a grade 4 bilirubin increase, grade 3 cholangitis and grade 3 hepatic failure and one patient developed a grade 4 GPT and GOT increase. There was no statistical significant difference ($p = 0.69$, fisher's exact test) in the incidence of toxicities between the two groups. Albumin-bilirubin (ALBI) grade, Child Pugh (CP) score and blood test changes over time are shown in Supplementary Tables 3, 4.

Local Progression, Progression Free Survival, and Overall Survival

The cumulative incidence of LP after 1-, 2-, and 3-years (where death without prior LP was defined as a competing event) was 6, 6, and 6% in the SBRT arm and 28, 39, and 65% in the TACE arm ($p = 0.02$ Gray test) (Figure 2A). The observation of LP might

have been prevented in the SBRT arm due to a higher incidence of intercurrent deaths within the first 3 months. No other factors except for the type of the treatment (HR 0.119, 0.015–0.993, $p = 0.04$ Fine and Gray regression model) were statistically significant concerning LP in univariate analysis (Table 2). The cumulative incidence rate of death (competing event) without prior documentation of LP after 1-, 2-, and 3 years were 52% in the SBRT group and 8% in the TACE group. The LCS (i.e., the time to LP or death) after 1-, 2-, and 3 years was 42.2, 42.2, and 42.2% in the SBRT group and 64, 53.3, and 26.7% in the TACE group ($p = 0.42$).

The median PFS was 4 months in the SBRT group and 11 months in the TACE group (HR: 2.172, 95% CI 0.988–4.775, $p = 0.05$, Figure 2B) which remained also significant on multivariate analysis (HR: 2.855, 95% CI: 1.227–6.644, $p = 0.02$). Patients with a BCLC stage A (HR: 0.208, 95% CI: 0.055–0.787, $p = 0.02$), with multiple HCC (HR: 2.759, 95% CI: 1.207–6.3006, $p = 0.02$) as well as patients with prior treatments (HR: 2.693, 95% CI: 1.199–6.046, $p = 0.02$) had a better PFS (Table 3).

The median OS, in the TACE group was 23 vs. 11 months in the SBRT group and the 1 and 2 years OS rates 84% and 47% in the TACE arm and 44% and 39% in the SBRT arm, respectively ($p = 0.20$, Figure 2C). Three patients in the SBRT arm died within 1 month after completion of therapy due to pneumonia, urosepsis and sepsis due to necrotizing fasciitis after hip-endoprosthesis. Patients with a higher CP score (HR 3.968, 95% CI: 1.419–11.096, $p = 0.01$) larger tumors (HR: 3.214, 95% CI: 1.355–7.624, $p = 0.01$) and PVT (HR: 3.107, 95% CI: 1.116–8.648 $p = 0.03$) had a worse OS, which remained significant on multivariate analysis (Table 2).

DISCUSSION

Over the past 10 years there have been significant advances in the treatment of HCC. Although in patients with BCLC stage B TACE appears to be the treatment with the best quality of evidence leading to an improvement of the OS, in advanced HCC, which poses a more heterogeneous group, the selection of treatment type depends on many factors such as the performance status of the patient, the underlying cirrhosis, the presence of metastases or the extent of macrovascular extension (9). To date there are no published results on randomized trials comparing SBRT with TACE in HCC, as randomized studies are still ongoing. This is the first prospective trial, including both treatment options, TACE and SBRT, avoiding randomization on the purpose of reflecting clinical needs prior to a randomized trial.

In the current prospective trial, patients in the SBRT arm were multi-morbid with advanced tumors and worse quality of life at baseline, not eligible for other treatments (Figure 3). Nevertheless, treatment was well-tolerated, while maintaining at least a stable QOL in the longitudinal assessment, independent of the comorbidities, and was similar for both SBRT and TACE. Similar results concerning the QOL after liver SBRT were also reported by Mendez Romero et al. (6) and Klein et al. (10) who

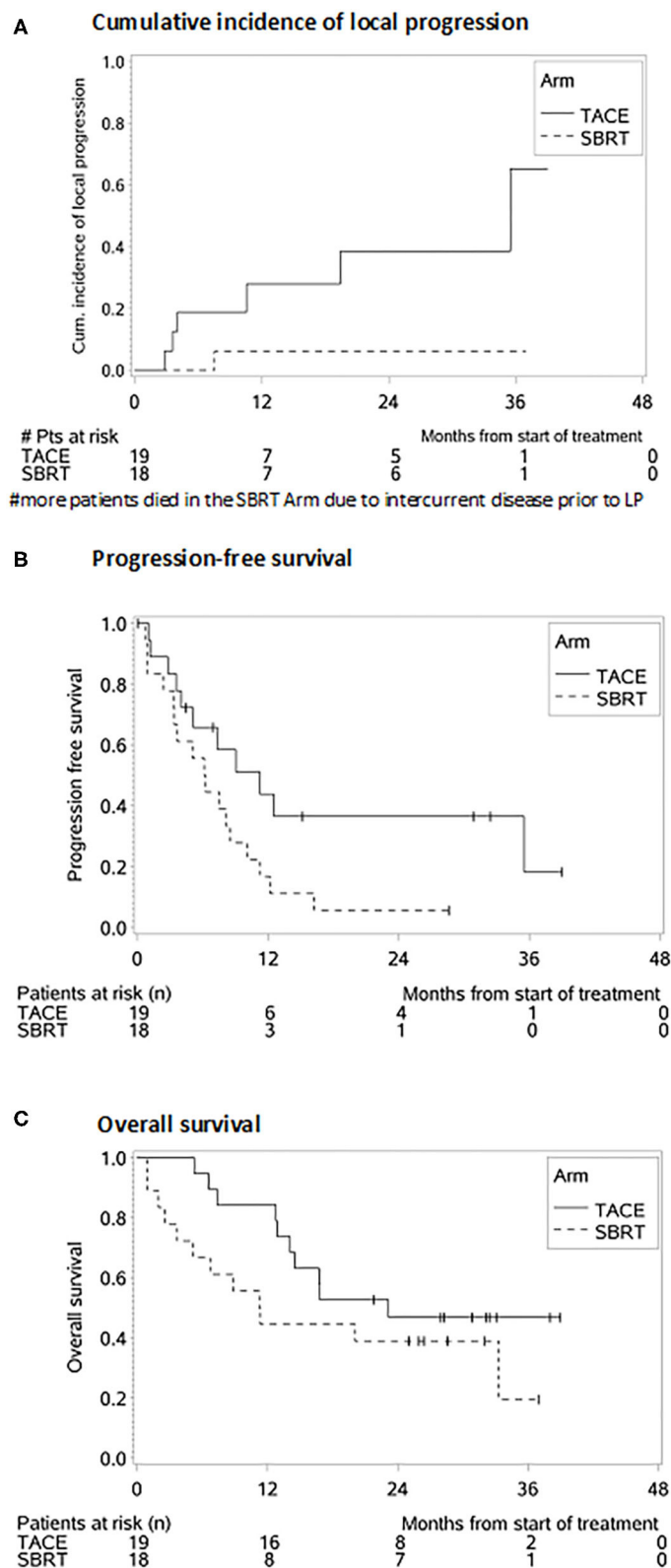


FIGURE 2 | Survival probabilities after SBRT and TACE. **(A)** Cumulative incidence of local progression. **(B)** Progression-free survival. **(C)** Overall survival.

observed a temporary worsening of appetite and fatigue, which was quickly resolved, resulting to an overall stable QOL, but there are no data comparing both treatments. Thus, patients ineligible for other local or system treatments tolerate the SBRT without impairing the QOL similar to patients with less advanced disease treated with TACE.

Additionally, the cumulative incidence of LP after 3-years of 6% in the SBRT group was high, similar to published literature, ranging between 64 and 96%, and 2-year OS rates ranging between 40 and 81% (11–20), corroborating the ablative potential of SBRT. Nevertheless, our results should be interpreted with caution under the consideration that in the 1st year, more deaths occurred in the SBRT group (as patients included in the SBRT arm were treatment-refractory and/or ineligible for

other treatments) preventing the observation of LP. This explains also the difference in the OS and PFS between the both groups and the modest OS and PFS in the SBRT arm. Although there was no statistically significant difference in the OS the PFS was statistically significant better in the TACE group probably due to patient selection, as patients in the SBRT had more advanced tumors. In our study TACE was also well-tolerated in terms of QOL and toxicity leading to a median OS of 26 months similar to published literature (21, 22) with a low incidence of LP. Due to the lack of randomization in our study, a direct comparison between SBRT and TACE is not possible, but both treatments show high efficacy.

Several, retrospective, studies that used propensity score matching in order to compare both treatments, indicate that SBRT could be an alternative to TACE in terms of local control. Bettinger et al. (23) showed similar local control rates after 1 year (TACE: 82%, SBRT 84.8%, $p = 0.8$) and OS (TACE: 11 months, SBRT 9 months, $p = 0.49$) for both treatments, with moderate toxicity, whereas Sapir et al. (24) showed that both LC at 1 year (SBRT 91%, TACE 47%, $p < 0.001$) and toxicity (TACE: 13%, SBRT: 8%, $p = 0.05$) favored SBRT, without any difference in the OS. Similarly, in a study by Shen et al. (25) SBRT showed a better in-field control after 3 years (77.5 vs. 55.6%) and OS rates (3-year OS of 55 vs. 13%) than TACE in patients with medium-sized HCC, particularly for recurrent cases. But also in comparison to RFA, Wahl et al. (26), using propensity score analysis, observed a similar freedom from LP (FFLP) 83.8 vs. 80.2% at 2 years, while for tumors > 2 cm, there was a decreased FFLP for RFA compared with SBRT (HR, 3.35; $P = 0.025$). In a another study, using propensity score matching in a cohort of 2,064 patients, after adjusting for clinical factors, SBRT was related to a significantly

TABLE 2 | Univariate fine and gray regression model for local progression.

Parameter	HR	95% CI	p
SBRT vs. TACE	0.119	0.015–0.933	0.04
ALBI grade (2–3 vs. 1)	0.222	0.029–1.702	0.15
Nodule (multiple vs. solitary)	2.602	0.557–12.154	0.22
Prior treatments (yes vs. no)	2.028	0.496–8.288	0.32
Tumor diameter ≥ 50 mm (yes vs. no)	0.581	0.129–2.614	0.48
BCLC (A vs. C)	1.438	0.094–22.086	0.79
BCLC (B vs. C)	3.040	0.385–24.022	0.29

CI, confidence interval; HR, Hazard ratio; TACE, transarterial chemoembolization; SBRT, stereotactic body radiation therapy; ALBI, albumin bilirubin grade; HCC, hepatocellular carcinoma, BCLC, Barcelona liver clinic classification.

TABLE 3 | Univariate and multivariate Cox-regression analysis of overall survival.

Parameter	Overall survival			Progression free survival		
	HR	95% CI	p	HR	95% CI	p
UNIVARIATE ANALYSIS						
SBRT vs. TACE	1.716	0.739–3.985	0.21	2.172	0.988–4.775	0.05
Child pugh score (7–9 vs. 5–6)	3.968	1.419–11.096	0.01	1.831	0.689–4.864	0.23
ALBI grade (2–3 vs. 1)	1.677	0.724–3.587	0.23	1.181	0.551–2.531	0.67
nodules (multiple vs. solitary)	1.530	0.653–3.587	0.33	2.759	1.207–6.306	0.02
Prior treatments (yes vs. no)	1.286	0.554–2.982	0.56	2.693	1.199–6.046	0.02
Metastases (yes vs. no)	1.728	0.499–5.980	0.39	2.260	0.634–8.052	0.21
Diameter ≥ 50 mm (yes vs. no)	3.214	1.355–7.624	0.01	1.740	0.782–3.873	0.18
BCLC (A vs. C)	0.514	0.161–1.638	0.26	0.208	0.055–0.787	0.02
BCLC (B vs. C)	0.478	0.177–1.289	0.15	0.471	0.197–1.126	0.09
Portal vein thrombosis (yes vs. no)	1.454	0.626–3.374	0.03	2.341	0.919–5.965	0.07
MULTIVARIATE ANALYSIS						
SBRT vs. TACE	1.948	0.778–4.879	0.15	2.855	1.227–6.644	0.02
Child pugh score (7–9 vs. 5–6)	8.866	2.355–33.376	<0.01	5.637	1.661–19.123	<0.01
Diameter ≥ 50 mm (yes vs. no)	4.695	1.810–12.177	<0.01			
HCC (multiple vs. solitary)	3.344	1.171–9.547	0.02	5.021	1.840–13.699	<0.01

CI, confidence interval; HR, Hazard ratio; TACE, transarterial chemoembolization; SBRT, stereotactic body radiation therapy; ALBI, albumin bilirubin grade; HCC, hepatocellular carcinoma, BCLC, Barcelona liver clinic classification.

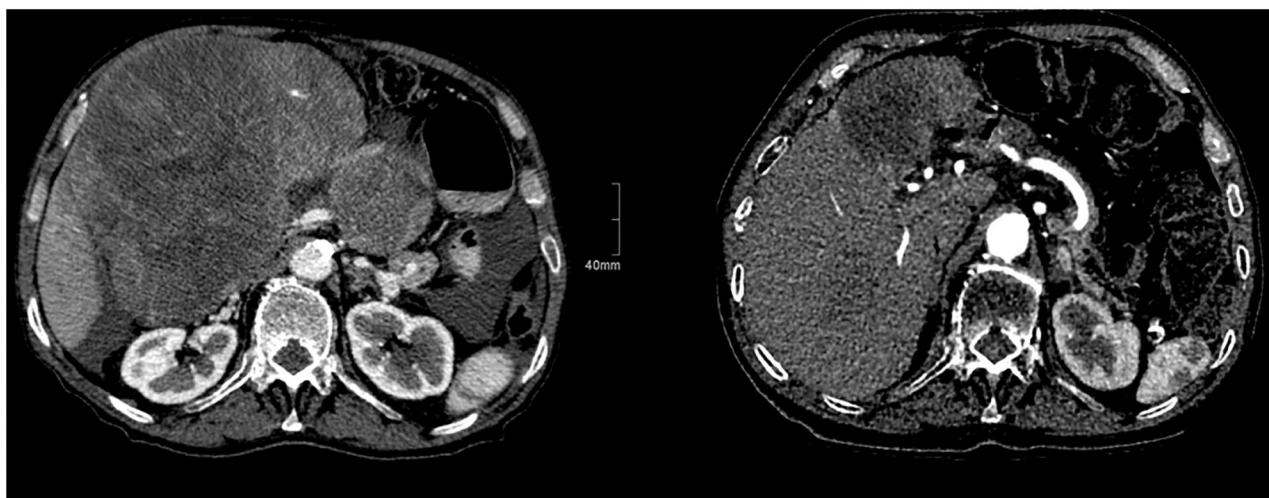
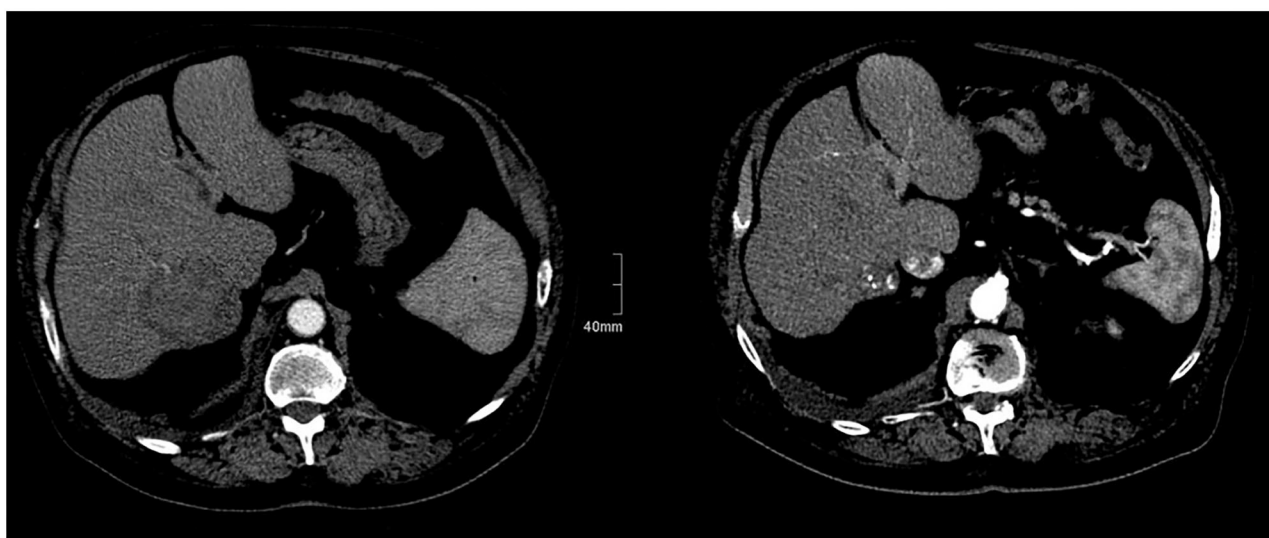
A**B**

FIGURE 3 | Patients with HCC before and after treatment. **(A)** Before SBRT and after SBRT. **(B)** Before and after TACE.

lower risk of local recurrence compared to RFA in both the entire (HR: 0.45, $p < 0.001$) and matched (HR 0.36, $p < 0.001$) cohorts (27). Similar results were also reported in a meta-analysis from Lee et al. (28) (SBRT vs. RFA: 84.5 vs. 79.5% $p = 0.431$). Yet, pooled analysis of OS in HCC studies showed an odds ratio of 1.43 (95% CI: 1.05–1.95, $p = 0.023$), favoring RFA. Additionally, radiotherapy shows similar results for TACE and RFA as bridging therapy (29). Of course, in the absence of prospective trials these results should be interpreted with caution, as some confounding cannot be ruled out, which could result in subtle biases.

Thus, SBRT is according to the NCCN guidelines (v5. 2020) reported not only as an alternative for patients ineligible for other

local treatments, but as a treatment option a priori equal to other local treatments, but due to the lack of randomized trials, SBRT is not yet included in the current Barcelona Clinic Liver Cancer (BCLC) classification (30).

But also, in more advanced stages, SBRT showed an OS benefit as compared to sorafenib in highly selected patients. Using two international cohorts of patients ($n = 1,023$) treated with sorafenib, Bettinger et al. (31), found in a propensity score analysis that patients treated with SBRT had an improved OS compared to sorafenib (17 vs. 10 months, $p = 0.012$). The rationale for taking an aggressive approach to treating large liver tumors is that patients often die from liver failure related to

disease progression regardless of the presence of extrahepatic disease (32). The clinical benefit of any local treatment option depends on the effectiveness of the modality and the a priori probability that LP will lead to mortality (32).

Currently checkpoint inhibitors play an increasingly important role in the treatment of several metastatic solid tumors as well as for primary liver tumors (33, 34). Ionizing radiation, apart from cytotoxicity, has been shown to additionally induce immune-modulatory effects, which trigger anti-tumor immune responses (35–40). SBRT, by applying a high single dose with a few but more than one fractions, seems to have the potential to lead to an activation of specific T-cell response in the tumor (41, 42). In pre-clinical models the most potent abscopal effects have been observed when CTLA4-antagonist treatment was applied during RT with 3X8Gy (vs. 5X6 Gy) in breast and colon cancer-bearing mice and not with a single dose of 20 or 30 Gy (42, 43). Grassberger et al. (44), reported on circulating immune cell populations in response to stereotactic body radiation therapy in patients with liver cancer showing that the fraction of activated mid-treatment CTLs was significantly associated with OS. Thus, there is a rationale for combining immunotherapies (IT) with RT as the radiation induced immune activation of CTLs can be boosted by checkpoint inhibitors.

Our study has several limitations such as the small sample size, the fact that some patients in the SBRT arm died shortly after treatment and the lack of a direct randomization between both arms so that a direct comparison is not possible. Patients in both arms received a number of subsequent treatments, ranging from transplantation and resection to systemic treatment and best supportive care which interfered with the outcome in both arms, especially in the SBRT arm where patients received more treatments. Additionally a few patients had metastatic disease in the SBRT arm which is a negative bias.

Moreover, statistical differences were revealed between the two groups, in terms of BCLC stage and portal vein thrombosis. However, due to the limited sample, it is likely that other types of variability exist, for example the presence of metastatic disease in SBRT group but not in TACE group, or range of tumor diameter. Furthermore, 42 % of the patients in the TACE arm were treated with conventional TACE, which might lead to a poorer survival, although DEB-TACE has not been shown to improve OS compared to conventional TACE in randomized trials or meta-analysis (9, 45, 46).

This is the first published trial evaluating TACE and SBRT in a prospective manner, showing that SBRT is a well-tolerated locally

effective treatment that does not impair the quality of life of multi-morbid patients, and could be considered as an alternative in carefully selected patients with contraindications for TACE.

DATA AVAILABILITY STATEMENT

The original contributions presented in the study are included in the article/**Supplementary Material**, further inquiries can be directed to the corresponding author/s.

ETHICS STATEMENT

The studies involving human participants were reviewed and approved by Ethics Committee University of Freiburg. The patients/participants provided their written informed consent to participate in this study.

AUTHOR CONTRIBUTIONS

TB, DB, MS, LM, A-LG, and EG: conceptualization. DB, MS, NB, IK, and EG: data curation. LM, GI, and EG: formal analysis. A-LG: funding acquisition. TB, DB, MS, LM, LS, NB, SK, HN, CG, FB, RT, A-LG, and EG: investigation. TB, DB, MS, LM, A-LG, and EG: methodology. TB, DB, MS, LM, and EG: project administration. TB, DB, LM, LS, NB, SK, HN, CG, FB, RT, and EG: resources. TB, MS, NN, and GI: software. TB, A-LG, and EG: supervision. GI: validation. GI and EG: visualization. TB, DB, MS, FB, NN, GI, A-LG, and EG: writing – original draft. TB, DB, MS, LM, LS, NB, IK, SK, HN, CG, NN, GI, FB, RT, A-LG, and EG: writing – review & editing. All authors contributed to the article and approved the submitted version.

FUNDING

This study was funded by the German Consortium for Translational Cancer Research (Deutsches Konsortium für Translationale Krebsforschung, DKTK)-Partner Site Freiburg. DB was funded by the Berta-Ottenstein-Programme for Advanced Clinician Scientists, Faculty of Medicine, University of Freiburg.

SUPPLEMENTARY MATERIAL

The Supplementary Material for this article can be found online at: <https://www.frontiersin.org/articles/10.3389/fonc.2021.653141/full#supplementary-material>

REFERENCES

1. Jemal A, Bray F, Center MM, Ferlay J, Ward E, Forman D. Global cancer statistics. *CA: Cancer J Clin.* (2011) 61:69–90. doi: 10.3322/caac.20107
2. Villanueva A, Hernandez-Gea V, Llovet JM. Medical therapies for hepatocellular carcinoma: a critical view of the evidence. *Nat Rev Gastroenterol Hepatol.* (2013) 10:34–42. doi: 10.1038/nrgastro.2012.199
3. Bruix J, Reig M, Sherman M. Evidence-based diagnosis, staging, and treatment of patients with hepatocellular Carcinoma. *Gastroenterology.* (2016) 150:835–53. doi: 10.1053/j.gastro.2015.12.041
4. Bujold A, Massey CA, Kim JJ, Brierley J, Cho C, Wong RK, et al. Sequential phase I and II trials of stereotactic body radiotherapy for locally advanced hepatocellular carcinoma. *J Clin Oncol.* (2013) 31:1631–9. doi: 10.1200/JCO.2012.44.1659

5. Measurements ICRU. ICRU Report 83: prescribing, recording and reporting photon-beam Intensity-Modulated Radiation Therapy (IMRT). *J ICRU*. (2010) 10:ndq001. doi: 10.1093/jicru/ndq001
6. Mendez Romero A, Wunderink W, van Os RM, Nowak PJ, Heijmen BJ, Nuytens JJ, et al. Quality of life after stereotactic body radiation therapy for primary and metastatic liver tumors. *Int J Radiation Oncol Biol Phys*. (2008) 70:1447–52. doi: 10.1016/j.ijrobp.2007.08.058
7. Brunner TB, Nestle U, Adebahr S, Gkika E, Wiehle R, Baltas D, et al. Simultaneous integrated protection: A new concept for high-precision radiation therapy. *Strahlentherapie Onkol*. (2016) 192:886–94. doi: 10.1007/s00066-016-1057-x
8. Lencioni R, Llovet JM. Modified RECIST (mRECIST) assessment for hepatocellular carcinoma. *Semin Liver Dis*. (2010) 30:52–60. doi: 10.1055/s-0030-1247132
9. Marrero JA, Kulik LM, Sirlin CB, Zhu AX, Finn RS, Abecassis MM, et al. Diagnosis, staging, and management of hepatocellular carcinoma: 2018 practice guidance by the American association for the study of liver diseases. *Hepatology*. (2018) 68:723–50. doi: 10.1002/hep.29913
10. Klein J, Dawson LA, Jiang H, Kim J, Dinniwell R, Brierley J, et al. Prospective longitudinal assessment of quality of life for liver cancer patients treated with stereotactic body radiation therapy. *Int J Radiat Oncol Biol Phys*. (2015) 93:16–25. doi: 10.1016/j.ijrobp.2015.04.016
11. Mendez Romero A, Wunderink W, Hussain SM, De Pooter JA, Heijmen BJ, Nowak PC, et al. Stereotactic body radiation therapy for primary and metastatic liver tumors: a single institution phase i-ii study. *Acta Oncol*. (2006) 45:831–7. doi: 10.1080/02841860600897934
12. Bujold A, Dawson LA. Stereotactic radiation therapy and selective internal radiation therapy for hepatocellular carcinoma. *Cancer Radiother*. (2011) 15:54–63. doi: 10.1016/j.canrad.2010.11.003
13. Moon DH, Wang AZ, Tepper JE. A prospective study of the safety and efficacy of liver stereotactic body radiotherapy in patients with and without prior liver-directed therapy. *Radiother Oncol*. (2018) 126:527–33. doi: 10.1016/j.radonc.2018.01.004
14. Takeda A, Sanuki N, Tsurugai Y, Iwabuchi S, Matsunaga K, Ebinuma H, et al. Phase 2 study of stereotactic body radiotherapy and optional transarterial chemoembolization for solitary hepatocellular carcinoma not amenable to resection and radiofrequency ablation. *Cancer*. (2016) 122:2041–9. doi: 10.1002/cncr.30008
15. Lasley FD, Mannina EM, Johnson CS, Perkins SM, Althouse S, Maluccio M, et al. Treatment variables related to liver toxicity in patients with hepatocellular carcinoma, Child-Pugh class A and B enrolled in a phase 1–2 trial of stereotactic body radiation therapy. *Pract Radiat Oncol*. (2015) 5:e443–9. doi: 10.1016/j.prro.2015.02.007
16. Scorsetti M, Comito T, Cozzi L, Clerici E, Tozzi A, Franzese C, et al. The challenge of inoperable hepatocellular carcinoma (HCC): results of a single-institutional experience on stereotactic body radiation therapy (SBRT). *J Cancer Res Clin Oncol*. (2015) 141:1301–9. doi: 10.1007/s00432-015-1929-y
17. Gkika E, Schultheiss M, Bettinger D, Maruschke L, Neeff HP, Schulenburg M, et al. Excellent local control and tolerance profile after stereotactic body radiotherapy of advanced hepatocellular carcinoma. *Radiat Oncol*. (2017) 12:116. doi: 10.1186/s13014-017-0851-7
18. Kang J-K, Kim M-S, Cho CK, Yang KM, Yoo HJ, Kim JH, et al. Stereotactic body radiation therapy for inoperable hepatocellular carcinoma as a local salvage treatment after incomplete transarterial chemoembolization. *Cancer*. (2012) 118:5424–31. doi: 10.1002/cncr.27533
19. Feng M, Suresh K, Schipper MJ, Bazzi L, Ben-Josef E, Matuszak MM, et al. Individualized adaptive stereotactic body radiotherapy for liver tumors in patients at high risk for liver damage: a phase 2 clinical trial. *JAMA Oncol*. (2018) 4:40–7. doi: 10.1001/jamaoncol.2017.2303
20. Kim JW, Seong J, Lee IJ, Woo JY, KH H. Phase I dose-escalation study of helical intensity-modulated radiotherapy-based stereotactic body radiotherapy for hepatocellular carcinoma. *Oncotarget*. (2016) 26:40756–66. doi: 10.18632/oncotarget.9450
21. Lo C-M, Ngan H, Tso W-K, Liu C-L, Lam C-M, Poon RT-P, et al. Randomized controlled trial of transarterial lipiodol chemoembolization for unresectable hepatocellular carcinoma. *Hepatology*. (2002) 35:1164–71. doi: 10.1053/jhep.2002.33156
22. Llovet JM, Real MI, Montaña X, Planas R, Coll S, Aponte J, et al. Arterial embolisation or chemoembolisation versus symptomatic treatment in patients with unresectable hepatocellular carcinoma: a randomised controlled trial. *Lancet*. (2002) 359:1734–9. doi: 10.1016/S0140-6736(02)08649-X
23. Bettinger D, Gkika E, Schultheiss M, Glaser N, Lange S, Maruschke L, et al. Comparison of local tumor control in patients with HCC treated with SBRT or TACE: a propensity score analysis. *BMC cancer*. (2018) 18:807. doi: 10.1186/s12885-018-4696-8
24. Sapir E, Tao Y, Schipper MJ, Bazzi L, Novelli PM, Devlin P, et al. Stereotactic body radiation therapy as an alternative to transarterial chemoembolization for hepatocellular carcinoma. *Int J Radiat Oncol Biol Phys*. (2018) 100:122–30. doi: 10.1016/j.ijrobp.2017.09.001
25. Shen PC, Chang WC, Lo CH, Yang JF, Lee MS, Dai YH, et al. Comparison of stereotactic body radiation therapy and transarterial chemoembolization for unresectable medium-sized hepatocellular carcinoma. *Int J Radiat Oncol Biol Phys*. (2019) 105:307–18. doi: 10.1016/j.ijrobp.2019.05.066
26. Wahl DR, Stenmark MH, Tao Y, Pollom EL, Caoili EM, Lawrence TS, et al. Outcomes after stereotactic body radiotherapy or radiofrequency ablation for hepatocellular carcinoma. *J Clin Oncol*. (2016) 34:452–9. doi: 10.1200/JCO.2015.61.4925
27. Kim N, Cheng J, Jung I, Liang J, Shih YL, Huang WY, et al. Stereotactic body radiation therapy vs. radiofrequency ablation in Asian patients with hepatocellular carcinoma. *J Hepatol*. (2020) 73:121–9. doi: 10.1016/j.jhep.2020.03.005
28. Lee J, Shin I-S, Yoon WS, Koom WS, Rim CH. Comparisons between radiofrequency ablation and stereotactic body radiotherapy for liver malignancies: Meta-analyses and a systematic review. *Radiother Oncol*. (2020) 145:63–70. doi: 10.1016/j.radonc.2019.12.004
29. Sapisochin G, Barry A, Doherty M, Fischer S, Goldaracena N, Rosales R, et al. Stereotactic body radiotherapy versus TACE or RFA as a bridge to transplant in patients with hepatocellular carcinoma. An intention-to-treat analysis. *J Hepatol*. (2017) 67:92–9. doi: 10.1016/j.jhep.2017.02.022
30. Bedenne L, Michel P, Bouche O, Milan C, Mariette C, Conroy T, et al. Chemoradiation followed by surgery compared with chemoradiation alone in squamous cancer of the esophagus: FFCD 9102. *J Clin Oncol*. (2007) 25:1160–8. doi: 10.1200/JCO.2005.04.7118
31. Bettinger D, Pinato DJ, Schultheiss M, Sharma R, Rimassa L, Pressiani T, et al. Stereotactic body radiation therapy as an alternative treatment for patients with hepatocellular carcinoma compared to sorafenib: a propensity score analysis. *Liver Cancer*. (2018) 8:281–94. doi: 10.1159/000490260
32. Crane CH, Koay EJ. Solutions that enable ablative radiotherapy for large liver tumors: fractionated dose painting, simultaneous integrated protection, motion management, and computed tomography image guidance. *Cancer*. (2016) 122:1974–86. doi: 10.1002/cncr.29878
33. Shigeta K, Datta M, Hato T, Kitahara S, Chen IX, Matsui A, et al. Dual programmed death receptor-1 and vascular endothelial growth factor receptor-2 blockade promotes vascular normalization and enhances antitumor immune responses in hepatocellular carcinoma. *Hepatology*. (2020) 71:1247–61. doi: 10.1002/hep.30889
34. Finn RS, Qin S, Ikeda M, Galle PR, Ducreux M, Kim T-Y, et al. Atezolizumab plus bevacizumab in unresectable hepatocellular carcinoma. *N Engl J Med*. (2020) 382:1894–905. doi: 10.1056/NEJMoa1915745
35. Mellman I, Coukos G, Dranoff G. Cancer immunotherapy comes of age. *Nature*. (2011) 480:480–9. doi: 10.1038/nature10673
36. Formenti SC, Demaria S. Radiation therapy to convert the tumor into an in situ vaccine. *Int J Radiat Oncol Biol Phys*. (2012) 84:879–80. doi: 10.1016/j.ijrobp.2012.06.020
37. Vatner RE, Cooper BT, Vanpouille-Box C, Demaria S, Formenti SC. Combinations of immunotherapy and radiation in cancer therapy. *Front Oncol*. (2014) 4:325. doi: 10.3389/fonc.2014.00325
38. Eckert F, Gaipil US, Niedermann G, Hettich M, Schilbach K, Huber SM, et al. Beyond checkpoint inhibition - Immunotherapeutic strategies in combination with radiation. *Clin Transl Radiat Oncol*. (2017) 2:29–35. doi: 10.1016/j.ctro.2016.12.006
39. Ko EC, Raben D, Formenti SC. The integration of radiotherapy with immunotherapy for the treatment of non-small cell lung cancer. *Clin Cancer Res*. (2018) 24:5792–806. doi: 10.1158/1078-0432.CCR-17-3620

40. Rodel F, Frey B, Multhoff G, Gaip U. Contribution of the immune system to bystander and non-targeted effects of ionizing radiation. *Cancer Lett.* (2015) 356:105–13. doi: 10.1016/j.canlet.2013.09.015
41. Dewan MZ, Galloway AE, Kawashima N, Dewynngaert JK, Babb JS, Formenti SC, et al. Fractionated but not single-dose radiotherapy induces an immune-mediated abscopal effect when combined with anti-CTLA-4 antibody. *Clin Cancer Res.* (2009) 15:5379–88. doi: 10.1158/1078-0432.CCR-09-0265
42. Demaria S, Kawashima N, Yang AM, Devitt ML, Babb JS, Allison JP, et al. Immune-mediated inhibition of metastases after treatment with local radiation and CTLA-4 blockade in a mouse model of breast cancer. *Clin Cancer Res.* (2005) 11:728–34.
43. Vanpouille-Box C, Alard A, Aryankalayil MJ, Sarfraz Y, Diamond JM, Schneider RJ, et al. DNA exonuclease Trex1 regulates radiotherapy-induced tumour immunogenicity. *Nat Commun.* (2017) 8:15618. doi: 10.1038/ncomms15618
44. Grassberger C, Hong TS, Hato T, Yeap BY, Wo JY, Tracy M, et al. Differential association between circulating lymphocyte populations with outcome after radiation therapy in subtypes of liver cancer. *Int J Radiat Oncol Biol Phys.* (2018) 101:1222–5. doi: 10.1016/j.ijrobp.2018.04.026
45. Lammer J, Malagari K, Vogl T, Pilleul F, Denys A, Watkinson A, et al. Prospective randomized study of doxorubicin-eluting-bead embolization in the treatment of hepatocellular carcinoma: results of the PRECISION V study. *Cardiovasc Intervent Radiol.* (2010) 33:41–52. doi: 10.1007/s00270-009-9711-7
46. Facciorusso A, Bellanti F, Villani R, Salvatore V, Muscatiello N, Piscaglia F, et al. Transarterial chemoembolization vs. bland embolization in hepatocellular carcinoma: a meta-analysis of randomized trials. *United Euro Gastroenterol J.* (2016) 5:511–8. doi: 10.1177/2050640616673516

Conflict of Interest: DB: consulting and advisory: Bayer Healthcare, Boston Scientific; teaching and speaking fees: Falk Foundation. MS: consulting and advisory: Bayer Healthcare; teaching and speaking fees: L.W. Gore, Falk Foundation.

The remaining authors declare that the research was conducted in the absence of any commercial or financial relationships that could be construed as a potential conflict of interest.

Copyright © 2021 Brunner, Bettinger, Schultheiss, Maruschke, Sturm, Bartl, Koundurdjieva, Kirste, Neeff, Goetz, Nicolay, Ihorst, Bamberg, Thimme, Grosu and Gkika. This is an open-access article distributed under the terms of the Creative Commons Attribution License (CC BY). The use, distribution or reproduction in other forums is permitted, provided the original author(s) and the copyright owner(s) are credited and that the original publication in this journal is cited, in accordance with accepted academic practice. No use, distribution or reproduction is permitted which does not comply with these terms.



Salvage Radiotherapy for Macroscopic Local Recurrence Following Radical Prostatectomy

Hind Zaine¹, Benjamin Vandendorpe¹, Benoit Bataille¹, Thomas Lacornerie², Jennifer Wallet³, Xavier Mirabel¹, Eric Lartigau^{1,4} and David Pasquier^{1,4*}

¹ Academic Department of Radiation Oncology, Centre Oscar Lambret, Lille, France, ² Department of Medical Physics, Centre O. Lambret, Lille, France, ³ Department of Biostatistics, Centre O. Lambret, Lille, France, ⁴ CRISTAL (Centre de Recherche en Informatique, Signal et Automatique de Lille [Research center in Computer Science, Signal and Automatic Control of Lille] UMR (Unité Mixte de Recherche [joint research center]) 9189, Lille University, Lille, France

OPEN ACCESS

Edited by:

Amar U. Kishan,
University of California, Los Angeles,
United States

Reviewed by:

Sean P. Collins,
Georgetown University,
United States
Laure Marignol,
Trinity College Dublin, Ireland

*Correspondence:

David Pasquier
d-pasquier@o-lambret.fr

Specialty section:

This article was submitted to
Radiation Oncology,
a section of the journal
Frontiers in Oncology

Received: 19 February 2021

Accepted: 29 March 2021

Published: 15 April 2021

Citation:

Zaine H, Vandendorpe B, Bataille B, Lacornerie T, Wallet J, Mirabel X, Lartigau E and Pasquier D (2021) Salvage Radiotherapy for Macroscopic Local Recurrence Following Radical Prostatectomy. *Front. Oncol.* 11:669261. doi: 10.3389/fonc.2021.669261

Introduction: Salvage radiotherapy is the only curative treatment for biochemical progression after radical prostatectomy. Macroscopic recurrence may be found in the prostatic bed. The purpose of our study is to evaluate the effectiveness of salvage radiotherapy of the prostate bed with a boost to the area of the macroscopic recurrence.

Material and Methods: From January 2005 to January 2020, 89 patients with macroscopic recurrence in the prostatectomy bed were treated with salvage radiotherapy +/- hormone therapy. The average PSA level prior to radiotherapy was 1.1 ng/mL (SD: 1.6). At the time of biochemical progression, 96% of the patients had a MRI that revealed the macroscopic recurrence, and 58% had an additional choline PET scan. 67.4% of the patients got a boost to the macroscopic nodule, while 32.5% of the patients only underwent radiotherapy of the prostate bed without a boost. The median total dose of radiotherapy was 70 Gy (Min.: 60 – Max.: 74). The most commonly-used regimen was radiotherapy of the prostatectomy bed with a concomitant boost. 48% of the patients were concomitantly treated with hormone therapy.

Results: After a median follow-up of 53.7 months, 77 patients were alive and 12 had died, of which 4 following metastatic progression. The 5-year and 8-year survival rates (CI95%) are, respectively, 90.2% (78.9-95.6%) and 69.8% (46.4-84.4%). The 5-year biochemical progression-free survival rate (CI95%) is 50.8% (36.7-63.3). Metastatic recurrence occurred in 11.2% of the patients. We did not find any statistically significant impact from the various known prognostic factors for biochemical progression-free survival. No toxicity with a grade of > or = to 3 was found.

Conclusions: Our series is one of the largest published to date. Salvage radiotherapy has its place in the management of patients with biochemical progression with local recurrence in the prostate bed, with an acceptable toxicity profile. The interest of the boost is to be evaluated in prospective trials.

Keywords: prostate cancer, macroscopic recurrence, salvage radiotherapy, boost, post-therapeutic toxicity

HIGHLIGHTS

- Salvage radiotherapy of the prostatectomy bed usually remains the only curative treatment for recurrence after prostatectomy for prostate cancer.
- Radiation oncologists are increasingly faced with macroscopic disease detected in the prostatectomy bed.
- There is no consensus and so there is considerable variability in the management of this category of patients.
- We present one of the largest series of patients with macroscopic recurrence treated by radiotherapy to date.
- Five years after radiotherapy, around half of the patients presented with a new relapse.
- A boost to the recurrence did not influence relapse free survival and toxicity was low.
- The interest of the boost is evaluated in prospective trials currently.

INTRODUCTION

Radical prostatectomy is an effective curative therapy and is widely used for localized prostate cancers. However, 15 to 40% of operated patients develop biochemical progression within five years after surgery (1, 2).

Salvage radiotherapy of the prostatectomy bed usually remains the only curative therapy indicated from a PSA level > 0.2 ng/mL. The effectiveness of this therapy depends on the PSA level, and some studies specify that the treatment is more effective when the pre-treatment PSA is less than 0.5 ng/mL (3, 4).

The benefits of additional hormone therapy vary depending on the pathological characteristics and make it possible to prolong metastasis-free survival (5, 6).

With the progress achieved in imaging (prostate MRIs, choline PET scans) and more recently PSMA PET CT, which is sensitive at PSA levels of less than 1 ng/mL or even 0.5 ng/mL (7, 8), radiation oncologists are increasingly faced with occurrences of biochemical progression with macroscopic disease found in the prostatectomy bed.

A 66 Gy dose, which is commonly used to treat biochemical progression, may be insufficient in cases of macroscopic recurrence, and increasing the doses applied to these recurrences is common.

To date, there is no consensus with regard to the application of a boost (target volumes, techniques, total dose, fractionation, etc.) and so there is considerable variability in the management of this category of patients with macroscopic recurrence.

The purpose of this analysis is to study this category of patients with macroscopic recurrence in the prostatectomy bed; to evaluate, retrospectively, the effectiveness of salvage radiotherapy with boost to the recurrence; and lastly, to define what place hormone therapy has in this situation.

MATERIAL AND METHODS

After having obtained the patients consent to the use of their data, we conducted a retrospective study of the patients treated by radiotherapy of the prostate bed at the Centre Oscar Lambret between January 2005 and January 2020 and who had an identified macroscopic recurrence. All patients treated consecutively were included.

A macroscopic local recurrence was defined by a relapse in prostatectomy bed visible on MRI and/or CT scan and/or choline PET and/or accessible to clinical examination by digital rectal examination.

89 patients were included; their average age when diagnosed was 61.3 years (SD = 5.7). The average pre-operation PSA level was 9.4 mg/mL (SD = 4.9). The surgical stage according to AJCC TNM, 8th Edition, was, for 36%, stage pT3a; for 20%, pT3b; and for 20%, pT2c. Lymph node dissection was performed in 67% of the patients and came back negative (pN0) for all of them. The Gleason score was 7 in 77% of the cases, less than 7 in 14% of the cases, and greater than 7 in 8.9% of the cases. The resection margin was R0 in 51% of the patients. The post-operation PSA nadir could not be measured in 87% of the patients. 53% of the patients developed post-operation urinary complications, mostly grade 1 (40% of the operated patients) (Table 1).

The median time to post-prostatectomy biochemical progression was 2.3 years (Min.: 0.1-Max.: 18.9)

Multiparameter magnetic resonance imaging was performed in all except four patients who had a prostate bed nodule that was palpable on digital rectal examination and visible in the pelvic computed tomography. The median size of the prostate bed nodule was 9.5 mm (Min.: 2-Max.: 35). The recurrence was most often localized in the perianastomotic position (38.8%). 58% of

TABLE 1 | Patient characteristics.

Radical prostatectomy	Population N = 89	
pTNM: T (MD = 5)		
pT2a	7	8%
pT2b	13	15%
pT2c	17	20%
pT3a	30	36%
pT3b	17	20%
pTNM: N (MD = 3)		
N0	58	67%
Nx (no lymph node dissection)	28	33%
Gleason Score (MD = 3)		
Gleason <= 7	78	91%
Gleason >= 8	8	9%
Resection margin (MD = 5)		
R0	43	51%
R1	41	49%
Post-op PSA		
Not measurable	77	87%
Measurable	12	13%
Postoperative urinary toxicities (MD=2)		
Grade 1	35	40.2%
Grade 2	11	12.6%

MD, missing data.

the patients had had a choline PET scan, which showed hyperfixation at the macroscopic nodule in 21% of cases. Pelvic lymph node recurrence was found in 6% of the patients. A biopsy of the prostate bed nodule was performed in 20% of the patients and was positive for 10% of the patients (**Table 2**).

15% of the patients had been treated prior to the salvage radiotherapy: 11% had had hormone therapy, 2% had had chemotherapy in combination with hormone therapy (Rising PSA clinical trial) and 2% had had stereotactic pelvic lymph node radiotherapy in combination with hormone therapy.

TABLE 2 | Characteristics of the macroscopic recurrence following radical prostatectomy.

Characteristics	Population N = 89	
Location of the macroscopic recurrence on the MRI (MD=4)		
Perianastomotic	33	38.8%
Periurethral	5	5.8%
Residual SV or SV bed	10	11.7%
Other	37	43.5%
Size of the macroscopic recurrence on the MRI, in mm (MD = 13)		
Median - (Range)	9.5	(2-35)
Mean – SD	11.3	6.6
PET scan		
Done	52	58%
Non-hypermetsabolic recurrence	33	37%
Hypermetsabolic recurrence	19	21%
Biopsy of the recurrence		
Done	18	20%
Negative	9	10%
Positive	9	10%

MD, Missing data; LR, Local recurrence.

The average PSA level prior to starting radiotherapy was 1.1 ng/mL (SD = 1.6). The average PSA doubling time was 10.7 months (SD = 11.7).

The radiotherapy techniques used were intensity-modulated radiotherapy in 77.5% of the patients and the three-dimensional technique in 22.4% of them.

The median total dose of radiotherapy was 70 Gy (Min.: 60 – Max.: 74); the median dose applied to the prostate bed was 66Gy (Min.:50– Max.:66.6). The median boost fractionation was 2.1 Gy/fraction (Min.: 1.8 – Max.: 6). The median duration of the radiotherapy was 48 days.

The most commonly-used regimen was radiotherapy of the prostatectomy bed with a concomitant supplementary dose (boost) to the macroscopic recurrence (**Figures 1A, B**). 67.4% of the patients treated by salvage radiotherapy received a boost to the macroscopic nodule, applied concomitantly with intensity modulation in 56.66% of them, and sequentially in 43.33% of them. 32.6% of the patients had radiotherapy of the prostate bed alone with no boost. 25% of patents underwent pelvic lymph node irradiation (**Table 3**).

We compared the two groups (with boost and without boost) in terms of median follow-up, baseline PSA, size of the macroscopic recurrence, the use or not of ADT and the choice of radiotherapy technique. The two groups were well balanced except for the technique and follow up. In the boost group, IMRT was used more often (90% vs 51.7%, $p < 0.001$) and the median follow up was shorter: 45 months (40-54 months) vs 61.4 months (51-72 months), $p = 0.03$.

We recorded the acute toxicities (during the radiotherapy and within three months post-treatment) and the delayed ones (more than three months after the end of the treatment). These toxicities were graded on the CTCAE scale, version 4.03.

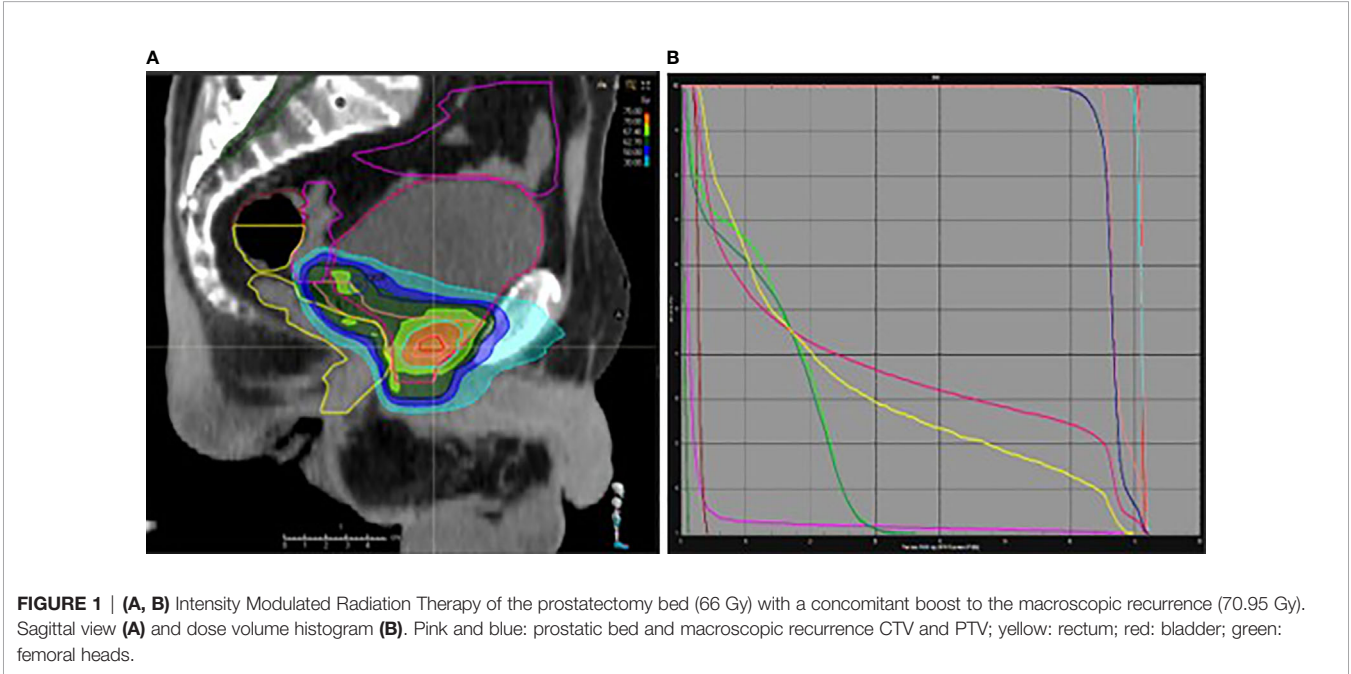


TABLE 3 | Radiotherapy treatment methods.

		Population treated	
Total RT dose, in Gy	Median - (Range) Mean - SD	70 68.8	(60; 74) (2.5)
RT techniques applied to the prostate bed	IMRT: 77.5% 3D: 22.4%		
Boost RT techniques	IMRT: 86.66% 3D: 6.66% Stereotactic: 6.66%		
Regimens and target volumes	Prostate bed + boost: 67.4%	Concomitant boost: 56.66% Sequential boost: 43.33%	Boost fractionation: Gy Median - (Range) 2.1 - (1.8; 6) Mean - SD: 2.3 - 0.9
	Prostate bed, no boost: 32.6% Pelvic lymph node irradiation: 25%		

RT, Radiotherapy; Boost, supplementary dose; IMRT, intensity-modulated radiotherapy; 3D, three-dimensional radiotherapy; Fr, fractionation.

48% of the patients had hormone therapy in combination with the radiotherapy, most often for a short period of time (6 months) (45%). Post-radiotherapy patient follow-up was carried out alternatively with the urologists, on a quarterly basis in the first year and then every six months, with a PSA screening performed prior to each consultation.

Remission is defined by a post-radiotherapy PSA nadir level less than the pre-radiotherapy PSA level. There being no consensual definition about biochemical progression after salvage radiotherapy, we opted for two definitions in our study: PSA > 0.2 ng/mL (definition 1) and post-radiotherapy PSA > PSA nadir + 0.5 ng/mL (definition 2). The latter definition was used in a recent retrospective study (9). Rising PSA was confirmed by two screenings one month apart.

Clinical recurrence is defined by the detection of a local, pelvic lymph node, recurrence or distant metastatic recurrence on imaging studies. A second imaging may be performed at the doctor's discretion.

Statistical Analysis

Biochemical progression-free survival (main criterion) with no metastatic or local recurrence and overall survival (secondary criteria) were estimated using the Kaplan-Meier method from the radiotherapy start date.

The prognostic value of the PSA level at the start of the treatment and the prognostic value of the boost with regard to biochemical progression-free survival were assessed using Cox regression models. The threshold of significance was set at 5%.

The software used was Stata v15.0 (StataCorp. 2009. Stata Statistical Software: Release 11. College Station, TX: StataCorp LP).

RESULTS

Post-radiotherapy remission was achieved in 93% of the patients, 79% of whom had a PSA nadir below 0.1 ng/mL.

The patients' follow-up, calculated using the Kaplan-Meier method, was 53.7 months (42.8-59.4 months). As of this follow-up, 77 patients were alive and 12 had died, of which 4 following metastatic progression. The 5-year (CI95%) and 8-year survival

rates were, respectively, 90.2% (78.9-95.6%) and 69.8% (46.4-84.4%) (**Figure 2**).

The median biochemical progression-free survival (CI95%) were 60.1 months (39.3 - 73.0) and 73.0 months (50.7 - 88.2), according to PSA > 0.2 ng/mL (Definition 1) or post-RT PSA nadir + 0.5 ng/mL (Definition 2), respectively. The 5-year biochemical progression-free survival rates (CI95%) were, respectively, 50.8% (36.7 - 63.3) (Definition 1) and 56.6% (42.7 - 68.2) (Definition 2) (**Table 4**, **Figure 3**).

The average time between the radiotherapy and the biochemical progression (Definition 2) was 2.8 years (SD = 1.9).

Metastatic recurrence occurred in 11.2% of the patients, with 7% of them presenting with bone metastasis.

We performed an analysis of the impact of the prognostic and therapeutic factors (tumoral stage, post-op Gleason score, resection margins, pre-RT PSA level, PSA kinetics, size of the macroscopic recurrence, boost to the macroscopic recurrence, hormone therapy, etc.) on the biochemical progression-free survival rate. None of these factors was significantly associated with biochemical progression-free survival in univariate analysis. Furthermore, we did not observe any significant heterogeneity of Boost effect in terms of biochemical progression-free survival according to the status of hormonotherapy.

With regard to the tolerance of the radiotherapy, 62% of the patients had acute urinary toxicity, of grade 1 in 47% of the cases. 53% of the patients developed delayed urinary toxicity of which 40% were grade 1. The side effects were mostly irritative signs of the lower urinary tract (pollakiuria, urgency). Late hematuria occurred in 4 patients in the Boost group and was grade 1 and 2.

20% and 8%, respectively, developed acute and delayed digestive toxicity. Escalating the radiotherapy dose to the macroscopic nodule in the prostate bed did not seem to increase either the risk or the severity of the acute or delayed urinary and digestive toxicity ($p > 0.5$).

DISCUSSION

Our work is a descriptive retrospective study of a series of 89 patients with a macroscopic recurrence in the prostate bed and who underwent radiation therapy at the Oscar Lambret Centre.

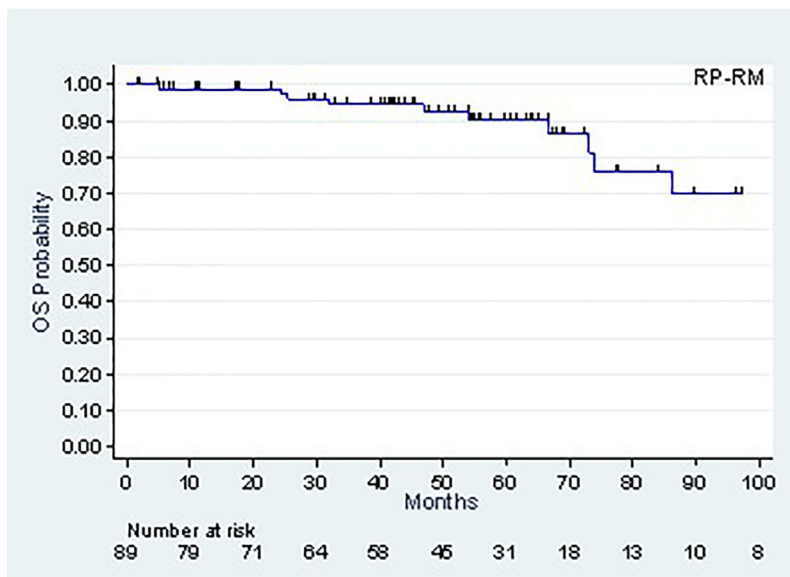


FIGURE 2 | Overall survival.

TABLE 4 | Biochemical progression-free survival.

Characteristics	According to PSA > 0.2 (Def. 1)		According to post-RT PSA nadir+ 0.5 (Def 2)	
Survived with no recurrence				
Number of progressions or deaths	37 ⁽¹⁾		33 ⁽²⁾	
Median (months) (CI95%)	60.1 months	(39.3 – 73.0)	73.0 months	(50.7 – 88.2)
5-year rate (%) (CI95%)	50.8%	(36.7 – 63.3)	56.6%	(42.7 – 68.2)
8-year rate (%) (CI95%)	16.4%	(3.3 – 38.4)	18.8%	(3.8 – 42.4)

⁽¹⁾32 biochemical progressions, PSA > 0.2 & 5 deaths with no prior biochemical progression.

⁽²⁾28 biochemical progressions, post-RT PSA nadir + 0.5 & 5 deaths with no prior biochemical progression.

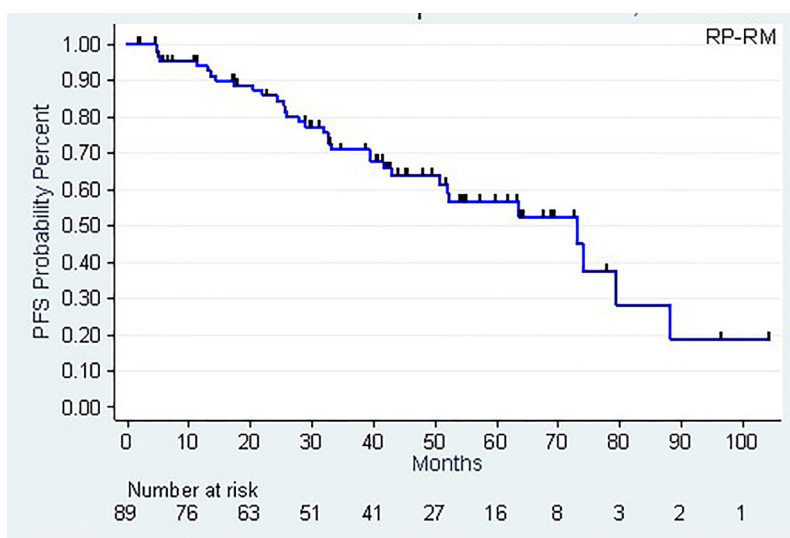


FIGURE 3 | Biochemical progression-free survival (PSA nadir + 0.5 ng/mL).

TABLE 5 | Comparative table of the results of the main retrospective studies.

	Number of pts	RT dose (Gy)	Median PSA (ng/mL)	Median follow-up	bPFS %	mPFS %	OS %
Shelan et al. (10)	69	PB: 64–66 Boost: 72–74 (2 Gy/Fr)	2.7 (0.9–6.5)	38 months	3 years 58% 5 years: 44%	3 years 91% 5 years: 76%	ND
A. Bruni et al. (11)	105	> 70: 58 pts, 66–70: 43 pts, < 66: 4 pts.	29 pts: PSA < 1.0 50 pts: 1.1–PSA < 5, 25 pts: > 5	52 months	5 years: 69.7% 10 years 57.7%	5 years: 86.1% 10 years 73.3%	5 years: 85.5% 10 years 76.1%
Zilli et al. (12)	171, of which 131 LR	PB: 64 (1.8–2 Gy/Fr) Boost: 74 (2 Gy/Fr)	0.75 (0.1–15.6)	36 months	3 years 64.2% Boost (n = 131) 68.4 No boost (n = 40) 49.7 p: 0.251	3 years 93.4 ± 3.3%, 5 years: 85.2 ± 3.2%	3 years 100% 5 years: 92.5%
Our series	89	Median - (Range) 70 (60; 74) Mean - SD 68.8 2.5	0.4 (0.19 – 8)	53.7 months	5 years: 45.6% 5 years: 50.8% 8 years 16.4%	5 years: 76.6% 8 years 57.2%	5 years: 90.2% 8 years 69.8%

pts, patients; RT, radiotherapy; LR, Local Recurrence; bPFS, biochemical-progression-free survival; mPFS, metastatic progression-free survival; OS, overall survival; ND, not documented; PB, Prostatectomy bed; Boost, supplementary dose.

It is one of the series with the largest number of participants published to date (10–12) (**Table 5**).

Salvage radiation is the only potentially curative therapy for biological progression after radical prostatectomy. It is associated with an improved biochemical progression-free survival rate, an improved metastatic progression-free survival rate, and an improved survival rate overall (13). Several studies have shown that the efficiency of salvage RT is highly dependent on the prostate-specific antigen (PSA) level prior to radiotherapy (14).

Magnetic resonance imaging appears to be one of the best diagnostic tools for detecting local recurrence when the PSA level is below < 1 ng/mL (8). Thus, radiation oncologists are increasingly faced with occurrences of macroscopic recurrences in the prostate bed. In our series, 58% of the patients with a macroscopic nodule visible under MRI have a PSA less than or equal to 0.5 ng/mL. Choline PET is associated with improved sensitivity and specificity on lymph node recurrences (15). PSMA PET CTs are more sensitive and can be suggested for patients whose PSA level is less than 0.5 ng/mL (16, 17).

The PSA level prior to salvage radiotherapy is a prognostic factor in the radiotherapy response. In a meta-analysis by Ohri et al, a 1 ng/mL increase in the pre-RT PSA reduces 5-year biochemical progression-free survival by 18.3% (CI of 95%: 10.4%–26.3%) (18). In our series, we did not find any statistically significant correlation between the pre-RT PSA level and the biochemical progression-free survival rate, though this may have been due to the hormone treatment prescribed for about half of the patients.

The optimal dose indicated to treat microscopic disease in the prostate bed is 64–66 Gy (19, 20), which may be insufficient if macroscopic disease is found in the bed. Increasing the dose in this category of patients may be necessary to get therapeutic results comparable to those of patients with no macroscopic disease.

In our analysis, the 5-year biochemical progression-free survival rate was 50.8% ((CI95%): 36.7–63.3); the 5-year metastatic progression-free survival rate was 76.6% ((CI95%): 62.7–85.9). Our results are very similar to those of the retrospective study by Shelan et al. (10); all of the patients in that study were treated uniformly with image-guided dose-escalated RT to the macroscopic recurrence: 3 to 5-year biochemical progression-free survival was 58% and 44%, respectively, and 3 to 5-year clinical survival was 91% and 76%.

In our analysis, we did not find any statistically significant difference between radiotherapy with or without boost, with regard to biochemical progression-free survival; nor did they in the retrospective study by A. Bruni et al. (11) in which no statistical advantage was found in the group receiving the increased dose (>70 Gy) with regard to OS or to mPFS. In another study by Zilli et al. (12), there is no significant difference in 3-year biochemical-progression-free survival between standard prostate bed therapy targeting a microscopic disease and boosted treatment if a nodule is identified by MRI (74 Gy: 68.4 months ± 4.6/64 Gy: 49.7 months ± 10.0).

These various results raise the question of whether there is any interest in escalating the dose to the macroscopic nodule; however, in these various studies, as in ours, the hormone therapy could have masked a potential benefit. In our study,

the increase in the dose to the macroscopic nodule was also limited and might explain these negative results.

With regard to post-radiotherapy toxicity, a prospective study that assesses the escalated dose of post-operation radiotherapy (64Gy vs.70Gy), in the absence of any detectable local recurrence, is the SAKK 09/10 study. This study showed low, grade 2 and grade 3 U and GI toxicity rates with minor impact on urinary quality of life (21). In the Ohri series (18), late GI and GU toxicity increased with salvage radiotherapy dose by 1.2% per Gy ($p=0.012$) and 0.7% per Gy ($p=0.010$), respectively. In our series, escalating the radiotherapy dose to the macroscopic nodule on the prostate bed did not significantly increase the risk and severity of acute and delayed post-radiation toxicity.

Due to the lack of standard management of this category of patients, a prospective study must be undertaken to better define the place of dose escalation, radiotherapy regimens, as well as that of hormone therapy, and thus to standardize care. In this regard, a prospective study, “The MAPS Trial” (NCT01411345) is underway. It assesses dose escalation in light of the recurrence detected in post-prostatectomy MRI (68 Gy, in 2 Gy/fraction to the prostatectomy site and concomitant boost of 2.25 Gy/fraction, for a total dose of 76.5 Gy).

CONCLUSION

Salvage radiotherapy has its place in the management of patients with biochemical progression with local recurrence in the

prostate bed, with an acceptable toxicity profile. The interest of the boost is to be evaluated in prospective trials.

DATA AVAILABILITY STATEMENT

The raw data supporting the conclusions of this article will be made available by the authors, without undue reservation.

ETHICS STATEMENT

Ethical review and approval was not required for the study on human participants in accordance with the local legislation and institutional requirements. Written informed consent for participation was not required for this study in accordance with the national legislation and the institutional requirements.

AUTHOR CONTRIBUTIONS

DP and HZ designed the study. HZ performed the data collection. DP, BV, BB, TL, XM and EL performed the patients' recruitment and the follow-up. JW performed the statistical analysis. HZ wrote the original draft. DP supervised the project. All authors helped revising and editing the manuscript.

REFERENCES

- Han M, Pound CR, Potter SR, Partin AW, Epstein JI, Walsh PC. Isolated local recurrence is rare after radical prostatectomy in men with gleason 7 prostate cancer and positive surgical margins: therapeutic implications. *J Urol* (2001) 165:864–6. doi: 10.1016/S0022-5347(05)66545-7
- Thompson IM, Valicenti RK, Albertsen P, Davis BJ, Goldenberg SL, Hahn C, et al. Adjuvant and salvage radiotherapy after prostatectomy: AUA/ASTRO Guideline. *J Urol* (2013) 190:441–9. doi: 10.1016/j.juro.2013.05.032
- Freedland SJ, Rumble RB, Finelli A, Chen RC, Slovin S, Stein MN, et al. Adjuvant and salvage radiotherapy after prostatectomy: american society of clinical oncology clinical practice guideline endorsement. *J Clin Oncol* (2017) 32:3892–8. doi: 10.1200/JCO.2014.58.8525
- Guidelines NCCN. (2018). <https://www.nccn.org/professionals/>.
- Shipley WU, Seiferheld W, Lukka HR, Major PP, Heney NM, Grignon DJ, et al. Radiation with or without Antiandrogen Therapy in Recurrent Prostate Cancer. NRG Oncology RTOG. *N Engl J Med* (2017) 376(5):417–28. doi: 10.1056/NEJMoa1607529
- Carrie C, Magné N, Burban-Provost P, Sargos P, Latorzeff I, Lagrange JL, et al. Short-term androgen deprivation therapy combined with radiotherapy as salvage treatment after radical prostatectomy for prostate cancer (GETUG-AFU 16): a 112-month follow-up of a phase 3, randomised trial. *Lancet Oncol* (2019) 20(12):1740–9. doi: 10.1016/S1470-2045(19)30486-3
- Umbehre MH, Muntener M, Hany T, Sulser T, Bachann LM. The role of 11c-choline and 18f-fluorocholine positron emission tomography (PET) and PET/CT in prostate cancer: a systematic review and meta-analysis. *Eur Urol* (2013) 64(1):106–17. doi: 10.1016/j.eururo.2013.04.019
- Buergy D, Sertdemir M, Weidner A, Shelan M, Lohr F, Wenz F, et al. Detection of local recurrence with 3-Tesla MRI after radical prostatectomy: a useful method for radiation treatment Planning. *In Vivo* (2018) 32(1):125–31. doi: 10.21873/invivo.11214
- Shelan M, Abo-Madyan Y, Welzel G, Bolenz C, Kosakowski J, Behnam N, et al. Dose-escalated salvage radiotherapy after radical prostatectomy in high risk prostate cancer patients without hormone therapy: outcome, prognostic factors and late toxicity. *Radiat Oncol* (2013) 27(8):276. doi: 10.1186/1748-717X-8-276
- Shelan M, Odermatt S, Bojaxhiu B, Nguyen DP, Thalmann GN, Aebbersold DM, et al. Disease Control With Delayed Salvage Radiotherapy for Macroscopic Local Recurrence Following Radical Prostatectomy. *Front Oncol* (2019) 9:12. doi: 10.3389/fonc.2019.00012
- Bruni A, Ingrosso G, Trippa F, Di Staso M, Lanfranchi B, Rubino L, et al. Macroscopic locoregional relapse from prostate cancer: which role for salvage radiotherapy. *Clin Trans Oncol* (2019) 21(11):1532–37. doi: 10.1007/s12094-019-02084-0
- Zilli T, Jorcano S, Peguret N, Caparrotti F, Hidalgo A, Khan HG, et al. Results of Dose-adapted Salvage Radiotherapy After Radical Prostatectomy Based on an Endorectal MRI Target Definition Model. *Am J Clin Oncol* (2017) 40(2):194–9. doi: 10.1097/COC.000000000000130
- King CR. The timing of salvage radiotherapy after radical prostatectomy: a systematic review. *Int J Radiat Oncol Biol Phys* (2012) 84(1):104–11. doi: 10.1016/j.ijrobp.2011.10.069
- Stephenson AJ, Scardino PT, Kattan MW, Pisansky TM, Slawin KM, Klein EA, et al. Predicting the outcome of salvage radiation therapy for recurrent prostate cancer after radical prostatectomy. *J Clin Oncol* (2009) 25:2035–41. doi: 10.1200/JCO.2006.08.9607
- Sandgren K, Westerlinck P, Jonsson JH, Blomqvist L, Thellenberg Karlsson C, Nyholm T, et al. Imaging for the detection of locoregional recurrences in biochemical progression after radical prostatectomy—a systematic review. *Eur Urol Focus* (2017) 5(4):550–60. doi: 10.1016/j.euf.2017.11.001
- Annunziata S, Pizzuto DA, Treglia G. Diagnostic Performance of PET Imaging Using Different Radiopharmaceuticals in Prostate Cancer According to Published Meta-Analyses. *Cancers (Basel)* (2020) 12(8):2153. doi: 10.3390/cancers12082153

17. Mottet N, Cornford P, van den Bergh RCN, Briers E, De Santis M, et al. EAU - EANM - ESTRO - ESUR - ISUP - SIOG Guidelines on Prostate Cancer. (2021). Available at: <https://uroweb.org/>.
18. Ohri N, Dicker AP, Trabulsi EJ, Showalter TN. Can early implementation of salvage radiotherapy for prostate cancer improve the therapeutic ratio? A systematic review and regression meta-analysis with radiobiological modelling. *Eur J Cancer* (2012) 48(6):837–44. doi: 10.1016/j.ejca.2011.08.013
19. Cox JD, Gallagher MJ, Hammond EH, Kaplan RS, Schellhammer PF. Consensus statements on radiation therapy of prostate cancer: guidelines for prostate re-biopsy after radiation and for radiation therapy with rising prostate-specific antigen levels after radical prostatectomy. American society for therapeutic radiology and oncology consensus panel. *J Clin Oncol* (1999) 17:1155. doi: 10.1200/JCO.1999.17.4.1155
20. Cornford P, Bellmunt J, Bolla M, Briers E, De Santis M, Gross T, et al. EAU-ESTRO-SIOG guidelines on prostate cancer. part II: treatment of relapsing, metastatic, and castration-resistant prostate cancer. *Eur Urol* (2017) 71(4):630–42. doi: 10.1016/j.eururo.2016.08.002
21. Ghadjar P, Hayoz S, Bernhard J, Zwahlen DR, Hölscher T, Gut P, et al. Acute toxicity and quality of life after dose-intensified salvage radiation therapy for biochemically recurrent prostate cancer after prostatectomy: first results of the randomized trial SAKK 09/10. *J Clin Oncol* (2017) 33:4158–66. doi: 10.1200/JCO.2015.63.3529

Conflict of Interest: The authors declare that the research was conducted in the absence of any commercial or financial relationships that could be construed as a potential conflict of interest.

Copyright © 2021 Zaine, Vandendorpe, Bataille, Lacornerie, Wallet, Mirabel, Lartigau and Pasquier. This is an open-access article distributed under the terms of the Creative Commons Attribution License (CC BY). The use, distribution or reproduction in other forums is permitted, provided the original author(s) and the copyright owner(s) are credited and that the original publication in this journal is cited, in accordance with accepted academic practice. No use, distribution or reproduction is permitted which does not comply with these terms.



Studies of Intra-Fraction Prostate Motion During Stereotactic Irradiation in First Irradiation and Re-Irradiation

Alexandre Taillez^{1,2}, Andre-Michel Bimbai³, Thomas Lacornerie⁴, Marie-Cecile Le Deley³, Eric F. Lartigau^{1,2,5} and David Pasquier^{1,2,5*}

¹ Academic Department of Radiation Oncology, Oscar Lambret Comprehensive Cancer Center, Lille, France, ² University of Lille, Lille, France, ³ Department of Biostatistics, Oscar Lambret Comprehensive Cancer Center, Lille, France, ⁴ Department of Medical Physics, Oscar Lambret Comprehensive Cancer Center, Lille, France, ⁵ CRISTAL UMR CNRS 9189, University of Lille, Lille, France

OPEN ACCESS

Edited by:

Sean P. Collins,
Georgetown University,
United States

Reviewed by:

Nils H. Nicolay,
University of Freiburg Medical
Center, Germany
Debra Freeman,
GenesisCare, United States

*Correspondence:

David Pasquier
d-pasquier@o-lambret.fr

Specialty section:

This article was submitted to
Radiation Oncology,
a section of the journal
Frontiers in Oncology

Received: 02 April 2021

Accepted: 28 June 2021

Published: 14 July 2021

Citation:

Taillez A, Bimbai A-M, Lacornerie T,
Le Deley M-C, Lartigau EF and
Pasquier D (2021) Studies of Intra-
Fraction Prostate Motion During
Stereotactic Irradiation in First
Irradiation and Re-Irradiation.
Front. Oncol. 11:690422.
doi: 10.3389/fonc.2021.690422

Background: Understanding intra-fractional prostate motions is crucial for stereotactic body radiation therapy (SBRT). No studies have focused on the intra-fractional prostate motions during re-irradiation with SBRT. The objective was to evaluate these translational and rotational motions in primary treated patients and in the context of re-irradiation.

Methods: From January 2011 to March 2020, 162 patients with histologically proven prostate cancer underwent prostate SBRT, including 58 as part of a re-irradiation treatment. We used the continuous coordinates of the fiducial markers collected by an orthogonal X-ray dual-image monitoring system. The translations and rotations of the prostate were calculated. Prostate deviations representing overall movement was defined as the length of the 3D-vectors.

Results: A total of 858 data files were analyzed. The deviations over time in the group of primary treated patients were significantly larger than that of the group of re-irradiation, leading to a mean deviation of 2.73 mm (SD =1.00) versus 1.90 mm (SD =0.79), $P < 0.001$. In the re-irradiation group, we identified displacements of -0.05 mm (SD =1.53), 0.20 mm (SD =1.46); and 0.42 mm (SD =1.24) in the left-right, superior-inferior and anterior-posterior planes. Overall, we observed increasing deviations over the first 30 min followed by a stabilization related to movements in the three translational axes.

Conclusion: This is the first study to focus on intrafraction prostate motions in the context of re-irradiation. We observed that intra-fraction prostate motions persisted in the setting of re-irradiation, although they showed a significant reduction when compared with the first irradiation. These results will help to better estimate random errors during SBRT treatment of intra-prostatic recurrence after irradiation.

Keywords: prostatic neoplasms, re-irradiation, stereotactic radiation therapy, motion, dose hypofractionation, salvage therapy, tracking

INTRODUCTION

With an estimated 1.4 million new cases and 375,000 deaths worldwide, prostate cancer was the second most frequent cancer and the fifth leading cause of cancer death among men in 2020 (1). Radiation therapy has been validated as a standard treatment for localized prostate cancer (2, 3) and several radiation therapy methods have been developed. Studies have shown that by delivering high doses of radiation per session, stereotactic radiation therapy (SBRT) provides a control similar to that obtained with standard techniques (4–6).

An intra-prostatic recurrence is the site of first recurrence after normal fractionated radiation therapy (7). Traditional treatment options for the local treatment of intra-prostatic recurrence include radical prostatectomy, brachytherapy, cryotherapy, and high-intensity focused ultrasound (HIFU) (2). Re-irradiation using SBRT has emerged as an important technique for this indication showing, with a short follow-up of 26 months, a good local control rate of 83.2% (95% CI, 75.5% – 90.9%), a survival without biological recurrence of 59.3% (95% CI, 47.9% – 70.7%) with a low severe toxicity rate Grade ≥ 2 for gastrointestinal (GI) 1.1% (95% CI, 0.1% – 2.0%), and genitourinary (GU) 10.5% (95% CI, 5.5% – 15.4%) (8–12).

Knowledge of the existence of intrafraction prostate motions during an extremely hypo-fractionated session is necessary to limit the volume already irradiated. The follow-up by X-ray orthogonal images of the Cyberknife® (Accuray Incorporated, Sunnyvale, CA, USA) fiducial markers implanted in the prostate gland makes it possible to monitor the position of the target to take it into account when performing the treatment.

Several studies with a small number of patients focused on the intra-fractional prostate motions during the first stereotactic irradiation using the Cyberknife®. Their findings showed that the prostate underwent translational and rotational motions during a session (13, 14). However, to date, no studies have focused on prostate motions in the context of re-irradiation using SBRT. Therefore, this study aimed to investigate the intra-fractional prostate motions in the first irradiation and in three re-irradiations using SBRT with a Cyberknife®.

MATERIALS AND METHODS

Screening of Patients

We collected the data from 162 patients treated at the Oscar Lambret Center (Lille, France), retrospectively. We included all the cancer patients treated with prostate SBRT using a dedicated Cyberknife® VSI or Cyberknife® M6 between January 1, 2011 and March 1, 2020.

Abbreviations: SBRT, stereotactic body radiation therapy; SD, standard deviation; HIFU, high-intensity focused ultrasound; EBRT, External Beam Radiation Therapy; GTV, Gross Tumor Volume; CTV, Clinical Target Volume; PTV, Planning Target Volume, DRR, Digitally Reconstructed Radiograph; LR, Left-Right; SI, Superior-Inferior, AP, Anterior-Posterior; AUC, area under the deviation curve; Kv, Kilovoltage; IMRT, intensity-modulated radiation therapy; MRI-magnetic resonance imaging; IGRT, image-guided radiation therapy; MRI-LINAC, magnetic resonance imaging-guided linear accelerator.

The patients were divided into two different population groups, with the first group comprising patients with an indication for SBRT as a treatment for localized prostate disease who had never received local treatment, and the second group comprising patients treated with SBRT for an intra-prostatic recurrence after the first radiation of the external beam radiation therapy (EBRT) type or brachytherapy. Hormone therapy was administered before or during irradiation. Prostate biopsy was systematic before treatment initiation in both groups. With regard to the group of patients receiving re-irradiation with SBRT, we enrolled primary patients treated for prostate adenocarcinoma or other pelvic neoplasia. There was no rectal preservation strategy using an endorectal balloon or gel spacer. An empty rectum was used as the half-full bladder preparation protocol.

In the context of the first irradiation using SBRT, the prescription dose was 36.25 Gy in five fractions for an isodose of 80%. The clinical target volume (CTV) included the entire prostate gland and the proximal part of the seminal vesicles from patients classified as the intermediate-risk group according to the D'Amico classification. The margins of the planning target volume (PTV) were 5 mm in all directions, except in the posterior direction which was 3 mm. During focal or whole gland re-irradiation, the prescription dose was 36 Gy in six fractions for a prescription dose of 80%. The PTV margin was 2 mm (9).

Acquisition of the Cyberknife® Data

Two pairs of gold fiducial markers were placed in all the enrolled patients with the implantation of one pair at the apex and the other pair at the prostate base (15). To determine the position of the target when the patient was placed on the table, the data from the double orthogonal X-ray images taken at 45° and 135° in the horizontal plane and data from the digitally reconstructed radiograph (DRR), were reset. The readjustment was applied automatically on the treatment table.

The acquisition images of the fiducial marker follow-up were made automatically with the In-tempo® system by adjusting the inter-image time according to the intra-fractional motions of the fiducial markers. In this system, the imaging and beam delivery was adapted to the rate and extent of tracked movements throughout the treatment, ensuring that accuracy is maintained from the first beam to the last. An automatic correction was then made to adjust the delivery of the beams (16). The deviations calculated from the radiographic images acquired in the time interval between the two motions of the table constituted a set of data.

The coordinates of the fiducial markers representing the prostate were collected throughout each session (with a median time of 50 s between two images) with treatment information for each beam, the beam and node number, and the movement of the target position.

Statistical Analyses

In each session with each patient, we analyzed the motions in relation to the reference point defined at the start of the session which corresponded to the barycenter of the fiducials after the first follow-up image.

The coordinates were recorded in three planes to measure the lateral, vertical, and longitudinal motions: “LR (Left-Right),” “SI (Superior-Inferior)” and “AP (Anterior-Posterior). Rotational motions were also recorded (“Roll,” “Pitch,” and “Yaw”). At each measurement time, we calculated the deviation from the reference point as the square root of the sum of the squares of the measurements “LR (Left-Right),” “SI (Superior-Inferior)” and “AP (Anterior-Posterior).” This deviation represented the overall prostate motion (length of the 3D vector).

For each session, we estimated the area under the deviation curve (AUC) for all treatment times up to 60 min; measurements after 60 min were ignored because of the low number of fractions that lasted more than 60 min. We then estimated the mean deviation for each session by dividing the AUC by the session’s treatment time (shortened to 60 min). The mean deviation was estimated per patient to compare the treatment groups (primary irradiation versus re-irradiation) using the Student’s t-test.

The deviation time variations were described considering the distribution of this parameter by 10-minute time interval, between 0 and 60 minutes, overall and by treatment group (primary irradiation vs. re-irradiation).

The deviation was modeled using a mixed linear regression which made it possible to estimate the mean difference between the two treatment groups. This took into account the time effect, overall, and according to treatment group (time \times treatment interaction) while considering the patient factor as a random factor. With regard to the six basic measurements of motion “LR (Left-Right),” “SI (Superior-Inferior),” “AP (Anterior-Posterior),” “Roll,” “Pitch” and “Yaw,” we calculated their means and standard deviations for each 10-minute time interval [(0,10), (10, 20)...(50-60)].

The significance of the test was set at $P < 0.05$. All the statistical analyses were performed using STATA v15.

RESULTS

Description of Populations

After excluding five patients who objected to the use of their medical data, the study population consisted of 162 patients whose median age at enrollment was 73 years old. Among the 162 patients, 58 (35.8%) received stereotactic re-irradiation, and 104 received their first stereotactic radiation (64.2%). A total of 858 sessions were analyzed. The patient and tumor characteristics during SBRT treatment are described in **Table 1**.

The initial characteristics of the patients who received SBRT after re-irradiation are described in **Table 2**. Among these 58 patients, 49 (84.5%) received the first irradiation for prostate neoplasia. Six re-irradiations were performed after the neoadjuvant treatment of rectal cancer and three after other indications (lymph nodes metastases of cutaneous neuroendocrine carcinoma, bladder urothelial carcinoma, and retroperitoneal liposarcoma). Three-dimensional conformal radiation therapy was the initial technique that was used, with 69% of the irradiation being in the context of a first indication. Prostate brachytherapy was performed in 14 patients (24.1%). Previously irradiated prostate disease was most often confined to the prostate gland (75.5% classified as cT1 and cT2).

Duration of Treatments

With regard to the duration of the sessions, they lasted on average 42.2 minutes (± 12.5) for primary irradiation and 40 minutes (± 17.3) for re-irradiation. Less than 10% of the sessions lasted more than 60 minutes (80/858). As shown in **Figure S1 (Appendix)**, most sessions lasted between 30 and 50 minutes (243 sessions, 28.3% between 30 and 40 minutes, and 234 sessions, 27.3%, between 40 and 50 minutes).

TABLE 1 | Patient and tumor characteristics at the time of SBRT (N=162).

Characteristics	1st irradiation N=104		Re-irradiation N=58		Total N =162	
Age (years)						
Median (min.; max.)	75	(54 – 85)	70	(51 – 87)	73	(51 – 87)
ECOG Performance Status		(M=4)				
0	77	77.0%	52	89.7%	129	81.6%
1	22	22.0%	6	10.3%	28	17.7%
2	1	1.0%	0	0.0%	1	0.6%
History of pelvic surgery						
No	103	99.0%	52	89.6%	155	95.7%
Yes	1	1.0%	6	10.3%	7	4.3%
PSA (ng/mL)						
Median (min.; max.)	8	(2.3 – 78.0)	5	(0.4 – 39.0)	7	(0.4 – 78.0)
Gleason score				(M=7)		(M=7)
≤ 6	48	46.2%	7	13.7%	55	35.5%
3+4	40	38.5%	8	15.7%	48	30.1%
4+3	12	11.5%	8	15.7%	20	12.9%
≥ 8	4	3.9%	22	43.1%	26	16.8%
N/A ¹	0	0%	6	11.8%	6	4.9%
Prognostic group of Amico						
Favorable	35	33.7%				
Favorable intermediate	40	38.5%				
Unfavorable intermediate	17	16.3%				
High risk	12	11.5%				

M, missing data; N/A¹, anatomical pathology analysis not feasible; ECOG, Eastern Cooperative Oncology Group; PSA, prostate-specific antigen.

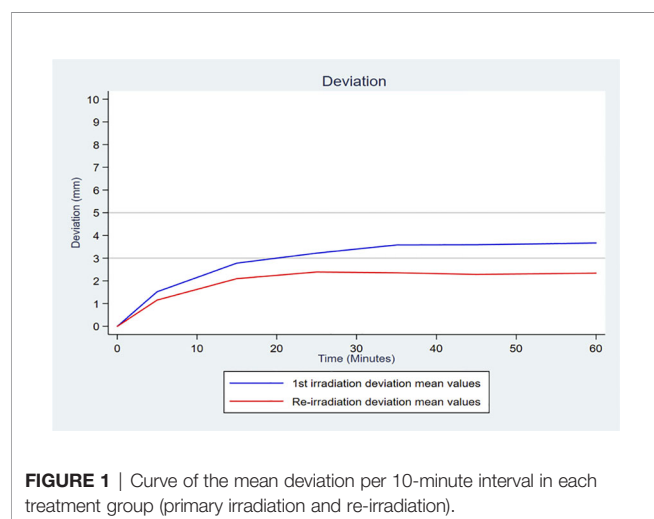
TABLE 2 | Patient, tumor and treatments characteristics at the time of first irradiation in patients who had SBRT as “re-irradiation” (N=58).

Characteristics		
Neoplasia related to 1st irradiation		
Prostate	49	84.5%
Rectum	6	10.3%
Other	3	5.2%
Technique used during the 1st irradiation		
IMRT	4	6.9%
3D-CRT	40	69.0%
Brachytherapy	14	24.1%
Abdominal-pelvic amputation		
Yes	0	0%
No	58	100%
Dose of the first radiation (Gy)		
Median (min.; max.)	70.1	(45 – 78)
D’AMICO prognostic group during the 1st irradiation (N=49)		
Favorable	16	34.0%
Favorable intermediate	8	17.0%
Unfavorable intermediate	2	4.3%
High risk	21	44.7%
TNM-staging of prostate cancer for a first irradiation (N=49)		
cT1a	1	2.2%
cT1b	1	2.2%
cT1c	14	31.1%
cT2a	10	22.2%
cT2b	3	6.7%
cT2c	5	11.1%
cT3a	6	13.3%
cT3b	3	6.7%
cT3aN1	1	2.2%
cT3bN1	1	2.2%

M, missing data; IMRT, intensity-modulated radiation therapy; 3D-CRT, three-dimensional conformal radiation therapy.

Description of Motions

Figure 1 describes the changes in the deviations over time according to the treatment group (primary irradiation and re-irradiation). The mean deviation over time in the primary irradiation group was significantly greater than that in the



re-irradiation group (mean deviation of 2.73, SD = 1.00, *versus* 1.90, SD = 0.79, respectively, $P < 0.001$), demonstrating an increased prostate mobility for primary irradiations.

The result of the mixed linear regression confirmed a significant temporal trend ($P < 10^{-4}$) and significant mean differences between the two groups, estimated at -0.71 mm (95% CI, -1.01 to -0.40; $P < 10^{-4}$) when the model was adjusted only over time. The model with interaction made it possible to conclude that not only was there was a significantly different mean deviation between the two groups, there was also a greater increase in the deviation over time in the primary irradiation group than in the re-irradiation group (the gradient being 0.51 mm and 0.43 mm for 10 minutes of time respectively, with a significant time x treatment interaction test, $P < 10^{-4}$) (**Table A1 in the Appendix**).

With regard to the variability over time of the prostate motion around the average, the results showed that motions of re-irradiation were -0.05 mm (SD = 1.53) for the LR translation, -0.2 mm (SD = 1.46) for the SI translation, and 0.42 mm (SD = 1.24) for the AP translation.

Concerning the temporal evolution of the prostate motions on the rotational axes in re-irradiation, it is noted that these motions remained close to the position observed at the beginning of the session, particularly for the roll (average = 0.02° , SD = 0.81°) and yaw (average = 0.05° , SD = 0.65°) axes. On the pitch, we observed a rotational average of -0.13° with a SD of 1.52° .

Figure 2 shows the changes in the deviations over time for the entire study population. Considering the 10-minute time intervals, there was an increase in the deviations over the first 30 minutes (median of 0.82, 1.94 and 2.37 mm in the intervals 0 – 10, 10 – 20, and 20 – 30, respectively) with a stabilization of the deviation after the first 30 minutes (median of 2.74, 2.75 and 2.82 mm in the intervals 30 – 40, 40 – 50, and 50 – 60, respectively). In the time intervals after the first 20 min, more than 35% of the recorded deviation values were measurements above 3 mm, and more than 14% were above 5 mm (**Figure S2 in the appendix**).

Figure 3 illustrates the mean motions and dispersion of these motions over time for all the sessions and patients. We observe more translational motions (for all the measurements, SD = 2.05, 1.86 and 1.60 mm for the LR, SI and AP translational motions respectively) and “Pitch” rotations (SD = 1.86°), contrasting with a low variability in “Roll” and “Yaw” rotations (SD = 0.88 and 0.81° respectively). The histogram of the distribution of the different measurements is illustrated by 20-minute intervals (0 – 20, 20 – 40, and 40 – 60) in **Appendix Figure S3**.

DISCUSSION

The delivery of a large number of small, non-isocentric, and non-coplanar beams directed at a target with a sub millimetric precision near the organs at risk, requires knowledge of prostate motions, especially since they are random and unpredictable (17). Our data suggested that during the first stereotactic irradiation of the prostate and during stereotactic re-irradiation after another radiation therapy technique, there were small but significant differences in the intra-fractional prostate motions.

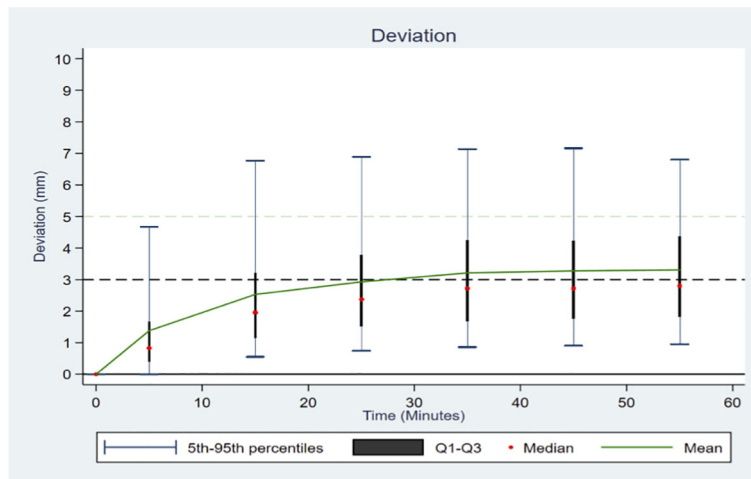


FIGURE 2 | Distribution of the deviation according to time in 10-minute intervals, across all patients.

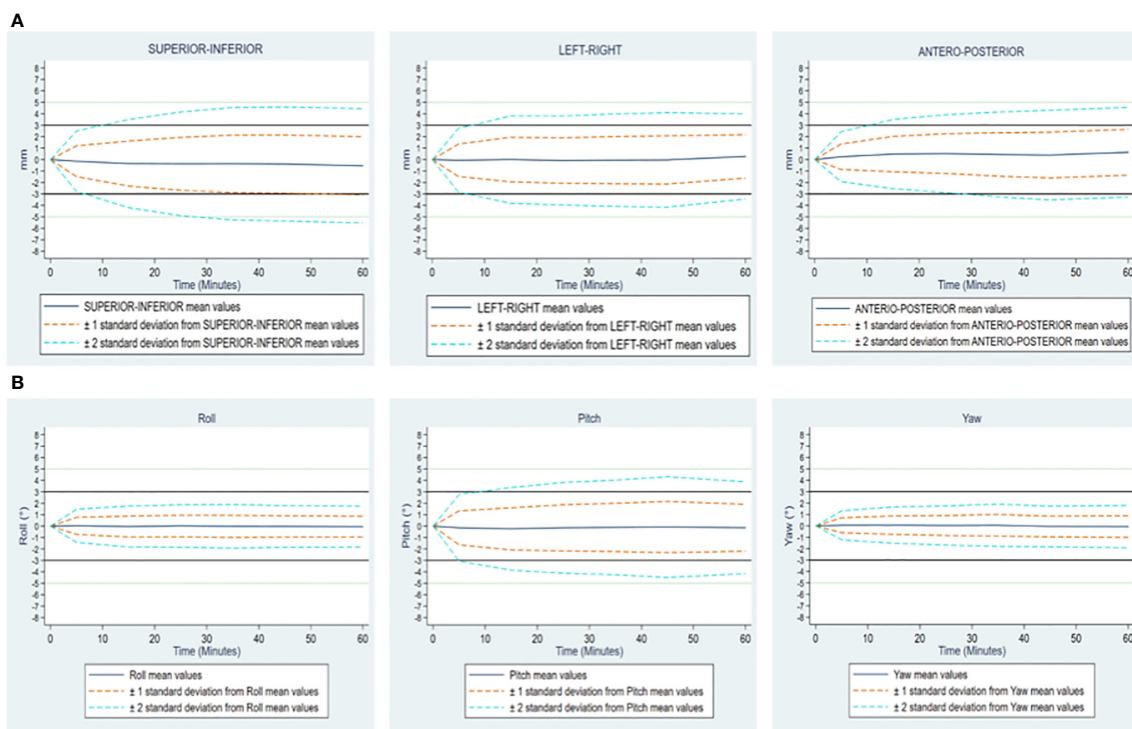


FIGURE 3 | (A) Translational motions Superio-Inferior, left-Right and antero-posterior expressed in mm. (B) Rational motions Roll, Pitch and Yaw expressed in degrees. Changes over time of translational and rotational motions of the prostate, in all patients. On each figure, mean values and standard deviations, by 10-minute time interval, overall considering both groups together.

To our knowledge, this is the first study to analyze intra-fractional prostate motions during stereotactic re-irradiation. This is a retrospective study but all treated patients have been included and we used technical data, so the retrospective nature does not influence the results.

One of the hypotheses for the weakest intra-fractional prostate motion is the onset of pelvic fibrosis following the first irradiation. Another hypothesis is better knowledge of preparation instructions during re-irradiation, since the patient had already applied them previously. Indeed, patients with

experience in long external radiation therapy (with almost 40 fractions) could be able to better apply preparations instructions when starting a new irradiation.

The extent of intra-fractional motions is disputed. Some studies that focused on the motions during a shorter irradiation with intensity-modulated radiation therapy (IMRT) have reported a significant number of necessary corrections, while others have described only more insignificant motions. These studies used different imaging systems as tools, such as the megavolt (18), megavolt-kilovolt imaging (19), Varian Calypso System (Varian Medical Systems, Palo Alto, CA, USA) (20, 21), and magnetic resonance imaging (MRI) (22).

With an increase in treatment duration, the significance of intra-fractional motion has grown, with appreciable variation being demonstrated. For the first 10 minutes of traditional radiation therapy, observations are similar to the multiple data that can be found in the literature focusing on prostatic motion.

Real-time tracking methods using orthogonal kV X-ray imaging with Exatrac Optical System showed average intra-fractional motion (± 1 SD) in the LR, SI, and AP directions of 0.7 ± 0.5 mm, 1.3 ± 0.7 mm, and 1.4 ± 0.9 mm respectively (23). Other studies such as Willoughby et al. have used an electromagnetic tracking system with Calypso® for prostate real-time tracking during external beam radiotherapy and their results showed that the average (SD) of the maximum differences were 0.91 ± 0.35 mm, 3.61 ± 3.13 mm, and 3.92 ± 4.32 mm in the lateral, longitudinal, vertical directions, respectively (24). Motion can also be studied with MRI. For instance, Mah D et al. showed prostate displacements (mean \pm SD) of: 0.2 ± 2.9 mm, 0.0 ± 3.4 mm, and 0.0 ± 1.5 mm in the anterior–posterior, superior–inferior, and left–right dimensions respectively (25).

The increase of motion with time has also been demonstrated in conventional fractionation by IMRT (26). For example, a study using a total of 68 sagittal cine-MRI sequences demonstrated an increasing displacement in the AP and SI planes during treatment with SD of 0.57 mm and 0.41 mm in the first two minutes increasing to 1.44 mm and 0.91 mm in the two to four minutes. This appears to be consistent with the increase in motion over time found in our study (27).

With the Cyberknife®, since the treatment time was close to 40 min per session, tracking was considered to be the most suitable solution. There is a tendency for more extensive motions when the session is long (17, 28, 29). Classic linear accelerators also allow stereotactic prostate radiotherapy to be performed. The treatment time is much shorter and image-guided radiation therapy (IGRT) techniques are different.

With regard to the translational components LR, SI, and AP during the first stereotactic irradiation by Cyberknife®, compared to the results of previous studies, our results were homogenous. Moreover, Koike et al. (30), based on the files of 16 patients, reported an LR of -0.09 ± 0.81 mm, a SI of 0.15 ± 2.06 mm, and an AP of 0.79 ± 1.99 mm, as well as an average deviation of 2.53 ± 1.77 mm. Similarly, Choi et al. (14), with data from 71 patients, found the translational averages for LR to be

0.12 ± 0.19 mm, SI 0.15 ± 0.31 mm, and AP 0.73 ± 0.32 mm with an average deviation of 1.0 ± 0.35 mm. Furthermore, Xie et al. (13) used data from 21 patients and found that for the LR, SI, and AP directions, values were 0.87 ± 1.17 mm, 1.55 ± 1.28 mm, and 1.80 ± 1.44 mm, respectively. Our average deviation data were consistent with the results of Xie et al. (13), showing a deviation of 2.61 mm (± 1.94 mm) during *de novo* irradiation. With regard to rotational prostate motions, in the work of Wolf et al. (31), the rotational data of 20 patients were evaluated, showing pitch rotations of 3.6° (SD 4.9°), roll 0.2° (SD 2.1°) and yaw 0.1° (SD 2.1°). The analysis by Cuccia et al. (32) showed rotations of the yaw at $0.09 \pm 0.10^\circ$, pitch $-0.04 \pm 0.33^\circ$, and roll $0.18 \pm 0.15^\circ$.

Other analyses of prostate motions were presented more recently as part of an irradiation with a magnetic resonance imaging-guided linear accelerator (MRI-LINAC), where the time per fraction was quite close to that performed with the Cyberknife®, that is, between 30 and 50 min per session (32, 33). Data from Cuccia et al. (32) on 100 fractions showed translational motions such as LR -0.24 ± 2.5 mm, SI 0.06 ± 0.46 mm and AP -0.17 ± 0.91 mm.

Our study found mainly translational motions in AP and SI, as observed by Langen et al. (28, 34), and there was a continuously increasing motion independent of the first irradiation or re-irradiation group, in line with the findings of other studies using prostate coordinates during irradiation by MRI-LINAC, particularly with respect to the findings of Keizer et al. (33).

The addition of a rectal preservation strategy has also been studied in the context of irradiation with SBRT. In other words, Cuccia et al. (32) were interested in the influence of the hydrogel spacer on the intra-fraction motions during irradiation with MRI-LINAC, and it was reported that the pitch rotation decreased significantly due to the use of this strategy. The use of the endorectal balloon or hydrogel spacer in SBRT is a possible option that has shown benefits, particularly in dosimetry (35, 36).

SBRT salvage therapy has been evaluated mainly retrospectively (8) and several prospective multicenter studies are ongoing (11, 12, 37).

Our study did not investigate the causes that could influence prostatic movements during a session, although displacements greater than 5 mm were observed in 14% of patients. However, several investigators have shown that non-resolving slow drift, mainly in the AP direction, is due to rectal filling, and that sudden transient motion, most frequent in AP and SI directions, is due to intestinal peristalsis. These are the two main types of prostate motion during a session. Pelvic muscle contraction can also contribute to AP plan. Systematic and random motions are significant in the AP and SI axes, while they are less significant in the LR axis (26, 38).

In our study, re-irradiation was the only factor that influenced prostate motion.

Several stereotactic radiation therapies exist in clinical routine and there are many IGRT methods. Image tracking with InTempo®, Exatrac® (ExacTrac, BrainLAB AG, Heimstetten, Germany) or transponders such as Calypso® (Varian Medical

Systems, Palo Alto, CA) are another way to track intra-fractional motion of a target. Real-time image tracking is all the more significant if the treatment time is long since we know that the movements can be more important (27, 39).

Currently, the only truly real-time IGRT methods are presented by MRI-Linac and Calypso® monitoring, however their accessibility is low worldwide. One of the strengths of the Cyberknife is that it can adapt the time between each image according to the motions previously recorded. It is therefore an adaptive discontinuous tracking almost in real time (Kv imaging between 15 and 150 seconds). Using Linac, a cone-beam-CT/Kilovoltage (Kv) follow-up can estimate the intra-fraction prostatic position between each arc but cannot be used during treatment delivery to assess for intrafraction organ motion especially because of prostate abrupt movements.

Some stereotactic irradiations are performed without real time tracking and we believe that in the context of a re-irradiation, real time tracking should be privileged although its clinical relevance is not established.

Finally, Choi et al. (14) showed that prostatic motion in the AP plane and global deviation had a possible association with digestive and urinary toxicities during Cyberknife® SBRT despite automatic correction. It therefore appears relevant to better understand prostatic motion in a context of increased risk of toxicity due to re-irradiation in order to better argue the practical management of the treatment.

The practices with regard to the implementation of the PTV in the context of re-irradiation with SBRT differ, being 0 mm in the study by Fuller et al. (11), 3 mm for Bergamin et al. (12), and 2 mm for Pasquier et al. GETUG 31 (37).

Reducing PTV margin is crucial since the reduction of the planned volume leads to less exposure to toxicity for organs at risk (40). PTV margin creates a fictitious volume that provides an acceptable probability of the delivery of CTV or GTV prescription dose. Although it is complex to calculate PTV margin in stereotactic radiotherapy, we can confirm that intra-fractional motions are essential for its estimation (41).

Since we observed less motion during re-irradiation it seems relevant to use a smaller margin compared to the margins used in first irradiation, especially since organs at risk are subject to strict constraints, dose gradient is high and the number of fraction is limited.

REFERENCES

1. Sung H, Ferlay J, Siegel RL, Laversanne M, Soerjomataram I, Jemal A, et al. Global Cancer Statistics 2020: GLOBOCAN Estimates of Incidence and Mortality Worldwide for 36 Cancers in 185 Countries. *CA A Cancer J Clin* (2021) 71(3):209–49. doi: 10.3322/caac.21660
2. Mohler JL, Antonarakis ES, Armstrong AJ, D'Amico AV, Davis BJ, Dorff T, et al. Prostate Cancer, Version 2.2019, NCCN Clinical Practice Guidelines in Oncology. *J Natl Compr Canc Netw* (2019) 17:479–505. doi: 10.6004/jnccn.2019.0023
3. Morgan SC, Hoffman K, Loblaw DA, Buyyounouski MK, Patton C, Barocas D, et al. Hypofractionated Radiation Therapy for Localized Prostate Cancer: Executive Summary of an ASTRO, ASCO, and AUA Evidence-Based

CONCLUSION

This study analyzed intra-fractional prostate motions during stereotactic irradiation as the first treatment and re-irradiation. Intra-fraction prostate motions persisted in the setting of re-irradiation, although a significant reduction was observed when compared to the first irradiation. The findings of our study make it possible to better understand prostate behavior at a time where re-irradiation by SBRT is being evaluated as a salvage therapy for intra-prostatic recurrence.

DATA AVAILABILITY STATEMENT

The raw data supporting the conclusions of this article will be made available by the authors, without undue reservation.

ETHICS STATEMENT

Ethical review and approval was not required for the study on human participants in accordance with the local legislation and institutional requirements. The patients/participants provided their written informed consent to participate in this study.

AUTHOR CONTRIBUTIONS

Conceptualization, DP and AT. Methodology, M-CLD, DP and AT. Formal analysis, A-MB. Investigation, AT and DP. Resources, TL and EFL. Writing—original draft preparation, AT. Writing—review and editing, DP, TL, and M-CLD. Supervision, DP and AT. Project administration, AT. All authors contributed to the article and approved the submitted version.

SUPPLEMENTARY MATERIAL

The Supplementary Material for this article can be found online at: <https://www.frontiersin.org/articles/10.3389/fonc.2021.690422/full#supplementary-material>

Guideline. *Pract Radiat Oncol* (2018) 8:354–60. doi: 10.1016/j.prro.2018.08.002

4. King CR, Freeman D, Kaplan I, Fuller D, Bolzicco G, Collins S, et al. Stereotactic Body Radiotherapy for Localized Prostate Cancer: Pooled Analysis From a Multi-Institutional Consortium of Prospective Phase II Trials. *Radiother Oncol* (2013) 109:217–21. doi: 10.1016/j.radonc.2013.08.030
5. Kishan AU, Dang A, Katz AJ, Mantz CA, Collins SP, Aghdam N, et al. Long-Term Outcomes of Stereotactic Body Radiotherapy for Low-Risk and Intermediate-Risk Prostate Cancer. *JAMA Netw Open* (2019) 2:e188006. doi: 10.1001/jamanetworkopen.2018.8006
6. Lehrer EJ, Kishan AU, Yu JB, Trifiletti DM, Showalter TN, Ellis R, et al. Ultrahypofractionated Versus Hypofractionated and Conventionally

- Fractionated Radiation Therapy for Localized Prostate Cancer: A Systematic Review and Meta-Analysis of Phase III Randomized Trials. *Radiother Oncol* (2020) 148:235–42. doi: 10.1016/j.radonc.2020.04.037
7. Zumsteg ZS, Spratt DE, Romesser PB, Pei X, Zhang Z, Kollmeier M, et al. Anatomical Patterns of Recurrence Following Biochemical Relapse in the Dose Escalation Era of External Beam Radiotherapy for Prostate Cancer. *J Urol* (2015) 194:1624–30. doi: 10.1016/j.juro.2015.06.100
 8. Corkum MT, Mendez LC, Chin J, D'Souza D, Boldt RG, Bauman GS. A Novel Salvage Option for Local Failure in Prostate Cancer, Reirradiation Using External Beam or Stereotactic Radiation Therapy: Systematic Review and Meta-Analysis. *Adv Radiat Oncol* (2020) 5:965–77. doi: 10.1016/j.adro.2020.04.022
 9. Pasquier D, Martinage G, Janoray G, Rojas DP, Zerini D, Goupy F, et al. Salvage Stereotactic Body Radiation Therapy for Local Prostate Cancer Recurrence After Radiation Therapy: A Retrospective Multicenter Study of the GETUG. *Int J Radiat OncologyBiologyPhys* (2019) 105:727–34. doi: 10.1016/j.ijrobp.2019.07.012
 10. Jereczek-Fossa BA, Rojas DP, Zerini D, Fodor C, Viola A, Fanetti G, et al. Reirradiation for Isolated Local Recurrence of Prostate Cancer: Mono-institutional Series of 64 Patients Treated With Salvage Stereotactic Body Radiotherapy (SBRT). *Br J Radiol* (2019) 92:20180494. doi: 10.1259/bjr.20180494
 11. Fuller D, Wurzer J, Shirazi R, Bridge S, Law J, Crabtree T, et al. Retreatment for Local Recurrence of Prostatic Carcinoma After Prior Therapeutic Irradiation: Efficacy and Toxicity of HDR-Like Sbrt. *Int J Radiat Oncol Biol Phys* (2020) 106:291–9. doi: 10.1016/j.ijrobp.2019.10.014
 12. Bergamin S, Eade T, Kneebone A, Booth J, Hsiao E, Schembri GP, et al. Interim Results of a Prospective Prostate-Specific Membrane Antigen-Directed Focal Stereotactic Reirradiation Trial for Locally Recurrent Prostate Cancer. *Int J Radiat Oncol Biol Phys* (2020) 108:1172–8. doi: 10.1016/j.ijrobp.2020.07.014
 13. Xie Y, Djajaputra D, King CR, Hossain S, Ma L, Xing L. Intrafractional Motion of the Prostate During Hypofractionated Radiotherapy. *Int J Radiat OncologyBiologyPhys* (2008) 72:236–46. doi: 10.1016/j.ijrobp.2008.04.051
 14. Choi HS, Kang KM, Jeong BK, Song JH, Lee YH, Ha IB, et al. Analysis of Motion-dependent Clinical Outcome of Tumor Tracking Stereotactic Body Radiotherapy for Prostate Cancer. *J Korean Med Sci* (2018) 33:e107. doi: 10.3346/jkms.2018.33.e107
 15. Cordoba A, Pasquier D, Nickers P, Lacornerie T, Lartigau É. Intraprostatic Fiducials in Stereotactic Radiotherapy for Prostate Cancer. *Cancer Radiother* (2016) 20:815–9. doi: 10.1016/j.canrad.2016.07.097
 16. Kilby W, Dooley JR, Kuduvali G, Sayeh S, Maurer CR. The CyberKnife Robotic Radiosurgery System in 2010. *Technol Cancer Res Treat* (2010) 9:433–52. doi: 10.1177/153303461000900502
 17. Ballhausen H, Li M, Hegemann N-S, Ganswindt U, Belka C. Intra-Fraction Motion of the Prostate is a Random Walk. *Phys Med Biol* (2015) 60:549–63. doi: 10.1088/0031-9155/60/2/549
 18. Azcona JD, Li R, Mok E, Hancock S, Xing L. Automatic Prostate Tracking and Motion Assessment in Volumetric Modulated Arc Therapy With an Electronic Portal Imaging Device. *Int J Radiat Oncol Biol Phys* (2013) 86:762–8. doi: 10.1016/j.ijrobp.2013.03.007
 19. Gorovets D, Bursleson S, Jacobs L, Ravindranath B, Tierney K, Kollmeier M, et al. Prostate SBRT With Intrafraction Motion Management Using a Novel Linear Accelerator-Based MV-Kv Imaging Method. *Pract Radiat Oncol* (2020) 10:e388–96. doi: 10.1016/j.prr.2020.04.013
 20. Kupelian P, Willoughby T, Mahadevan A, Djemil T, Weinstein G, Jani S, et al. Multi-Institutional Clinical Experience With the Calypso System in Localization and Continuous, Real-Time Monitoring of the Prostate Gland During External Radiotherapy. *Int J Radiat OncologyBiologyPhys* (2007) 67:1088–98. doi: 10.1016/j.ijrobp.2006.10.026
 21. Litzenberg DW, Balter JM, Hadley SW, Sandler HM, Willoughby TR, Kupelian PA, et al. Influence of Intrafraction Motion on Margins for Prostate Radiotherapy. *Int J Radiat OncologyBiologyPhys* (2006) 65:548–53. doi: 10.1016/j.ijrobp.2005.12.033
 22. McPartlin AJ, Li XA, Kershaw LE, Heide U, Kerkmeijer L, Lawton C, et al. MRI-Guided Prostate Adaptive Radiotherapy – A Systematic Review. *Radiation Oncol* (2016) 119:371–80. doi: 10.1016/j.radonc.2016.04.014
 23. Levin-Epstein R, Qiao-Guan G, Juarez JE, Shen Z, Steinberg ML, Ruan D, et al. Clinical Assessment of Prostate Displacement and Planning Target Volume Margins for Stereotactic Body Radiotherapy of Prostate Cancer. *Front Oncol* (2020) 10:539. doi: 10.3389/fonc.2020.00539
 24. Willoughby TR, Kupelian PA, Pouliot J, Shinohara K, Aubin M, Roach M, et al. Target Localization and Real-Time Tracking Using the Calypso 4D Localization System in Patients With Localized Prostate Cancer. *Int J Radiat OncologyBiologyPhys* (2006) 65:528–34. doi: 10.1016/j.ijrobp.2006.01.050
 25. Mah D, Freedman G, Milestone B, Hanlon A, Palacio E, Richardson T, et al. Measurement of Intrafractional Prostate Motion Using Magnetic Resonance Imaging. *Int J Radiat OncologyBiologyPhys* (2002) 54:568–75. doi: 10.1016/S0360-3016(02)03008-0
 26. Ghadjar P, Fiorino C, Munck af Rosenschöld P, Pinkawa M, Zilli T, van der Heide UA. ESTRO ACROP Consensus Guideline on the Use of Image Guided Radiation Therapy for Localized Prostate Cancer. *Radiother Oncol* (2019) 141:5–13. doi: 10.1016/j.radonc.2019.08.027
 27. Vargas C, Saito AI, Hsi WC, Indelicato D, Falchook A, Zengm Q, et al. Cine-Magnetic Resonance Imaging Assessment of Intrafraction Motion for Prostate Cancer Patients Supine or Prone With and Without a Rectal Balloon. *Am J Clin Oncol* (2010) 33:11–6. doi: 10.1097/COC.0b013e31819fd7c
 28. Langen KM, Willoughby TR, Meeks SL, Santhanam A, Cunningham A, Levine L, et al. Observations on Real-Time Prostate Gland Motion Using Electromagnetic Tracking. *Int J Radiat Oncol Biol Phys* (2008) 71:1084–90. doi: 10.1016/j.ijrobp.2007.11.054
 29. Kotte ANTJ, Hofman P, Legendijk JJW, van Vulpen M, van der Heide UA. Intrafraction Motion of the Prostate During External-Beam Radiation Therapy: Analysis of 427 Patients With Implanted Fiducial Markers. *Int J Radiat OncologyBiologyPhys* (2007) 69:419–25. doi: 10.1016/j.ijrobp.2007.03.029
 30. Koike Y, Sumida I, Mizuno H, Shiomi H, Kurosu K, Ota S, et al. Dosimetric Impact of Intra-Fraction Prostate Motion Under a Tumour-Tracking System in Hypofractionated Robotic Radiosurgery. *PLoS One* (2018) 13(4):1–10. doi: 10.1371/journal.pone.0195296
 31. Wolf J, Nicholls J, Hunter P, Nguyen DT, Keall P, Martin J. Dosimetric Impact of Intrafraction Rotations in Stereotactic Prostate Radiotherapy: A Subset Analysis of the TROG 15.01 SPARK Trial. *Radiother Oncol* (2019) 136:143–7. doi: 10.1016/j.radonc.2019.04.013
 32. Cuccia F, Mazzola R, Nicosia L, Figlia V, Gaj-Levra N, Ricchetti F, et al. Impact of Hydrogel Peri-Rectal Spacer Insertion on Prostate Gland Intra-Fraction Motion During 1.5 T MR-Guided Stereotactic Body Radiotherapy. *Radiat Oncol* (2020) 15:178. doi: 10.1186/s13014-020-01622-3
 33. de Muinck Keizer DM, Kerkmeijer LGW, Willigenburg T, van Lier ALHMW, Hartogh MDd, van der Voort van Zyp JRN, et al. Prostate Intrafraction Motion During the Preparation and Delivery of MR-guided Radiotherapy Sessions on a 1.5T Mr-Linac. *Radiother Oncol* (2020) 151:88–94. doi: 10.1016/j.radonc.2020.06.044
 34. Langen KM, Jones DT. Organ Motion and its Management. *Int J Radiat Oncol Biol Phys* (2001) 50:265–78. doi: 10.1016/s0360-3016(01)01453-5
 35. de Leon J, Jameson MG, Rivest-Henault D, Keats S, Rai R, Arumugam S, et al. Reduced Motion and Improved Rectal Dosimetry Through Endorectal Immobilization for Prostate Stereotactic Body Radiotherapy. *BJR* (2019) 92:20190056. doi: 10.1259/bjr.20190056
 36. Hwang ME, Mayeda M, Liz M, Goode-Marshall B, Gonzalez L, Elliston CD, et al. Stereotactic Body Radiotherapy With Periprostatic Hydrogel Spacer for Localized Prostate Cancer: Toxicity Profile and Early Oncologic Outcomes. *Radiat Oncol* (2019) 14:136. doi: 10.1186/s13014-019-1346-5
 37. Pasquier D, Le Deley M-C, Tresch E, Cormier L, Dutreque M, Nenat S, et al. Getug-AFU 31: A Phase I/II Multicentre Study Evaluating the Safety and Efficacy of Salvage Stereotactic Radiation in Patients With Intraprostatic Tumour Recurrence After External Radiation Therapy—Study Protocol. *BMJ Open* (2019) 9:e026666. doi: 10.1136/bmjopen-2018-026666
 38. McNair HA, Wedlake L, Lips IM, Andreyev J, Van Vulpen M, Dearnaley D. A Systematic Review: Effectiveness of Rectal Emptying Preparation in Prostate Cancer Patients. *Pract Radiat Oncol* (2014) 4:437–47. doi: 10.1016/j.prr.2014.06.005
 39. Gill S, Dang K, Fox C, Bressel M, Kron T, Bergen N, et al. Seminal Vesicle Intrafraction Motion Analysed With Cinematic Magnetic Resonance Imaging. *Radiat Oncol* (2014) 9:174. doi: 10.1186/1748-717X-9-174
 40. Verellen D, Ridder MD, Linthout N, Tournel K, Soete G, Storme G. Innovations in Image-Guided Radiotherapy. *Nat Rev Cancer* (2007) 7:949–60. doi: 10.1038/nrc2288

41. Seuntjens J, Lartigau EF, Cora S, Ding GX, Goetsch S, Nuytens J, et al. Report 91. Prescribing, Recording, and Reporting of Stereotactic Treatments With Small Photon Beams. *J ICRU* (2014) 14(2):1–160. doi: 10.1093/jicru/ndx017

Conflict of Interest: The authors declare that the research was conducted in the absence of any commercial or financial relationships that could be construed as a potential conflict of interest.

Copyright © 2021 Taillez, Bimbai, Lacornerie, Le Deley, Lartigau and Pasquier. This is an open-access article distributed under the terms of the Creative Commons Attribution License (CC BY). The use, distribution or reproduction in other forums is permitted, provided the original author(s) and the copyright owner(s) are credited and that the original publication in this journal is cited, in accordance with accepted academic practice. No use, distribution or reproduction is permitted which does not comply with these terms.



Use of a Biodegradable, Contrast-Filled Rectal Spacer Balloon in Intensity-Modulated Radiotherapy for Intermediate-Risk Prostate Cancer Patients: Dosimetric Gains in the BioPro-RCMI-1505 Study

Igor Latorzeff^{1*}, Eric Bruguière², Emilie Bogart³, Marie-Cécile Le Deley³, Eric Lartigau^{4,5}, Delphine Marre⁶ and David Pasquier^{4,5}

OPEN ACCESS

Edited by:

Valdir Carlos Colussi,
University Hospitals Cleveland Medical
Center, United States

Reviewed by:

Ben GL Vanneste,
Maastricht Clinic, Netherlands
Tiziana Rancati,
Istituto Nazionale dei Tumori (IRCCS),
Italy

*Correspondence:

Igor Latorzeff
ilatorzeff@clinique-pasteur.com

Specialty section:

This article was submitted to
Radiation Oncology,
a section of the journal
Frontiers in Oncology

Received: 28 April 2021

Accepted: 21 July 2021

Published: 26 August 2021

Citation:

Latorzeff I, Bruguière E, Bogart E,
Le Deley M-C, Lartigau E,
Marre D and Pasquier D (2021) Use of
a Biodegradable, Contrast-Filled
Rectal Spacer Balloon in Intensity-
Modulated Radiotherapy for
Intermediate-Risk Prostate Cancer
Patients: Dosimetric Gains in the
BioPro-RCMI-1505 Study.
Front. Oncol. 11:701998.
doi: 10.3389/fonc.2021.701998

¹ Department of Radiotherapy, Clinique Pasteur, Toulouse, France, ² Department of Imaging, Clinique Pasteur, Toulouse, France, ³ Methodology and Biostatistics Unit, Centre Oscar Lambret, Lille, France, ⁴ Academic Department of Radiation Oncology, Centre Oscar Lambret, Lille, France, ⁵ CRISTAL UMR CNRS 9189, Lille University, Lille, France, ⁶ Department of Physics, Clinique Pasteur, Toulouse, France

Background/purpose: Dose-escalated external beam radiotherapy (RT) is effective in the control of prostate cancer but is associated with a greater incidence of rectal adverse events. We assessed the dosimetric gain and safety profile associated with implantation of a new biodegradable rectal spacer balloon.

Materials/methods: Patients scheduled for image-guided, intensity-modulated RT for intermediate-risk prostate cancer were prospectively included in the French multicenter BioPro-RCMI-1505 study (NCT02478112). We evaluated the dosimetric gain, implantation feasibility, adverse events (AEs), and prostate-cancer-specific quality of life associated with use of the balloon spacer.

Results: After a scheduled review of the initial recruitment target of 50 patients by the study's independent data monitoring committee (IDMC), a total of 24 patients (including 22 with dosimetry data) were included by a single center between November 2016 and May 2018. The interventional radiologist who implanted the balloons considered that 86% of the procedures were easy. 20 of the 24 patients (83.3%) received IMRT and 4 (16.7%) received volumetric modulated arc therapy (78–80 Gy delivered in 39 fractions). The dosimetric gains associated with spacer implantation were highly significant ($p < 0.001$) for most variables. For the rectum, the median (range) relative gain ranged from 15.4% (–9.2–47.5) for D20cc to 91.4% (36.8–100.0) for V70 Gy (%). 15 patients (62%) experienced an acute grade 1 AE, 8 (33%) experienced a late grade 1 AE, 1 (4.2%) experienced an acute grade 2 AE, and 3 experienced a late grade 2 AE. No grade 3 AEs were reported. Quality of life was good at baseline (except for sexual activity) and did not markedly worsen during RT and up to 24 months afterwards.

Conclusion: The use of a biodegradable rectal spacer balloon is safe, effective and associated with dosimetric gains in modern RT for intermediate-risk prostate cancer.

Keywords: prostate cancer, intermediate risk group, intensity-modulated radiotherapy, prospective study, spacer with biodegradable contrast-filled rectal balloon, organs at risk, dosimetric analyses, quality of life

INTRODUCTION

A number of randomized clinical trials have notably demonstrated that dose-escalated external beam radiotherapy (RT) can effectively achieve good biochemical and clinical outcomes in prostate cancer (1–6). In the multicenter Medical Research Council RT01 trial, patients were randomized to conformal RT with either 64 or 74 Gy (2 Gy/session) plus 3 to 6 months of neoadjuvant hormone therapy; the 5-year biochemical relapse-free survival rate was 71% in the 74 Gy group and 60% in the 64 Gy group ($p=0.0007$) (3). Likewise, the GETUG 06 trial showed that dose escalation from 70 to 80 Gy provided a better 5-year biochemical outcome but slightly more adverse events (AEs) (1). However, the anatomic proximity between the prostate, the urinary tract and the rectum means that the latter are also exposed to the toxic effects of ionizing radiation. Hence, dose escalation is associated with a higher relapse-free survival rate but also with a greater frequency of urinary tract and rectal AEs and erectile dysfunction. The development of modern, intensity-modulated RT (IMRT) enabled escalation of the prostate dose to 78 Gy with the same risk of rectal toxicity as three-dimensional conformal RT at 70 Gy (3). Furthermore, the use of volume-modulated arc therapy has shortened treatment times without sacrificing tissue coverage (7, 8). Lastly, irradiation of the urinary tract and rectum can be minimized by targeting the dose to the prostate as accurately as possible with using image-guided RT (IGRT). In a comparative study, the use of IGRT was associated with a lower rate of grade ≥ 2 urinary tract AEs at 3 years (10.4%, vs. 20% in a control group) (5).

Despite these technical advances, however, the dose delivered to the rectum (*via* external beam RT or brachytherapy) remains a limiting factor in dose escalation. A number of researchers reasoned that the incidence and severity of rectal AEs could be reduced by increasing the distance between the prostate and the rectum *via* the insertion or injection of spacers made of biodegradable material [e.g. hyaluronic acid (HA)] or non-biodegradable material [e.g. polyethylene glycol (PEG)] into the perirectal fat. Indeed, the use of spacers is associated with

less rectal AEs (9–11). By way of an example, 222 patients with stage T1 or T2 prostate cancer and undergoing image-guided IMRT (79.2 Gy in 1.8-Gy fractions) were randomized to spacer implantation or no implantation (12, 13). The incidence of rectal AEs 3 to 15 months after treatment was significantly lower in the spacer group (2.0%) than in the control group (7.0%; $p=0.04$). Furthermore, bowel-related quality of life (QoL) 6, 12, and 15 months after the end of IMRT was significantly better in the spacer group (12, 13).

The ProSpace[®] biodegradable fillable balloon (BioProtect Ltd, Tzur Yigal, Israel) is a rectal spacer with confirmed safety and efficacy in preclinical and clinical studies (14–19).

Although the insertion procedure is slightly more invasive than for HA and PEG spacers (a small perineal incision and a special dilator and sheath are required), inflation of the balloon with sterile diluted iodine contrast solution (or physiological saline solution, if iodine is contraindicated) avoids the potential lateral and craniocaudal dispersion of spacer material (18). In a Phase II multicenter study, the mean \pm standard deviation (SD) prostate-rectum distance was 0.22 ± 0.2 cm before insertion and 2.47 ± 0.47 cm after insertion; this distance was maintained during RT (20).

The present prospective, interventional, multicenter study was designed to assess the dosimetric gain, implantation procedure, and acute and late AEs associated with use of the contrast-filled ProSpace[®] balloon for better image-guided targeting in patients undergoing IMRT of intermediate-risk prostate cancer (16). Here, we report the final results for the primary efficacy criterion (dosimetric gain) and some of the secondary criteria, together with intermediate results for other secondary criteria (notably QoL and safety).

METHODS AND MATERIALS

The study's rationale and protocol (including the study objectives, inclusion and exclusion criteria, device characteristics, device implantation, dosimetric criteria, safety evaluation and patient-reported outcomes) have been described in detail elsewhere (16). Briefly, adult patients scheduled for IGRT (with cone-beam CT) and IMRT (78 Gy, 2 Gy/fraction) for intermediate-risk prostate cancer [according to the D'Amico classification (21)] were prospectively screened for eligibility in six French cancer centers. The study's main inclusion and exclusion criteria are listed in **Supplementary Table 1**, and the study visits and procedures are summarized in **Supplementary Table 2**. The primary objective was to evaluate the dosimetric gain for the organs at risk (OAR) associated with use of the ProSpace[®] biodegradable balloon. The secondary objectives were to evaluate (i) the technical feasibility of the balloon's implantation, (ii) AEs (evaluated according to the

Abbreviations: AE, adverse event; BMI, body mass index; CI, confidence interval; CTV, clinical target volume; DXcc, dose delivered to X cc of the designated anatomic structure; ECOG PS, Eastern Cooperative Oncology Group Performance Status; EORTC QLQ-C30, European Organisation for Research and Treatment of Cancer Core Quality of Life Questionnaire; EORTC QLQ-PR25, European Organisation for Research and Treatment of Cancer Prostate Cancer-Specific Quality of Life Questionnaire; IMRT, intensity-modulated radiation therapy; OAR, organs at risk; OR, odds ratio; PSA, prostate-specific antigen; QoL, quality of life; SD, standard deviation; V70 Gy, volume of the indicated anatomic structure receiving 70 Gy; VX%, volume receiving X% of the prescribed dose.

National Cancer Institute – Common Terminology Criteria for Adverse Events (CTCAE, version 4.0; https://ctep.cancer.gov/protocoldevelopment/electronic_applications/ctc.htm#ctc_40), (iii) the time interval between implantation and the initiation of radiotherapy and the relationship with implantation-related complications, (iv) the association between ProSpace® use and treatments for acute proctitis and (v) QoL (using the European Organisation for Research and Treatment of Cancer (EORTC) score QoL self-questionnaire (QLQ-C30) and the prostate-cancer-specific PR25 module (22, 23). “Early” AEs were defined as those arising within 6 months (rather than 3 months, in the CTCAE) of RT.

The dosimetry plans before and after ProSpace® implantation were calculated using Eclipse treatment planning software (Varian, Palo Alto, CA). For the purposes of the present publication, data were collected and doses were reported and analyzed using the Aquilab SharePlace platform (including ArtiviewTM 3.20.1 software) from Aquilab SAS (Loos Les Lille, France). Aquilab SAS also managed the study’s electronic case report form, the study database, and the on-line patient self-questionnaires.

In all cases, the ProSpace® was implanted in an operating room by the same interventional radiologist. During inflation of the balloon with saline solution, the investigators added 1 ml of iodine contrast enhancer in order to improve the IGRT procedure and enhance the balloon’s delineation on the planning CT. The implantation of a contrast-filled ProSpace® balloon has been described in detail by Vanneste et al. (18).

The study was approved by an institutional review board (*Comité de Protection des Personnes Nord Ouest I*, Lille, France; reference: 13/10/2016) and registered at ClinicalTrials.gov (NCT02478112). All included patients received information on the study’s objectives and procedures and gave their written consent to participation.

RESULTS

Study Population and Treatment

A total of 24 patients were included in the study between November 28th, 2016, and May 28th, 2018. Initially, 50 patients were planned for accrual but an intermediate, scheduled review by the study’s independent data monitoring committee (IDMC) stopped patient enrolment after the first 24, since the primary objective had been achieved. Hence, although the study had a multicenter design, all 24 patients came from a single cancer center (Toulouse, France). The characteristics of the study population on inclusion are summarized in **Table 1**. All patients were evaluated with MRI before study entry and the cancer was staged as T2 in all cases. Two patients lacked dosimetry data after ProSpace® implantation. Hence, 22 patients were included in the dosimetry analysis.

21 of the 24 patients received a contrast-filling balloon, and 3 patients received a balloon without contrast (iodine allergy: n=2;

TABLE 1 | Characteristics of the study population on inclusion.

Variables (n=24)			Characteristics (n=24)		
Age (years)			Medical history		
median (range)	75.5	(61.0–81.0)	infectious disease	0	0%
mean ± SD	74.1	± 5.2	digestive tract disease	1*	4.2%
Clinical T stage			prostate resection	5	20.8%
T1c	4	16.7%	cardiovascular disease	15	62.5%
T2a	16	66.7%	type II diabetes	3	12.5%
T2b	2	8.3%	pelvic surgery	0	0%
T2c	2	8.3%	Androgen deprivation therapy	11	45.8%
N0 status	24	100.0%	Medications other than androgen deprivation therapy*	16	66.7%
M0 status	24	100.0%	Anticoagulants	0	0%
Initial serum PSA (ng/ml)			Biopsies		
median (range)	7.1	(0.6–19.6)	Number of biopsy cores		
mean ± SD	8.0	± 4.2	median (range)	14.5	(5.0–24.0)
Prostate volume (cc)			mean ± SD	14.8	± 4.6
median (range)	34.0	(15.0–89.0)	Number of positive biopsy cores		
mean ± SD	36.7	± 17.2	median (range)	4.0	(1.0–13.0)
ECOG PS = 0	24	100.0%	mean ± SD	4.8	± 3.2
Total Gleason score			Total length of positive biopsies (mm)		
6	2	8.3%	median (range)	20.0	(1.0–50.0)
7	22	91.7%	mean ± SD	20.4	± 12.8
			Proportion of positive biopsies (%)		
			median (range)	30.0	(7.1–86.7)
			mean ± SD	35.3	± 22.1
			Side(s) invaded		
			left only	7	29.2%
			right only	4	16.7%
			left and right	13	54.2%

SD, standard deviation; PSA, prostate-specific antigen; ECOG PS, Eastern Cooperative Oncology Group Performance Status; BMI, body mass index.

*medications other than androgen deprivation therapy included treatments for diabetes and other metabolic diseases, arterial hypertension and other cardiovascular diseases, gout, allergy, asthma, arthritis, insomnia, stress, and glaucoma.

protocol deviation: $n=1$). The interventional radiologist considered that the implantation was easy or very easy in 19 of the 22 cases (86%). Difficulties were noted in three cases (14%): incomplete inflation of the balloon due to resistance; difficulty crossing the perineal region and slight displacement of the balloon at the end of

the inflation; failure to inflate the balloon (though a second balloon inflated with no problems) (**Figure 1A**). Further results for the implantation procedures are given in **Table 2**.

With regard to treatment, 20 of the 24 patients (83.3%) received IMRT and 4 (16.7%) received volumetric modulated arc therapy.

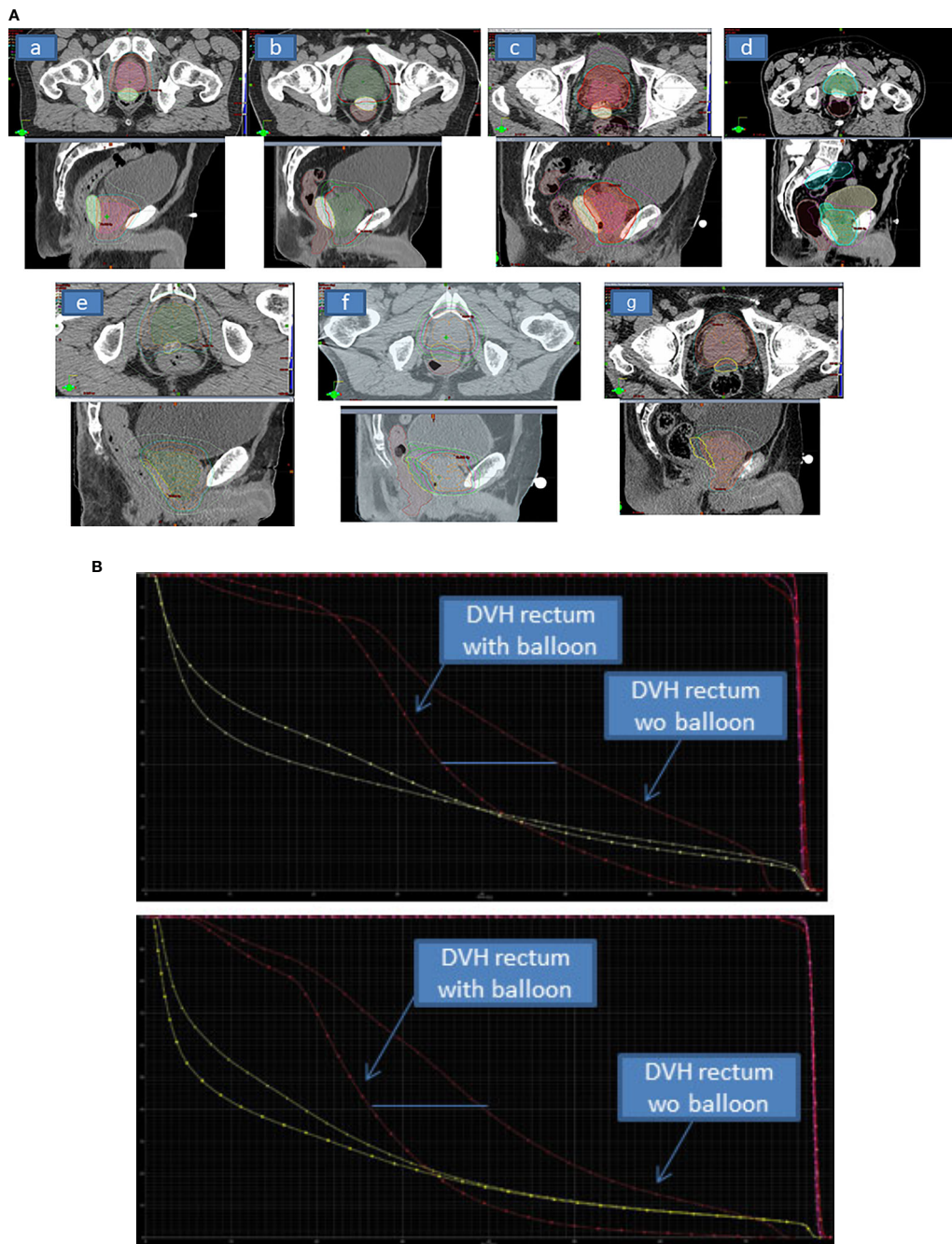


FIGURE 1 | (A) The planning CT axial and sagittal views of delineated volumes of interest (prostate gland and the ProSpace® biodegradable balloon) showing good quality of delineation with iodinated contrast-filling balloon (a–g). For 1 patient (e) iodine contrast product was too much diluted. For 2 patients (f, g), the procedure was performed without iodine contrast enhancement, and so delineation of the balloon was less easy. **(B)** The dose-volume histogram (DVH) for the rectum pre-balloon and post-balloon for 2 patients, showing the dosimetric benefit achieved with the balloon. The DVH for bladder (also shown, in yellow) is not modified. With regard to the clinical target volume and the planned treatment volume (shown in pink and red, respectively), balloon implantation was associated with greater homogeneity.

TABLE 2 | Characteristics of the ProSpace[®] balloon implantation.

Variables (n=24)		
Time interval between implantation and the start of RT (days)		
median (range)	23.0	(21.0–35.0)
mean \pm SD	24.5	\pm 4.2
missing data	6	
Type of anesthesia		
general	22	91.7%
local	2	8.3%
Duration of the surgical session (min)		
median (range)	36.0	(13.0–64.0)
mean \pm SD	33.5	\pm 12.9
Duration of the implantation (min)		
median (range)	14.0	(1.0–23.0)
mean \pm SD	14.2	\pm 6.2
missing data	1	

RT, radiotherapy; SD, standard deviation.

The median (range) duration of RT was 58.5 days (55.0–68.0), and the mean \pm SD duration was 59.3 \pm 3.5 days. In all cases, contrast-free CT was used for contouring. The treatment volume included the seminal vesicles in 22 of the 24 cases (91.7%) and the pelvis in 2 (8.3%) to a dose of 46 Gy. In all 24 cases, the total planned dose was 78 Gy delivered in 39 fractions.

Dosimetry Data

As mentioned above, dosimetry data before and after ProSpace[®] implantation were available for 22 patients (**Table 3**). The median dosimetric gains (whether expressed in absolute or relative terms) associated with ProSpace[®] implantation were highly significant ($p < 0.001$) for the majority of the dosimetric variables. For the rectum, the median (range) relative gain ranged from 15.4% (–9.2–47.5) for D20cc to 91.4% (36.8–100.0) for V70 Gy (the percentage volume of the rectum receiving 70 Gy radiation). Non-significant differences were observed for Dmax (rectum), V50% (rectum), V70% (bladder, cc), V60% (bladder, cc) and V50% (bladder, cc) (**Figure 1B**). The absolute dosimetric gains were significant for D2.5cc, D5cc, D10cc, D15cc, D20cc, V70 Gy, V90%, V80%, and V60% (all $p < 0.001$) (**Table 3**).

With regard to safety, 5 of the 24 patients (21%) did not experience any AEs, 15 (62%) experienced a grade 1 AE, and 4 (17%) experienced a grade 2 AE. No grade 3 AEs were reported. Sixteen patients (67%) experienced an acute AE (grade 1 or 2), and 11 (46%) experienced a late AE. Urinary frequency was the most common acute AE (grade 1 for 13 patients and grade 2 for 1) and the most common late AE (grade 1 for 5 patients and grade 2 for 2). Only one AE (proctitis) was considered by an investigator to be related to ProSpace[®] implantation, although the event started a week after the first RT session and a month after the implantation. As this was the only AE thought to be related to ProSpace[®] implantation, we were unable to assess the relationship between complications on one hand and the time interval between implantation and the start of RT on the other.

Before and after RT, the median International Prostate Symptom Score (IPSS) ranged from 3 to 5 (**Table 4**). The IPSS increased during RT, and 5 patients had experienced severe symptoms at this point.

Quality of Life

At baseline, the QLQ-C30 and PR25 questionnaires gave mean values of >80 for the “functioning” domains and <20 for the symptom domains. The exception was the PR25 sexual activity score, with a mean (range) value of 66.7 (0–100) at baseline. We then observed (i) a slight worsening of the scores for fatigue, loss of appetite, constipation and diarrhea, and urinary symptoms and problems during and immediately after RT, and (ii) worsening of the score of dyspnea during the post-RT follow-up (**Figure 2**). The other domain scores remained stable during RT and up to 24 months thereafter.

DISCUSSION

In the prospective BioPro-RCMI-1505 study, we evaluated the routine use of a relatively new rectal spacer as part of a modern IMRT/IGRT protocol. Our present results indicate that the balloon is a safe, efficacious adjunct to IMRT for prostate cancer; it was associated with dosimetric gains that help to spare the wall of the rectum from the effects of a higher dose to the prostate. Placement of the balloon spacer was relatively easy for physicians with experience of transrectal prostate procedures. Filling the balloon with contrast solution facilitates delineation of the spacer volume on the planning CT (18). The level of patient satisfaction was high, and the patients reported good QoL before and after the procedure. The delivery of a high dose of radiation (~ 78 Gy) to the prostate in IMRT increases the likelihood of tumor control; the percentage of patients with a grade 2 gastro-intestinal AE ranges from 1% to 23%, and the percentage with a grade 3 AE is very low (0% to 3%) (2). In a retrospective study performed in the USA, the combination of image guidance with IMRT dose escalation was associated with a low proportion of patients with late grade 2 genitourinary tract AEs (5). In a randomized phase III study of a PEG hydrogel spacer (SpaceOAR, Augmenix, Inc., Bedford, MA) in modern IMRT/IGRT for prostate cancer, the dosimetric gains were associated with a lower incidence of late grade ≥ 1 rectal AEs (24).

TABLE 3 | Dosimetry parameters before and after ProSpace® balloon implantation.

Variables (n=22)	Before Balloonimplantation		After Balloonimplantation		Relative Gain (%)		Absolute Gain		p*
Dmax - rectum (Gy)									0.067
median (range)	76.2	(75.1–77.1)	75.8	(66.8–77.4)	0.4	(-2.3–12.1)	0.3	(-1.7–9.2)	
mean ± SD	76.1	± 0.5	75.3	± 2.2	1.1	± 2.9	0.8	± 2.2	
D2.5cc - rectum (Gy)									<0.001
median (range)	73.6	(71.8–73.9)	63.5	(47.2–73.8)	13.7	(- 0.1–35.0)	10.1	(- 0.1–25.4)	
mean ± SD	73.4	± 0.5	61.3	± 8.1	16.5	± 10.7	12.1	± 7.8	
D5cc - rectum (Gy)									<0.001
median (range)	71.9	(66.0–73.3)	56.6	(40.7–70.8)	20.9	(2.8–40.1)	14.8	(2.0–27.8)	
mean ± SD	71.4	± 2.0	55.6	± 8.0	22.1	± 10.3	15.7	± 7.2	
D10cc - rectum (Gy)									<0.001
median (range)	65.0	(52.7–69.4)	50.7	(34.0–59.4)	20.9	(9.6–44.4)	13.1	(6.1–30.2)	
mean ± SD	63.7	± 4.5	49.1	± 7.6	22.8	± 10.8	14.6	± 7.1	
D15cc - rectum (Gy)									<0.001
median (range)	56.9	(43.9–63.1)	45.7	(30.0–54.0)	17.0	(2.6–46.5)	10.3	(1.4–29.3)	
mean ± SD	55.7	± 5.5	44.6	± 7.2	19.6	± 13.1	11.2	± 7.8	
D20cc - rectum (Gy)									<0.001
median (range)	50.9	(36.6–58.7)	41.1	(26.9–51.3)	15.4	(-9.2–47.5)	8.6	(-3.7–27.9)	
mean ± SD	49.3	± 6.3	40.9	± 6.9	16.0	± 16.2	8.4	± 8.4	
V90% - rectum (cc)									<0.001
median (range)	6.6	(3.5–9.3)	0.6	(0.0–5.3)	90.2	(32.5–100.0)	5.1	(2.5–8.4)	
mean ± SD	6.5	± 1.6	1.1	± 1.3	84.2	± 17.1	5.3	± 1.5	
V80% - rectum (cc)									<0.001
median (range)	11.4	(6.2–15.8)	2.7	(0.1–8.4)	78.0	(26.4–99.1)	7.5	(3.0–15.4)	
mean ± SD	11.3	± 2.6	2.9	± 2.3	74.4	± 19.5	8.3	± 2.9	
V60% - rectum (cc)									0.001
median (range)	24.1	(13.1–35.3)	14.0	(2.6–31.3)	37.1	(-21.6–88.1)	9.5	(-5.6–29.0)	
mean ± SD	23.3	± 6.0	13.8	± 8.4	39.9	± 34.0	9.5	± 8.8	
V50% - rectum (cc)									0.058
median (range)	30.9	(18.5–50.3)	22.2	(5.9–62.6)	16.6	(-67.7–81.2)	5.6	(-25.3–37.7)	
mean ± SD	31.9	± 9.1	25.3	± 14.2	18.4	± 39.3	6.6	± 14.6	
V70 Gy - rectum (cc)									<0.001
median (range)	6.7	(3.5–9.5)	0.6	(0.0–5.3)	90.0	(32.5–100.0)	5.2	(2.6–8.6)	
mean ± SD	6.6	± 1.7	1.2	± 1.3	84.1	± 17.1	5.4	± 1.5	
V70 Gy - rectum (%)									<0.001
median (range)	9.7	(5.2–19.6)	0.7	(0.0–8.1)	91.4	(36.8–100.0)	8.5	(4.7–15.6)	
mean ± SD	10.7	± 3.9	1.8	± 2.2	85.2	± 16.4	8.9	± 3.1	
V70% - bladder (cc)									0.10
median (range)	59.0	(18.5–103.7)	49.6	(21.5–95.3)	8.2	(-38.9–62.7)	4.9	(-22.5–39.8)	
mean ± SD	58.3	± 18.9	53.2	± 20.4	7.7	± 21.3	5.2	± 12.1	
V60% - bladder (cc)									0.22
median (range)	72.0	(23.6–126.5)	64.0	(27.5–111.0)	8.1	(-41.2–62.0)	6.2	(-27.5–58.3)	
mean ± SD	74.0	± 22.5	67.3	± 22.5	6.6	± 22.3	6.7	± 17.0	
V50% - bladder (cc)									0.39
median (range)	90.8	(31.3–147.1)	88.1	(36.4–133.3)	5.6	(-41.2–63.4)	5.7	(-31.1–92.3)	
mean ± SD	93.3	± 28.8	85.5	± 25.3	4.5	± 23.0	7.8	± 24.5	
Homogeneity of the prostate CTV (10³)									0.002
median (range)	29.5	(22.0–70.0)	21.5	(14.0–146.0)	29.4	(-108.6–56.3)	8.0	(-76.0–19.0)	
mean ± SD	31.2	± 9.9	26.8	± 26.9	20.4	± 33.8	4.4	± 18.8	

DXcc, dose delivered to *X* cc of the indicated anatomic structure; *VX%*, volume receiving *X%* of the prescribed dose; *V70 Gy*, volume of the indicated anatomic structure receiving 70 Gy; *CTV*, clinical target volume. *calculated for the relative gain, using Wilcoxon's test.

Bold values: *p* < 0.05.

When considering the primary objective, we found that use of the balloon spacer resulted in statistically significant dosimetric gains for the rectum. Moreover, the adjunction of a spacer between the prostate and the rectum increased CTV homogeneity in our cohort. This result could lead to a difference for bladder dose coverage with IMRT dosimetry. Basically to spare the rectum wall without spacer, IMRT planning is performed with CTV heterogeneity with the maximum dose to the prostate located at the anterior part of the prostate, close to the bladder neck. Adding spacer allows

better dose CTV homogeneity and we reported bladder dose distribution V70%, V60% and V50% differences but these findings didn't reach statistical significance level.

Our present dosimetric and safety results for a balloon spacer are in line with the literature data for PEG and HA gel spacers (12, 24, 25). In the randomized study of a PEG gel spacer described by Karsh et al., the median rectal V70 dose was 2.3% in the spacer and 10.5% in the control group; this corresponded to a relative reduction of 78% (*p* ≤ 0.0001). There were no intergroup differences in the incidence of acute grade ≥2

TABLE 4 | Prostate symptoms before, during and after RT, as rated on the IPSS.

IPSS	Baselines=21		Start of RTn=20		Mid-RTn=22		End of RTn=23		3 months post-RTn=23		6 months post-RTn=23		12 months post-RTn=24		24 months post-RTn=12	
Median (range)	5.0	(1.0–17.0)	3.5	(0.0–18.0)	7.0	(2.0–28.0)	11.0	(2.0–28.0)	4.0	(0.0–15.0)	3.0	(0.0–18.0)	3.5	(0.0–15.0)	3.5	(1.0–13.0)
Mean \pm SD	5.4	\pm 3.9	4.8	\pm 4.5	9.8	\pm 6.6	12.2	\pm 8.2	5.0	\pm 3.5	5.0	\pm 4.3	5.3	\pm 4.5	5.8	\pm 4.4
Mild symptoms (0-7), n (%)	16	76.2%	15	75.0%	12	54.5%	9	39.1%	18	78.3%	17	73.9%	17	70.8%	7	58.3%
Moderate symptoms (8-19), n (%)	5	23.8%	5	25.0%	8	36.4%	9	39.1%	5	21.7%	6	26.1%	7	29.2%	5	41.7%
Severe symptoms (20-35), n (%)	0	0.0%	0	0.0%	2	9.1%	5	21.7%	0	0.0%	0	0.0%	0	0.0%	0	0.0%

IPSS, International Prostate Symptom Score; RT, radiotherapy; SD, standard deviation.

rectal AEs (4.1% vs. 4.2% in the spacer and control groups, respectively; $p=0.5$) or acute grade ≥ 2 urinary tract AEs (37.8% vs 44.4%, $p=0.5$). The incidence of late grade ≥ 1 rectal AEs at 37 months was significantly lower in the spacer arm (2%) than in the control arm (9%; $p<0.03$). Moreover, none of the patients in the spacer group experienced a late grade ≥ 2 rectal AE (24). QoL was significantly better in the spacer group; at 3 years, the proportions of men in the control and spacer groups experiencing a QoL decline beyond the established threshold for a minimally important difference were 41% vs. 14% ($p=0.002$) for bowel QoL and 30% vs. 17% ($p=0.04$) for urinary QoL (12). Chapet et al. investigated the injection of HA to preserve the rectal wall during hypofractionated RT for prostate cancer. They first published on the dosimetric gains resulting from the implantation of the HA gel in a cohort of 16 patients (26). Our findings are consistent with the dose and volume reductions following injection of HA, which resulted in significantly limitation of the radiation dose delivered to the rectal wall (26). A subsequent multicenter phase II trial (from 2010 to 2012) included 36 patients with low-risk to intermediate-risk prostate cancer. With regard to acute toxicity, the injection of HA was associated with a mean \pm SD pain score (on a 0 to 10 scale) of 4.6 ± 2.3 . Grade 2 AEs were reported for 20 patients (19 with urinary obstruction, urinary frequency, or both, and 1 with proctitis) (27).

More recently, in a systematic review and meta-analysis based on 7 studies (1 randomized clinical trial and 6 cohort studies) involving 1011 men (of whom 486 received a PEG hydrogel spacer), the prostate-rectum separation produced by the spacer was sufficient to reduce V70 rectal irradiation (25). The authors of the review also showed that a PEG spacer was associated with fewer rectal toxic effects and better bowel-related quality of life (25).

Lastly, the ProSpace balloon was first investigated by Gez et al. in a multicenter study of 27 patients (20). Although Vanneste et al.'s report in 2017 described filling the ProSpace balloon with iodine contrast solution in 15 cases, Gez et al.'s publication from 2013 did not mention contrast solution. Gez et al.'s results for the dose reduction on rectal volumes were similar to our present results, and acute toxicity was also limited (20). Most of the AEs correspond to mild pain in the perineal area after implantation. Three cases of acute urinary retention resolved in a few hours (20). The results of subsequent studies suggested that although balloon spacers are associated with a significant reduction in rectal doses and are relatively easy to implant, volume loss (i.e. leakage of saline from the

balloon) over the course of treatment is a problem (28, 15). Despite the volume loss, the spacing between the prostate and the rectal wall was nevertheless maintained (19). Lastly, in a large, comparative, non-randomized study of patients receiving a gel spacer ($n=139$) or a balloon spacer ($n=264$), Schörghofer et al. reported that although use of either spacer reduced the incidence of grade 1 and 3 AEs, grade 3 AEs (rectal perforation) occurred only in patients ($n=6$) having received the balloon spacer (17). The researchers suggested that this rectal perforation might have been due to the balloon spacer's rigidity and size (17). In view of the rectal dosimetric gains observed with the balloon spacer and the low frequency of gastrointestinal adverse events during and after implantation, we suggest that this procedure should be used in the next generation of clinical trials on dose escalation as a means of improving the curability of prostate cancer. It would be interesting to investigate the putative benefit of a rectal spacer for hypofractionated dose regimens or intraprostatic dose-boosting procedures with either conventional fractionation or a stereotactic boost, such as the ongoing Simultaneous Integrated Boost for Prostate Cancer study (NCT03664193).

The present study had a number of limitations. Firstly, the inclusion of patients at a single-center (despite an initially multicenter design) means that the results cannot be readily extended to other institutions and settings. Secondly, the study design (i.e. termination once the dosimetric gain had been demonstrated) limited the number of study participants and thus restricted the volume of clinically interesting data on adverse events. Thirdly, we did not include a comparator group, e.g. patients treated with another type of spacer or treated in the absence of a rectal spacer. Fourthly, we lacked some IPSS and QoL data at 24 months post-RT for some patients, and only a small proportion of patients answered the PR25 module's questions on sexual function (although half the study population received a 6-month course of androgen deprivation therapy). Fifthly, we did not report the rectal spacer balloon's volume stability (while using daily cone beam CT IGRT quality control insurance during treatment course) during therapy. We didn't observe any loss of balloon during treatment course.

CONCLUSION

A biodegradable rectal spacer balloon was found to be a safe, effective means of obtaining dosimetric gains in the RT of intermediate-risk prostate cancer. The implantation was easy,

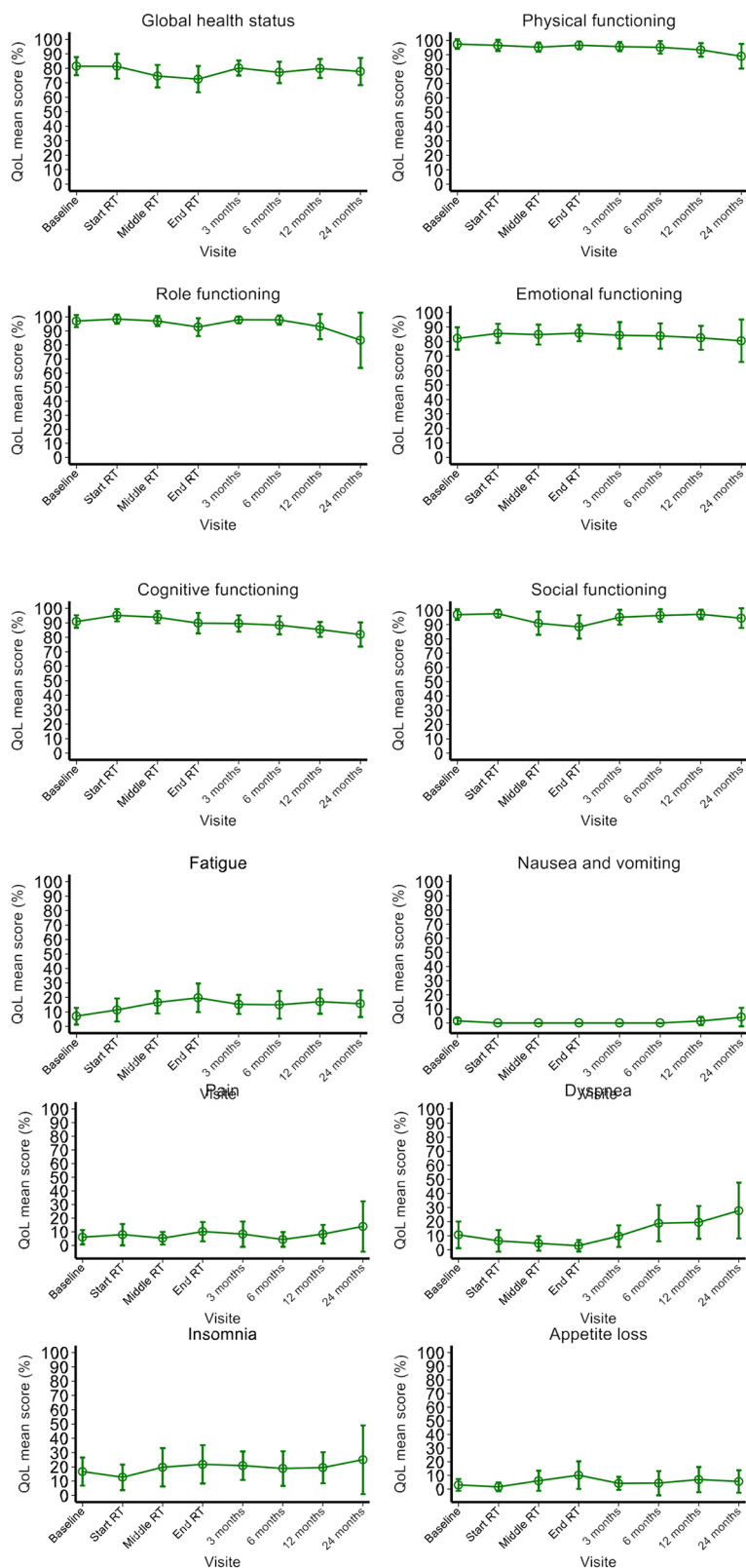


FIGURE 2 | Prostate cancer-specific QoL before, during and after RT, as assessed with the EORTC QLQ-C30 and the EORTC QLQ-PR25 self-questionnaires.

and the few technical difficulties experienced did not compromise the treatment's safety or effectiveness.

DATA AVAILABILITY STATEMENT

The raw data supporting the conclusions of this article will be made available by the authors, without undue reservation.

ETHICS STATEMENT

The studies involving human participants were reviewed and approved by Comité de Protection des Personnes Nord Ouest I, Lille, France; reference: 13/10/2016. Written informed consent for participation was not required for this study in accordance with the national legislation and the institutional requirements.

AUTHOR CONTRIBUTIONS

IL, EBr, and DP conceived and designed the study, acquired, analyzed and interpreted, and drafted the manuscript. EBo and MC-D contributed to the statistical analysis and interpretation of data. IL, EBr, DP, EBo, MC-D, EL, and DM helped to supervise

the work and revised the article for critical content. All authors contributed to the article and approved the submitted version.

FUNDING

The study was funded by Centre Oscar Lambret (Lille, France) and AQUILAB (Loos, France). ProSpace® biodegradable balloons were provided at cost price by BioProtect Ltd (Tzur Yigal, Israel).

ACKNOWLEDGMENTS

We thank all the patients, physicians, nurses, and data managers who participated in the study. Medical writing support was provided by David Fraser PhD (Biotech Communication SARL, Ploudalmézeau, France) and funded by Centre Oscar Lambret.

SUPPLEMENTARY MATERIAL

The Supplementary Material for this article can be found online at: <https://www.frontiersin.org/articles/10.3389/fonc.2021.701998/full#supplementary-material>

REFERENCES

- Beckendorf V, Guerif S, Le Prise E, Cosset JM, Bougnoux A, Chauvet B, et al. 70 Gy Versus 80 Gy in Localized Prostate Cancer: 5-Year Results of GETUG 06 Randomized Trial. *Int J Radiat Oncol Biol Phys* (2011) 80:1056–63. doi: 10.1016/j.ijrobp.2010.03.049
- Cahlon O, Hunt M, Zelefsky MJ. Intensity-Modulated Radiation Therapy: Supportive Data for Prostate Cancer. *Semin Radiat Oncol* (2008) 18:48–57. doi: 10.1016/j.semradonc.2007.09.007
- Dearnaley DP, Jovic G, Syndikus I, Khoo V, Cowan RA, Graham JD, et al. Escalated-Dose Versus Control-Dose Conformal Radiotherapy for Prostate Cancer: Long-Term Results From the MRC RT01 Randomised Controlled Trial. *Lancet Oncol* (2014) 15:464–73. doi: 10.1016/S1470-2045(14)70040-3
- Peeters ST, Heemsbergen WD, Koper PC, van Putten WL, Slot A, Dierlwart MF, et al. Dose-Response in Radiotherapy for Localized Prostate Cancer: Results of the Dutch Multicenter Randomized Phase III Trial Comparing 68 Gy of Radiotherapy With 78 Gy. *J Clin Oncol* (2006) 24:1990–6. doi: 10.1200/JCO.2005.05.2530
- Zelefsky MJ, Kollmeier M, Cox B, Fidaleo A, Sperling D, Pei X, et al. Improved Clinical Outcomes With High-Dose Image Guided Radiotherapy Compared With Non-IGRT for the Treatment of Clinically Localized Prostate Cancer. *Int J Radiat Oncol Biol Phys* (2012) 84:125–9. doi: 10.1016/j.ijrobp.2011.11.047
- Zelefsky MJ, Pei X, Chou JF, Schechter M, Kollmeier M, Cox B, et al. Dose Escalation for Prostate Cancer Radiotherapy: Predictors of Long-Term Biochemical Tumor Control and Distant Metastases-Free Survival Outcomes. *Eur Urol* (2011) 60:1133–9. doi: 10.1016/j.eururo.2011.08.029
- Hall WA, Fox TH, Jiang X, Prabhu RS, Rossi PJ, Godette K, et al. Treatment Efficiency of Volumetric Modulated Arc Therapy in Comparison With Intensity-Modulated Radiotherapy in the Treatment of Prostate Cancer. *J Am Coll Radiol* (2013) 10:128–34. doi: 10.1016/j.jacr.2012.06.014
- Khan MI, Jiang R, Kiciak A, Ur Rehman J, Afzal M, Chow JC. Dosimetric and Radiobiological Characterizations of Prostate Intensity-Modulated Radiotherapy and Volumetric-Modulated Arc Therapy: A Single-Institution Review of Ninety Cases. *J Med Phys* (2016) 41:162–8. doi: 10.4103/0971-6203.189479
- Leiker AJ, Desai NB, Folkert MR. Rectal Radiation Dose-Reduction Techniques in Prostate Cancer: A Focus on the Rectal Spacer. *Future Oncol* (2018) 14:2773–88. doi: 10.2217/fon-2018-0286
- Mok G, Benz E, Vallee JP, Miralbell R, Zilli T. Optimization of Radiation Therapy Techniques for Prostate Cancer With Prostate-Rectum Spacers: A Systematic Review. *Int J Radiat Oncol Biol Phys* (2014) 90:278–88. doi: 10.1016/j.ijrobp.2014.06.044
- Vaggers S, Rai BP, Chedgy ECP, de la Taille A, Somani BK. Polyethylene Glycol-Based Hydrogel Rectal Spacers for Prostate Brachytherapy: A Systematic Review With a Focus on Technique. *World J Urol* (2021) 39 (6):1769–80. doi: 10.1007/s00345-020-03414-6
- Hamstra DA, Mariados N, Sylvester J, Shah D, Karsh L, Hudes R, et al. Continued Benefit to Rectal Separation for Prostate Radiation Therapy: Final Results of a Phase III Trial. *Int J Radiat Oncol Biol Phys* (2017) 97(5):976–85. doi: 10.1016/j.ijrobp.2016.12.024
- Mariados N, Sylvester J, Shah D, Karsh L, Hudes R, Beyer D, et al. Hydrogel Spacer Prospective Multicenter Randomized Controlled Pivotal Trial: Dosimetric and Clinical Effects of Perirectal Spacer Application in Men Undergoing Prostate Image Guided Intensity Modulated Radiation Therapy. *Int J Radiat Oncol Biol Phys* (2015) 92:971–7. doi: 10.1016/j.ijrobp.2015.04.030
- Ben-Yosef R, Paz A, Levy Y, Alani S, Muncher Y, Shohat S, et al. A Novel Device for Protecting Rectum During Prostate Cancer Irradiation: *In Vivo* Data on a Large Mammal Model. *J Urol* (2009) 181:1401–6. doi: 10.1016/j.juro.2008.11.010
- Melchert C, Gez E, Bohlen G, Scarzello G, Koziol I, Anscher M, et al. Interstitial Biodegradable Balloon for Reduced Rectal Dose During Prostate Radiotherapy: Results of a Virtual Planning Investigation Based on the Pre- and Post-Implant Imaging Data of an International Multicenter Study. *Radiation Oncol* (2013) 106:210–4. doi: 10.1016/j.radonc.2013.01.007
- Pasquier D, Bogart E, Bonodeau F, Lacornerie T, Lartigau E, Latorzeff I. BioPro-RCMI-1505 Trial: Multicenter Study Evaluating the Use of a Biodegradable Balloon for the Treatment of Intermediate Risk Prostate Cancer by Intensity Modulated Radiotherapy: Study Protocol. *BMC Cancer* (2018) 18:566. doi: 10.1186/s12885-018-4492-5
- Schorghofer A, Drerup M, Kunit T, Lusuardi L, Holzinger J, Karner J, et al. Rectum-Spacer Related Acute Toxicity - Endoscopy Results of 403 Prostate Cancer Patients After Implantation of Gel or Balloon Spacers. *Radiat Oncol* (2019) 14:47. doi: 10.1186/s13014-019-1248-6
- Vanneste BGL, van De Beek K, Lutgens L, Lambin P. Implantation of a Biodegradable Rectum Balloon Implant: Tips, Tricks and Pitfalls. *Int Braz J Urol* (2017) 43:1033–42. doi: 10.1590/s1677-5538.10.2016.0494

19. Vanneste BGL, van Wijk Y, Lutgens LC, Van Limbergen EJ, van Lin EN, van de Beek K, et al. Dynamics of Rectal Balloon Implant Shrinkage in Prostate VMAT: Influence on Anorectal Dose and Late Rectal Complication Risk. *Strahlenther Onkol* (2018) 194:31–40. doi: 10.1007/s00066-017-1222-x
20. Gez E, Cytron S, Ben Yosef R, London D, Corn BW, Alani S, et al. Application of an Interstitial and Biodegradable Balloon System for Prostate-Rectum Separation During Prostate Cancer Radiotherapy: A Prospective Multi-Center Study. *Radiat Oncol* (2013) 8:96. doi: 10.1186/1748-717X-8-96
21. D'Amico AV, Whittington R, Malkowicz SB, Schultz D, Blank K, Broderick GA, et al. Biochemical Outcome After Radical Prostatectomy, External Beam Radiation Therapy, or Interstitial Radiation Therapy for Clinically Localized Prostate Cancer. *JAMA* (1998) 280:969–74. doi: 10.1001/jama.280.11.969
22. Fayers P, Bottomley A, Group EQoL, and Quality of Life U. Quality of Life Research Within the EORTC-The EORTC QLQ-C30. European Organisation for Research and Treatment of Cancer. *Eur J Cancer* (2002) 38 Suppl 4:S125–33. doi: 10.1016/S0959-8049(01)00448-8
23. van Andel G, Bottomley A, Fossa SD, Efficace F, Coens C, Guerif S, et al. An International Field Study of the EORTC QLQ-PR25: A Questionnaire for Assessing the Health-Related Quality of Life of Patients With Prostate Cancer. *Eur J Cancer* (2008) 44:2418–24. doi: 10.1016/j.ejca.2008.07.030
24. Karsh LI, Gross ET, Pieczonka CM, Aliotta PJ, Skomra CJ, Ponsky LE, et al. Absorbable Hydrogel Spacer Use in Prostate Radiotherapy: A Comprehensive Review of Phase 3 Clinical Trial Published Data. *Urology* (2018) 115:39–44. doi: 10.1016/j.urology.2017.11.016
25. Miller LE, Efsthathiou JA, Bhattacharyya SK, Payne HA, Woodward E, Pinkawa M. Association of the Placement of a Perirectal Hydrogel Spacer With the Clinical Outcomes of Men Receiving Radiotherapy for Prostate Cancer: A Systematic Review and Meta-Analysis. *JAMA Netw Open* (2020) 3:e208221. doi: 10.1001/jamanetworkopen.2020.8221
26. Chapet O, Udrescu C, Devonec M, Tanguy R, Sotton MP, Enachescu C, et al. Prostate Hypofractionated Radiation Therapy: Injection of Hyaluronic Acid to Better Preserve the Rectal Wall. *Int J Radiat Oncol Biol Phys* (2013) 86:72–6. doi: 10.1016/j.ijrobp.2012.11.027
27. Chapet O, Decullier E, Bin S, Faix A, Ruffion A, Jalade P, et al. Prostate Hypofractionated Radiation Therapy With Injection of Hyaluronic Acid: Acute Toxicities in a Phase 2 Study. *Int J Radiat Oncol Biol Phys* (2015) 91:730–6. doi: 10.1016/j.ijrobp.2014.11.027
28. Wolf F, Gaisberger C, Ziegler I, Krenn E, Scherer P, Hraby S, et al. Comparison of Two Different Rectal Spacers in Prostate Cancer External Beam Radiotherapy in Terms of Rectal Sparing and Volume Consistency. *Radiother Oncol* (2015) 116:221–5. doi: 10.1016/j.radonc.2015.07.027

Conflict of Interest: The authors declare that this study received funding from BioProtect Ltd and AQUILAB. The funder was not involved in the study design, collection, analysis, interpretation of data, the writing of this article or the decision to submit it for publication.

Publisher's Note: All claims expressed in this article are solely those of the authors and do not necessarily represent those of their affiliated organizations, or those of the publisher, the editors and the reviewers. Any product that may be evaluated in this article, or claim that may be made by its manufacturer, is not guaranteed or endorsed by the publisher.

Copyright © 2021 Latorzeff, Bruguère, Bogart, Le Deley, Lartigau, Marre and Pasquier. This is an open-access article distributed under the terms of the Creative Commons Attribution License (CC BY). The use, distribution or reproduction in other forums is permitted, provided the original author(s) and the copyright owner(s) are credited and that the original publication in this journal is cited, in accordance with accepted academic practice. No use, distribution or reproduction is permitted which does not comply with these terms.



A Real-World, Multicenter, Observational Retrospective Study of Durvalumab After Concomitant or Sequential Chemoradiation for Unresectable Stage III Non-Small Cell Lung Cancer

OPEN ACCESS

Edited by:

Aditya Juloori,
University of Chicago Medical Center,
United States

Reviewed by:

Jiamei Fu,
Shanghai Pulmonary Hospital, China
Henry Soo-Min Park,
Yale University, United States

*Correspondence:

Alessio Bruni
bruni.alessio@aou.mo.it

[†]These authors have contributed
equally to this work and share
first authorship

[‡]These authors have contributed
equally to this work and share
last authorship

Specialty section:

This article was submitted to
Radiation Oncology,
a section of the journal
Frontiers in Oncology

Received: 21 July 2021

Accepted: 06 September 2021

Published: 28 September 2021

Citation:

Bruni A, Scotti V, Borghetti P,
Vagge S, Cozzi S, D'Angelo E,
Gajj Lepra N, Fozza A, Taraborrelli M,
Piperno G, Vanoni V, Sepulcri M,
Trovò M, Nardone V, Lattanzi E,
Bou Selman S, Bertolini F,
Franceschini D, Agustoni F,
Jereczek-Fossa BA, Magrini SM, Livi L,
Lohr F and Filippi AR (2021) A Real-
World, Multicenter, Observational
Retrospective Study of Durvalumab
After Concomitant or Sequential
Chemoradiation for Unresectable
Stage III Non-Small Cell Lung Cancer.
Front. Oncol. 11:744956.
doi: 10.3389/fonc.2021.744956

Alessio Bruni^{1†}, Vieri Scotti^{2†}, Paolo Borghetti³, Stefano Vagge⁴, Salvatore Cozzi⁵,
Elisa D'Angelo¹, Niccolò Gajj Lepra⁶, Alessandra Fozza⁴, Maria Taraborrelli⁷,
Gaia Piperno⁸, Valentina Vanoni⁹, Matteo Sepulcri¹⁰, Marco Trovò¹¹, Valerio Nardone¹²,
Elisabetta Lattanzi¹³, Said Bou Selman¹⁴, Federica Bertolini¹⁵, Davide Franceschini¹⁶,
Francesco Agustoni¹⁷, Barbara Alicja Jereczek-Fossa^{8,18}, Stefano Maria Magrini³,
Lorenzo Livi², Frank Lohr¹⁴ and Andrea Riccardo Filippi^{19‡}

¹ Radiotherapy Unit, Department of Oncology and Hematology, University Hospital of Modena, Modena, Italy, ² Department of Oncology, Radiation Therapy Unit, Careggi University Hospital, Florence, Italy, ³ Radiation Oncology Department, Spedali Civili and University of Brescia, Brescia, Italy, ⁴ Department of Radiation Oncology, Istituto di Ricovero e Cura a Carattere Scientifico (IRCCS) Policlinico San Martino, Genova, Italy, ⁵ Radiation Therapy Department, Arcispedale di Santa Maria Nuova IRCCS (Istituto di Ricovero e Cura a Carattere Scientifico), Reggio Emilia, Italy, ⁶ Advanced Radiation Oncology Department, Istituto di Ricovero e Cura a Carattere Scientifico (IRCCS), Sacro Cuore Don Calabria Hospital, Verona, Italy, ⁷ Radiation Oncology Department, SS. Annunziata Hospital, "G. D'Annunzio" University of Chieti, Chieti, Italy, ⁸ Division of Radiotherapy, European Institute of Oncology (IEO), Istituto di Ricovero e Cura a Carattere Scientifico (IRCCS) European Institute of Oncology, Milan, Italy, ⁹ Radiation Oncology Department, S. Chiara Hospital, Trento, Italy, ¹⁰ Radiation Oncology Unit, Veneto Institute of Oncology Istituto Oncologico Veneto (IOV), Istituto di Ricovero e Cura a Carattere Scientifico (IRCCS), Padua, Italy, ¹¹ Radiation Oncology Department, Azienda Sanitaria Universitaria Integrata, Udine, Italy, ¹² Radiotherapy Unit, "Ospedale del Mare", Naples, Italy, ¹³ Radiotherapy Unit, University Hospital of Parma, Parma, Italy, ¹⁴ Department of Radiotherapy, Bolzano Hospital, Bolzano, Italy, ¹⁵ Medical Oncology Unit, Department of Oncology and Hematology, University Hospital of Modena, Modena, Italy, ¹⁶ Department of Radiotherapy and Radiosurgery, Humanitas Research Hospital, Istituto di Ricovero e Cura a Carattere Scientifico (IRCCS)-Humanitas Research Hospital, Milan, Italy, ¹⁷ Medical Oncology, Fondazione Istituto di Ricovero e Cura a Carattere Scientifico (IRCCS) Policlinico San Matteo, Pavia, Italy, ¹⁸ Department of Oncology and Hemato-Oncology, University of Milan, Milan, Italy, ¹⁹ Department of Radiation Oncology, Fondazione Istituto di Ricovero e Cura a Carattere Scientifico (IRCCS) Policlinico San Matteo and University of Pavia, Pavia, Italy

Introduction: For unresectable stage III non-small cell lung cancer (NSCLC), the standard therapy consists of chemoradiotherapy (CRT) followed by durvalumab maintenance for responding patients. The present study reports on the safety and outcome of durvalumab use after CRT in a real-world, multicenter, retrospective cohort.

Methods: Two hundred thirty-eight patients have been included. We collected data on systemic therapy, radiation therapy, the timing between CRT and durvalumab, number of durvalumab cycles, reasons for non-starting or discontinuation, incidence and grade of adverse events (AEs), and progression-free survival (PFS) and overall survival (OS).

Results: One hundred fifty-five patients out of 238 (65.1%) received at least one durvalumab dose: 91 (58.7%) after concomitant CRT (cCRT) and 64 (41.3%) after sequential CRT (sCRT). Programmed-death ligand 1 (PD-L1) status was unknown in

7/155 (4.5%), negative in 14 (9.1%), and positive $\geq 1\%$ in 134/155 (86.4%). The main reasons for non-starting durvalumab were progression (10.1%), PD-L1 negativity (7.5%), and lung toxicity (4.6%). Median follow-up time was 14 months (range 2–29); 1-year PFS and OS were 65.5% (95%CI: 57.6–74.4) and 87.9% (95%CI: 82.26–93.9), respectively. No significant differences in PFS or OS were detected for cCRT vs. sCRT, but the median PFS was 13.5 months for sCRT vs. 23 months for cCRT. Potentially immune-related AEs were recorded in 76/155 patients (49.0%). Pneumonitis was the most frequent, leading to discontinuation in 11/155 patients (7.1%).

Conclusions: Durvalumab maintenance after concurrent or sequential chemoradiation for unresectable, stage III NSCLC showed very promising short-term survival results in a large, multicenter, retrospective, real-world study. Durvalumab was the first drug obtaining a survival benefit over CRT within the past two decades, and the present study contributes to validating its use in clinical practice.

Keywords: chemoradiotherapy, immunotherapy, stage III, unresectable, NSCLC

INTRODUCTION

The randomized phase 3 PACIFIC trial established a new standard for unresectable stage III non-small cell lung cancer (NSCLC), introducing immunotherapy maintenance with the anti-programmed-death ligand 1 (anti-PD-L1) agent durvalumab after chemoradiotherapy (CRT). The use of durvalumab substantially improved both progression-free survival (PFS) and overall survival (OS) in patients responding to CRT (1–3). The subsequent registration and clinical use of durvalumab varied across countries. According to the European Medicines Agency (EMA) recommendations, durvalumab use was approved in Italy in September 2018, restricted to patients with a PD-L1 tumor proportion score (TPS) $>1\%$, following a post-hoc analysis showing that patients with tumors expressing PD-L1 below 1% lacked any survival advantage over control.

As unresectable stage III NSCLC presents heterogeneous clinical features, the therapeutic approach may vary widely across centers. Therefore, in this study, we aimed to describe the use of durvalumab in a real-life context, on a multicenter basis, assessing the adherence to EMA indications and providing information on patients' demographics, treatment tolerance, and survival.

MATERIAL AND METHODS

Study Population and Outcome Assessment

In June 2020, we invited Italian Centers participating in the Association of Radiotherapy and Clinical Oncology (AIRO) thoracic oncology network to include in this observational study all stage III patients referred to radiotherapy, which would have been candidates for CRT and durvalumab after approval in Italy from September 2018 to March 2020. Sixteen centers agreed, for a total of 238 enrolled patients.

Patient demographics, tumor characteristics, and treatment-related information were collected in a centralized digital database.

According to standard practice, during durvalumab administration and subsequent follow-up, restaging with total body CT scan was performed every 3 months during the first 2 years and then every 6 months, with variations according to each institution's preference.

We defined locoregional relapse as either local (primary tumor) or mediastinal failure, while systemic progression as the occurrence of extra-thoracic visceral or nodal metastases. OS probability was calculated from the end of CRT to death for any cause (or last assessment of vital status); PFS was calculated from the end of CRT to any disease progression (local failure and distant progression) or death.

All adverse events (AEs) were categorized using Common Terminology Criteria for Adverse Events (CTCAE) version 4.0.

The Ethical Committee of the Coordinating Center in Modena first reviewed and approved the study (approval number 59/2021/OSS/AOUMO) and then each participating center.

Statistical Analysis

The univariate Cox proportional-hazards models were performed to screen the effect of the clinical and demographic variables on the PFS and OS. The hazard ratios associated with the PFS and OS were calculated with their 95% confidence interval for each factor from the Cox proportional-hazards model. Those covariates with a p-value <0.05 were then selected for the multivariate analysis, where the PFS and OS were the dependent variable. Multivariate analysis was performed using again the Cox proportional-hazards model.

The likelihood ratio test was used as a test of statistical significance, and the multiple comparisons correction was not performed. Differences, with a p-value less than 0.05, were selected as significant, and data were acquired and analyzed in R v4.0.3 software environment.

RESULTS

At the end of CRT, 83/238 (34.8%) patients did not start durvalumab. The main reasons were the absence of PD-L1

expression (n = 18; 7.5%), persistent CRT-related toxicities (n = 14; 5.9%), disease progression (n = 24; 10%), denial of consent (n = 2; 0.8%), death due to other causes (n = 2; 0.8%), viral infections (n = 5; 2.2%, including SARS-CoV-2), and acute renal injury (n = 1; 0.4%). The remaining 17 patients (7.2%) did not start durvalumab due to unknown causes.

One hundred fifty-five out of 238 patients (65.2%) received at least one durvalumab dose after CRT. Main patients and tumors characteristics are reported in **Table 1**; 150/155 (95.5%) underwent fluorine-18-deoxyglucose positron emission tomography (¹⁸FDG-PET) for staging and 141 (90.9%) brain CT scan or MRI. One hundred twelve patients (77.5%) received 60 Gray (Gy) in 30 fractions, 10 (6.5%) received 66 Gy in 33 fractions, and 10 (6.5%) received 44–54 Gy in 22–27 fractions; 15 patients (9.5%) received 51–55 Gy in 17–20 fractions. All patients received platinum-based chemotherapy, mostly weekly carboplatin/taxanes (33.5%), and platinum/etoposide every 3 weeks (20.6%).

Concomitant CRT (cCRT) has been administered in 91 patients (58.8%) and sequential CRT (sCRT) in 64 (41.2%). **Table 2** describes patients' and tumor characteristics of these two subgroups. As expected, those who received sCRT were older, with larger tumors, and more likely to receive hypofractionated RT.

TABLE 1 | Patients' characteristics.

Category	Variables	Percentage (%)
Age (mean)	66 (40–82)	
Gender	Male	109 (70.3%)
	Female	46 (29.7%)
Smoking habit	Active smokers	11 (7.1%)
	Former smokers	88 (56.8%)
	Never smokers	56 (36.1%)
Performance status (ECOG)	0	93 (60.0%)
	1	57 (36.8%)
	2	5 (3.2%)
Cardiac comorbidities	Yes	50 (32.2%)
	No	105 (67.8%)
Hypertension	Yes	75 (48.4%)
	No	80 (51.6%)
Histology	Adenocarcinoma	92 (59.3%)
	SCC	49 (31.6%)
	Other	14 (9.1%)
PD-L1 expression	<1%	14 (9.1%)
	1–50%	71 (45.8%)
	>50%	63 (40.6%)
	Unknown	7 (4.5%)
T stage	T1	21 (13.5%)
	T2	46 (29.7%)
	T3	44 (28.4%)
	T4	44 (28.4%)
N stage	N0	4 (2.5%)
	N1	13 (8.4%)
	N2	94 (60.7%)
	N3	44 (28.4%)
TNM staging (9th edition)	IIIA	51 (32.9%)
	IIIB	85 (54.9%)
	IIIC	19 (12.2%)
Chemoradiotherapy	Concomitant	91 (58.8%)
	Sequential	64 (41.2%)

TNM, tumor node metastasis; ECOG, Eastern Cooperative Oncology Group; PD-L1, programmed-death ligand 1.

Twenty-two percent of patients started durvalumab <42 days from CRT and 78% after 42 days. The median time from CRT to first durvalumab dose was 52 days (range 9–245).

At the time of writing, 54 of 155 (35.4%) patients were still on treatment. The main reasons for durvalumab discontinuation are reported in **Table 3**. The mean and median numbers of durvalumab cycles were 14 and 13 (range 1–34), respectively.

Survival

The median follow-up time was 14 months (range 2–29). PFS at 6, 12, and 18 months was 83.5% (95%CI: 77.6–89.7), 65.5% (95%

TABLE 2 | Patients' characteristics for concomitant vs. sequential chemoradiotherapy.

Category		Concomitant CRT	Sequential CRT
Patients	Total number	91	64
Age	Mean (range)	64 (40–80)	69 (43–82)
	Median (range)	66 (40–80)	72 (43–82)
Gender	Male (%)	61 (67.1%)	48 (75%)
	Female (%)	30 (32.9%)	16 (25%)
Smoke habit	Active smokers	37 (40.7%)	19 (29.7%)
	Former smokers	48 (52.8%)	40 (62.5%)
	Never smokers	6 (6.5%)	5 (7.8%)
Cardiac comorbidities	No (%)	68 (74.7%)	37 (57.8%)
	Yes (%)	23 (25.3%)	27 (42.2%)
Histology	Adenocarcinoma	51 (56.1%)	41 (64.1%)
	SCC	31 (34.1%)	18 (28.1%)
	Other	9 (9.8%)	5 (7.8%)
PD-L1 expression	<1%	8 (8.7%)	6 (9.3%)
	1%–25%	36 (39.6%)	22 (34.4%)
	25%–50%	3 (3.3%)	10 (15.6%)
	>50%	38 (41.8%)	25 (39.1%)
	Unknown	7 (7.6%)	1 (1.6%)
T stage	T1	16 (17.6%)	5 (7.8%)
	T2	31 (34.1%)	15 (23.4%)
	T3	26 (28.6%)	18 (25.0%)
	T4	18 (19.7%)	26 (40.8%)
N Stage	N0	2 (2.2%)	2 (3.2%)
	N1	8 (8.8%)	5 (7.8%)
	N2	59 (64.8%)	35 (54.7%)
	N3	22 (24.2%)	22 (34.3%)
¹⁸ FDG-PET	Yes	89 (97.8%)	61 (95.3%)
	No	2 (2.2%)	3 (4.7%)
Clinical stage	IIIA	37 (40.6%)	14 (21.9%)
	IIIB	44 (48.3%)	41 (64.1%)
	IIIC	10 (11.1%)	9 (14.0%)
Chemotherapy cycles	Median (range)	4 (1–9)	4 (3–8)
	Two to three	28 (30.7%)	26 (40.6%)
	Four	22 (24.2%)	29 (45.3%)
	More than four	36 (39.6%)	9 (13.6%)
RT schedule	Conventional	81 (89.1%)	49 (76.5%)
	Hypofractionation	10 (9.9%)	15 (23.5%)
RT total dose	>66 Gy	10 (10.9%)	2 (3.2%)
	60–66 Gy	76 (83.6%)	51 (79.7%)
	<60 Gy	5 (5.5%)	11 (17.1%)
Clinical response	Complete response	4 (4.4%)	2 (3.2%)
	Partial response	71 (78.1%)	45 (70.3%)
	Stable disease	14 (15.3%)	16 (25.0%)
	Unknown	2 (2.2%)	1 (1.5%)
Time interval CRT—durvalumab first dose	Days (range)	56 (10–245)	51 (9–153)

TABLE 3 | Reasons for treatment discontinuation.

Reasons for durvalumab discontinuation	n. of patients (%)
Achieving planned total dose as per PACIFIC study	36 (23.4%)
Disease progression	35 (22.6%)
Pneumonitis	11 (7.1%)
Diarrhea	4 (2.6%)
Thyroiditis	3 (1.9%)
Cardiovascular disease	3 (1.9%)
Liver dysfunction	2 (1.3%)
Neutropenia	2 (1.3%)
Skin reactions	1 (0.6%)
Pancreatic failure	1 (0.6%)
COVID-19	1 (0.6%)
Other	2 (1.3%)
Total	101/155 (65.2%)

Covid19, Coronavirus Disease 2019.

CI: 57.6–74.4), and 53.1% (95%CI: 43.8–64.3), respectively (**Figure 1**). OS at 6, 12, and 18 months was 97.2% (95%CI: 94.6–99.9), 87.9% (95%CI: 82.26–93.9), and 79.3% (95%CI: 71.1–88.4), respectively (**Figure 1**). Median PFS was 23 months, and median OS was not reached.

We did not detect any significant difference in PFS (log-rank $p = 0.2$) or OS (log-rank $p = 0.7$) between concurrent and sCRT plus durvalumab (**Figure 2**). However, the median PFS was 13.5 and 23.0 months for sCRT and cCRT, respectively.

The univariate analysis demonstrated a significant association among TNM staging, histology, and PFS (p -value ≤ 0.05). The multivariate analysis confirmed a statistically significant effect of staging and histology on PFS (p -values: 0.022 and 0.016, respectively). In particular, the risk of progression was about 2.5 times more likely in patients with stage IIIC vs. IIIA, keeping constant histology (HR = 2.53). In addition, the risk of progression was about 1.9 times more likely in patients with squamous cell carcinoma (SCC) vs. non-squamous histology, maintaining constant TNM staging (HR = 1.92).

A significant association between histology and OS was also observed (p -values = 0.039). In particular, the risk of death was about 2.4 times more likely in patients with SCC vs. non-squamous histology (HR = 2.39).

Pattern of Relapse

At the time of writing, 55 patients (35.5%) relapsed locally or systemically; 32 (20.6%) had locoregional progression [as the only site of disease progression in nine (5.8%)], and 46 (29.7%) developed systemic metastases; 23 patients (14.8%) had both local and systemic relapse, and 23 (14.8%) had systemic relapses alone. Primary metastatic sites were the brain, lung (ipsilateral and contralateral), liver, and bone. More than one metastatic site was found in 17 patients. Nine patients had less than five metastatic sites (5/46, 10.8%), while 37/46 (89.2%) experienced poly-metastatic spread.

At progression, 30/55 patients (54.5%) received systemic treatment (26 with chemotherapy and four with pembrolizumab), and nine (16.3%) received metastasis-directed stereotactic RT (exclusive salvage in five patients at the time of analysis). The remaining 16 patients (29%) were referred to palliative care.

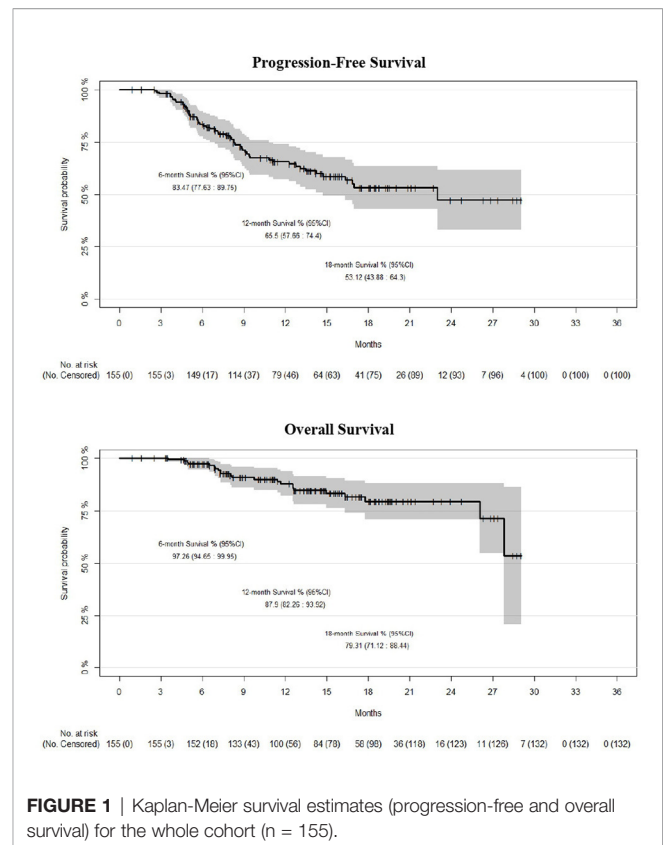


FIGURE 1 | Kaplan-Meier survival estimates (progression-free and overall survival) for the whole cohort ($n = 155$).

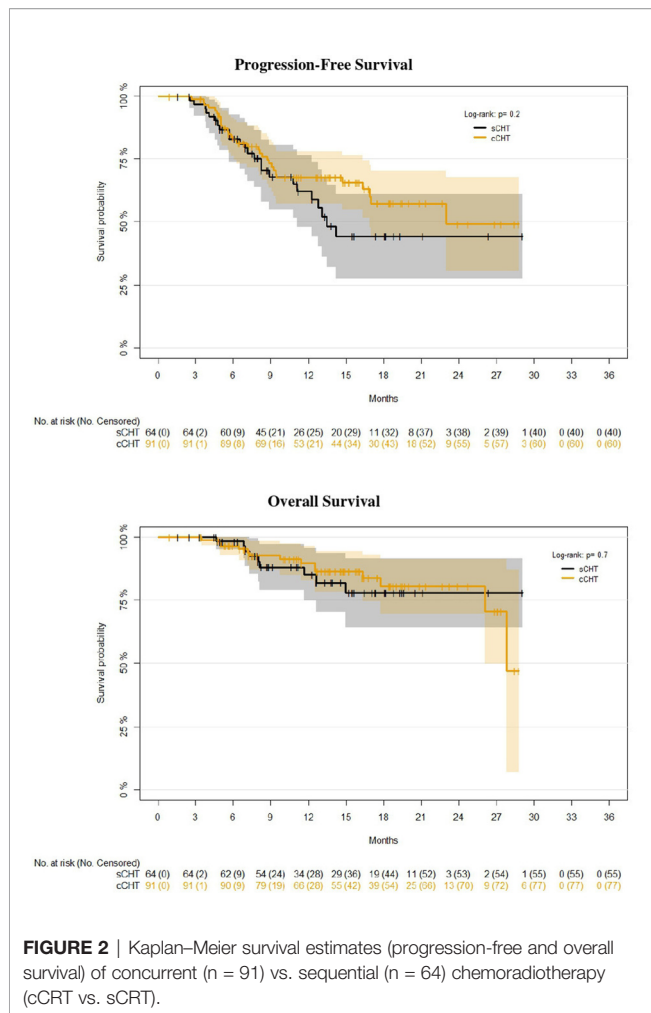
Toxicity

We defined AEs occurring before the first durvalumab dose as CRT-related, while all other AEs were defined as potentially immune-related. We report in details AEs recorded in patients receiving at least one durvalumab dose ($n = 155$). One hundred five patients experienced at least one AE related to CRT administration. Grade 1–2 esophagitis was the most common (80/155, 50.3%), followed by grade 1–2 lung toxicity recorded in 36/155 patients (23.2%). In comparison, only three patients experienced grade 3 pneumonitis (1.9%). Hematological toxicity was recorded in 13 patients (four patients with grade 2, two with grade 3, and two with grade 4).

Potentially immune-related AEs (defined as a “side effect occurred after at least one cycle of durvalumab and not previously reported”) were recorded in 76/155 patients (49.0%). The most frequent were pneumonitis (27/155, 17.4%; 85.2% of whom were G1–2, 11.1% G3, and 3.7% G4), causing definitive discontinuation of durvalumab in 11 patients (7.1%) and then myalgia/asthenia (27/155, 17.4%; all were G1–G2) and thyroiditis (11/155, 7.1%; of whom 91.9% were G1–G2 and 9.1% were G3). We report all reasons for durvalumab permanent discontinuation in **Table 2**.

DISCUSSION

We report the findings of a multicenter, observational, retrospective study in patients with unresectable stage III NSCLC candidates to CRT and durvalumab outside clinical trials or expanded access programs (EAPs).



A consistent proportion of the whole cohort ($n = 83$; 34.8%) did not receive durvalumab after CRT, primarily for PD-L1 negativity or CRT-related toxicity. For those receiving at least one durvalumab dose ($n = 155$), demographic characteristics were quite similar to the PACIFIC trial, with a median age of 66 but a prevalence of PD-L1-positive patients (86.4%) and a higher rate of stage IIIB or IIIC (67.1%, **Table 1**). Considering the limited follow-up, PFS and OS are slightly higher than in PACIFIC trial^{1,2,3}, and in line with the very positive findings of previously published observational series (4–6) including comparisons with historical cohorts treated in the pre-immunotherapy era. In the most extensive retrospective series reported so far, including 147 patients treated with durvalumab after concurrent CRT, from Canadian and Japanese Centers (6), 12 months' OS was above 90%, reaching 100% for patients affected with tumors expressing PD-L1 >50%. The median time to durvalumab first dose was 33 days, relatively short for a real-life study; no impact on survival was detected for patients initiating durvalumab >42 days after CRT.

In our study, 12-month PFS was 65.5%, and OS 87.9%, and the crude rate of local failure was 21%. In assessing these values,

we should take into account the methodological limitations of any direct comparison between different study designs and patient populations and, in particular, the uncertainties in PFS assessment (influenced by the absence of a clear follow-up protocol and RECIST use in our study), which might lead to PFS overestimation.

A detailed analysis of the pattern of relapse suggested that most of the patients relapsed outside the thorax, many with poly-metastatic disease (60.9%). This latter finding is partially in contrast with the PACIFIC trial, in which intrathoracic progression was the most common compared with metastatic progression (80.6% vs. 15.3%, respectively, in the durvalumab arm, 74.5% vs. 20.3%, respectively, in the placebo arm) (7). At the time of progression, 16.3% of patients did receive local therapy alone and 54.5% chemotherapy. These preliminary data, which need to be confirmed by larger observational series, are relevant for the design of future clinical trials dedicated to progressors after CRT plus durvalumab.

Of particular interest with this series is the inclusion of patients treated with sCRT, who were eligible for durvalumab maintenance according to EMA indications. They represent a meaningful proportion of our cohort (41.2%), reflecting national preferences. We found no significant differences in PFS or OS for these patients when compared with patients receiving concurrent CRT; however, median PFS was remarkably higher for patients receiving concurrent CRT (23 vs. 13.5 months), and this result is mainly due to progressions after the first 12 months from RT (taking into account the low number of patients at risk and events, with related statistical uncertainties). These are probably the most interesting and novel findings of this study, suggesting that the two approaches (cCRT or sCRT) might achieve similar survival rates (especially OS), despite some differences in patients and tumor characteristics (**Table 2**), but with different median PFS. Notably, PFS and OS were calculated from the end of RT, with the aim of comparing these data with the PACIFIC survival data, which have been calculated from the date of randomization post-CRT.

The prospective ongoing PACIFIC-6 trial (NCT03693300) will better clarify the safety (first objective) and efficacy (secondary objective) of sCRT plus durvalumab, and additional information is expected from the publication of the survival data of the PACIFIC-R real-world study (NCT03798535). However, in the PACIFIC-R study, only 14% of patients received sCRT (based on EAP data). Notably, the median time interval between RT and durvalumab first dose was 52 days, as reported for our cohort (8).

At multivariate analysis, we found that patients affected with SCC are more likely to progress and die, confirming what was already shown by other studies (6).

The safety profile was in general analogous to other series, with the most common cause for durvalumab discontinuation being pneumonitis (7.1%) (1–6). Many research strategies are currently being investigated to further improve the outcomes of CRT and immunotherapy combinations (9); the present study results, together with similar findings, support the feasibility and the translation to practice of phase 3 trials' results in this particular setting.

The strength points of the study are as follows: a) a very homogeneous cohort of patients affected by stage III PD-L1 >1% NSCLC; b) to our knowledge, the first study reporting the main reasons why durvalumab was not started after CRT; and c) the results of sCRT showed from a real world series. On the other hand, the main limitations of our study are represented by its retrospective nature and, secondly, by the relatively short follow-up time, which may influence survival projections in the mid-term to long term.

In conclusion, maintenance therapy with durvalumab, for stage III unresectable NSCLC, PD-L1 >1%, responding to cCRT or sCRT, was associated with very promising short-term survival rates in a large multicenter, retrospective, real-world series. Durvalumab was confirmed to be the first drug obtaining a survival benefit over CRT within the past two decades, and the present study contributes to validating its use in clinical practice.

DATA AVAILABILITY STATEMENT

The original contributions presented in the study are included in the article/supplementary material. Further inquiries can be directed to the corresponding author.

ETHICS STATEMENT

The studies involving human participants were reviewed and approved by the Ethical Committee of “Area Vasta Emilia Nord”—University Hospital of Modena. The patients/

participants provided their written informed consent to participate in this study.

AUTHOR CONTRIBUTIONS

AB, VS, PB, SV, and ARF: conceptualization. AB, SC, ED'A, NG, AF, MTa, GP, VV, MS, MTr, VN, EL, SS, FB, DF, and FA: data curation. AB and ARF: formal analysis. AB, ARF, and FL: original draft writing. AB, ARF, BJ-F, SM, LL, and FL: review and editing. All authors contributed to the article and approved the submitted version.

ACKNOWLEDGMENTS

The authors thank the following for their contribution to the study: Prof. Filippo Alongi, Dr. Giovanni Aluisio, Dr. Marco Banini, Dr. Fausto Barbieri, Dr. Patrizia Ciammella, Dr. G. Scarzello, Prof. Renzo Corvo, Dr. Nunziata D' Abbiero, Dr.ssa Lucrezia Gasparini, Prof. Domenico Genovesi, Dr.ssa Jessica Imbrescia, Dr. Cinzia Iotti, Dr. Martin Maffei, Dr. Marco Perna, Dr. Tiziana Proto, Dr. Valeria Santoro, Prof. Marta Scorsetti, Prof. Marcello Tiseo, and Dr. Giulia Volpi. This work has been conducted on behalf of the Thoracic Oncology Group of the Italian Association of Radiotherapy and Clinical Oncology (AIRO). The authors thank the AIRO Scientific Committee and the Board for the critical revision of the manuscript. Data were presented in part at the virtual AIRO National Meeting, November 2020. Editorial support in the preparation of this article was provided by Edra S.p.A. and unconditionally funded by AstraZeneca.

REFERENCES

1. Antonia SJ, Villegas A, Daniel D, Vicente D, Murakami S, Hui R, et al. Durvalumab After Chemoradiotherapy in Stage III Non-Small-Cell Lung Cancer. *N Engl J Med* (2017) 377:1919–29. doi: 10.1056/NEJMoa1709937
2. Antonia SJ, Villegas A, Daniel D, Vicente D, Murakami S, Hui R, et al. Overall Survival With Durvalumab After Chemoradiotherapy in Stage III NSCLC. *N Engl J Med* (2018) 379:2342–50. doi: 10.1056/NEJMoa1809697
3. Faivre-Finn C, Vicente D, Kurata T, Planchard D, Paz-Ares L, Vansteenkiste JF, et al. Four-Year Survival With Durvalumab After Chemoradiotherapy in Stage III NSCLC—An Update From the PACIFIC Trial. *J Thorac Oncol* (2021) 16:860–67. doi: 10.1016/j.jtho.2020.12.015
4. Offin M, Shaverdian N, Rimmer A, Lobaugh S, Shepherd AF, Simone CB 2nd, et al. Clinical Outcomes, Local-Regional Control and the Role for Metastasis-Directed Therapies in Stage III Non-Small-Cell Lung Cancers Treated With Chemoradiation and Durvalumab. *Radiother Oncol* (2020) 149:205–11. doi: 10.1016/j.radonc.2020.04.047
5. Faehling M, Schumann C, Christopoulos P, Hoffknecht P, Alt J, Horn M, et al. Durvalumab After Definitive Radiochemotherapy (RCT) in Locally Advanced Unresectable NSCLC: Real-World Data on Survival and Safety From the German Expanded Access Program (EAP). *Lung Cancer* (2020) 150:114–22. doi: 10.1016/j.lungcan.2020.10.006
6. Desilets A, Blanc-Durand F, Lau S, Hakoziaki T, Kitadai R, Malo J, et al. Durvalumab Therapy Following Chemoradiation Compared With a Historical Cohort Treated With Chemoradiation Alone in Patients With Stage III Non-Small-Cell Lung Cancer: A Real-World Multicentre Study. *Eur J Cancer* (2021) 142:83–91. doi: 10.1016/j.ejca.2020.10.008
7. Raben D, Rimmer A, Senan S, Broadhurst H, Pellas T, Dennis PA, et al. Patterns of Disease Progression With Durvalumab in Stage III NSCLC (PACIFIC). Proceedings of the 61st Annual Meeting of the American Society for Radiation Oncology (ASTRO). *Int J Radiat Oncol Biol Phys* (2019) 105: P683. doi: 10.1016/j.ijrobp.2019.08.034
8. McDonald F, Mornex F, Garassino MC, Filippi AR, Christoph D, Haakensen VD, et al. PACIFIC-R: Real-World Characteristics of Unresectable Stage III NSCLC Patients Treated With Durvalumab After Chemoradiotherapy. *J Thorac Oncol* (2021) 16:S738–9. doi: 10.1016/S1556-0864(21)01921-3
9. Passiglia F, Leone G, Olmetto E, Delcuratolo MD, Tabbò F, Reale ML, et al. Immune-Checkpoint Inhibition in Stage III Unresectable NSCLC: Challenges and Opportunities in the Post-PACIFIC Era. *Lung Cancer* (2021) 157:85–91. doi: 10.1016/j.lungcan.2021.05.009

Conflict of Interest: AB: speakers' bureau from Astra Zeneca, MSD, Technologie Avanzate; and advisory role for Astra Zeneca. VS: speakers' bureau for Astra Zeneca, Roche, Accuray Int.; and advisory role for Astra Zeneca. PB: speakers' bureau for Astra Zeneca. SV: speakers' bureau for Astra Zeneca, Roche, Accuray Int. ED'A: speaker's bureau from Nestlé, MSD, Astra Zeneca; travel expenses: IPSEN; and expert testimony: Nestlé. NG: speakers' bureau for Astra Zeneca. DF: speakers' bureau for Astra Zeneca; and advisory role for AstraZeneca. FA: speakers' bureau for Astra Zeneca, Roche, BMS, Boehringer Ingelheim, MSD; and advisory role for Boehringer Ingelheim, MSD. BJ-F: personal fees from Janssen, Roche, Astra Zeneca, and Accuray, and institutional grants from AIRC, FIEO-CCM and Accuray Int., all outside of the submitted work. ARF: speakers' bureau for Astra Zeneca, MSD, Roche, Ipsen; advisory role for Astra Zeneca, Roche; institutional research funding: Astra Zeneca; and honoraria for study conduction (not related to the present study): Astra Zeneca.

The remaining author declares that the research was conducted in the absence of any commercial or financial relationships that could be construed as a potential conflict of interest.

Publisher's Note: All claims expressed in this article are solely those of the authors and do not necessarily represent those of their affiliated organizations, or those of the publisher, the editors and the reviewers. Any product that may be evaluated in this article, or claim that may be made by its manufacturer, is not guaranteed or endorsed by the publisher.

Copyright © 2021 Bruni, Scotti, Borghetti, Vagge, Cozzi, D'Angelo, Giaj Levra, Fozza, Taraborrelli, Piperno, Vanoni, Sepulcri, Trovò, Nardone, Lattanzi, Bou Selmán, Bertolini, Franceschini, Agustoni, Jereczek-Fossa, Magrini, Livi, Lohr and Filippi. This is an open-access article distributed under the terms of the Creative Commons Attribution License (CC BY). The use, distribution or reproduction in other forums is permitted, provided the original author(s) and the copyright owner(s) are credited and that the original publication in this journal is cited, in accordance with accepted academic practice. No use, distribution or reproduction is permitted which does not comply with these terms.



Comparative Analyses of Two Established Scores to Assess the Stability of Spinal Bone Metastases Before and After Palliative Radiotherapy

OPEN ACCESS

Edited by:

Dinesh Thotala,
Washington University in St. Louis,
United States

Reviewed by:

Yingming Sun,
Fujian Medical University, China
Alba Fiorentino,
Ospedale Generale Regionale
Francesco Miulli, Italy

*Correspondence:

Tilman Bostel
tilman.bostel@unimedizin-mainz.de

[†]These authors have contributed
equally to this work and share
first authorship

Specialty section:

This article was submitted to
Radiation Oncology,
a section of the journal
Frontiers in Oncology

Received: 05 August 2021

Accepted: 21 September 2021

Published: 19 October 2021

Citation:

Bostel T, Akbaba S,
Wollschläger D, Klodt T, Oebel L,
Mayer A, Drabke S, Sprave T,
Debus J, Förster R, Rief H, Rühle A,
Grosu A-L, Schmidberger H and
Nicolay NH (2021) Comparative
Analyses of Two Established Scores
to Assess the Stability of Spinal
Bone Metastases Before and
After Palliative Radiotherapy.
Front. Oncol. 11:753768.
doi: 10.3389/fonc.2021.753768

Tilman Bostel^{1,2*†}, Sati Akbaba^{1,2†}, Daniel Wollschläger³, Tristan Klodt^{1,2}, Laura Oebel^{1,2}, Arnulf Mayer^{1,2}, Sophia Drabke^{1,2}, Tanja Sprave^{4,5}, Jürgen Debus^{6,7}, Robert Förster⁸, Harald Rief⁹, Alexander Rühle^{4,5}, Anca-Ligia Grosu^{4,5}, Heinz Schmidberger^{1,2} and Nils H. Nicolay^{4,5}

¹ Department of Radiation Oncology and Radiation Therapy, University Medical Center Mainz, Mainz, Germany, ² German Cancer Consortium (DKTK) Partner Site Mainz, German Cancer Research Center, Heidelberg, Germany, ³ Institute of Medical Biostatistics, Epidemiology and Informatics (IMBEI), University Medical Center Mainz, Mainz, Germany, ⁴ Department of Radiation Oncology, University Hospital of Freiburg, Freiburg, Germany, ⁵ German Cancer Consortium (DKTK) Partner Site Freiburg, German Cancer Research Center, Heidelberg, Germany, ⁶ Department of Radiation Oncology, University Hospital of Heidelberg, Heidelberg, Germany, ⁷ German Cancer Consortium (DKTK) Partner Site Heidelberg, German Cancer Research Center, Heidelberg, Germany, ⁸ Institute of Radiation Oncology, Cantonal Hospital Winterthur, University of Zurich, Winterthur, Switzerland, ⁹ Radiation Therapy Practice Bonn-Rhein-Sieg, Bad Godesberg site, Bonn, Germany

Background and Purpose: To compare two validated spinal instability scores regarding the stabilizing effects and skeletal-related events (SREs) of palliative radiotherapy (RT) in patients with spinal bone metastases (SBM).

Materials and Methods: Two hundred eighty-two osteolytic SBM of lung or breast cancer patients were analyzed for stability before and following RT based on the Spinal Instability Neoplastic Score (SINS) or the Taneichi score. Score concordance was quantified by absolute agreement and Cohen's kappa coefficient. SREs were defined as fractures or local progression after RT. OS was quantified as the time between the start of RT and death from any cause.

Results: At 3 and 6 months after RT, 35 and 50% of initially unstable SBM were re-stabilized according to SINS in patients still alive. Corresponding Taneichi score-based stabilization proportions were 25 and 46%, respectively. Comparison of both stability scores showed high absolute agreement for all time-points (range 71–78%, kappa range 0.35–0.44). SRE occurred more frequently in initially unstable SBM compared to stable SBM according to SINS (14 vs. 5%), but no such association could be shown for the Taneichi-based instability criterion. Poor general condition of patients was negatively associated with SINS-measured re-stabilization after 6 months, but no predictive factor for re-stabilization could be found for the Taneichi score.

Conclusions: Despite the relatively high agreement between both stabilization scores, the SINS should be considered the standard for future studies on the stabilization effects of RT in SBM.

Keywords: spinal bone metastases, instability, radiotherapy, SINS, skeletal-related events

INTRODUCTION

Spinal bone metastases (SBM) occur in up to 80% of patients with advanced solid tumors (1, 2). Affected patients often suffer from severe pain, movement restrictions, and/or neurological deficits. Radiotherapy (RT) is a key treatment for symptomatic SBM (3). In addition to the elimination of pain symptoms and restoration of skeletal function, instability of SBM with impending or manifest fractures represents another frequent indication for palliative RT. Unstable SBM not only affect spinal statics but may also threaten the integrity of the spinal cord and the branching nerves with potentially significant negative impact on the patients' quality of life (4, 5). However, stability assessment of the spinal column is a major challenge in clinical practice and is often only carried out on the basis of clinical experience. This may result in under- or overdiagnosis of spinal instability, making communication between physicians of different disciplines very difficult, and leading to inconsistent therapeutic approaches. For this reason, the Spinal Instability Neoplastic Score (SINS) was introduced in 2010 by the Spinal Oncology Study Group and has since become the most adopted stability score for assessing SBM (6). Based on six categories, the SINS is a highly reliable tool to classify the stability of metastatically affected vertebral bodies into stable, potentially unstable, and unstable lesions (7). For unstable vertebral bodies, the SINS gives a clear recommendation for a stabilizing surgery and postoperative RT. In the case of potentially unstable vertebral body metastases, palliative RT is often preferred to surgery, especially for patients with poor prognosis. Unfortunately, there are only very limited SINS-based data on the effect of RT in unstable SBM (8). Instead, the data available so far are mainly based on the Taneichi score, which has also been validated (9–15).

Therefore, this retrospective study aimed to assess pre- and post-RT stability of spinal metastases using the SINS and Taneichi score, in order to verify their agreement, establish potential predictive factors for stability, and analyze skeletal-related events (SRE) and overall survival (OS) following RT.

MATERIAL AND METHODS

Patient Selection

A total of 221 patients with a median age of 63 years (range 34–88 years) and osteolytic SBM of the thoracic or lumbar spine with underlying breast (38%) or bronchial carcinoma (62%) were included in this retrospective study. All patients received one or more palliative RT at the University Hospitals of Mainz and Heidelberg between 2006 and 2012. The required patient data

were taken from the medical records and cancer registers of the participating centers. The diagnosis of SBM was based on imaging techniques such as CT, MRI, or bone scintigraphy. As inclusion criteria, the spinal metastases had to have an osteolytic phenotype and be located in the thoracic or lumbar spine. This analysis has been approved by the independent ethics committees of the medical faculties of the universities of Heidelberg and Mainz (Heidelberg: S-513/2012, Mainz: 2020-15282).

Stability Assessment

At baseline, as well as 3 and 6 months after palliative RT, the stability of metastatically affected vertebral bodies was assessed by CT imaging using the SINS and Taneichi scores. The Taneichi score is only validated for osteolytic bone metastases in the thoracic and lumbar spinal column. It is based purely on radiological criteria (degree of vertebral body destruction, involvement of the costovertebral joint and/or pedicle) to identify spinal lesions that have a very high risk of impending vertebral body collapse. The SINS, on the other hand, is validated for bone metastases of any phenotype throughout the entire spinal column. It is based on six criteria (location, type of pain, type of lesions, spinal alignment, presence of vertebral compression fractures, affection of posterolateral elements) to classify the affected vertebral bodies as stable, potentially unstable, and unstable. In this analysis, the instability criteria of the original publication were used (6, 16), i.e., all vertebral body metastases that were classified as at least potentially unstable (≥ 7 points) according to SINS or had a fracture risk of at least 50% according to Taneichi Score were evaluated as unstable. For both scores, the shift in stability from (potentially) unstable to stable and from stable to (potentially) unstable was independently determined by a board-certified radiologist in patients still alive at the time of evaluation. Furthermore, SREs after palliative RT were assessed, defined as new fractures or progressive sintering of SBM-affected vertebral bodies, or the need for re-irradiation. In the case of multiple bone metastases in a vertebral body or within the target volume, only the most severe lesion was evaluated. If several spinal regions were irradiated in a given patient, each region was evaluated separately in our analysis. A pain response was documented based on reduction of ≥ 2 points on the 10-point visual analogue scale according to the international consensus criteria (17). For partial and complete pain response to RT, the SINS criterion “*type of pain*” was rated with 1 and 0 points in our analysis, respectively.

Treatment

Radiation treatment planning was based on planning CT examinations and, in the case of paravertebral tumor spread, supplemented with MRI scans. The radiation dose was

administered *via* one or more dorsal or oblique dorsal photon fields (6 or 18 MV photon energy). The planning target volume (PTV) included the metastatically affected vertebral body or bodies and the adjacent intervertebral discs, and in most cases also the caudally and cranially adjacent vertebral bodies. Palliative RT was indicated if SBM caused pain symptoms, spinal instability, or neurological deficits. None of the patients in this analysis received additional surgery or other invasive procedures.

Statistical Analysis

Overall survival (OS) was defined as the period from the beginning of first RT until death from any cause and estimated using the Kaplan-Meier method. Group differences in OS after first RT were assessed using the log-rank test. Logistic regression using generalized estimating equations was used to test whether the probability of stable lesions according to SINS and Taneichi score changed from baseline to 3 and 6 months after RT. Logistic regression using generalized estimating equations was used to test the association between the occurrence of any SRE and baseline instability of SBM. Association of prognostic factors “age at RT”, “tumor histology”, “KPS <70 vs. ≥70”, and “fractures prior to RT” with the SINS and Taneichi scores at 3 and 6 months post-RT was tested using separate univariate mixed ordinal logistic regression models. The concordance of the SINS and Taneichi scores in the patient cohort was checked using absolute agreement, and with Cohen’s kappa coefficient. Statistical analysis was done using the R statistical environment, version 4.0.2 (R Core Team 2020, Vienna, Austria). P values of $p < 0.05$ were considered statistically significant.

RESULTS

A total of 221 patients with 282 target volumes and 792 SBM (range 1–14 metastases per patient) of lung and breast carcinomas that were treated with palliative RT were assessed according to SINS and Taneichi score. Median follow-up after RT was 10.9 months (range 0.1–100.6 months). Further detailed information on patient and treatment characteristics is provided in **Table 1**.

Stability Assessment

Most patients exhibited unstable SBM prior to RT according to the SINS (217/282 SBM; 77%) and Taneichi score (224/282 SBM; 79%), respectively. The majority of these lesions (SINS: 88%, Taneichi: 82%) were associated with pain before the start of irradiation. In patients still alive at 3 and 6 months after RT, the change from baseline in the proportion of stable SBM was statistically significant ($p < 0.001$) at each time point with 35% (50/143) and 50% (52/104) of the primarily unstable SBM becoming stabilized according to SINS. Our analysis showed no statistically significant differences in the stabilization proportion between SBM of lung and breast cancer patients (see **Tables 2, 3A, and 3B**).

Prior to RT, the average SINS was 8.3 [standard deviation (SD) 2.3, range 3–15]. After palliative RT, the average SINS

decreased to 6.7 (SD 2.4, range 2–12) after 3 months and to 6.0 (SD 2.2, range 1–12) after 6 months. According to the Taneichi score, the corresponding 3- and 6-month stabilization proportions were 25% (39/154 SBM) and 46% (53/115 SBM), respectively, representing a statistically significant change from baseline ($p < 0.001$ for each time point; see **Table 4**). The exact distribution of Taneichi scores before and after palliative RT is summarized in detail in **Table 4**.

Our analysis showed only slightly different 3- and 6-month stabilization proportions of SBM in breast and lung cancer patients who were still alive at the time of evaluation (see **Table 2**). Taking into account patients who died, the SINS-based stabilization proportions of SBM in the entire study population at 3 and 6 months after palliative RT were only 23% (50/217) and 24% (52/217), respectively. The corresponding Taneichi-based stabilization proportions were 17% (39/224) and 24% (53/224). The different survival prognosis of breast and lung cancer patients had a substantial impact on stabilization probability of primary unstable SBM. In breast cancer patients, the 6-month stabilization probability was 43% (40/93 SBM) and 41% (39/96 SBM) according to the SINS and Taneichi scores, while in lung cancer patients the corresponding values for both scores were only 10 and 11% (SINS: 12/124 SBM, Taneichi: 14/128 SBM).

In our analysis, the SINS criteria “*type of lesions*”, “*type of pain*”, and “*presence of vertebral compression fractures*” were decisive for the change in stability assessment of primary unstable SBM, while the scores in the other SINS criteria remained stable over time. Regarding the “*type of lesions*” criterion, recalcification was responsible for an improvement in the SINS stability category (i.e., shift from potentially unstable to stable) in 56% of initially unstable osteolytic SBM 3 months after RT (28/50; mixed type of lesions 50%, blastic lesions 6%, no recalcification 44%) and 81% of SBM 6 months after RT (42/52; mixed type of lesions 62%, blastic lesions 19%, no recalcification 19%), respectively. Regarding the “*type of pain*” criterion, an improvement of the stability due to an RT-induced pain response was present in 75% of symptomatic primary unstable SBM in our analysis (117/157; partial response 40%, complete response 35%).

A shift in stability from stable to (potentially) unstable according to both scores was only rarely observed following RT (see **Table 2**). In SINS, a Karnofsky Performance Score of less than 70% had a statistically significant association with worse stabilization probability in the univariate mixed ordinal logistic regression for patients still alive 6 months after palliative RT (see **Table 3A**); in contrast, no predictive factors could be identified for the Taneichi Score in patients still alive 3 and 6 months after palliative RT that could prospectively predict stabilization of primarily unstable SBM (see **Table 3B**).

When comparing the two stability scores, absolute agreement both before and at 3 and 6 months after RT was high (78, 71, and 73%, respectively), but Cohen’s kappa coefficients were low due to inhomogeneous marginal frequencies (0.35, 0.41 and 0.44, respectively).

Skeletal-Related Events

Pathologic fractures were detected in 38% of SBM prior to RT (106/282). Up to 6 months after RT, new fractures and

TABLE 1 | Patients' and treatment characteristics.

Characteristics	Value	Percent
Age (y)		
Median	63	
Range	34–88	
Gender (n)		
Female	124	56.1
Male	97	43.9
KPS (nRTc)		
100	5	2.0
90	41	16.6
80	78	31.6
70	74	30.0
60	36	14.6
50	9	3.6
40	3	1.2
30	1	0.4
Number of bone metastases (nRTvol)		
Median	2	
Range	1–14	
Solitary	130	46.1
Multiple	152	53.9
Spine involvement (nRTvol)		
Thoracic	139	49.3
Thoracolumbar	66	23.4
Lumbar	77	27.3
Primary tumor (n)		
Breast carcinoma	83	37.6
NSCLC	126	57.0
SCLC	12	5.4
Distant extraskelatal metastases (n)		
Brain	29	13.1
Lung	33	14.9
Liver	38	17.2
Adrenal glands	15	6.8
Visceral	84	38.0
Other locations	15	6.8
Single radiation dose (Gy)		
Median	3	
Range	2–4	
Cumulative dose (Gy)		
Median	30	
Range	8–40	
Fractionation of RT (nRTvol)		
20 × 2.0 Gy	31	11.0
10 × 2.5 Gy	1	0.4
14 × 2.5 Gy	27	9.6
15 × 2.5 Gy	1	0.4
1 × 3.0 Gy	1	0.4
3 × 3.0 Gy	2	0.7
5 × 3.0 Gy	1	0.4
7 × 3.0 Gy	1	0.4
9 × 3.0 Gy	1	0.4
10 × 3.0 Gy	208	73.8
11 × 3.0 Gy	1	0.4
12 × 3.0 Gy	3	1.1
2 × 4.0 Gy	1	0.4
5 × 4.0 Gy	3	1.1
Indications for RT		
Pain (nRTvol)	235	83.3
Instability (nRTvol according to SINS)	218	77.3
Neurologic deficit (nRTc)	8	3.2
Chemotherapy (n)	150	60.7
Other treatments for bone metastases		
Orthopedic corset (nRTvol)	151	53.5
Bisphosphonates (nRTc)	217	87.9

KPS, Karnofsky performance score; y, years; RT, radiotherapy; Gy, Gray; n, number of patients (in total 221); nRTvol, number of RT volumes (in total 282); nRTc, number of RT courses (in total 247).

progressive sintering of pre-existing fractures within the vertebral bodies were observed in 3% (8/282) and 8% of SBM (22/282), respectively. According to SINS and Taneichi Score, the majority of these post-RT fractures were already initially assessed unstable (90 and 87%, respectively).

Most patients with post-RT fractures received osteoprotective therapy with bisphosphonates or RANK ligand inhibitors (90%) and had already been provided with a corset (66%) before the fracture. Associated pain was reported in 67% of post-RT fractures (20/30 SBM). In addition to post-RT fractures, three SBMs were locally progressive at follow-up with a need for re-irradiation due to new neurological deficits, resulting in an overall SRE proportion of 12% (33/282 target volumes). The presence of an initial pathological fracture in the irradiated area resulted in increased SRE proportions compared to unfractured metastatic lesions (21 vs. 6%). Furthermore, SINS-based initial vertebral body instability was significantly associated with the occurrence of SRE after palliative RT ($p = 0.046$, OR 3.38, 95% CI 1.02–11.22, Wald test), which was the case in 14% of primary unstable SBM (30/217) compared to only 5% of primary stable SBM (3/65). In contrast, this association could not be shown for the Taneichi-based instability criterion ($p = 0.22$, OR 1.97, 95% CI 0.66–5.81, Wald test).

Overall Survival

For the entire study population, median OS after first palliative RT of SBM amounted to 4.8 months (95% CI 3.8–6.0 months); the corresponding 6-, 12-, and 24-month OS was 42% (95% CI 36–49%), 29% (95% CI 23–35%), and 12% (95% CI 8–17%), respectively. Our analysis showed significantly worse OS after first RT for patients with Karnofsky Performance Scores below 70% compared to patients with scores of $\geq 70\%$ ($p < 0.001$) (see **Figure 1**).

Tumor histology was significantly associated with OS after palliative RT of SBM, with breast cancer patients having a considerably better prognosis than lung cancer patients ($p < 0.001$, median OS 12.9 months vs. 3.2 months) (see **Figure 2**).

DISCUSSION

Vertebral instability of SBM represents a key indication for palliative RT, which aims to support recalcification and to improve bone stability. Despite the clinical significance, data on RT-induced stabilization of primarily unstable SBM are limited (18). In particular, the role of stability scores in the context of assessing radiation-induced stabilization remains largely unknown (8).

In our dataset, palliative RT of primarily unstable SBM rarely lead to stabilization in lung cancer patients, whereas nearly half of unstable SBM of breast cancer patients re-stabilized within 6 months after RT. Regarding OS after RT, our evaluation showed significant differences between patients with osseous metastatic lung and breast cancer (median OS 12.9 months vs. 3.2 months). Consequently, the likelihood of stabilization of primarily unstable SBM depends to a large extent on the prognosis of

TABLE 2 | Radiogenic changes in vertebral body stability according to SINS and Taneichi Score.

Stability assessment of SBMs	SINS	Taneichi score
Prior to RT (total study population)		
- stable (%)	64 (23%)	58 (21%)
- unstable (%)	218 (77%)	224 (79%)
Shift from unstable to stable 3 mo. after RT (only SBM of the surviving patients in the <u>entire study population</u>)		
- stable (%)	50 (35%)	39 (25%)
- unchanged unstable (%)	93 (65%)	115 (75%)
Shift from stable to unstable 3 mo. after RT (only SBM of the surviving patients in the <u>entire study population</u>)		
- unchanged stable (%)	40 (95%)	29 (94%)
- unstable (%)	2 (5%)	2 (6%)
Shift from unstable to stable 6 mo. after RT (only SBM of the surviving patients in the <u>entire study population</u>)		
- stable (%)	52 (50%)	53 (46%)
- unchanged unstable (%)	52 (50%)	62 (54%)
Shift from stable to unstable 6 mo. after RT (only SBM of the surviving patients in the <u>entire study population</u>)		
- unchanged stable (%)	29 (97%)	20 (100%)
- unstable (%)	1 (3%)	0 (0%)
Shift from unstable to stable 6 mo. after RT (only SBM of the surviving <u>breast cancer patients</u>)		
- stable (%)	40 (51%)	39 (48%)
- unchanged unstable (%)	39 (49%)	42 (52%)
Shift from unstable to stable 6 mo. after RT (only SBM of the surviving <u>lung cancer patients</u>)		
- stable (%)	12 (48%)	14 (41%)
- unchanged unstable (%)	13 (52%)	20 (59%)

SBM, spinal bone metastases; SINS, Spine Instability Neoplastic Score; RT, radiotherapy; NA, not analyzable, because the follow-up examination was missing due to a deterioration of the general condition or death.

the patients, as recalcification of osteolytic SBM is not expected before 3–6 months after palliative RT (19).

Thus, the relevance of stabilization of unstable SBM is higher for patients with a median OS exceeding 6 months. In our study, tumor histology and the Karnofsky Performance Score were found to be the crucial prognostic factors for OS, which is consistent with the results of previous studies predicting OS in patients with bone metastases (20, 21). Differences in recalcification and stabilization rates between different tumor entities are to a large extent due to the different prognoses, but other factors may also play important roles, such as the individual radiation sensitivity of the respective tumor cell types, the individual tumor microenvironment, the radiation dose or simultaneous systemic treatments. To date, the exact

underlying mechanism of radiation-induced recalcification of osteolytic bone metastases remains incompletely understood.

For patients with a low chance of achieving bone stability 6 months after conventional palliative RT, alternative approaches to improve metastatic spinal stability may be considered. For such situations, further dose escalation in the bone metastases through simultaneous integrated boost (i.e., hypofractionated ablative radiotherapy) or even stereotactic body radiotherapy (SBRT) may be promising options. Dose escalation strategies have the potential to improve stabilization in patients with unstable SBM, particularly in patients with good life expectancy and SBM from tumor entities with a relatively low chance of bone stability at 6 months or those with oligometastatic disease. However, potential benefits of SBRT

TABLE 3A | Univariate analysis of prognostic factors related to stabilization of initially unstable SBM according to SINS.

Predictor	3 months after RT			6 months after RT		
	p-value	OR	CI	p-value	OR	CI
Age	0.99	1.001	0.941–1.064	0.80	0.995	0.954–1.037
Lung cancer (vs. breast cancer)	0.41	1.829	0.434–7.713	0.16	2.196	0.742–6.500
KPS (<70% vs. ≥70%)	0.20	0.273	0.037–1.996	0.02	0.158	0.032–0.790
Fractures before RT (yes vs. no)	0.88	0.919	0.294–2.868	0.73	0.850	0.337–2.142

TABLE 3B | Univariate analysis of prognostic factors related to stabilization of initially unstable SBM according to Taneichi score.

Predictor	3 months after RT			6 months after RT		
	p-value	OR	CI	p-value	OR	CI
Age	NA	1.006	NA	0.65	1.008	0.975–1.042
Lung cancer (vs. breast cancer)	0.09	1.537	0.929–2.543	0.21	1.717	0.740–3.983
KPS (<70% vs. ≥70%)	0.63	0.845	0.424–1.683	0.69	0.775	0.223–2.698
Fractures before RT (yes vs. no)	0.60	0.874	0.527–1.448	0.58	0.805	0.373–1.736

must be balanced against the increased risk of side effects such as fractures or neurologic deficits (22, 23). Surgical stabilization options may also become more relevant to patients. However, compared to SBRT or conventional palliative RT, surgery may interrupt necessary systemic treatments for a considerable time due to perioperative comorbidities.

In assessing vertebral body stability, our analysis showed a relatively good agreement between the SINS and Taneichi scores, with slightly better stabilization rates as assessed by the SINS. This is primarily explained by the inclusion of clinical assessment parameters. Therefore, improved stability scores in our evaluation were also measured by the SINS in case of only a pain response in the absence of recalcification. Nevertheless, our study has shown that previously reported stabilizing effects of palliative RT, based on the Taneichi Score, can be transferred relatively well to the SINS (9, 11, 13, 14, 16, 18, 24). In spinally metastasized head-and-neck tumors, a recent publication assessed stability also on the basis of the SINS (8).

TABLE 4 | Stability assessment of irradiated SBM before and after palliative RT according to the Taneichi score.

Stability assessment of irradiated SBM	n (%)
Taneichi classification prior to RT	
- A	31 (11.0)
- B	48 (17.0)
- C	32 (11.3)
- D	55 (19.5)
- E	67 (23.8)
- F	47 (16.7)
- G	2 (0.7)
Taneichi classification 3 months after RT	
- A	55 (29.7)
- B	29 (15.7)
- C	19 (10.3)
- D	25 (13.5)
- E	35 (18.9)
- F	21 (11.4)
- G	1 (0.5)
Taneichi classification 6 months after RT	
- A	62 (45.9)
- B	20 (14.8)
- C	9 (6.7)
- D	17 (12.6)
- E	15 (11.1)
- F	11 (8.1)
- G	1 (0.7)

SBM, spinal bone metastases; RT, radiotherapy; n, number of patients.

For the SINS, a Karnofsky Performance Score of less than 70% had a statistically significant negative association with the probability of stabilization in our analysis for patients still alive at 6 months after palliative RT. This can be potentially explained by a reduced physical activity of patients with reduced performance, which could negatively impact bony mineralization. In contrast to the results of a recently published study, we could not identify any predictive factors for the Taneichi score in patients still alive at 3 and 6 months after palliative RT that could predict stabilization of primarily unstable SBM (24).

In our study population, pathologic fractures of unstable SBM were shown to be a common clinical problem before starting irradiation. After palliative RT, SRE occurred in 12% of irradiated SBM due to new fractures (3%), progressive fractures (8%), and local progression with the need for re-irradiation (1%). Most post-RT fractures occurred in patients with initial fractures and unstable SBM, and two-thirds of patients with a post-RT fracture reported associated pain. In the literature, secondary fractures, spinal cord compression, and re-irradiation rates after palliative multifractional RT were reported in 2–5, 4–6, and 7–9% of cases, respectively (25–28). The higher number of fractures in our study population can be explained by the high proportion of initially complicated SBM that were not adequately considered in the landmark studies and large literature reviews (25–28).

The presence of a pathologic fracture prior to RT resulted in an increase of SRE in our analysis compared to unfractured metastatic bone (21 vs. 6%). Furthermore, SINS-based initial vertebral instability was found to be significantly associated with the occurrence of SRE, whereas no such association could be demonstrated for Taneichi-based vertebral instability.

Our study has some limitations, especially considering the retrospective character of this patient cohort. For instance, data on clinical factors that may influence bone stabilization and fracture probability such as, e.g., osteoporosis, medication or physical activity could not be systematically collected in our cohort. Furthermore, patients' quality of life could not be assessed retrospectively and requires further prospective investigation. Our evaluation did not include cervical and sacral SBM, as the Taneichi Score is only validated for osteolytic thoracic and lumbar SBM.

For this analysis, we intentionally included only patients who had not received RT in recent years to exclude potential effects of modern systemic therapies such as immunotherapy on bony remineralization. Thus, as a result of improved survival, SRE and stabilization rates of

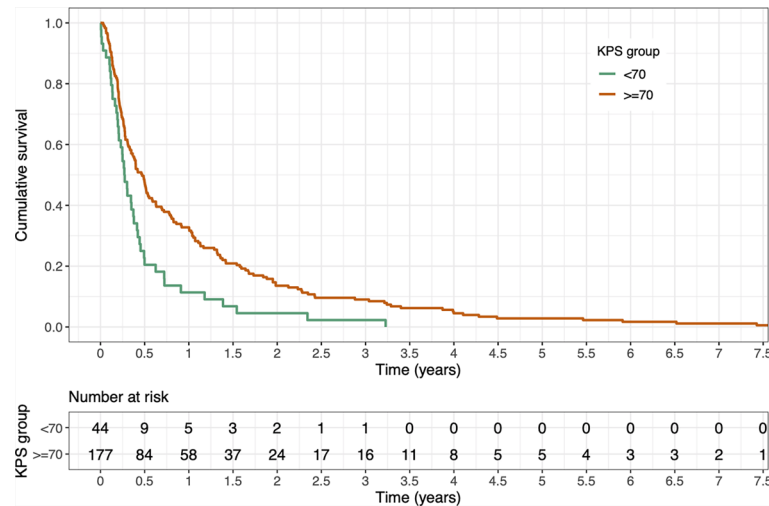


FIGURE 1 | Kaplan-Meier estimate of overall survival (OS) after first radiotherapy stratified by Karnofsky Performance Score (KPS) <70 vs. ≥70. OS was significantly better for patients with a KPS of ≥70% ($p < 0.001$, log-rank test).

patients with more recently treated unstable SBM may be higher than reported here. Therefore, the current analysis intends to serve as baseline examination for subsequent histology-specific stability analyses of SBM irradiated in recent years.

In summary, the choice of radiation dose and fractionation should take into account not only the therapeutic goal but also clinical factors such as patients' general condition and comorbidities, the extent of metastatic disease, and the overall prognosis of the patients, since significant recalcification of osteolytic SBM can first be detected at 3–6 months after palliative RT. The results of our retrospective evaluation support the urgent need to initiate prospective studies to

systematically assess irradiation effects and complication rates (SRE) as a function of initial SINS-based vertebral body instability in the era of modern systemic therapies.

CONCLUSION

Our analysis showed a relatively high agreement between two widely available clinical stabilization scores. The data published so far based on the Taneichi score can therefore be transferred relatively well to the SINS. However, compared to the SINS, the Taneichi Score has some important limitations (i.e., validation

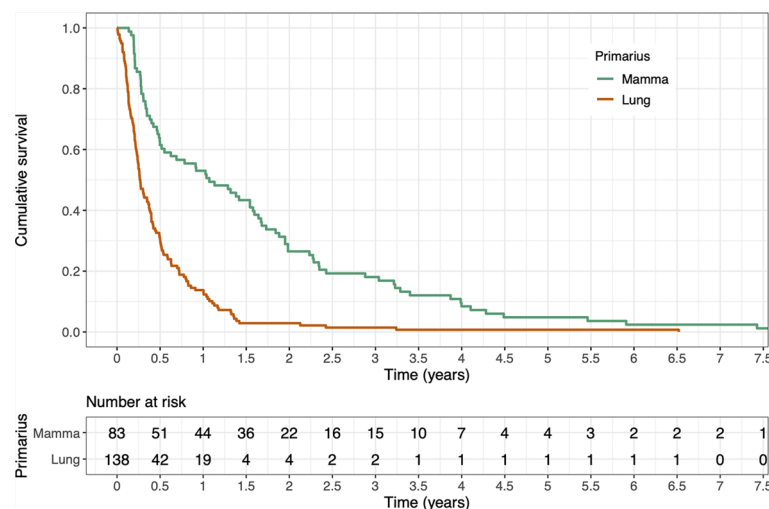


FIGURE 2 | Kaplan-Meier estimate of overall survival after first radiotherapy stratified by tumor histology. OS was significantly better for breast cancer patients compared to lung cancer patients ($p < 0.001$, log-rank test).

only for osteolytic SBM and thoracolumbar lesions), so the SINS should be further considered in future studies on the stabilization effects and complications of palliative RT in SBM. In this regard, initial vertebral body instability according to SINS and pre-existing fractures seemed to increase the risk for SRE after RT.

DATA AVAILABILITY STATEMENT

The raw data supporting the conclusions of this article will be made available by the authors, without undue reservation.

ETHICS STATEMENT

The studies involving human participants were reviewed and approved by the independent ethics committees of the medical faculties of the universities of Heidelberg and Mainz (Heidelberg: S-513/2012, Mainz: 2020-15282). Written informed consent for

participation was not required for this study in accordance with the national legislation and the institutional requirements.

AUTHOR CONTRIBUTIONS

TB and SA equally contributed to this manuscript. TB, SA, and NN developed and planned the retrospective analysis. DW is responsible for statistical considerations/basis of the analysis. TB, SA, TK, LO, AM, SD, TS, JD, RF, HR, AR, A-LG, HS, and NN participated in data collection and/or interpretation of the results. TB wrote the manuscript. All authors contributed to the article and approved the submitted version.

ACKNOWLEDGMENTS

We thank Jessica Lüder, Pia Fischer, and Alex Diwo for participating in data collection.

REFERENCES

- Mundy GR. Metastasis to Bone: Causes, Consequences and Therapeutic Opportunities. *Nat Rev Cancer* (2002) 2(8):584–93. doi: 10.1038/nrc867
- Nielsen OS. Palliative Radiotherapy of Bone Metastases: There Is Now Evidence for the Use of Single Fractions. *Radiother Oncol: J Eur Soc Ther Radiol Oncol* (1999) 52(2):95–6. doi: 10.1016/s0167-8140(99)00109-7
- Lutz S, Balboni T, Jones J, Lo S, Petit J, Rich SE, et al. Palliative Radiation Therapy for Bone Metastases: Update of an ASTRO Evidence-Based Guideline. *Pract Radiat Oncol* (2017) 7(1):4–12. doi: 10.1016/j.prro.2016.08.001
- Patchell RA, Tibbs PA, Regine WF, Payne R, Saris S, Kryscio RJ, et al. Direct Decompressive Surgical Resection in the Treatment of Spinal Cord Compression Caused by Metastatic Cancer: A Randomised Trial. *Lancet* (2005) 366(9486):643–8. doi: 10.1016/S0140-6736(05)66954-1
- Rades D, Segedin B, Conde-Moreno AJ, Garcia R, Perpar A, Metz M, et al. Radiotherapy With 4 Gy X 5 Versus 3 Gy X 10 for Metastatic Epidural Spinal Cord Compression: Final Results of the SCORE-2 Trial (ARO 2009/01). *J Clin Oncol: Off J Am Soc Clin Oncol* (2016) 34(6):597–602. doi: 10.1200/JCO.2015.64.0862
- Fisher CG, DiPaola CP, Ryken TC, Bilsky MH, Shaffrey CI, Berven SH, et al. A Novel Classification System for Spinal Instability in Neoplastic Disease: An Evidence-Based Approach and Expert Consensus From the Spine Oncology Study Group. *Spine* (2010) 35(22):E1221–9. doi: 10.1097/BRS.0b013e3181e16ae2
- Fourney DR, Frangou EM, Ryken TC, DiPaola CP, Shaffrey CI, Berven SH, et al. Spinal Instability Neoplastic Score: An Analysis of Reliability and Validity From the Spine Oncology Study Group. *J Clin Oncol: Off J Am Soc Clin Oncol* (2011) 29(22):3072–7. doi: 10.1200/JCO.2010.34.3897
- Bostel T, Rühle A, Rackwitz T, Mayer A, Klodt T, Oebel L, et al. The Role of Palliative Radiotherapy in the Treatment of Spinal Bone Metastases From Head and Neck Tumors—A Multicenter Analysis of a Rare Event. *Cancers (Basel)* (2020) 12(7):1950. doi: 10.3390/cancers12071950
- Bostel T, Forster R, Schlamp I, Sprave T, Bruckner T, Nicolay NH, et al. Spinal Bone Metastases in Colorectal Cancer: A Retrospective Analysis of Stability, Prognostic Factors and Survival After Palliative Radiotherapy. *Radiat Oncol* (2017) 12(1):115. doi: 10.1186/s13014-017-0852-6
- Bostel T, Forster R, Schlamp I, Wolf R, Serras AF, Mayer A, et al. Stability, Prognostic Factors and Survival of Spinal Bone Metastases in Malignant Melanoma Patients After Palliative Radiotherapy. *Tumori* (2016) 102(2):156–61. doi: 10.5301/tj.5000382
- Foerster R, Habermehl D, Bruckner T, Bostel T, Schlamp I, Welzel T, et al. Spinal Bone Metastases in Gynecologic Malignancies: A Retrospective Analysis of Stability, Prognostic Factors and Survival. *Radiat Oncol* (2014) 9:194. doi: 10.1186/1748-717X-9-194
- Foerster R, Hees K, Bruckner T, Bostel T, Schlamp I, Sprave T, et al. Survival and Stability of Patients With Urothelial Cancer and Spinal Bone Metastases After Palliative Radiotherapy. *Radiol Oncol* (2018) 52(2):189–94. doi: 10.1515/raon-2017-0038
- Rief H, Bischof M, Bruckner T, Welzel T, Askoxylakis V, Rieken S, et al. The Stability of Osseous Metastases of the Spine in Lung Cancer—a Retrospective Analysis of 338 Cases. *Radiat Oncol* (2013) 8(1):200. doi: 10.1186/1748-717X-8-200
- Schlamp I, Rieken S, Habermehl D, Bruckner T, Forster R, Debus J, et al. Stability of Spinal Bone Metastases in Breast Cancer After Radiotherapy: A Retrospective Analysis of 157 Cases. *Strahlenther Onkol* (2014) 190(9):792–7. doi: 10.1007/s00066-014-0651-z
- Schlamp I, Lang H, Forster R, Wolf R, Bostel T, Bruckner T, et al. Stability of Spinal Bone Metastases and Survival Analysis in Renal Cancer After Radiotherapy. *Tumori* (2015) 101(6):614–20. doi: 10.5301/tj.5000370
- Taneichi H, Kaneda K, Takeda N, Abumi K, Satoh S. Risk Factors and Probability of Vertebral Body Collapse in Metastases of the Thoracic and Lumbar Spine. *Spine (Phila Pa 1976)* (1997) 22(3):239–45. doi: 10.1097/00007632-199702010-00002
- Chow E, Hoskin P, Mitera G, Zeng L, Lutz S, Roos D, et al. Update of the International Consensus on Palliative Radiotherapy Endpoints for Future Clinical Trials in Bone Metastases. *Int J Radiat Oncol Biol Phys* (2012) 82(5):1730–7. doi: 10.1016/j.ijrobp.2011.02.008
- Sprave T, Hees K, Bruckner T, Foerster R, Bostel T, Schlamp I, et al. The Influence of Fractionated Radiotherapy on the Stability of Spinal Bone Metastases: A Retrospective Analysis From 1047 Cases. *Radiat Oncol* (2018) 13(1):134. doi: 10.1186/s13014-018-1082-2
- Koswig S, Budach V. Remineralization and Pain Relief in Bone Metastases After After Different Radiotherapy Fractions (10 Times 3 Gy vs. 1 Time 8 Gy). A Prospective Study. *Strahlenther Onkol* (1999) 175(10):500–8. doi: 10.1007/s000660050061
- Bollen L, Jacobs WCH, van der Linden YM, van der Hel O, Taal W, Dijkstra PDS. A Systematic Review of Prognostic Factors Predicting Survival in Patients With Spinal Bone Metastases. *Eur Spine J* (2018) 27(4):799–805. doi: 10.1007/s00586-017-5320-3
- Rades D, Haus R, Schild SE, Janssen S. Prognostic Factors and a New Scoring System for Survival of Patients Irradiated for Bone Metastases. *BMC Cancer* (2019) 19(1):1156. doi: 10.1186/s12885-019-6385-7
- Sahgal A, Atenafu EG, Chao S, Al-Omar A, Boehling N, Balagamwala EH, et al. Vertebral Compression Fracture After Spine Stereotactic Body Radiotherapy: A Multi-Institutional Analysis With a Focus on Radiation

- Dose and the Spinal Instability Neoplastic Score. *J Clin Oncol* (2013) 31 (27):3426–31. doi: 10.1200/JCO.2013.50.1411
23. Garg AK, Shiu AS, Yang J, Wang XS, Allen P, Brown BW, et al. Phase 1/2 Trial of Single-Session Stereotactic Body Radiotherapy for Previously Unirradiated Spinal Metastases. *Cancer* (2012) 118(20):5069–77. doi: 10.1002/cncr.27530
 24. Bostel T, Forster R, Schlampp I, Sprave T, Akbaba S, Wollschläger D, et al. Stability and Survival Analysis of Elderly Patients With Osteolytic Spinal Bone Metastases After Palliative Radiotherapy: Results From a Large Multicenter Cohort. *Strahlenther Onkol* (2019) 195(12):1074–85. doi: 10.1007/s00066-019-01482-1
 25. Steenland E, Leer JW, van Houwelingen H, Post WJ, van den Hout WB, Kievit J, et al. The Effect of a Single Fraction Compared to Multiple Fractions on Painful Bone Metastases: A Global Analysis of the Dutch Bone Metastasis Study. *Radiother Oncol* (1999) 52(2):101–9. doi: 10.1016/S0167-8140(99)00110-3
 26. Hartsell WF, Scott CB, Bruner DW, Scarantino CW, Ivker RA, Roach M3rd, et al. Randomized Trial of Short- Versus Long-Course Radiotherapy for Palliation of Painful Bone Metastases. *J Natl Cancer Inst* (2005) 97(11):798–804. doi: 10.1093/jnci/dji139
 27. Chow E, Harris K, Fan G, Tsao M, Sze WM. Palliative Radiotherapy Trials for Bone Metastases: A Systematic Review. *J Clin Oncol* (2007) 25(11):1423–36. doi: 10.1200/JCO.2006.09.5281
 28. Chow E, Zeng L, Salvo N, Dennis K, Tsao M, Lutz S. Update on the Systematic Review of Palliative Radiotherapy Trials for Bone Metastases. *Clin Oncol (R Coll Radiol)* (2012) 24(2):112–24. doi: 10.1016/j.clon.2011.11.004

Conflict of Interest: The authors declare that the research was conducted in the absence of any commercial or financial relationships that could be construed as a potential conflict of interest.

Publisher's Note: All claims expressed in this article are solely those of the authors and do not necessarily represent those of their affiliated organizations, or those of the publisher, the editors and the reviewers. Any product that may be evaluated in this article, or claim that may be made by its manufacturer, is not guaranteed or endorsed by the publisher.

Copyright © 2021 Bostel, Akbaba, Wollschläger, Klodt, Oebel, Mayer, Drabke, Sprave, Debus, Förster, Rief, Rühle, Grosu, Schmidberger and Nicolay. This is an open-access article distributed under the terms of the Creative Commons Attribution License (CC BY). The use, distribution or reproduction in other forums is permitted, provided the original author(s) and the copyright owner(s) are credited and that the original publication in this journal is cited, in accordance with accepted academic practice. No use, distribution or reproduction is permitted which does not comply with these terms.



Clinical Studies on Ultrafractionated Chemoradiation: A Systematic Review

Erica Scirocco^{1,2*}, Francesco Cellini^{3,4}, Alice Zamagni^{1,2}, Gabriella Macchia⁵,
Francesco Deodato⁵, Savino Cilla⁶, Lidia Strigari⁷, Milly Buwenge², Stefania Rizzo⁸,
Silvia Cammelli^{1,2†} and Alessio Giuseppe Morganti^{1,2†}

¹ Radiation Oncology, Istituto di Ricovero e Cura a Carattere Scientifico (IRCCS) Azienda Ospedaliero-Universitaria di Bologna, Bologna, Italy, ² Department of Experimental, Diagnostic and Specialty Medicine—Alma Mater Studiorum Bologna University, Bologna, Italy, ³ Università Cattolica del Sacro Cuore, Dipartimento Universitario Diagnostica per immagini, Radioterapia Oncologica ed Ematologia, Roma, Italy, ⁴ Fondazione Policlinico Universitario “A. Gemelli” Istituto di Ricovero e Cura a Carattere Scientifico (IRCCS), Dipartimento di Diagnostica per Immagini, Radioterapia Oncologica ed Ematologia, Roma, Italy, ⁵ Radiotherapy Unit, Gemelli Molise Hospital, Catholic University of Sacred Heart, Campobasso, Italy, ⁶ Medical Physic Unit, Gemelli Molise Hospital, Catholic University of Sacred Heart, Campobasso, Italy, ⁷ Medical Physics Unit, Istituto di Ricovero e Cura a Carattere Scientifico (IRCCS) Azienda Ospedaliero-Universitaria di Bologna, Bologna, Italy, ⁸ Service of Radiology, Imaging Institute of Southern Switzerland, Ente Ospedaliero Cantonale (EOC), Lugano, Switzerland

OPEN ACCESS

Edited by:

Alessio Bruni,
University Hospital of Modena, Italy

Reviewed by:

Elvira V. Grigorieva,
Institute of Molecular Biology and
Biophysics (RAS), Russia
Andra Valentina Krauze,
National Cancer Institute,
United States

*Correspondence:

Erica Scirocco
erica.scirocco@studio.unibo.it

[†]These authors share senior
authorship

Specialty section:

This article was submitted to
Radiation Oncology,
a section of the journal
Frontiers in Oncology

Received: 27 July 2021

Accepted: 25 October 2021

Published: 16 November 2021

Citation:

Scirocco E, Cellini F, Zamagni A,
Macchia G, Deodato F, Cilla S,
Strigari L, Buwenge M, Rizzo S,
Cammelli S and Morganti AG
(2021) Clinical Studies on
Ultrafractionated Chemoradiation:
A Systematic Review.
Front. Oncol. 11:748200.
doi: 10.3389/fonc.2021.748200

Aim: The efficacy of low-dose fractionated radiotherapy (LDFRT) and chemotherapy (CHT) combination has large preclinical but little clinical evidence. Therefore, the aim of this review was to collect and analyze the clinical results of LDRT plus concurrent CHT in patients with advanced cancers.

Methods: A systematic literature search was conducted on PubMed using the PRISMA methodology. Only studies based on the combination of LDFRT (< 1 Gy/fraction) and CHT were included. Endpoints of the analysis were tumor response, toxicity, and overall survival, with particular focus on any differences between LDFRT-CHT and CHT alone.

Results: Twelve studies (307 patients) fulfilled the selection criteria and were included in this review. Two studies were retrospective, one was a prospective pilot trial, six were phase II studies, two were phase I trials, and one was a phase I/II open label study. No randomized controlled trials were found. Seven out of eight studies comparing clinical response showed higher rates after LDFRT-CHT compared to CHT alone. Three out of four studies comparing survival reported improved results after combined treatment. Three studies compared toxicity of CHT and LDFRT plus CHT, and all of them reported similar adverse events rates. In most cases, toxicity was manageable with only three likely LDFRT-unrelated fatal events (1%), all recorded in the same series on LDFRT plus temozolomide in glioblastoma multiforme patients.

Conclusion: None of the analyzed studies provided level I evidence on the clinical impact of LDFRT plus CHT. However, it should be noted that, apart from two small series of breast cancers, all studies reported improved therapeutic outcomes and similar tolerability compared to CHT alone.

Systematic Review Registration: www.crd.york.ac.uk/prospero/, identifier CRD42020206639.

Keywords: chemo-sensitization, low-dose radiotherapy, systematic review, clinical trials, combined modality treatment

INTRODUCTION

Conventionally fractionated curative radiotherapy (RT) is delivered in 1.8–2.0 Gy daily fractions. Conversely, low-dose fractionated RT (LDFRT) is defined as the use of very small dose per fraction (< 1.0 Gy). In some experimental models, LDFRT resulted more effective than predicted by the linear quadratic model in terms of improved cell kill (1, 2). In particular, *in vitro* experiments showed this phenomenon in several cell lines (3–5). Interestingly, the higher efficacy of LDFRT was confirmed in human cells by several laboratories using different assay techniques, conditions of cell growth, handling, and irradiation (1). On the contrary, a relative tumor cell radiation resistance was recorded when higher doses per fraction were used (6). The low-dose hyper-radiation sensitivity (HRS) phenomenon has been interpreted on the basis of a threshold effect in radiation-induced damage repair. In fact, DNA-repair mechanisms are triggered only above certain dose levels, while lower doses are ineffective in arresting irradiated cells in the G2 cell-cycle phase (7, 8).

The peculiar efficacy of LDFRT has been interpreted also on the basis of immunological mechanisms. For example, Klug and colleagues (9) reported that local LDFRT produces efficient recruitment of tumor-specific T cells in human pancreatic carcinomas with T-cell-mediated tumor rejection and prolonged survival in otherwise immune refractory spontaneous and xenotransplant mouse tumor models. The authors used one single fraction with doses ranging between 0.5 and 6.0 Gy. They observed that the number of intratumoral T lymphocytes was higher after irradiation with the lowest dose (0.5 Gy) (9). Based on this preclinical evidence, LDFRT was tested also in a clinical study (10).

Concurrent chemoradiation is a standard treatment option in several tumors since CHT is able to act as a radiosensitizer. Interestingly, when delivered as LDFRT, also RT may act as a chemosensitizer. This peculiar synergistic effect of LDFRT and CHT was demonstrated by several preclinical studies, in different cell lines, and using different drugs such as cisplatin, carboplatin, docetaxel, and paclitaxel (11–15). It is worth noting that LDFRT-induced toxicity is significantly lower compared to conventional fractionation or hypofractionation. This higher tolerability allows LDFRT to be associated with “full-dose” CHT, with a clear benefit in terms not only of local response but also of systemic tumor control (16).

Considering these aspects, interest in the combination of LDFRT with CHT in the clinical management of cancer patients grew. LDFRT was proposed as a new systemic agent labeled with an “r” (e.g., gemcitabine plus LDFRT: rG) (17). Although some preliminary studies suggested the effectiveness of this combination (16, 17), randomized trials, meta-analyses, and

systematic reviews on this topic are lacking. Therefore, the aim of this review was to collect and analyze the results of LDFRT plus CHT, currently available in literature, in terms of tumor response, clinical outcomes, and treatment tolerability.

METHODS AND MATERIALS

Our systematic review protocol was registered (registration number: CRD42020206639) within the International Prospective Register of Systematic Reviews (PROSPERO, www.crd.york.ac.uk/prospero/) on 31 August 2020.

Inclusion Criteria

Human studies of any design, without limitations in terms of the number of enrolled patients, and based on LDFRT plus CHT combination, were included. Studies based on LDFRT without concurrent CHT were excluded. No restriction about total delivered dose, biological effective dose (BED), and RT technique was imposed.

Outcome Measures

We reported the main findings of the analyzed papers with particular focus on clinical tumor response, overall survival, and treatment-related toxicity. Moreover, any differences between LDFRT-CHT and CHT alone were recorded and reported.

Bibliographic Search

We conducted a search based on PubMed from the earliest date to 20 May 2020. In our review, we considered only studies published in the English language. We used various combinations of the subsequent terms in PubMed such as low-dose, radiotherapy, ultra-fractionation, hyper-radiation-sensitivity, chemosensitization, concurrent, and chemotherapy. Finally, the following two search strategies were used in PubMed: i) low-dose[All Fields] AND (“radiotherapy”[Subheading] OR “radiotherapy”[All Fields] OR “radiotherapy”[MeSH Terms]) AND concurrent[All Fields] AND (“drug therapy”[Subheading] OR (“drug”[All Fields] AND “therapy”[All Fields]) OR “drug therapy”[All Fields] OR “chemotherapy”[All Fields] OR “drug therapy”[MeSH Terms] OR (“drug”[All Fields] AND “therapy”[All Fields]) OR “chemotherapy”[All Fields]); and ii) “hyper radiation sensitivity” OR (“ultrafractionation” OR “ultrafractionated”) AND (“radiotherapy” OR “irradiation” OR “radiation”) OR (“chemosensitization” AND (“radiotherapy” OR “irradiation” OR “radiation”)). We found 396 studies with the first strategy and 253 with the second one. We removed duplicates, and we made the first selection based on titles and abstracts. Moreover, a further search through the references of the selected studies was performed. After

reading the full-text articles, six studies were excluded: three used the term “ultrafractionation” or “low-dose RT,” but the delivered dose/fraction was ≥ 1 Gy; two studies did not use LDFRT plus CHT combination, and one study reported duplicated patients. Finally, 12 articles fulfilled our criteria (16–27).

Study Selection and Quality Assessment

We used the PRISMA guidelines as a guide to select the items to be included within the review (28, 29). Title, abstract, and keywords of the identified articles were independently analyzed by two researchers (ES, AZ), and disagreements were solved by the senior author (AM). Potentially eligible studies were retrieved, and full-text evaluation was performed based on the inclusion and exclusion criteria by two different authors (ES, AZ) with disagreements resolved by consensus-based discussion. Subsequently, the following data were collected independently by two authors (ES, MB) from each article, with disagreements resolved by the senior author (AM): authors' name and year of publication, study design, accrual period, patients and setting, treatment (LDFRT and CHT), and main outcomes. Papers were evaluated based on the ROBINS-I Risk of Bias tool (30). Two reviewers (ES, AZ) assessed the quality of the included studies, and discrepancies were resolved on agreement.

RESULTS

Search Results

Twelve articles (16–27) including 307 patients fulfilled the inclusion criteria for this review. Accrual period of all the studies ranged from 2000 to 2014. Details on the analyzed studies are reported in **Table 1**, while the flowchart of the literature search process is shown in **Figure 1**.

Study Design and Risk of Bias

Two studies were retrospective (22, 26), one was a prospective pilot trial (18), six were phase II studies (16, 19, 21, 23, 25, 27), two were phase I trials (20, 24), and one was a phase I/II open label study (17). No randomized controlled trials were found. All were considered to own moderate to serious risk of bias according to the ROBINS-I tool (30). **Appendix 1** shows the risk of bias rating per study based on the ROBINS-I tool.

Analysis of the Selected Studies

Treated Tumors

The characteristics and stage of primary tumors in the analyzed papers are shown in **Table 1**.

Patients and Treatment

Patients' median age ranged from 21 to 84 years (median 57.6) (16–18, 20, 22–26). Median follow-up ranged from 6.5 to 48 months (median: 22.5 months). The RT total dose ranged from 1.6 to 67.5 Gy. CHT was based on different schedules depending

on tumor features. RT details and CHT schedules are shown in **Table 1**.

Evaluations

Response was reported in different ways in all the studies (16–27), while overall survival (OS) rates were reported in six studies (18, 19, 21–23, 27). Toxicity was reported in 11 studies (16–21, 23–27), mainly using the Common Toxicity Criteria for Adverse Events scale (31).

Treatment Results

Toxicity results are shown in **Table 2**. In most studies, the treatment was reasonably tolerated, despite obvious differences due to the different used CHT regimens (16–21, 23–27). In the phase II trial conducted by Beauchesne et al. (19) on LDFRT plus temozolomide in glioblastoma multiforme (GBM), three cases of fatal adverse events were reported: one due to hematological toxicity and two due to pulmonary infections. Moreover, Regine and colleagues (17), in their trial on gemcitabine plus LDFRT in pancreatic and small bowel cancers, reported one grade 3 infection out of six patients treated with 0.6 Gy/fraction and one grade 3 infection and one grade 3 diarrhea out of four patients treated with 0.7 Gy/fraction. **Table 3** reports details on tumor response and outcome. The results are very inhomogeneous as expected considering the different treated tumors and clinical settings.

Comparisons

Among all the studies included in our review, only Morganti and colleagues compared irradiated (LDFRT) and non-irradiated sites in patients with metastatic colorectal cancer treated with FOLFIRI-Bevacizumab (23). The authors reported 83.4% and 33.3% overall response rate (ORR) in irradiated and non-irradiated metastases, respectively (p : 0.02). Moreover, the 2-year progression rate was 63.9% and 31.2% in irradiated and non-irradiated sites, respectively (p : 0.08) (23). In other publications, the results of LDFRT-CHT were compared to those of CHT alone as reported in other studies (**Table 4**) (16–22, 24–27).

DISCUSSION

To the best of our knowledge, this is the first review of clinical studies on combined LDFRT plus CHT. Five studies compared clinical response rates after LDFRT-CHT with literature data on CHT in similar patients, reporting higher ORR rates (16, 21, 23, 26, 27). Similarly, four studies compared OS after LDFRT-CHT and reported improved outcome compared to CHT alone (17, 19, 20, 22). Finally, four studies compared toxicity after LDFRT plus CHT versus CHT alone reporting similar adverse event rates (16, 21, 24, 25). Interestingly, clinical findings regarding LDFRT-CHT were published in 12 studies between 2004 and 2017, and no further studies were published thereafter. The lack of prospective studies, moreover with no control groups, could explain the disinterest in this combined modality therapy.

TABLE 1 | Studies characteristics.

Study	Study design	No of patients	Median FUP	Setting	Treatment	
					Radiotherapy total dose (dose per fraction)	Chemotherapy
Arnold 2004 (16)	Phase II	40	18	Locally advanced SCCHN	3.2 Gy/4 fx (0.8 Gy, days: 1, 2, 22, 23)	Paclitaxel 225 mg/m ² i.v. (days 1, 22) + Carboplatin 10 mg/ml (within 30 min after Paclitaxel)
Regine 2007 (17)	Phase I/II	10	NR	Unresectable (5) or M1 pancreatic (liver) (4) or unresectable small bowel ca (1)	2 dose levels: 0.6 and 0.7 Gy/fx, BID, days: 1, 2, 8, 9. Four cycles planned	Gem 1,250 mg/m ² days: 1 and 8 at 10 mg/m ² /min of a 3-week cycle
Valentini 2010 (26)	Retrospect.	22	6.5	Relapsed or metastatic ca of lung (12), H&N (7), breast (2); esophagus (1)	0.4 Gy BID repeated over 2 (lung, breast, and esophagus) or 4 (H&N) consecutive days, depending on the CHT schedule. Median total dose 8 Gy (range, 3.2–12.8 Gy).	Gem (1) or Cisplatin+Gem (1) or Pemetrexed (8) or Carboplatin (2) or Cisplatin+Fluorouracil (7) or Capecitabine (1) or Fluorouracil (1) or Docetaxel (1)
Mantini 2012 (21)	Phase II	19	6.5	Advanced NSCLC	1.6 Gy (0.4 Gy BID, days 1,2)	Concurrent Pemetrexed 500 mg/m ² IV (cycles repeated fourfold every 21 days)
Nardone 2012 (24)	Phase I	10	NR	Breast cancer stage IIA/B-IIIa	0.4 Gy BID for 2 days every 21 days for 8–6 cycles	2 CHT schedules: 1) 4 cycles of nonpegylated liposomal doxorubicin sequentially followed by 4 cycles of docetaxel; 2) 6 cycles of nonpegylated liposomal doxorubicin + concurrent docetaxel
Nardone 2014 (25)	Phase II	21	31	Breast cancer stage IIA-IIIa	0.4 Gy BID, days: 1, 2, 6 of every cycle. First RT fraction delivered before CHT, the second fraction given at least 5–6 h later; cycle repeated every 21 days; total dose: 9.6 Gy (6 cycles)	6 cycles of liposomal anthracycline (50 mg/mq) and docetaxel (75 mg/mq) on day 1 of a 21-day cycle; cycle repeated every 21 days
Konski 2014 (20)	Phase I	27	8.4	Locally advanced or metastatic pancreatic cancer	3 RT dose level: 1) 28.8 Gy (0.4 Gy BID); 2) 28 Gy (0.5 Gy BID); 3) 28.8 Gy (0.6 Gy BID) days 1,2,8,9	Gem IV days 1, 8 + Erlotinib once PO (21 day cycles)
Balducci 2014 (18)	Prospective	32	22.5	Recurrent/progressive GBM	Two schedules: 1) 0.3 Gy BID, days: 1, 2, 8, 9, 15, 16, every 42 days (2 cycles: total dose of 7.2 Gy); 2) 0.4 Gy BID over 5 consecutive days, every 28 days (2 cycles: total dose of 8 Gy)	Two schedules: 1) Cisplatin (30 mg/m ² on days 1, 8, 15) + Ftemustine (40 mg/m ² on days 2,9,16) if recurrent or progressive disease during adjuvant TMZ, on days 1, 2, 8, 9, 15, and 16, every 42 days; 2) TMZ rechallenged (150/200 mg/m ²) if recurrent or progressive disease more than 4 months after adjuvant TMZ, over 5 consecutive days, every 28 days
Beauchesne 2015 (19)	Phase II	40	48	Newly diagnosed inoperable GBM	67.5 Gy/90 fx (0.75 Gy each 3 daily doses, at least a 4-h interfraction interval; 5 days a week)	Concurrent TMZ (dose of 75 mg/m ² for 7 days a week). At the end of a 4-week break, CHT was resumed for up to 6 cycles of adjuvant TMZ treatment, every 28 days according to the standard 5-day regimen.
Das 2015 (27)	Phase II	24	30	Locally advanced SCC of the cervix (stage IIB–IIIB)	3.2 Gy/4fx (0.8 Gy BID)	Paclitaxel (175 mg/m ²) + Carboplatin (AUC X 5) 3 weekly for 2 cycles followed by radical chemoradiation
Morganti 2016 (23)	Phase II	18	30	Metastatic colorectal cancer	2.4 Gy (0.2 Gy BID, days: 1, 2 of every cycle)	12 FOLFIRI-B cycles (bevacizumab, irinotecan, bolus fluorouracil, and leucovorin with a 46-h infusion of fluorouracil, every 2 weeks)
Mattoli 2017 (22)	Retrospect.	44	NR	NSCLC (stage IIIA-IIIb)	100% patients: induction CHT + 0.4 Gy BID (days: 1,2 and 8,9 every cycle); 45% surgery; 59% neo-adjuvant CHT-RT (50.4Gy)	100% patients: 2 cycles of concurrent Platinum; 59% neo-adjuvant CHT+RT

FUP, follow-up; RT, radiotherapy; CHT, chemotherapy; SCCHN, squamous cell carcinoma of the head and neck; SCC, squamous cell carcinoma; RR, response rate; CR, complete response; PR, partial response; PFS, progression free survival; BID, bis in die; NRC, neoadjuvant radiochemotherapy; NAC, conventional neoadjuvant chemotherapy; PO, per oral; PMRR, pathological major response rate; TRG, tumor regression grade; GBM: glioblastoma multiforme, TMZ, temozolomide; Gem, gemcitabine.

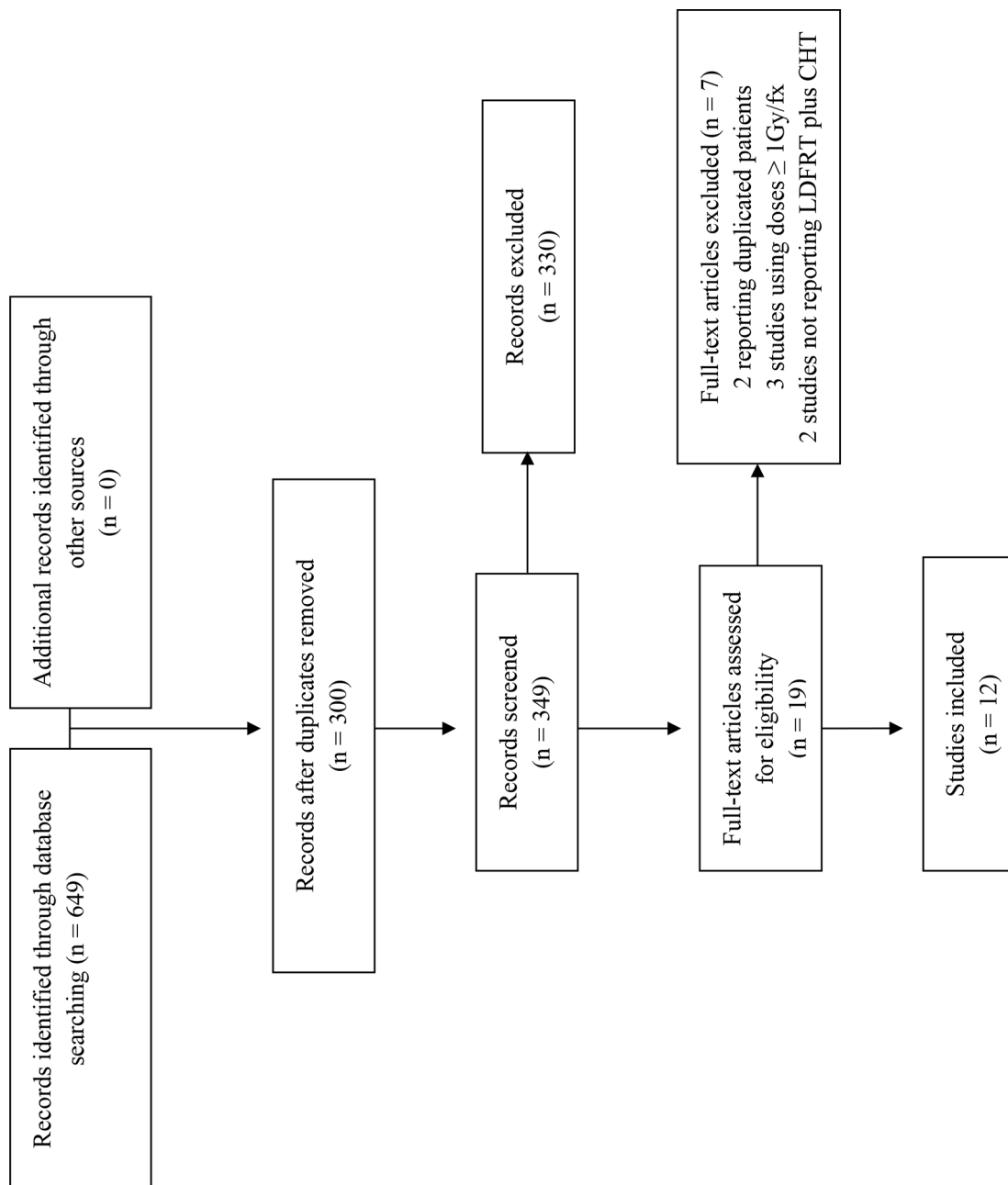
**FIGURE 1** | Process of paper selection.

TABLE 2 | Toxicity.

Study	Main findings
Arnold et al., 2004 (16)	Grade 3,4 toxicities: neutropenia (50%), infection (8%), dermatologic reactions (8%), allergic reactions (3%), pulmonary reactions (3%), myalgia (3%). No grade 5 toxicity. Toxicity profile similar to CHT alone
Regine et al., 2007 (17)	1/6 experienced DLT at dose level 1 (0.6 Gy/fx): grade 3 infection; 2/4 experienced DLT at dose level 2 (0.7 Gy/fx): grade 3 nonhematologic infection and grade 3 diarrhea
Valentini et al., 2010 (26)	Grade 3–4 hematologic toxicities (9%); at a median follow-up of 6.5 months no local toxicity observed
Mantini et al., 2012 (21)	Neutropenia grade 4 (1 patient: 5.2%), already experienced during the prior CHT regimen (cisplatin and gemcitabine). Toxicity profile similar to CHT alone
Nardone et al., 2012 (24)	No grade 3, 4 toxicities. Toxicity profile similar to CHT alone
Nardone et al., 2014 (25)	No grade 2–4 hematological toxicities; no cardiac events
Konski et al., 2014 (20)	Very little > grade 3 toxicity; in cycle 4, one grade 5 bowel perforation in dose level 1 in one patient (3.7%) with a very large tumor with invasion of the duodenum; grade 3 ileus in the first cycle of therapy with dose level 1 in 1 patient (3.7%)
Balducci et al., 2014 (18)	Toxicities reversible without treatment-related death. Grade 2 fatigue (37.5%), grade 2 alopecia (50%), grade 1 skin reaction (9.3%), grade 1 headache (3.1%). Hematological toxicity (28.1%), with grade 1, 2 and 3, 4 in 18.7% and 9.4%, respectively. No late toxicity observed in retreated patients. LDFRT + CHT showed better toxicity profile when compared to the same group of patients treated with the different approaches available in this setting (re-resection, re-irradiation, different chemotherapy schedules)
Beauchesne et al., 2015 (19)	Fatal grade 4 hematological toxicity (2.5%), fatal pulmonary infection (5%)
Das et al., 2015 (27)	Grade 3, 4 hematological toxicity (24%)
Morganti et al., 2016 (23)	Grade 3, 4 toxicities 11.1%
Mattoli et al., 2017 (22)	Toxicity NR

RT, radiotherapy; LDFRT, low-dose fraction radiotherapy; CHT, chemotherapy; DLT, dose-limiting toxicity; NR, not reported.

However, in most cases, the analyzed studies included only patients undergoing LDFRT plus CHT, without direct comparisons with patients undergoing CHT alone. In fact, differences were almost always tested against CHT results from other published studies.

Arnold et al. (16) reported higher ORR (90%), in advanced head and neck squamous cell carcinoma treated with LDFRT plus CHT, compared to literature data (55–75%) on similar patients treated with the same drug combination (carboplatin plus paclitaxel) (32–35). Regine et al. (17) reported prolonged OS after LDFRT plus gemcitabine, in locally advanced pancreatic adenocarcinoma, compared to literature data (36, 37) on gemcitabine alone (median OS: 11 months versus 4.8–5.6 months, respectively). Konski et al. (20) reported on locally advanced pancreatic cancer, with or without small burden metastatic disease, recording improved OS after LDFRT plus erlotinib and gemcitabine (9.1 months) compared to a study on erlotinib and gemcitabine alone (6.2 months) (38). Mattoli et al. (22) reported prolonged median OS in stage IIIA–IIIB non-small cell lung cancer treated with LDFRT plus concurrent induction CHT compared to another study (39) based on induction CHT alone in a similar patient population (median OS: 51 months versus 12.5 months, respectively). Beauchesne et al. published the results of their phase II trial (19) on inoperable GBM treated with LDFRT plus temozolomide reporting 16 months median OS. Surprisingly, this result is at least comparable with the outcome

(median OS: 14.6 months) recorded in the EORTC/NCIC trial after standard RT plus temozolomide in patients with resected disease (40). Mantini et al. (21) reported 42% ORR and 17 months median OS in stage III–IV non-small cell lung cancer treated with LDFRT plus concurrent pemetrexed. These results were better compared to 9.1% ORR and 8.3 months median OS recorded in a similar patient population treated with pemetrexed alone (41). Valentini et al. (26) reported higher response rates in patients with lung (ORR: 41.6%) and head and neck cancer (ORR: 57%) treated with LDFRT–CHT compared to literature data on lung (ORR: 5–10%) (42, 43) and head and neck tumors (ORR: 10–35%) (44–47) treated with CHT alone (similar regimens). Das et al. (27) reported 100% ORR and 100% 2-year OS in locally advanced carcinoma of the uterine cervix treated with LDFRT plus induction CHT followed by radical chemoradiation. These figures were higher compared to the ones registered in a similar patient population treated with the same CHT induction regimen followed by standard chemoradiation (48). Only two studies did not show improved results after LDFRT plus CHT compared to CHT alone. In fact, Nardone et al. (24, 25) treated stage IIA/B–IIIA breast cancer patients with LDFRT plus CHT and reported similar response rates compared to CHT alone. However, it should be noted that the sample size of these studies was particularly small, with only 10 (24) and 21 patients (25) enrolled, respectively.

TABLE 3 | Response and outcome.

Study	Main findings
Arnold et al., 2004 (16)	ORR: 82% (assessed radiographically); RR: 90% at the primary site; RR: 69% at nodal site
Regine et al., 2007 (17)	ORR 30% (assessed radiographically); median OS 11 months (range: 4–37 months)
Valentini et al., 2010 (26)	ORR 45% (42% in previously treated patients); ORR of 57.1% and 41.6% in HN and lung cancer, respectively; with a median follow-up of 6.5 months no local toxicity observed
Mantini et al., 2012 (21)	ORR 42%; median OS 17 months. RR and median OS higher than CHT alone.
Nardone et al., 2012 (24)	50% clinical CR; TRG 1 (absence of residual cancer) 10%; TRG 2 (residual isolated cells scattered through fibrosis) 40%; PMRR 20% with LDFRT + sequential CHT and 40% with LDFRT + concurrent CHT
Nardone et al., 2014 (25)	PMRR: 33.3%; TRG1: 14.3%; TRG2: 19%
Konski et al., 2014 (20)	PR (30%), stable (55.5%), PD (3.7%); median OS 9.1 months
Balducci et al., 2014 (18)	CR 3.1%, PR 9.4%, stable disease 25% for at least 8 weeks after the end of treatment, 62.5% PD. Clinical benefit 37.5%. Median PFS and OS 5 and 8 months. Survival rate at 12 months 27.8%
Beauchesne et al., 2015 (19)	2y-OS 32.4%; 3-y OS 17.2%; median PFS 9.6 months; CR (10%); PR (17.5%). No improved OS (9.53 months) compared to unresectable GBM reported in literature
Das et al., 2015 (27)	OS and PFS at 2.5 years 84%. ORR (100% with 40% CR and 60% PR, based on MRI findings) and 3y-OS (80%)
Morganti et al., 2016 (23)	38.9% clinical or pathological CR; median OS 38 months; 2y PFS: 63.9 and 31.2% and ORR: 83.3% and 33.3% in irradiated and not irradiated lesions, respectively
Mattoli et al., 2017 (22)	Response assessed by ¹⁸ F-FDG PET-CT; at early PET-CT, 47.6% responders. At final PET-CT, 83% responders, 17.4% nonresponders (all nonresponders at early PET-CT). Early responders had higher PFS and OS than early nonresponders. Locoregional recurrence < 30%; 2-y OS rate was 59%; median OS 51 months

RT, radiotherapy; CHT, chemotherapy; LDFRT, low-dose fraction radiotherapy; ORR, response rate; CR, complete response; PR, partial response; PD, progression disease; PFS, progression-free survival; RECIST, response evaluation criteria in solid tumors; BID, bis in die (twice daily); GBM, glioblastoma multiforme; NRC, neoadjuvant radiochemotherapy; NAC, conventional neoadjuvant chemotherapy; PO, per oral; PMRR, pathological major response rate; TRG, tumor regression grade; HN, head and neck; ¹⁸F-FDG PET-CT, [18F]Fluoro-2-Deoxy-d-Glucose positron emission tomography/computed tomography.

In terms of toxicity, Arnold et al. (16), Nardone et al. (24, 25), and Mantini et al. (21) reported similar toxicity profile in patients treated with LDFRT plus CHT compared to studies on CHT alone. Moreover, Balducci et al. (18) reported lower toxicity rates with LDFRT plus CHT compared to similar patient groups with recurrent GBM (49, 50) treated with several different approaches (second-line CHT, re-irradiation, re-resection). The worse complications recorded in the analyzed papers were reported in Beauchesne et al.'s (19) and Regine et al.'s studies (17). The first series included GBM patients treated with LDFRT plus temozolomide. Three cases of fatal adverse events were recorded: one after severe hematological toxicity and two due to pulmonary infections (19). It should be noted that these complications are not uncommon in patients treated with temozolomide alone. In particular, pneumonitis can occur when prophylactic treatment against pneumocystis carinii infections is not prescribed. In the second study, based on LDFRT plus gemcitabine in pancreatic and small bowel cancers, two grade 3 infections and one grade 3 diarrhea were reported (17). The irradiation of the entire upper abdomen could almost partially explain these adverse events.

A comparison within the same study between LDFRT-CHT and CHT was reported only by Morganti et al. As previously described, after CHT based on the FOLFIRI-bevacizumab regimen, the ORR

rate was 83.4% in metastatic lesions undergoing LDFRT and 33.3% in non-irradiated lesions (p: 0.02) (23).

This review has several limitations including lack of randomized trials, heterogeneity of the study design with inclusion of two retrospective studies (22, 26), small sample size with a median number of 23 patients per study (range: 6–44) and four studies with less than 20 patients, and heterogeneity in terms of tumor and treatment characteristics. More specifically, the outcome results reported in two phase I (24) and phase I/II (17) trials, each enrolling only 10 patients, must be interpreted with caution due to the very small sample size. The usefulness of a literature review with these limitations could be debatable. However, due to lack of evidence from large prospective trials, we considered it useful to review the available data. Furthermore, it should be emphasized the uniformity between the analyzed series in terms of results, since all studies reported better outcomes after LDFRT-CHT compared to CHT alone, apart from two small studies on breast cancer (24, 25).

Based on the low level of evidence of the selected studies, the use of LDFRT-CHT in current clinical practice does not seem justified. However, especially in advanced cancers resistant to systemic therapies, enrollment of patients in prospective studies would be useful.

TABLE 4 | Comparisons with chemotherapy alone.

Study	Main findings
Arnold et al., 2004 (16)	LDFRT + CHT well tolerated with higher RR delivering less CHT cycles compared to CHT alone. Toxicity profile similar to CHT alone
Regine et al., 2007 (17)	RR and survival rates higher than CHT alone
Valentini et al., 2010 (26)	ORR higher than CHT alone seen in different settings
Mantini et al., 2012 (21)	RR and median OS higher than CHT alone. Toxicity profile similar to CHT alone
Nardone et al., 2012 (24)	Toxicity profile similar to CHT alone
Nardone et al., 2014 (25)	PMRR was 33.3%, similar to CHT alone
Konski et al., 2014 (20)	Efficacy results compared to CHT alone (median OS of metastatic patients around 6 months in locally advanced disease with gemcitabine alone versus 9.1 months with LDFRT + CHT)
Balducci et al., 2014 (18)	LDFRT + CHT showed a very low toxicity profile when compared to the same group of patients treated with different approaches (36)
Beauchesne et al., 2015 (19)	Median OS of 16 months higher than OS rates reported in EORTC/NCIC trial (conventional RT + CHT versus conventional RT alone)
Das et al., 2015 (27)	ORR (100% with 40% CR and 60% PR, based on MRI findings) and 3y-OS (80%) with LDFRT + CHT followed by CHT + RT versus RR (70%) and 3y-OS (68%) with CHT + RT (the latter treatment scheme done with more CHT cycles). Lower toxicity grade with LDFRT+CHT followed by CHT + RT compared to treatment scheme using CHT+RT (the latter done with higher cycles of CHT)
Morganti et al., 2016 (23)	2y PFS: 63.9 and 31.2%, ORR: 83.3% and 33.3% in irradiated and not irradiated lesions, respectively
Mattoli et al., 2017 (22)	Median OS higher than CHT alone

RT, radiotherapy; CHT, chemotherapy; SCCHN, advanced squamous cell carcinoma of the head and neck; HN, head and neck; ORR, response rate; CR, complete response; PR, partial response; PD, progression disease; PFS, progression free survival; RECIST, response evaluation criteria in solid tumors; BID, bis in die (twice daily); NRC, neoadjuvant radiochemotherapy; NAC, conventional neoadjuvant chemotherapy; PO, per oral; PMRR, pathological major response rate; TRG, tumor regression grade; DLT, dose-limiting toxicity.

Further studies in this field could have the following design or aims: (i) randomized comparison between LDFRT-CHT versus CHT alone; (ii) definition of the optimal dose and fractionation in LDFRT-CHT; (iii) definition of the optimal CHT regimens in this setting; and (iv) evaluation of LDFRT plus immunotherapy combination, given some evidence on the immune-enhancement effect of LDFRT (51).

DATA AVAILABILITY STATEMENT

The original contributions presented in the study are included in the article/**Supplementary Material**. Further inquiries can be directed to the corresponding author.

REFERENCES

- Joiner MC, Marples B, Lambin P, Short SC, Turesson I. Low-Dose Hypersensitivity: Current Status and Possible Mechanisms. *Int J Radiat Oncol Biol Phys* (2001) 49(2):379–89. doi: 10.1016/s0360-3016(00)01471-1
- Lambin P, Marples B, Fertl B, Malaise EP, Joiner MC. Hypersensitivity of a Human Tumour Cell Line to Very Low Radiation Doses. *Int J Radiat Biol* (1993) 63(5):639–50. doi: 10.1080/09553009314450831
- Joiner MC. Induced Radioresistance: An Overview and Historical Perspective. *Int J Radiat Biol* (1994) 65(1):79–84. doi: 10.1080/09553009414550111
- Wouters BG, Sy AM, Skarsgard LD. Low-Dose Hypersensitivity and Increased Radioresistance in a Panel of Human Tumor Cell Lines With Different Radiosensitivity. *Radiat Res* (1996) 146(4):399–413. doi: 10.2307/3579302
- Marples B, Lambin P, Skov KA, Joiner MC. Low Dose Hyper-Radiosensitivity and Increased Radioresistance in Mammalian Cells. *Int J Radiat Biol* (1997) 71(6):721–35. doi: 10.1080/095530097143725

AUTHOR CONTRIBUTIONS

Conception and design: ES, FC, AZ, and AM. Data extraction from included studies: ES, FC, GM, FD, and AGM. Analysis and interpretation of data: ES, FD, SCi, LS, MB, SR, SCa, and AM. Manuscript writing: all authors. All authors contributed to the article and approved the submitted version.

SUPPLEMENTARY MATERIAL

The Supplementary Material for this article can be found online at: <https://www.frontiersin.org/articles/10.3389/fonc.2021.748200/full#supplementary-material>

6. Lambin P, Malaise EP, Joiner MC. Might Intrinsic Radioresistance of Human Tumour Cells be Induced by Radiation? *Int J Radiat Biol* (1996) 69(3):279–90. doi: 10.1080/095530096145832
7. Marples B, Wouters BG, Joiner MC. An Association Between the Radiation-Induced Arrest of G2-Phase Cells and Low-Dose Hyper-Radiosensitivity: A Plausible Underlying Mechanism? *Radiat Res* (2003) 160(1):38–45. doi: 10.1667/rr3103
8. Marples B, Wouters BG, Collis SJ, Chalmers AJ, Joiner MC. Low-Dose Hyper-Radiosensitivity: A Consequence of Ineffective Cell Cycle Arrest of Radiation-Damaged G2-Phase Cells. *Radiat Res* (2004) 161(3):247–55. doi: 10.1667/rr3130
9. Klug F, Prakash H, Huber PE, Seibel T, Bender N, Halama N, et al. Low-Dose Irradiation Programs Macrophage Differentiation to an iNOS/M1 Phenotype That Orchestrates Effective T Cell Immunotherapy. *Cancer Cell* (2013) 24(5):589–602. doi: 10.1016/j.ccr.2013.09.014
10. Beauchesne P. Three-Times Daily Ultrafractionated Radiation Therapy, a Novel and Promising Regimen for Glioblastoma Patients. *Cancers (Basel)* (2013) 5(4):1199–211. doi: 10.3390/cancers5041199
11. Chendil D, Oakes R, Mohiuddin M, Alcock RA, Gallicchio VS, Ahmed MM, et al. Low Dose Fractionated Radiation Enhances the Radiosensitization Effect of Paclitaxel in Colorectal Tumor Cells With Mutant P53. *Cancer* (2000) 89(9):1893–900. doi: 10.1002/1097-0142(20001101)89:9<1893::aid-cncr4>3.3.co;2-2
12. Dey S, Spring PM, Arnold S, Valentino J, Chendil D, Regine WF, et al. Low-Dose Fractionated Radiation Potentiates the Effects of Paclitaxel in Wild-Type and Mutant P53 Head and Neck Tumor Cell Lines. *Clin Cancer Res* (2003) 9(4):1557–65.
13. Gupta S, Koru-Sengul T, Arnold SM, Devi GR, Mohiuddin M, Ahmed MM, et al. Low-Dose Fractionated Radiation Potentiates the Effects of Cisplatin Independent of the Hyper-Radiation Sensitivity in Human Lung Cancer Cells. *Mol Cancer Ther* (2011) 10(2):292–302. doi: 10.1158/1535-7163.MCT-10-0630
14. Spring PM, Arnold SM, Shajahan S, Brown B, Dey S, Lele SM, et al. Low Dose Fractionated Radiation Potentiates the Effects of Taxotere in Nude Mice Xenografts of Squamous Cell Carcinoma of Head and Neck. *Cell Cycle* (2004) 3(4):479–85. doi: 10.4161/cc.3.4.786
15. Beauchesne PD, Bertrand S, Branche R, Linke SP, Revel R, Dore JF, et al. Human Malignant Glioma Cell Lines Are Sensitive to Low Radiation Doses. *Int J Cancer* (2003) 105(1):33–40. doi: 10.1002/ijc.11033
16. Arnold SM, Regine WF, Ahmed MM, Valentino J, Spring P, Kudrimoti M, et al. Low-Dose Fractionated Radiation as a Chemopotentiator of Neoadjuvant Paclitaxel and Carboplatin for Locally Advanced Squamous Cell Carcinoma of the Head and Neck: Results of a New Treatment Paradigm. *Int J Radiat Oncol Biol Phys* (2004) 58(5):1411–7. doi: 10.1016/j.ijrobp.2003.09.019
17. Regine WF, Hanna N, Garofalo MC, Doyle A, Arnold S, Kataria R, et al. Low-Dose Radiotherapy as a Chemopotentiator of Gemcitabine in Tumors of the Pancreas or Small Bowel: A Phase I Study Exploring a New Treatment Paradigm. *Int J Radiat Oncol Biol Phys* (2007) 68(1):172–7. doi: 10.1016/j.ijrobp.2006.11.045
18. Balducci M, Diletto B, Chiesa S, D'Agostino GR, Gambacorta MA, Ferro M, et al. Low-Dose Fractionated Radiotherapy and Concomitant Chemotherapy for Recurrent or Progressive Glioblastoma: Final Report of a Pilot Study. *Strahlenther Onkol* (2014) 190(4):370–6. doi: 10.1007/s00066-013-0506-z
19. Beauchesne P, Quillien V, Faure G, Bernier V, Noel G, Quetin P, et al. A Concurrent Ultra-Fractionated Radiation Therapy and Temozolomide Treatment: A Promising Therapy for Newly Diagnosed, Inoperable Glioblastoma. *Int J Cancer* (2016) 138(6):1538–44. doi: 10.1002/ijc.29898
20. Kanski A, Meyer JE, Joiner M, Hall MJ, Philip P, Shields A, et al. Multi-Institutional Phase I Study of Low-Dose Ultra-Fractionated Radiotherapy as a Chemosensitizer for Gemcitabine and Erlotinib in Patients With Locally Advanced or Limited Metastatic Pancreatic Cancer. *Radiother Oncol* (2014) 113(1):35–40. doi: 10.1016/j.radonc.2014.08.014
21. Mantini G, Valentini V, Meduri B, Margaritora S, Balducci M, Micciché F, et al. Low-Dose Radiotherapy as a Chemo-Potentiator of a Chemotherapy Regimen With Pemetrexed for Recurrent Non-Small-Cell Lung Cancer: A Prospective Phase II Study. *Radiother Oncol* (2012) 105(2):161–6. doi: 10.1016/j.radonc.2012.09.006
22. Mattoli MV, Massacesi M, Castellucci A, Scolozzi V, Mantini G, Calcagni ML, et al. The Predictive Value of 18F-FDG PET-CT for Assessing the Clinical Outcomes in Locally Advanced NSCLC Patients After a New Induction Treatment: Low-Dose Fractionated Radiotherapy With Concurrent Chemotherapy. *Radiat Oncol* (2017) 12(1):4. doi: 10.1186/s13014-016-0737-0
23. Morganti AG, Cellini F, Mignogna S, Padula GDA, Caravatta L, Deodato F, et al. Low-Dose Radiotherapy and Concurrent FOLFIRI-Bevacizumab: A Phase II Study. *Future Oncol* (2016) 12(6):779–87. doi: 10.2217/fon.15.350
24. Nardone L, Valentini V, Marino L, De Santis MC, Terribile D, Franceschini G, et al. A Feasibility Study of Neo-Adjuvant Low-Dose Fractionated Radiotherapy With Two Different Concurrent Anthracycline-Docetaxel Schedules in Stage IIA/B-III A Breast Cancer. *Tumori* (2012) 98(1):79–85. doi: 10.1700/1053.11503
25. Nardone L, Diletto B, De Santis MC, D'Agostino GR, Belli P, Bufi E, et al. Primary Systemic Treatment and Concomitant Low Dose Radiotherapy for Breast Cancer: Final Results of a Prospective Phase II Study. *Breast* (2014) 23(5):597–602. doi: 10.1016/j.breast.2014.06.005
26. Valentini V, Massacesi M, Balducci M, Mantini G, Micciché F, Mattiucci GC, et al. Low-Dose Hyperradiosensitivity: Is There a Place for Future Investigation in Clinical Settings? *Int J Radiat Oncol Biol Phys* (2010) 76(2):535–9. doi: 10.1016/j.ijrobp.2009.02.075
27. Das S, Subhashini J, Rami Reddy JK, KantiPal S, Isiah R, Oommen R, et al. Low-Dose Fractionated Radiation and Chemotherapy Prior to Definitive Chemoradiation in Locally Advanced Carcinoma of the Uterine Cervix: Results of a Prospective Phase II Clinical Trial. *Gynecol Oncol* (2015) 138(2):292–8. doi: 10.1016/j.ygyno.2015.05.020
28. Shamseer L, Moher D, Clarke M, Ghersi D, Liberati A, Petticrew M, et al. PRISMA-P Group. Preferred Reporting Items for Systematic Review and Meta-Analysis Protocols (PRISMA-P) 2015: Elaboration and Explanation. *BMJ* (2015) 350:g7647. doi: 10.1136/bmj.g7647
29. Hutton B, Salanti G, Caldwell DM, Chaimani A, Schmid CH, Cameron C, et al. The PRISMA Extension Statement for Reporting of Systematic Reviews Incorporating Network Meta-Analyses of Health Care Interventions: Checklist and Explanations. *Ann Intern Med* (2015) 162(11):777–84. doi: 10.7326/M14-2385
30. Sterne JA, Hernán MA, Reeves BC, Savović J, Berkman ND, Viswanathan M, et al. ROBINS-I: A Tool for Assessing Risk of Bias in Non-Randomised Studies of Interventions. *BMJ* (2016) 355:i4919. doi: 10.1136/bmj.i4919
31. Common Terminology Criteria for Adverse Events (CTCAE). Available at: https://ctep.cancer.gov/protocoldevelopment/electronic_applications/ctc.htm (Accessed 26 December 2020).
32. Vokes EE, Stenson K, Rosen FR, Kies MS, Rademaker AW, Witt ME, et al. Weekly Carboplatin and Paclitaxel Followed by Concomitant Paclitaxel, Fluorouracil, and Hydroxyurea Chemoradiotherapy: Curative and Organ-Preserving Therapy for Advanced Head and Neck Cancer. *J Clin Oncol* (2003) 21(2):320–6. doi: 10.1200/JCO.2003.06.006
33. Bouillet T, Morere J, Depreaux G. Phase II Study of Paclitaxel (P) Twice a Week as a Radiosensitizer, After Paclitaxel-Carboplatin (C) Induction in Stage III-IV Head and Neck Carcinoma. *Proc Am Soc Clin Oncol* (1999) 18:403a. doi: 10.1016/S0959-8049(99)81076-4
34. Dunphy FR, Dunleavy TL, Harrison BR, Trinkaus KM, Kim HJ, Stack BC Jr, et al. Induction Paclitaxel and Carboplatin for Patients With Head and Neck Carcinoma. Analysis of 62 Patients Treated Between 1994 and 1999. *Cancer* (2001) 91(5):940–8. doi: 10.1002/1097-0142(20010301)91:5<940::AID-CNCR1083>3.0.CO;2-A
35. Machtay M, Rosenthal DI, Hershock D, Jones H, Williamson S, Greenberg MJ, et al. Penn Cancer Center Clinical Trials Group. Organ Preservation Therapy Using Induction Plus Concurrent Chemoradiation for Advanced Resectable Oropharyngeal Carcinoma: A University of Pennsylvania Phase II Trial. *J Clin Oncol* (2002) 20(19):3964–71. doi: 10.1200/JCO.2002.11.026
36. Storniolo AM, Enas NH, Brown CA, Voi M, Rothenberg ML, Schilsky R. An Investigational New Drug Treatment Program for Patients With Gemcitabine: Results for Over 3000 Patients With Pancreatic Carcinoma. *Cancer* (1999) 85(6):1261–8. doi: 10.1002/(SICI)1097-0142(19990315)85:6<1261::AID-CNCR7>3.0.CO;2-T
37. Burris HA 3rd, Moore MJ, Andersen J, Green MR, Rothenberg ML, Modiano MR, et al. Improvements in Survival and Clinical Benefit With Gemcitabine as First-Line Therapy for Patients With Advanced Pancreas Cancer: A Randomized Trial. *J Clin Oncol* (1997) 15(6):2403–13. doi: 10.1200/JCO.1997.15.6.2403

38. Moore MJ, Goldstein D, Hamm J, Figer A, Hecht JR, Gallinger S, et al. National Cancer Institute of Canada Clinical Trials Group. Erlotinib Plus Gemcitabine Compared With Gemcitabine Alone in Patients With Advanced Pancreatic Cancer: A Phase III Trial of the National Cancer Institute of Canada Clinical Trials Group. *J Clin Oncol* (2007) 25(15):1960–6. doi: 10.1200/JCO.2006.07.9525
39. Ardizzoni A, Grossi F, Scolaro T, Giudici S, Foppiano F, Boni L, et al. Induction Chemotherapy Followed by Concurrent Standard Radiotherapy and Daily Low-Dose Cisplatin in Locally Advanced Non-Small-Cell Lung Cancer. *Br J Cancer* (1999) 81(2):310–5. doi: 10.1038/sj.bjc.6990693
40. Stupp R, Mason WP, van den Bent MJ, Weller M, Fisher B, Taphoorn MJ, et al. European Organisation for Research and Treatment of Cancer Brain Tumor and Radiotherapy Groups; National Cancer Institute of Canada Clinical Trials Group. Radiotherapy Plus Concomitant and Adjuvant Temozolomide for Glioblastoma. *N Engl J Med* (2005) 352(10):987–96. doi: 10.1056/NEJMoa043330
41. Hanna N, Shepherd FA, Fossella FV, Pereira JR, De Marinis F, von Pawel J, et al. Randomized Phase III Trial of Pemetrexed Versus Docetaxel in Patients With Non-Small-Cell Lung Cancer Previously Treated With Chemotherapy. *J Clin Oncol* (2004) 22(9):1589–97. doi: 10.1200/JCO.2004.08.163
42. Shepherd FA, Dancey J, Ramlau R, Mattson K, Gralla R, O'Rourke M, et al. Prospective Randomized Trial of Docetaxel Versus Best Supportive Care in Patients With Non-Small-Cell Lung Cancer Previously Treated With Platinum-Based Chemotherapy. *J Clin Oncol* (2000) 18(10):2095–103. doi: 10.1200/JCO.2000.18.10.2095
43. Fossella FV, DeVore R, Kerr RN, Crawford J, Natale RR, Dunphy F, et al. Randomized Phase III Trial of Docetaxel Versus Vinorelbine or Ifosfamide in Patients With Advanced Non-Small-Cell Lung Cancer Previously Treated With Platinum-Containing Chemotherapy Regimens. The TAX 320 Non-Small Cell Lung Cancer Study Group. *J Clin Oncol* (2000) 18(12):2354–62. doi: 10.1200/JCO.2000.18.12.2354. Erratum in: *J Clin Oncol.* (2004); 22(1):209. PMID: 10856094.
44. Forastiere AA, Metch B, Schuller DE, Ensley JF, Hutchins LF, Triozzi P, et al. Randomized Comparison of Cisplatin Plus Fluorouracil and Carboplatin Plus Fluorouracil Versus Methotrexate in Advanced Squamous-Cell Carcinoma of the Head and Neck: A Southwest Oncology Group Study. *J Clin Oncol* (1992) 10(8):1245–51. doi: 10.1200/JCO.1992.10.8.1245
45. Forastiere AA, Leong T, Rowinsky E, Murphy BA, Vlock DR, DeConti RC, et al. Phase III Comparison of High-Dose Paclitaxel + Cisplatin + Granulocyte Colony-Stimulating Factor Versus Low-Dose Paclitaxel + Cisplatin in Advanced Head and Neck Cancer: Eastern Cooperative Oncology Group Study E1393. *J Clin Oncol* (2001) 19(4):1088–95. doi: 10.1200/JCO.2001.19.4.1088
46. Gibson MK, Li Y, Murphy B, Hussain MH, DeConti RC, Ensley J, et al. Eastern Cooperative Oncology Group. Randomized Phase III Evaluation of Cisplatin Plus Fluorouracil Versus Cisplatin Plus Paclitaxel in Advanced Head and Neck Cancer (E1395): An Intergroup Trial of the Eastern Cooperative Oncology Group. *J Clin Oncol* (2005) 23(15):3562–7. doi: 10.1200/JCO.2005.01.057
47. Soulieres D, Senzer NN, Vokes EE, Hidalgo M, Agarwala SS, et al. Multicenter Phase II Study of Erlotinib, an Oral Epidermal Growth Factor Receptor Tyrosine Kinase Inhibitor, in Patients With Recurrent or Metastatic Squamous Cell Cancer of the Head and Neck. *J Clin Oncol* (2004) 22(1):77–85. doi: 10.1200/JCO.2004.06.075
48. McCormack M, Kadalayil L, Hackshaw A, Hall-Craggs MA, Symonds RP, Warwick V, et al. A Phase II Study of Weekly Neoadjuvant Chemotherapy Followed by Radical Chemoradiation for Locally Advanced Cervical Cancer. *Br J Cancer* (2013) 108(12):2464–9. doi: 10.1038/bjc.2013.230
49. Niyazi M, Siefert A, Schwarz SB, Ganswindt U, Kreth FW, Tonn JC, et al. Therapeutic Options for Recurrent Malignant Glioma. *Radiother Oncol* (2011) 98(1):1–14. doi: 10.1016/j.radonc.2010.11.006
50. Gilbert MR. Recurrent Glioblastoma: A Fresh Look at Current Therapies and Emerging Novel Approaches. *Semin Oncol* (2011) 38(Suppl;4):S21–33. doi: 10.1053/j.seminoncol.2011.09.008
51. Reissfelder C, Timke C, Schmitz-Winnenthal H, Rahbari NN, Koch M, Klug F, et al. A Randomized Controlled Trial to Investigate the Influence of Low Dose Radiotherapy on Immune Stimulatory Effects in Liver Metastases of Colorectal Cancer. *BMC Cancer* (2011) 11:419. doi: 10.1186/1471-2407-11-419

Conflict of Interest: The authors declare that the research was conducted in the absence of any commercial or financial relationships that could be construed as a potential conflict of interest.

Publisher's Note: All claims expressed in this article are solely those of the authors and do not necessarily represent those of their affiliated organizations, or those of the publisher, the editors and the reviewers. Any product that may be evaluated in this article, or claim that may be made by its manufacturer, is not guaranteed or endorsed by the publisher.

Copyright © 2021 Scirocco, Cellini, Zamagni, Macchia, Deodato, Cilla, Strigari, Buwenge, Rizzo, Cammelli and Morganti. This is an open-access article distributed under the terms of the Creative Commons Attribution License (CC BY). The use, distribution or reproduction in other forums is permitted, provided the original author(s) and the copyright owner(s) are credited and that the original publication in this journal is cited, in accordance with accepted academic practice. No use, distribution or reproduction is permitted which does not comply with these terms.

APPENDIX TABLE 1 | Overall risk of bias rating by study and corresponding reasons.

Component study	Overall “ROBINS-I Risk of Bias tool” judgment	Comments
Arnold et al. 2004 (16)	Serious	Bias in measurement of outcomes (one patient was removed from the study but included in the toxicity and response analysis; one refused additional chemotherapy after his first cycle but was analyzed in the treatment group)
Regine et al., 2007 (17)	Moderate	Bias due to confounding (heterogeneous setting of tumors)
Valentini et al., 2010 (26)	Moderate	Bias due to confounding (heterogeneous setting of tumors)
Mantini et al. 2012 (21)	Moderate	Bias due to confounding (heterogeneous setting of NSCLC)
Nardone et al. 2012 (24)	Moderate	Bias due to confounding (heterogeneous setting of breast cancer)
Nardone et al., 2014 (25)	Moderate	Bias due to confounding (heterogeneous setting of breast cancer)
Konski et al. 2014 (20)	Serious	Bias due to selection of participants into the study (select group of advanced pancreatic cancer patients with limited metastatic disease) Bias due to deviation from intended interventions (10/26 patients completed treatment; patients underwent chemotherapy schedule, which is currently reserved for those patients who cannot tolerate more intensive therapy)
Balducci et al. 2014 (18)	Moderate	Bias due to deviations from intended interventions (patients' compliance was 78.1%)
Beauchesne et al. 2015 (19)	Moderate	Bias due to deviations from intended interventions (when tumor progression was found, patients were treated at investigator's discretion)
Das et al. 2015 (27)	Moderate	Bias due to deviation from intended interventions (in 3 patients, delay in administered second cycle of low-dose fraction radiation therapy for personal reasons)
Morganti et al. 2016 (23)	Moderate	Bias in measurement of outcomes (3 patients underwent a subsequent resection of metastatic disease in the irradiated sites, rising the complete response rate up to 38.9% for irradiated lesions)
Mattoli et al. 2017 (22)	Moderate	Bias due to confounding (selection criteria not reported, heterogeneous setting of NSCLC and different strategy of treatment)



Clinical Evaluation of the Inverse Planning System Utilized in Gamma Knife Lightning

Taoran Cui¹, Ke Nie¹, Jiahua Zhu^{1,2}, Shabbar Danish³, Joseph Weiner¹, Anupama Chundury¹, Nisha Ohri¹, Yin Zhang¹, Irina Vergalasova¹, Ning Yue¹ and Xiao Wang^{1*}

¹ Department of Radiation Oncology, Rutgers-Cancer Institute of New Jersey, Rutgers-Robert Wood Johnson Medical School, New Brunswick, NJ, United States, ² Department of Radiation Oncology, Reading Hospital, Tower Health, West Reading, PA, United States, ³ Department of Neurosurgery, Jersey Shore University Medical Center, Neptune City, NJ, United States

OPEN ACCESS

Edited by:

Tonghe Wang,
Emory University, United States

Reviewed by:

Justin Visak,
University of Texas Southwestern
Medical Center, United States
Brígida Ferreira,
University of Lisbon, Portugal
Ranjini Tolakanahalli,
Baptist Hospital of Miami,
United States

*Correspondence:

Xiao Wang
xw240@cinj.rutgers.edu

Specialty section:

This article was submitted to
Radiation Oncology,
a section of the journal
Frontiers in Oncology

Received: 10 December 2021

Accepted: 31 January 2022

Published: 23 February 2022

Citation:

Cui T, Nie K, Zhu J, Danish S, Weiner J, Chundury A, Ohri N, Zhang Y, Vergalasova I, Yue N and Wang X (2022) Clinical Evaluation of the Inverse Planning System Utilized in Gamma Knife Lightning. *Front. Oncol.* 12:832656. doi: 10.3389/fonc.2022.832656

Objectives: The purpose of this study is to independently compare the performance of the inverse planning algorithm utilized in Gamma Knife (GK) Lightning Treatment Planning System (TPS) to manual forward planning, between experienced and inexperienced users, for different types of targets.

Materials and Methods: Forty patients treated with GK stereotactic radiosurgery (SRS) for pituitary adenoma (PA), vestibular schwannoma (VS), post-operative brain metastases (pBM), and intact brain metastases (iBM) were randomly selected, ten for each site. Three inversely optimized plans were generated for each case by two experienced planners (OptExp1 and OptExp2) and a novice planner (OptNov) using GK Lightning TPS. For each treatment site, the Gradient Index (GI), the Paddick Conformity Index (PCI), the prescription percentage, the scaled beam-on time (sBOT), the number of shots used, and dosimetric metrics to OARs were compared first between the inversely optimized plans and the manually generated clinical plans, and then among the inversely optimized plans. Statistical analyses were performed using the Student's t-test and the ANOVA followed by the post-hoc Tukey tests.

Results: The GI for the inversely optimized plans significantly outperformed the clinical plans for all sites. PCIs were similar between the inversely optimized and clinical plans for PA and VS, but were significantly improved in the inversely optimized plans for iBM and pBM. There were no significant differences in the sBOT between the inversely optimized and clinical plans, except for the PA cases. No significant differences were observed in dosimetric metrics, except for lower brain V_{12Gy} and PTV $D_{98\%}$ in the inversely optimized plans for iBM. There were no noticeable differences in plan qualities among the inversely optimized plans created by the novice and experienced planners.

Conclusion: Inverse planning in GK Lightning TPS produces GK SRS plans at least equivalent in plan quality and similar in sBOT compared to manual forward planning in this independent validation study. The automatic workflow of inversed planning ensures a consistent plan quality regardless of a planner's experience.

Keywords: inverse planning, Gamma Knife Icon™®, GammaPlan®, Gamma Knife® Lightning, stereotactic radiosurgery (SRS), pituitary adenoma, vestibular schwannoma, brain metastases (BM)

INTRODUCTION

The Leksell Gamma Knife (GK) is considered an effective stereotactic radiosurgery (SRS) platform for various cranial diseases. Although initially designed for small and well-circumscribed lesions, such as targets in functional brain surgery or solitary brain metastasis (1), GK continues to evolve with advanced technologies of variable collimator sizes, motor-driven sector, and image-guided cone-beam CT (CBCT), to allow for SRS for targets of non-spherical and irregular shapes. There have been excellent clinical outcomes reported on the management of post-operative brain metastases (2), acoustic neuroma (3), pituitary adenoma (4), and arteriovenous malformations (5) using GK SRS.

During an SRS treatment delivered by a GK Perfexion/ICON™ unit, 8 sectors with ^{60}Co sources can be independently modulated with collimators of three different sizes to achieve a variable irradiated volume at the isocenter. A patient receiving GK SRS is supported and moved by a high-precision treatment couch which aligns the irradiation focal point to a pre-defined cranial location, and the radiation is delivered at the location with a given set of collimators, which is usually referred as a “shot”. A single shot or multiple shots with various weights can be used to achieve desired coverage or conformity for targets of different volumes or shapes. The treatment planning for GK SRS is therefore defined as the adjustments of collimator selection, isocenter location, and relative weight of multiple shots to create a GK SRS plan that meets the pre-defined requirements.

Traditionally, the design of a GK SRS plan is performed manually, in a forward, trial-and-error approach. The quality of a GK SRS plan generated in this approach significantly relies on the prior experiences of a planner, the time and effort spent on planning, and different planning approaches applied among various planners. Hence, the plan quality of a GK SRS plan usually suffers from inter-planner variabilities and it is often challenging to ensure consistent plan quality. In addition, the improvement of plan quality of GK SRS plans is usually accompanied by the inflation of beam-on time (BOT) (6) which could result in prolonged treatment time and patient discomfort. Therefore, it is desirable to have an efficient and effective automatic treatment planning system available for clinical application independent of planner's experiences to assure consistent plan quality for GK SRS.

Multiple inverse planning approaches have been proposed for GK SRS using morphology guided (7), non-linear programming (8), multiresolution-level (9) techniques. Whereas these approaches presented promising results, they were never integrated with the treatment planning system (TPS) thus not ideal for real-time clinical application. More recently, a new inverse planning technology has become clinically available in the latest GK Lightning TPS which enables an automatic workflow for GK treatment planning with minimum manual inputs (10). While the initial study performed by the vendor has demonstrated encouraging results, only two independent studies on GK Lightning have been recently published (11, 12), and independent evaluations of the inverse planning technology with broader clinical relevance are still in need. In the current manuscript, we aim to evaluate this new inverse planning technology by comparing the inversely optimized plan

generated with this technology to clinically approved forward-based plans for a variety of disease types. The inversely optimized plans generated by different planners with various experience levels were also compared for all plans to assess the readiness of this new technology.

MATERIALS AND METHODS

Patients treated with GK SRS at our institution for pituitary adenoma (PA), vestibular schwannoma (VS), postoperative surgical bed of brain metastases (pBM), and intact brain metastases (iBM) were randomly selected for this retrospective, institutional IRB approved (Pro2018000227) study.

Per departmental protocol, series of T1- and T2-weighted MRI were acquired prior to treatment planning. Gross tumor volumes (GTVs) were contoured as radiographic enhancements on contrast-enhanced T1-weighted FSPGR MRI in 1.5mm axial cuts, and verified on an independent series of contrast-enhanced T1-weighted MRI in coronal cuts. Clinical target volumes (CTVs) were the same as GTVs, except for post-operative brain metastasis cases, where there was no GTV and a CTV was created by adding a 2-mm isotropic margin to a surgical cavity. All the selected clinical plans were initially treated with frame fixation and therefore setup margin was not used. Therefore, planning target volumes (PTVs) was identical to CTVs. The original clinical plans were manually designed to achieve at least 99% target coverage by prescribed doses, unless at the discretion of physicians. The dose constraints to organs-at-risk (OARs) were strictly followed with AAPM Task Group report 101 (13), that $D_{0.035\text{cc}} < 10\text{ Gy}$ and $D_{0.2\text{cc}} < 8\text{ Gy}$ for the optical apparatus, $D_{0.035\text{cc}} < 15\text{ Gy}$ and $D_{0.5\text{cc}} < 10\text{ Gy}$ for the brainstem, and $D_{0.035\text{cc}} < 9\text{ Gy}$ for the cochlea.

To compare the differences between the manual forward planning and the new inverse planning technology, each patient was replanned by two experienced planners (OptExp1 and OptExp2) and one novice planner (OptNov) utilizing the inverse planning technology in the GK Lightning TPS (10). The experienced users have at least 5 years of GK planning experience, while the novice planner has less than 3 months experience. The implementation of the inverse planning technology was discussed in detail by Sjölund et al. (10). Briefly, a cost function is first constructed to include various planning objectives defined by a planner, including the prescription dose coverage of multiple targets, the maximum dose delivered to targets and OARs, low dose spillage, and BOT, in order to encourage higher target coverage and lower selectivity and to penalize higher dose to the OARs and longer BOT. The optimizer then adjusts the position and weight of each shot by minimizing the cost function using linear programming until an optimal solution to the cost function is achieved. Neither shot placement nor shot opening selection is required prior to optimization. Furthermore, multiple targets could be inversely optimized at the same time.

In this study, the same original clinical plan prescription dose was chosen to cover the target, and target coverage was selected as a mandatory constraint. Similarly, the maximum dose to OARs was defined using the same dose constraints as the

approved clinical plan. There were no new requirements on the weights of low dose spillage or BOT, for both the weights were frequently adjusted by a planner in a trial-and-error approach. Manual modifications of shot position and weight after the optimization were allowed to either increase target coverage or reduce OAR dose, if necessary. The planning goal was to achieve at least 99% target coverage and as good a Paddick Conformity Index (PCI) (14) and Gradient Index (GI) (15) as possible, with the goal of $PCI > 0.75$ and $GI < 3$. In order to compare the BOT between the clinical and inversely optimized plans generated at different dose-rates, the BOTs were scaled to the same dose rate of 3.5 Gy per minute (sBOT).

The inversely optimized plans were compared to the original clinical plan using several metrics including target coverage, prescription percentage, PCI, GI, sBOTs, number of shots, and number of different utilized sectors. The prescription percentage is defined as the percentage of the dose maximum that is normalized with the prescription dose. $D_{0.035cc}$ and $D_{0.5cc}$ of the brainstem, $D_{0.035cc}$ of the optic chiasm/nerves, and the ipsilateral cochlea were evaluated if these OARs were present. Furthermore, V_{12Gy} of the brain was also included for analysis for postoperative and intact brain metastases cases.

For each disease site, the Student's t-test was first applied to compare the metrics between clinical and inversely optimized plans. Specifically, the Chi-square test was used to demonstrate if there was any difference in the numbers of sectors used per plan. Then, the one-way ANOVA test was performed to determine if there were any differences in the metrics among the inversely optimized plans created by different planners, followed by the post-hoc Tukey Test to determine the metrics of which specific inversely optimized plans were different. A p-value less than 0.05 was considered statistically significant.

RESULTS

Dosimetric Metrics

Forty patients treated with GK SRS were identified from our institutional database with 10 patients for each of the pre-defined

disease sites. The prior clinical plans were all manually generated without using any optimization algorithms. All optimized plans generated using the inverse planning technology of the GK Lighting TPS were reviewed to ensure that target coverage and dosimetric OAR constraints all met the clinical criteria. Although manual modification was allowed, none of the planners reported necessity of manual tweaking of shots, since all dosimetric criteria were met after iterative inverse optimization. A comparison of dose distribution and shot placement between the clinical plan and inversely optimized plan for a representative pBM case is shown in **Figure 1**. Compared to the clinical plan, the inversely optimized plan has similar coverage, but greater number of shots with different isocenters.

Results for Each Site

Figure 2, **Tables 1** and **2** summarized the comparison of plan qualities among the inversely optimized and clinical plans for patients treated for PA, VS, pBM, and iBM.

For PA cases, the GI and sBOT were both significantly improved in the inversely optimized plans at the expense of larger number of shots utilized per plan compared to the corresponding clinical plans. No significant differences were observed for any other metrics between the inversely optimized and clinical plans. The results of the ANOVA test indicated that there were no differences in the metrics among the inversely optimized plans by the three planners, except that GIs in the inversely optimized plans created by the novice planner were significantly lower than those in the inversely optimized plans by the two experienced planners.

For VS cases, the low dose spillages were better controlled with significantly lower GIs in the inversely optimized plans compared to the clinical plans, whereas the numbers of shots used per plan were also significantly higher in the inversely optimized plans. No other statistically significant differences in the other metrics were observed between the inversely optimized and clinical plans. Furthermore, all three inversely optimized plans had similar metric values with the only significant differences observed in the PCIs.

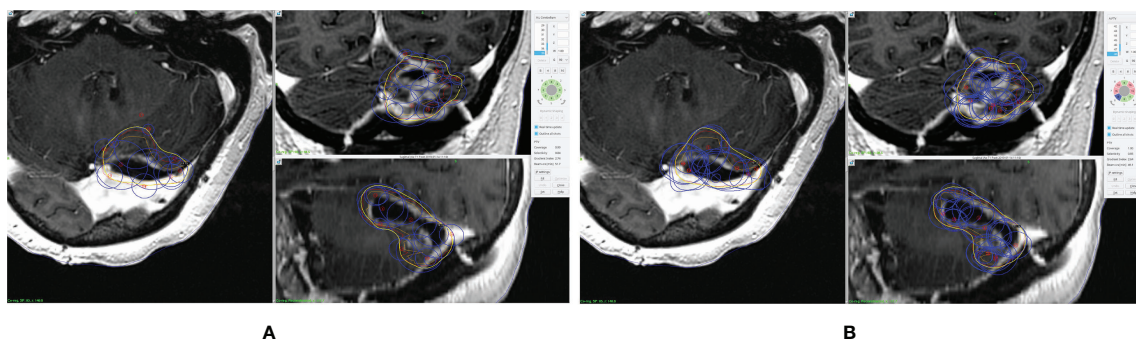
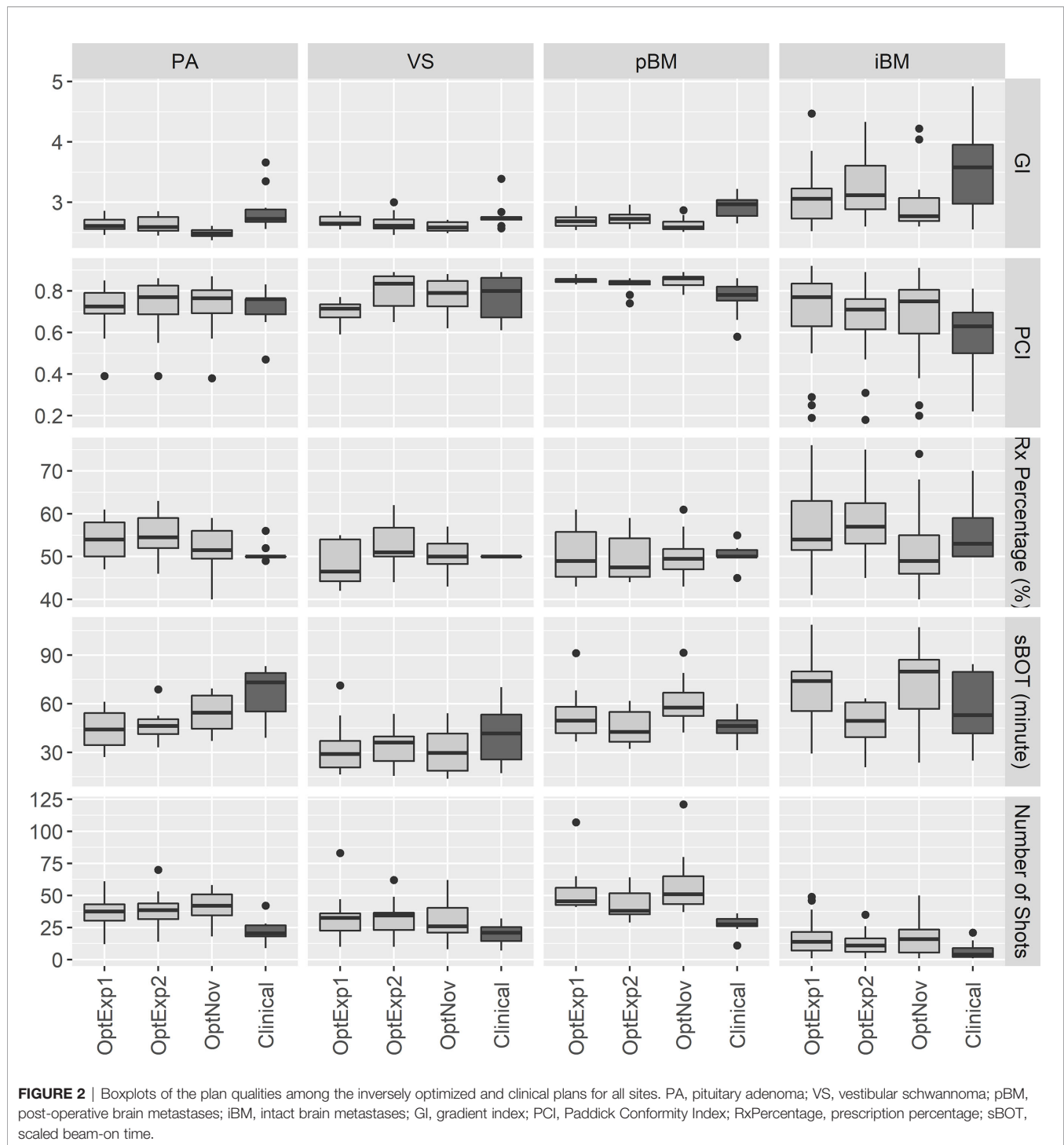


FIGURE 1 | An example of prescription dose coverage and shot placement in **(A)** clinical plan and **(B)** inversely optimized plan. The surgical cavity is delineated in orange, and the CTV is in red. The blue lines represent the shots, and the yellow lines represent the isodose lines of the prescription dose.



For pBM cases, the inversely optimized plans presented better plan qualities with significantly higher PCI and lower GI, but more shots per plan compared to the clinical plans, and there were no significant differences observed among the three inversely optimized plans. For each PTV treated in the iBM cases, despite all PTVs covered with at least 99% of prescription dose, there were significant differences in $D_{98\%}$ of PTV, PCI, and

GI between the clinical and inversely optimized plans. The volumes of PTV in iBM cases range from 0.02 to 17.62 cc, with a mean of 2.19 cc and a standard deviation of 3.25 cc. While the inversely optimized plans had higher conformality and tighter low dose spillage, which also resulted in lower V_{12Gy} of normal brain tissue, the clinical plans delivered higher radiation dose to the PTVs with higher $D_{98\%}$. These differences could

TABLE 1 | Summary of the target metrics among the inversely optimized and clinical plans for all sites.

Metrics	Site	OptExp1	OptExp2	OptNov	Clinical	p-value Student's t-test	ANOVA
GI	PA	2.64 ± 0.13 (2.46-2.86)	2.63 ± 0.14 (2.45-2.85)	2.49 ± 0.07 (2.37-2.61)	2.88 ± 0.35 (2.56-3.66)	p < 0.05	p<0.05; OptNov
	VS	2.68 ± 0.10 (2.55-2.85)	2.67 ± 0.16 (2.46-3.00)	2.59 ± 0.08 (2.49-2.71)	2.78 ± 0.23 (2.57-3.39)	p < 0.05	
	pBM	2.69 ± 0.13 (2.54-2.94)	2.73 ± 0.12 (2.56-2.96)	2.63 ± 0.12 (2.51-2.87)	2.93 ± 0.20 (2.65-3.22)	p < 0.05	
	iBM	3.13 ± 0.51 (2.52-4.47)	3.25 ± 0.54 (2.60-4.33)	2.95 ± 0.43 (2.60-4.22)	3.55 ± 0.68 (2.55-4.92)	p < 0.05	
PCI	PA	0.71 ± 0.14 (0.39-0.85)	0.72 ± 0.15 (0.39-0.86)	0.72 ± 0.15 (0.38-0.87)	0.72 ± 0.11 (0.47-0.83)		p<0.05; OptExp1
	VS	0.70 ± 0.06 (0.59-0.77)	0.80 ± 0.09 (0.65-0.89)	0.78 ± 0.09 (0.62-0.88)	0.77 ± 0.11 (0.61-0.89)		
	pBM	0.85 ± 0.01 (0.83-0.88)	0.83 ± 0.04 (0.74-0.86)	0.85 ± 0.03 (0.78-0.89)	0.77 ± 0.09 (0.58-0.86)	p < 0.05	
	iBM	0.71 ± 0.19 (0.19-0.92)	0.67 ± 0.16 (0.18-0.89)	0.68 ± 0.19 (0.20-0.91)	0.59 ± 0.15 (0.22-0.81)	p < 0.05	
RxPercentage (%)	PA	54.20 ± 5.05 (47.00-61.00)	55.10 ± 5.63 (46.00-63.00)	51.90 ± 5.53 (40.00-59.00)	50.70 ± 2.00 (49.00-56.00)		p<0.05; OptNov
	VS	48.30 ± 5.23 (42.00-55.00)	52.80 ± 5.81 (44.00-62.00)	50.40 ± 4.77 (43.00-57.00)	50.00 ± 0.00 (50.00-50.00)		
	pBM	50.50 ± 6.33 (43.00-61.00)	49.60 ± 5.87 (44.00-59.00)	50.20 ± 5.45 (43.00-61.00)	50.40 ± 2.50 (45.00-55.00)		
	iBM	56.77 ± 8.21 (41.00-76.00)	58.23 ± 7.27 (45.00-75.00)	51.58 ± 8.17 (40.00-74.00)	55.42 ± 6.11 (50.00-70.00)		
sBOT (min)	PA	44.12 ± 11.67 (27.06-61.17)	46.60 ± 9.98 (33.09-68.80)	54.68 ± 11.64 (37.07-69.42)	67.09 ± 15.53 (38.97-83.10)	p < 0.05	p<0.05; OptExp2
	VS	33.22 ± 17.30 (16.36-71.30)	33.22 ± 11.73 (15.48-53.67)	31.15 ± 13.91 (13.71-54.13)	40.05 ± 17.65 (17.17-70.15)		
	pBM	53.25 ± 16.46 (36.69-91.17)	45.03 ± 10.96 (32.10-61.73)	61.49 ± 14.96 (42.24-91.49)	45.65 ± 7.79 (31.34-59.88)		
	iBM	68.46 ± 23.73 (29.33-108.60)	49.26 ± 13.63 (20.87-63.27)	73.88 ± 22.63 (23.74-107.11)	58.51 ± 19.59 (24.92-84.38)		
Number of Shots	PA	37.30 ± 13.65 (12.00-61.00)	39.10 ± 15.39 (14.00-70.00)	41.50 ± 12.89 (18.00-58.00)	22.60 ± 8.87 (9.00-42.00)	p < 0.05	p < 0.05
	VS	33.90 ± 20.71 (10.00-83.00)	32.20 ± 15.83 (10.00-62.00)	30.20 ± 17.16 (8.00-62.00)	19.80 ± 8.53 (7.00-32.00)	p < 0.05	
	pBM	53.70 ± 20.37 (41.00-107.00)	43.30 ± 12.49 (29.00-64.00)	59.40 ± 25.26 (37.00-121.00)	27.40 ± 6.87 (11.00-36.00)	p < 0.05	
	iBM	16.84 ± 12.53 (1.00-49.00)	11.97 ± 8.36 (1.00-35.00)	17.35 ± 14.04 (1.00-50.00)	6.00 ± 5.22 (1.00-21.00)	p < 0.05	

OptExp1 and OptExp2 are from two experienced planners and OptNov is from one novice planner.

PA, pituitary adenoma; VS, vestibular schwannoma; pBM, post-operative brain metastases; iBM, intact brain metastases; GI, gradient index; PCI, Paddick Conformity Index;

RxPercentage, prescription percentage; sBOT, scaled beam-on time.

The bold values mean the difference is significant with $p < 0.05$.

probably be explained by the margin deliberately created between the prescription isodose line and PTVs during the manual planning process, especially for small brain metastases. The inversely optimized plans again presented similar plan qualities, except for that the sBOTs in the OptExp2 plans were significantly shorter than those in the OptExp1 and OptNov plans, and that the PTVs in the OptNov plans were prescribed to a significantly lower percentage isodose line.

BOT Comparison

Figure 3 summarizes the average numbers of shots and compositions of sectors in the inversely optimized and clinical plans for the four disease sites included in the study. As shown previously, the number of shots used per plan was significantly higher in the inversely optimized plans regardless of treatment sites. Furthermore, the number of shots used per target in the inversely optimized plans positively correlated with the target volume, as illustrated in **Figure 4**. We should also note that significantly more blocked sectors were used in the inversely

optimized plans (Chi-squared test; $p < 0.001$) than clinical plans, since planners barely used blocked sectors during the manual planning process in order to avoid the lengthening of sBOTs as a consequence of reduced effective dose rate. The reduction of effective dose rate due to the usage of blocked sector in the inversely optimized plans was compensated by more utilized shots, therefore the sBOTs in the inversely optimized plans remained no worse than those in the clinical plans.

DISCUSSION

The results of the study revealed that inversely optimized plans generated using the new inverse planning technology in GK Lightning TPS presented comparable quality to clinically approved plans. No consistent differences between the inversely optimized plans generated by experienced and inexperienced users were observed, which implied the persistent performance of the inverse planning technology in GK Lightning TPS which was

TABLE 2 | Summary of the dosimetric metrics among the inversely optimized and clinical plans for all sites.

Metrics	Site	OptExp1	OptExp2	OptNov	Clinical	p-value Student's t-test	ANOVA
LON_D0.03cc (Gy)	PA	4.88 ± 2.17 (1.40-7.90)	5.28 ± 2.61 (1.40-9.00)	5.38 ± 2.49 (1.70-8.90)	5.39 ± 2.17 (1.40-8.10)		
RON_D0.03cc (Gy)	PA	4.86 ± 2.09 (2.30-8.70)	5.00 ± 2.46 (2.30-9.80)	5.11 ± 2.34 (2.10-9.10)	5.26 ± 2.78 (2.30-9.80)		
BS_D0.03cc (Gy)	PA	8.09 ± 2.86 (4.40-11.40)	9.58 ± 3.66 (5.30-14.10)	9.02 ± 3.20 (5.10-13.30)	9.45 ± 3.41 (4.90-13.10)		
BS_D0.5cc (Gy)	PA	5.97 ± 2.00 (3.50-8.30)	6.50 ± 2.35 (3.30-9.50)	6.35 ± 2.18 (3.40-9.20)	6.48 ± 2.34 (3.20-8.80)		
Chiams_D0.03cc (Gy)	PA	5.15 ± 0.98 (3.80-6.90)	5.17 ± 1.30 (3.50-7.70)	5.20 ± 1.09 (3.40-6.80)	5.51 ± 1.25 (3.70-7.40)		
BS_D0.03cc (Gy)	VS	10.40 ± 3.32 (3.70-14.10)	11.24 ± 3.24 (5.20-14.00)	11.60 ± 3.42 (4.90-14.70)	10.84 ± 3.19 (4.90-14.40)		
BS_D0.5cc (Gy)	VS	7.51 ± 3.18 (1.80-11.30)	7.62 ± 3.09 (2.50-11.10)	7.84 ± 3.20 (2.30-11.70)	7.65 ± 3.10 (2.30-11.20)		
Cochlea_D0.03cc (Gy)	VS	5.64 ± 2.71 (2.30-11.20)	5.56 ± 2.61 (1.90-10.40)	5.30 ± 1.87 (2.20-8.10)	5.52 ± 2.87 (2.50-12.60)		
Brain_V12Gy (cc)	pBM	38.42 ± 15.34 (11.51-65.28)	40.11 ± 16.99 (12.14-74.12)	37.98 ± 15.94 (11.19-67.02)	43.53 ± 19.86 (17.42-89.79)		
PTV_D 98% (Gy)	pBM	17.04 ± 1.44 (15.30-18.70)	17.13 ± 1.41 (15.40-18.70)	17.20 ± 1.39 (15.50-18.80)	17.06 ± 1.89 (13.90-20.00)		
Cavity_D 98% (Gy)	pBM	19.39 ± 2.19 (15.90-22.10)	19.48 ± 2.16 (16.00-22.20)	19.80 ± 2.31 (16.50-22.40)	18.97 ± 2.11 (15.50-21.60)		
Brain_V12Gy (cc)	iBM	16.88 ± 10.02 (0.45-36.06)	18.86 ± 11.44 (0.57-41.06)	16.98 ± 10.10 (0.58-35.21)	22.16 ± 13.20 (0.54-46.61)	p < 0.05	
PTV_D 98% (Gy)	iBM	20.28 ± 2.07 (13.40-25.70)	20.51 ± 1.92 (14.10-23.00)	20.97 ± 2.05 (13.70-24.50)	21.16 ± 2.22 (13.50-24.70)	p < 0.05	

OptExp1 and OptExp2 are from two experienced planners and OptNov is from one novice planner.

PA, pituitary adenoma; VS, vestibular schwannoma; pBM, post-operative brain metastases; iBM, intact brain metastases; L/RON, left/right optic nerve; BS, brainstem.

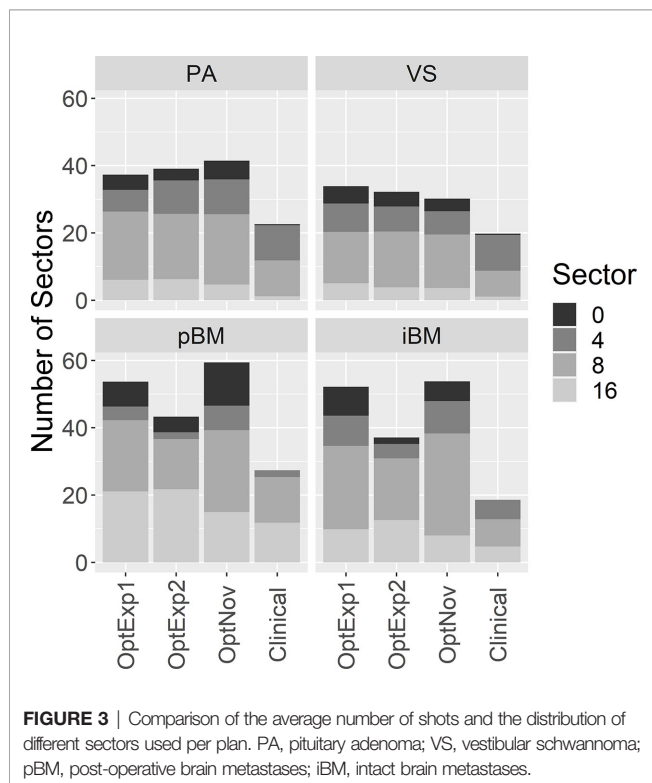
The bold values mean the difference is significant with $p < 0.05$.

independent of planner's experiences. Hence, the implementation of the inverse planning technology may potentially help flatten the learning curve for inexperienced users. To date, the research on

the clinical applications of the inverse planning technology in GK is still limited. Wiczorek et al. (11) compared inverse plans optimized by GK Lightning with manual forward plans on 115 lesions and demonstrated that the inverse plans were comparable or superior to forward plans with regard to plan quality metrics. Spaniol et al. (12) performed similar analyses on 38 patients' plans, as well as evaluated inter-operator variability on one plan for every pathology type. They also showed improved plan quality with GK Lightning, with minimal variability on the operator's experience. Compared with previous studies, our study not only classified plan quality comparisons into different diagnoses with a wider range of treatment sites, but also investigated planner dependence for all forty plans. Our study provides an independent evaluation of the inverse planning technology and a comparison of GK plans created by experienced and inexperienced users with various disease sites clinically treated with GK.

Overall, the plan quality of inversely optimized plans generated with the inverse planning technology was at least equivalent to the plan quality of those manually created by experienced planners across all disease types, especially the PCI of the inversely optimized plans was significantly better in the pBM and iBM cases. This is primarily due to the nature of malignancy type of lesions and the large separation between the targets and critical organs, so that large shots were often used in forward planning for multiple brain metastases cases to reduce overall treatment time.

The traditional manual forward planning for GK is usually complex and nonintuitive, mostly due to the high degrees-of-freedom of a GK plan. Because of the high dimension of the search space (8), the plan quality of a manually created GK plan



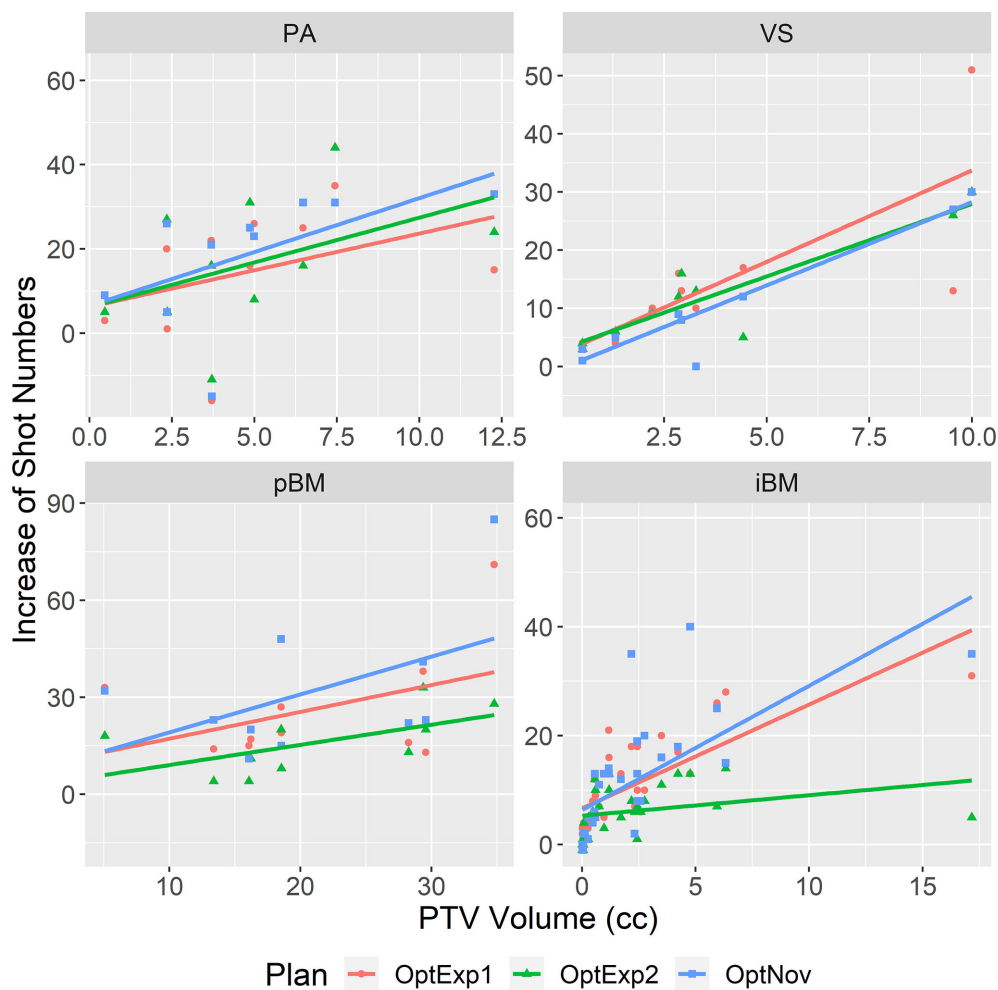


FIGURE 4 | Correlations between the increase of number of shots in the inversely optimized plans and the PTV volume. The linear regression for each site was shown in the straight line. PA, pituitary adenoma; VS, vestibular schwannoma; pBM, post-operative brain metastases; iBM, intact brain metastases.

largely depends on the experience of the planner, and therefore it can be challenging for an inexperienced planner to create an acceptable GK plan. Even for plans created by experienced planners, it is very likely that these plans are not the optimal solution, especially when the target is large and complex with adjacent OARs present. It was not until the release of Leksell GammaPlan V10.0 (2010) that resolving this limitation of manual forward planning became possible with an inverse planning tool (16). This commercially available tool provides a solution with a two-step optimization process that first identifying the number and location of shots then adjusting the weighting of each shot to achieve the desired plan quality. However, the implementation of this first version of the inverse planning technology has been limited with several drawbacks. The inverse planning tool is unable to create a plan equivalent to a manual plan created by an expert planner unless the targets are regular-shaped with no adjacent OARs. Additionally, it is only suitable for the optimization of one target at a time and it doesn't

account for the existing dose spillage from nearby targets during the optimization.

The optimization technology in GK Lightning has been substantially improved from the previous version. The simultaneous optimization of multiple targets is allowed in GK Lightning and is integrated as a single-step procedure where the placement of shots and the pre-selection of sectors are no longer needed. Furthermore, prescription doses to targets and maximum doses to OARs can be specified prior to optimization, which are especially beneficial for the planning of benign cases presented with adjacent OARs. Additionally, planners only need to manipulate optimization with respect to two optimization objectives: low dose spillage and BOT. This has been simplified compared to prior versions where planners needed to specify coverage, selectivity, GI, and BOT.

We should note that the isodose line prescription percentage is implicitly determined during the optimization. Whereas the lower bound of the prescription percentage of a target is directly

correlated with the maximum dose of the target, which can also be specified in the optimization, the upper bound of the prescription percentage can only be adjusted indirectly by increasing the penalty on low dose spillage. This lack of direct manipulation of the prescription percentage imposes challenges to control the dose homogeneity of a target. It has been argued that the internal hotspot created by prescribing to a lower percentage would increase the response of the central hypoxic region of the tumor and therefore result in a higher local control (17), whereas it was also reported that prescribing to a percentage of 70% or higher would not affect local control (18). Despite the lack of consensus, the optimum prescription percentage of 50% is usually preferred at our institution in order to take the advantage of the steepest dose fall-off, with up to 70% isodose line prescriptions allowed in certain cases to increase target conformity; however, when using GK Lightning for small intact brain metastases, we have noticed that the prescription isodose line could be increased to higher than 80% because of the preset penalties on lower target conformity and longer BOT. Therefore, for small intact brain metastases cases, it might be necessary to manually adjust prescription percentage or re-optimize by assigning a higher weighting to low dose spillage and lower weighting to BOT to achieve satisfactory treatment plans.

It is worth noting that the actual delivery time is the sum of the BOT and transition times between consecutive shots. The more shots used in a GK plan, the longer transition time will be added to the total delivery time. In general, inversely optimized plans have a higher number of shots, since the algorithm in the GK Lightning tends to deploy multiple shots of different sector combinations at a single location (10). Thus, the actual delivery time of an inversely optimized plan will be longer than that of a manual forward plan with similar plan quality and BOT. On average, adding one more shot in a GK plan will add an approximately 5-second transition time. Therefore, an inversely optimized plan with 30 more shots would result in additional two and a half minutes in the actual delivery time. Although the impacts are expected to be small for patients immobilized with frame fixation, this increase in the actual delivery time may affect patients treated with frameless fixation in several aspects, including higher likelihood of treatment interruptions due to the intrafraction motion and patient discomfort.

Nevertheless, the inverse planning in GK Lightning improve the workflow of GK treatment. Experienced users may find the automatic planning process advantageous to free themselves from the tedious and lengthy manual planning while focusing on other aspects that need their clinical knowledge and judgments. The overall good quality of inversely optimized plans is beneficial especially for inexperienced users, in that inexperienced users could create plans of comparable quality to those created by experienced users with similar planning time. It should be noted that manual contouring is needed for the inverse planning, thereby additional contouring time is required and should be considered for clinics where the manual forward planning is conducted without contouring.

One limitation of the study is that there was no direct comparison of the treatment planning time between the

inversely optimized and clinical plans, since the study was retrospective and treatment planning times were not recorded for manually generated clinical plans. Although treatment planning time of a GK plan, regardless of whether the plan is created manually or with inverse planning, increases for more complex plans, it usually takes substantially more time to manually create plans for multiple large and irregular targets. While the planning time of a manual plan varies from 5 minutes for a single, regular brain metastasis to more than half an hour for a large post-operative cavity, the optimizing of a plan with the inverse planning usually takes less than 15 minutes, despite several iterations of re-optimization. It can be inferred from clinical experiences that the implementation of the inverse planning technology in GK Lightning will help reduce treatment planning time and improve planning efficiency.

CONCLUSION

The dosimetric quality of the plans inversely optimized with GK Lightning TPS are comparable to those forwardly planned by an experienced user. The performance of the inverse optimization is user independent, making the inverse planning technology in GK Lightning TPS a promising tool to enable efficient clinical workflow.

DATA AVAILABILITY STATEMENT

The original contributions presented in the study are included in the article/supplementary material. Further inquiries can be directed to the corresponding author.

ETHICS STATEMENT

The studies involving human participants were reviewed and approved by Rutgers University Institutional Review Board. Written informed consent for participation was not required for this study in accordance with the national legislation and the institutional requirements.

AUTHOR CONTRIBUTIONS

XW, TC, and KN led the conception and design of the study. XW, TC, JZ, KN, SD, JW, AC, and NO contributed to acquisition of data. TC, XW, and KN contributed to analysis and interpretation of data. TC, XW, KN, SD, JW, AC, and NY drafted and revised the article. All authors contributed to the article and approved the submitted version.

REFERENCES

- Leksell L. Stereotactic Radiosurgery. *J Neurol Neurosurg Psychiatry* (1983) 46 (9):797–803. doi: 10.1136/jnnp.46.9.797
- Jagannathan J, Yen CP, Ray DK, Schlesinger D, Oskouian RJ, Pouratian N, et al. Gamma Knife Radiosurgery to the Surgical Cavity Following Resection of Brain Metastases. *J Neurosurg* (2009) 111(3):431–8. doi: 10.3171/2008.11.JNS08818
- Foote RL, Coffey RJ, Swanson JW, Harner SG, Beatty CW, Kline RW, et al. Stereotactic Radiosurgery Using the Gamma Knife for Acoustic Neuromas. *Int J Radiat Oncol Biol Phys* (1995) 32(4):1153–60. doi: 10.1016/0360-3016(94)00454-s
- Izawa M, Hayashi M, Nakaya K, Satoh H, Ochiai T, Hori T, et al. Gamma Knife Radiosurgery for Pituitary Adenomas. *J Neurosurg* (2000) 93(Suppl 3):19–22. doi: 10.3171/jns.2000.93.supplement
- Pan DH, Guo WY, Chung WY, Shiao CY, Chang YC, Wang LW. Gamma Knife Radiosurgery as a Single Treatment Modality for Large Cerebral Arteriovenous Malformations. *J Neurosurg* (2000) 93 Suppl 3:113–9. doi: 10.3171/jns.2000.93.supplement
- Petti PL, Larson DA, Kunwar S. Use of Hybrid Shots in Planning Perfixion Gamma Knife Treatments for Lesions Close to Critical Structures. *J Neurosurg* (2008) 109 Suppl:34–40. doi: 10.3171/JNS/2008/109/12/S7
- Wu QJ, Chankong V, Jitprapaikularn S, Wessels BW, Einstein DB, Mathayomchan B, et al. Real-Time Inverse Planning for Gamma Knife Radiosurgery. *Med Phys* (2003) 30(11):2988–95. doi: 10.1118/1.1621463
- Shepard DM, Ferris MC, Ove R, Ma L. Inverse Treatment Planning for Gamma Knife Radiosurgery. *Med Phys* (2000) 27(12):2748–56. doi: 10.1118/1.1328080
- Tian Z, Yang X, Giles M, Wang T, Gao H, Butker E, et al. A Preliminary Study on a Multiresolution-Level Inverse Planning Approach for Gamma Knife Radiosurgery. *Med Phys* (2020) 47(4):1523–32. doi: 10.1002/mp.14078
- Sjolund J, Riad S, Hennix M, Nordstrom H. A Linear Programming Approach to Inverse Planning in Gamma Knife Radiosurgery. *Med Phys* (2019) 46 (4):1533–44. doi: 10.1002/mp.13440
- Wieczorek DJ, Kotecha R, Hall MD, Tom MC, Davis S, Ahluwalia MS, et al. Systematic Evaluation and Plan Quality Assessment of the Leksell(R) Gamma Knife(R) Lightning Dose Optimizer. *Med Dosim* (2021) 47(1):70–8. doi: 10.1016/j.meddos.2021.08.006
- Spaniol M, Mai S, Zakrzewski T, Ehmann M, Stieler F. Inverse Planning in Gamma Knife Radiosurgery: A Comparative Planning Study. *Phys Med* (2021) 82:269–78. doi: 10.1016/j.ejmp.2021.02.019
- Benedict SH, Yenice KM, Followill D, Galvin JM, Hinson W, Kavanagh B, et al. Stereotactic Body Radiation Therapy: The Report of AAPM Task Group 101. *Med Phys* (2010) 37(8):4078–101. doi: 10.1118/1.3438081
- Paddick I, Lippitz B. A Simple Dose Gradient Measurement Tool to Complement the Conformity Index. *J Neurosurg* (2006) 105 Suppl :194–201. doi: 10.3171/sup.2006.105.7.194
- Paddick I. A Simple Scoring Ratio to Index the Conformity of Radiosurgical Treatment Plans. Technical Note. *J Neurosurg* (2000) 93(Suppl 3):219–22. doi: 10.3171/jns.2000.93.supplement
- Schlesinger DJ, Sayer FT, Yen CP, Sheehan JP. Leksell GammaPlan Version 10.0 Preview: Performance of the New Inverse Treatment Planning Algorithm Applied to Gamma Knife Surgery for Pituitary Adenoma. *J Neurosurg* (2010) 113 Suppl:144–8. doi: 10.3171/2010.7.GKS101033
- Shaw E, Scott C, Souhami L, Dinapoli R, Kline R, Loeffler J, et al. Single Dose Radiosurgical Treatment of Recurrent Previously Irradiated Primary Brain Tumors and Brain Metastases: Final Report of RTOG Protocol 90-05. *Int J Radiat Oncol Biol Phys* (2000) 47(2):291–8. doi: 10.1016/s0360-3016(99)00507-6
- Shiue K, Barnett GH, Suh JH, Vogelbaum MA, Reddy CA, Weil RJ, et al. Using Higher Isodose Lines for Gamma Knife Treatment of 1 to 3 Brain Metastases Is Safe and Effective. *Neurosurgery* (2014) 74(4):360–4; discussion 364–5; quiz 365–6. doi: 10.1227/NEU.0000000000000289

Conflict of Interest: The authors declare that the research was conducted in the absence of any commercial or financial relationships that could be construed as a potential conflict of interest.

Publisher's Note: All claims expressed in this article are solely those of the authors and do not necessarily represent those of their affiliated organizations, or those of the publisher, the editors and the reviewers. Any product that may be evaluated in this article, or claim that may be made by its manufacturer, is not guaranteed or endorsed by the publisher.

Copyright © 2022 Cui, Nie, Zhu, Danish, Weiner, Chundury, Ohri, Zhang, Vergalasova, Yue and Wang. This is an open-access article distributed under the terms of the Creative Commons Attribution License (CC BY). The use, distribution or reproduction in other forums is permitted, provided the original author(s) and the copyright owner(s) are credited and that the original publication in this journal is cited, in accordance with accepted academic practice. No use, distribution or reproduction is permitted which does not comply with these terms.



The Impact of Optic Nerve Movement on Intracranial Radiation Treatment

Kun Qing^{1,2,3}, Ke Nie^{1*}, Bo Liu¹, Xue Feng², James R. Stone², Taoran Cui¹, Yin Zhang¹, Jiahua Zhu¹, Quan Chen⁴, Xiao Wang¹, Li Zhao⁵, Shreel Parikh⁶, John P. Mugler III², Sung Kim¹, Joseph Weiner¹, Ning Yue¹ and Anupama Chundury^{1*}

¹ Department of Radiation Oncology, Rutgers-Cancer Institute of New Jersey, Rutgers-Robert Wood Johnson Medical School, New Brunswick, NJ, United States, ² Department of Radiology, University of Virginia, Charlottesville, VA, United States, ³ Department of Radiation Oncology, City of Hope Medical Center, Duarte, CA, United States, ⁴ Department of Radiation Oncology, University of Kentucky, Lexington, KY, United States, ⁵ Department of Biomedical Engineering, Zhejiang University, Hangzhou, China, ⁶ Department of Medicine, Tuoro School of Osteopathic Medicine, New York, NY, United States

OPEN ACCESS

Edited by:

Brian Timothy Collins,
Georgetown University, United States

Reviewed by:

John E. Mignano,
Tufts University School of Medicine,
United States
Vanessa Figlia,
Advanced Radiation Oncology
Department, Italy

*Correspondence:

Anupama Chundury
ac1807@cinj.rutgers.edu
Ke Nie
kn231@cinj.rutgers.edu

Specialty section:

This article was submitted to
Radiation Oncology,
a section of the journal
Frontiers in Oncology

Received: 27 October 2021

Accepted: 24 January 2022

Published: 24 February 2022

Citation:

Qing K, Nie K, Liu B, Feng X,
Stone JR, Cui T, Zhang Y, Zhu J,
Chen Q, Wang X, Zhao L, Parikh S,
Mugler JP III, Kim S, Weiner J,
Yue N and Chundury A (2022)
The Impact of Optic Nerve Movement
on Intracranial Radiation Treatment.
Front. Oncol. 12:803329.
doi: 10.3389/fonc.2022.803329

Purpose: In radiotherapy, high radiation exposure to optic nerve (ON) can cause optic neuropathy or vision loss. In this study, we evaluated the pattern and extent of the ON movement using MRI, and investigated the potential dosimetric effect of this movement on radiotherapy.

Methods: MRI was performed in multiple planes in 5 human subjects without optic pathway abnormalities to determine optic nerve motion in different scenarios. The subjects were requested to gaze toward five directions during MRI acquisitions, including neutral (straight forward), left/right (horizontal movement), and up/down (vertical movement). Subsequently, the measured displacement was applied to patients with peri-optic tumors to evaluate the potential dosimetric effect of this motion.

Results: The motion of ON followed a nearly conical shape. By average, the anterior end of ONs moved with 10.8 ± 2.2 mm horizontally and 9.3 ± 0.8 mm vertically, while posterior end has negligible displacement. For patients who underwent stereotactic radiotherapy to a peri-optic tumors, the movement of ON in this measured range introduced non-negligible dosimetric effect.

Conclusion: The range of motion of the anterior portions of the optic nerves is on the order of centimeters, which may need to be considered with extra attention during radiation therapy in treating peri-optic lesions.

Keywords: radiation-induced optic neuropathy, MRI, optical nerve, stereotactic radiodirtherapy, radiation therapy

INTRODUCTION

Radiation-induced optic neuropathy (RION) can be a severe ocular complication in patients treated with radiotherapy (1). It often presents as an acute, profound, and irreversible loss of vision about 10–20 months after radiation exposure (2). It is believed that necrosis resulting from an overdose of radiation to the anterior visual pathway (AVP) is the primary cause of RION. Dosimetric studies have demonstrated that RION can occur when the cumulative dose to the AVP exceeds 50 Gy for conventional fractionation, or beyond 10Gy in a single fraction (2).

During radiation treatment, a planning margin, either a planning target volume (PTV) relative to clinical target volume (CTV) or planning risk volume (PRV) relative to organs at risk (OAR), is typically given to compensate for inter-/intrafractional motion and setup uncertainties. A 3-5 mm expansion is used for the optic apparatus in conventional radiation treatment, and a 0-1 mm expansion is used for single-/hypofractionated stereotactic radiosurgery (SRS). This concept is particularly crucial in SRS treatments, as the sharp dose falloff required near critical structures necessitates the reduction of small positional uncertainties that could have a sizable effect on radiation dose.

Compared to the optic chiasm (3), the range of movement for the optic nerve is known to be higher (4). Furthermore, instructing patients to fix their eyes on a single point for 5 minutes, or to close their eyes, did not significantly reduce movement (5). These findings implied the occurrence of non-negligible movement of the optic nerve, which may affect the dose exposure during radiotherapy. An accurate understanding of the magnitude of optic nerve movement is fundamental to the development of intracranial radiation treatment plans that minimize the risk of RION. The purpose of this study is to investigate the pattern and extent of optic nerve motion using serial MRI scans, and evaluate the potential dosimetric influence of this motion in representative patients with peri-optic tumors.

METHODS

Human Subjects and Image Acquisition

The MRI study was approved by the Institutional Review Board at University of Virginia. Five healthy subjects without any orbital or optic apparatus abnormalities were recruited, including three young subjects (ages 24, 30, and 35 yrs., all males) and two older subjects (a 65-year-old female and a 67-year-old male). MRIs were performed on a 3T MR scanner (Siemens Magnetom Prisma, Erlangen, Germany) with a 64-channel head/neck coil. Images were taken with T2-weighted FLAIR-HASTE acquisition (duration: 50-74 seconds, resolution: $0.7 \times 0.7 \times 3.0 \text{ mm}^3$, slice number 8-12 slices, TE/TR=90/3060ms, GRAPPA factor=4). All subjects were scanned in the supine position and were instructed to gaze in five different directions during MRI acquisitions: neutral (straight forward), left/right (horizontal movement), and up/down (vertical movement). Axial plane images were acquired for both eyes to assess horizontal motion and sagittal plane images of the right eyes were obtained to evaluate vertical motion. To be able to reproduce eye motion, extra scans assessing horizontal movement were taken on two different days within a 14-day window for the three younger subjects.

Motion Assessment

On day 1, a baseline was established using the acquired MRI with the eyes in the neutral position. All other scans captured at different eye positions or on different days were rigidly aligned to the baseline using Velocity (Varian Medical Systems, Palo Alto, CA). Three measurement points were created, an anterior end

connecting to the globe, a posterior end connecting to the optic canal along each optic nerve, and a middle point with equal distance between the optic nerve and the anterior/posterior ends. The L-R displacement was calculated along the axial plane to represent the horizontal movement of the eyes, while the S-I motion was assessed along the sagittal plane to represent vertical movement. The reproducibility of these points was also evaluated by comparing the repeated results to the initial ones. The extent of movement was further determined from the average displacement of the optic nerve as measured in the all subjects. Finally, a new motion-inclusive model was constructed based on the pattern of physiological movement of the optic nerve established from this study using Solidworks (Dassault Systèmes, Velizy-Villacoublay).

Dosimetric Impact

To evaluate the potential dosimetric effect of optic nerve movement, three patients with peri-optic tumors (defined as a lesion within 3-5 mm of the optic nerve) were identified: Patient #1 was diagnosed with a meningioma that was treated with external beam radiation utilizing two partial arcs to a total dose of 6600 cGy in 33 fractions on a Truebeam (Varian Medical Systems, Palo Alto, CA); Patient #2, was diagnosed with a pituitary adenoma that was treated with hypofractionated stereotactic radiosurgery to a total dose of 2500 cGy in 5 fractions using the Gamma Knife Icon™ (Elekta, Stockholm, Sweden); and Patient #3, who was diagnosed with an optic nerve sheath meningioma treated with proton beam therapy to a total dose of 5220cGy RBE in 29 fractions with the Mevion S250 Proton Therapy System (Mevion Medical Systems, Littleton, MA).

The planning images (CT or MRI), plan dose, and contours were transferred to Eclipse (Varian Medical Systems, Palo Alto, CA) for direct comparison. We then further simulated the effect of optic nerve movement by creating a new estimated contour that was conically expanded from the original contour, effectively generating a motion-inclusive margin. The maximum point dose (D_{\max} or $D_{0.035\text{cc}}$) and $D_{0.2\text{cc}}$ to the optic nerve on both the conventional and motion-inclusive margin models were obtained, while the D_{\min} to the GTV and D_{95} for the PTV were reported in the worst-case scenarios and then compared with the actual/original values.

RESULTS

Representative Images Showing Movement Pattern

A representative case showing optic nerve movement in the left-right (L-R, axial plane) and superior-inferior (S-I, sagittal plane) directions is displayed in **Figures 1** and **2**. The middle images demonstrate the neutral position with the subject looking straight forward, while the others show the subject gazing in different directions. It is evident that the optic nerves move in the opposite direction relative to the lens. When the subject's gaze was guided to the left, the optic nerves moved to the right,

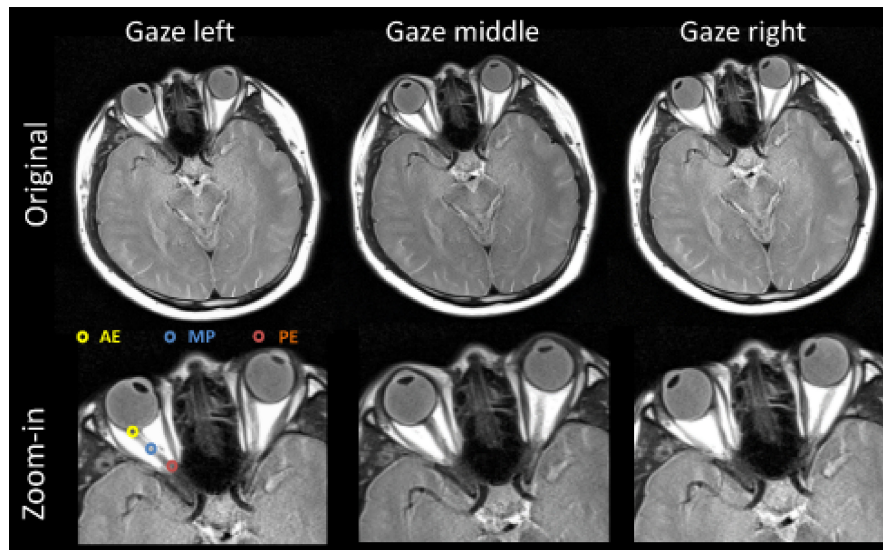


FIGURE 1 | Representative axial view images obtained from subject S1 (29-year-old male). Optic nerve structure and measurement points are shown as: the anterior end (AE) of the optic nerve connects to the globe, the posterior end (PE) connects to the optic canal, and the middle point (MP) is the midpoint of the optic nerve. It is quite evident that the anterior ends of both optic nerves move quite substantially in the opposite direction of the motion of the eyes (lens), as compared to their locations when the subject is looking straight forward (gaze middle).

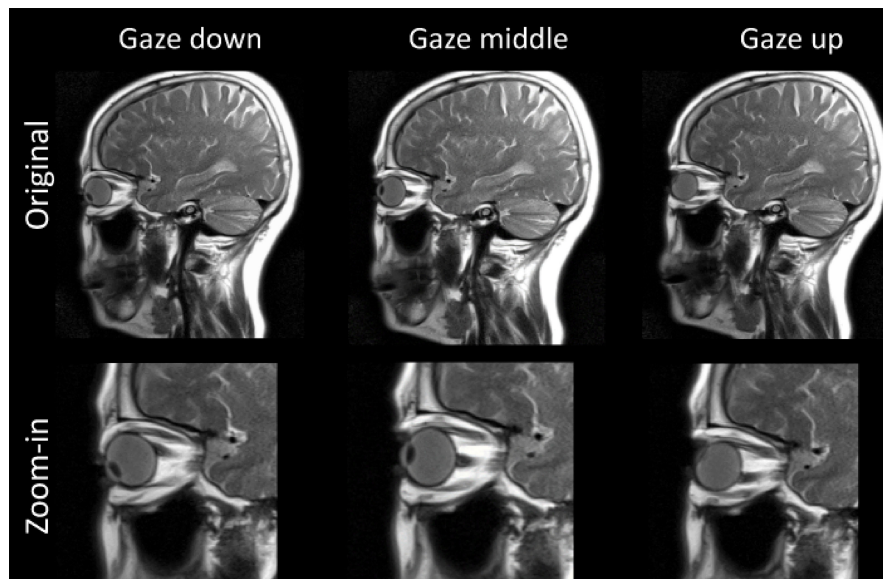


FIGURE 2 | Representative images obtained from subject S4 (65-year-old female) for vertical movement of the eyes. Similarly, the anterior ends of both optic nerves move in the opposite direction of the vertical motion of the eyes (lens).

whereas when the subject was instructed to gaze upwards, the optic nerves moved downwards. Additionally, regardless of eye movement, the posterior end of the optic nerve, where it exits the optic canal, demonstrated minimal movement. Overall, the anterior end had a larger magnitude of displacement relative to the posterior end.

Motion Assessment

Movement was assessed *via* both horizontal and vertical movement. As shown in **Table 1**, the anterior end (AE) moved in the range of centimeters horizontally, with an average of 10.4 ± 2.2 mm and 11.1 ± 1.4 mm for the left and right eyes, respectively. Conversely, the posterior end (PE) had minimal

TABLE 1 | Horizontal movement of the optic nerves.

	Horizontal Movement						Vertical Movement		
	Right Eye			Left Eye			Right Eye		
	L*->C*	C->R*	L->R	L->C	C->R	L->R	U*->C	C->D	U->D
Anterior(mm)	4.9±0.8	6.2±0.3	11.1±1.4	5.9±0.7	4.6±1.3	10.4±2.2	5.311.7	4.212.1	9.310.8
Middle(mm)	2.6±0.5	3.0±0.6	5.2±0.6	3.2±0.3	2.1±0.8	5.111.3	3.110.9	2.1±1.1	5.110.8
Posterior(mm)	0.7±0.3	0.5±0.2	0.8±0.3	0.3±0.4	0.3±0.2	0.410.2	0.4±0.3	0.4±0.3	0.5±0.3

*denotes five directions: L, Left; C, Center; R, Right; U, Upwards; D, Downwards.

movement, being within 1 mm. The middle point (MP) movement is equivalent for both eyes and is about half of the AE movement, with 5.1 ± 1.3 mm both the left and right eyes. The same motion pattern was observed regarding vertical movement. The anterior end moved with an average distance of 9.3 ± 0.8 mm going up/down, and the posterior end connecting to the optic canal showed minimal motion. From these results, it can be postulated that the optic nerve rotates around the PE, where it exits the optic canal, and moves within a conical shape, as shown in **Figure 3**.

Repeatability:

Horizontal movement was tested in the three younger subjects (S1-S3). The mean differences were 1.1 mm for left eye and 1.2 mm for the right eye while the maximal differences for the left and right eyes were 2.7 and 3.8 mm respectively.

Dosimetric Impact

Three clinical cases were selected to evaluate the dosimetric impact of possible optic nerve motion. Two cases (Patients #1 and 2) had optic nerves in close proximity to the target volumes, while a third case (Patient #3) had an optic nerve sheath meningioma where the nerve was part of the target volume itself. A conical shape with fixed PE and a 5 mm expansion for the AE was used to create a

motion-inclusive planning optic nerve margin for all cases to evaluate the dosimetric impact further.

Patient #1, as shown in **Figure 4**, was diagnosed with a meningioma that treated with two partial arcs to a total dose of 6600 cGy in 33 fractions. In the original treatment plan, a conventional 3 mm expansion was used to create the optic nerve PRV. According to the latest QUANTEC recommendation for conventional fractionation (6), the estimated risk of toxicity for the optic apparatus is < 3% when the maximum point dose, D_{\max} is less than 55Gy, 3%-7% if D_{\max} is within 55-60Gy, and 7-20% when D_{\max} is larger than 60Gy. In the patient's original plan the D_{\max} of the optic nerve is approximately 52 Gy (**Table 2**), which is within the tolerance limit; however, with the consideration of possible optic nerve movement, the D_{\max} could have increased to 56 Gy, falling into the range of increased risk (3-7%) for developing optic neuropathy (RION).

Patient #2, as shown in **Figure 5**, was diagnosed with a peri-optic pituitary adenoma treated with hypofractionated SRS to a total dose of 2500 cGy in 5 fractions. When utilizing the motion-inclusive margin, the maximum point dose $D_{0.035\text{ cc}}$ (the dose covering the 0.035cc volume receiving highest dose), as shown in **Table 2**, increased from 24.4 Gy (clinically acceptable) to 25.2 Gy, which is above the dose constraint of 25 Gy, in accordance with AAPM TG-101 (7). The $D_{0.2\text{ cc}}$ (the dose covering the 0.2cc

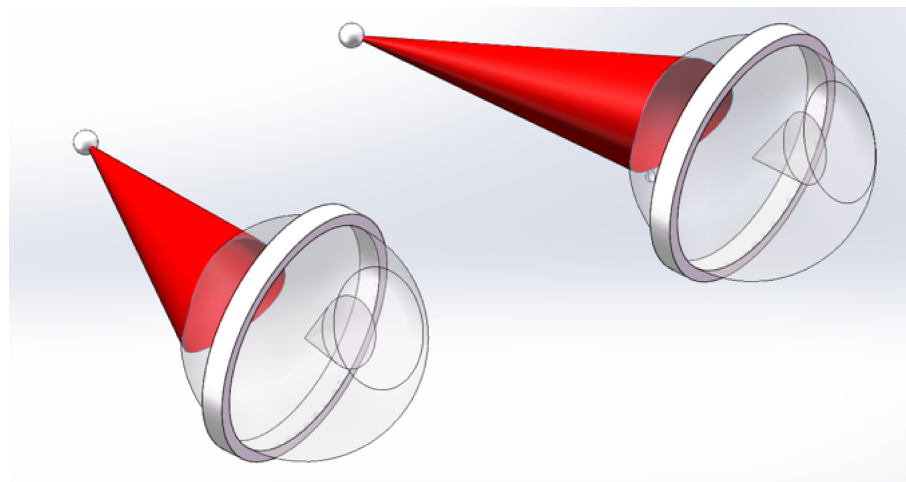


FIGURE 3 | Images generated by Solidworks (Dassault Systèmes, Velizy-Villacoublay), showing the range of motion (red) for the optic nerves based on measurement of anatomy gathered from MRI of subject S1.

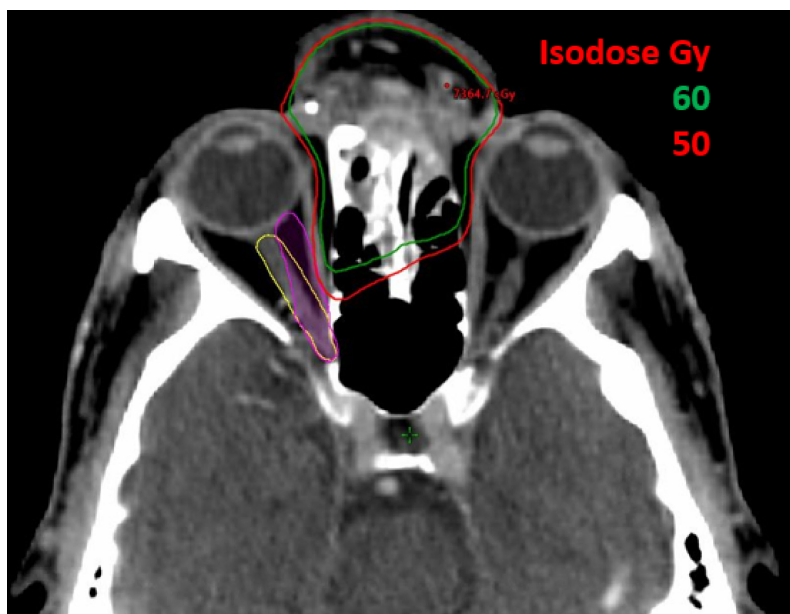


FIGURE 4 | A 61-year-old male patient with skin cancer who was previously treated on Truebeam (Varian Medical Systems, Palo Alto, CA) for 66 Gy in 33 fractions. Original contour for optic nerve is shown in yellow and optic nerve with motion in worst scenario is shown in purple contour.

TABLE 2 | Changes of maximal doses due to potential movement of optic nerves.

	D_{max} (Gy)	D_{0.035cc} (Gy)	D_{0.2cc} (Gy)	D_{0.5cc} (Gy)
Patient #1	52.0→55.7	50.0→51.6	47.1→49.4	42.9→45.3
Patient #2	26.9→31.6	25.6→26.3	22.9→23.4	13.4→12.8*

Values before and after symbol → are original doses and doses after potential movement of optic nerve. * decrease of D_{0.5cc} is because the total volume of the optic nerve is 0.7cc. Even though the maximal dose increases, the minimal dose covering the 0.5cc volume decreases.

volume receiving highest dose) increased from 22.9 Gy to 23.4 Gy, which also exceeded the recommended dose constraints (≤ 23 Gy) as per protocol (7).

Patient #3, as shown in **Figure 6**, was diagnosed with an optic nerve sheath meningioma with a large portion of the optic nerve itself being targeted with proton beam therapy to a total relative biologically effective (RBE) dose of 5220 cGy in 29 fractions. The PTV percent volume that received at least 95% of the prescription dose (D₉₅, yellow) with conventional 3 mm expansion from the GTV was 95% of the prescription dose in the treated plan; however if the motion-inclusive expansion PTV (purple) was utilized, the D₉₅ target coverage actually dropped to 92%, as shown in **Figure 6**. The minimum dose, D_{min}, to the gross tumor volume (GTV) also dropped from 95% of the prescription dose in the treated plan to 90% with the motion-inclusive expansion as shown in **Figure 6**.

DISCUSSION

The purpose of this study was to identify the extent of optic nerve motion using MRI and to further evaluate the dosimetric impact on periorbital lesions that have undergone radiation treatment. Optic

nerve motion was found to be in the opposite direction of globe motion and followed a nearly conical shape. The displacement of the PEs of the optic nerves, where they adjoin the optic canal, was minimal (within 1 mm) in all subjects, yet the displacement of the AEs of the nerves, where they connect to the globes, could be over 10 mm. A simple rigid motion model was applied to three clinical scenarios to evaluate the dosimetric effects of optic nerve movement based on the finding of this study. In these three cases, non-negligible dosimetric changes were observed.

A few studies have investigated optic nerve motion previously. Clarke et al. (8) demonstrated that by having patients look at different sides the optic nerves could move up to 6 mm as compared to the neutral position, based on CBCT images of four patients. In a study investigating optimal MRI sequence design for optic nerve disease by Moodley et al. (4), it was found that the mean total distance that the optic nerves travel during eye movement was 11.8 mm; however, none of these prior studies systematically evaluated the movement patterns for the optic nerves in multiple directions, nor did they further assess the dosimetric impact of these movements.

Although the absolute risks of RION remain relatively low in most patients, the risk for toxicity increases exponentially as

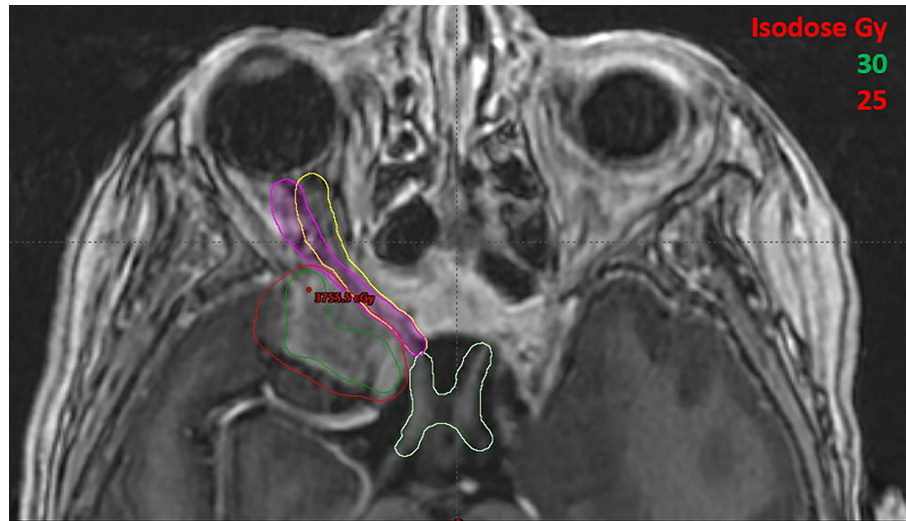


FIGURE 5 | A female patient with a peri-optic pituitary adenoma treated with hypofractionated SRS for 2500 cGy in 5 fractions. Original contour for optic nerve is shown in yellow and optic nerve with motion in worst scenario is shown in purple contour.

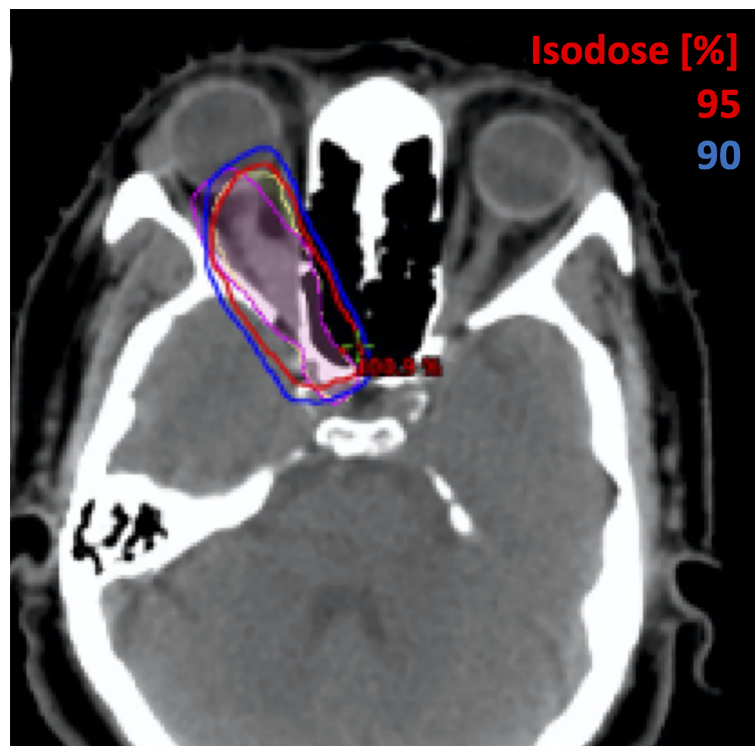


FIGURE 6 | A 51-year-old female with a benign meningioma treated on the Mevion S250 Proton Therapy System (Mevion Medical Systems, Littleton, MA) for 52.2 Gy in 29 fractions. Original contours for GTV and PTV are shown in yellow and GTV and PTV moving with optic nerve in worst scenario are shown in purple contours.

therapeutic dose increases. This is especially true in patients with peri-optic lesions such as meningiomas, pituitary adenomas etc., where hypofractionated SRS can be the definitive treatment. Due to sharp dose falloff required near critical structures with SRS,

even small uncertainties in position could have a sizeable effect on the radiation dose delivered. The risk of RION can be further increased in patients who have undergone prior radiation treatments to the same area, where avoiding excessive dose to

the optic nerve is crucial. For SRS, most clinical sites use either no margin or 1 mm margins for the optic nerve contours/PRV. For conventional external beam treatment, a 3 to 5 mm margin is generally used, pending image guidance and treatment technique. The results obtained from this study demonstrated that the displacement of the optic nerves as patients change the direction of their gaze can exceed these defined margins, and this may lead to insufficient dosing to the target volume if the tumor is of the optic nerve (i.e., optic sheath meningioma), or excessive dosage to the organs at risk (i.e., optic nerve itself) if the PTV is adjacent to the nerve. One may argue that for conventionally fractionated external beam radiation therapy, treatment is divided into multiple fractions over a long course. The eyeball movement is likely be averaged out in all directions. However, for single-fraction SRS or hypofractionated SRT, the optic nerve motion could result in a higher impact, especially when patients are treated with high-dose-rate beams (e.g. 1400MU/min for 6FFF beam). Additionally, majority of patients treated in radiation oncology are simulated with CT images, which only take a few seconds. If the patient is simulated with optic nerves at non-neutral positions the dosimetric estimation regarding the nerves itself could be inaccurate since the treatment plan was purely generated based on that image set. A possible solution to this could be that patients may need to be counseled to look straight ahead (or in a pre-determined direction based on target location) or to utilize eye-tracking if deemed necessary (9, 10). Furthermore, during treatment, it may be beneficial to guide the patient to look towards the desired optimal side/direction, in order to minimize the radiation dose to the optic nerve. Nevertheless, data on how far and frequently the patients move their eyes during the entire course of radiation treatment and how stable the optic nerve can stay at neutral position with/without couching, although beyond the scope of the current study, warrants larger-scale clinical investigations.

This study has a few limitations. First, to shorten the imaging acquisition time for improved patient comfort, two-dimensional imaging sequences with relatively thick slices (3mm) were used. Even though the in-plane resolution is relatively high (0.7 mm), the thicker slices could still lead to uncertainty in the measured range of movement. Given the imaging parameters, this uncertainty should not exceed 1-2 mm, which does not affect the conclusion of this study. In addition, a rigid movement model was assumed throughout the course of the study. The optic nerve, being an organ consisting of soft tissue, deforms with motion. Based on imaging results, the anterior portion of the optic nerves, which are close to the posterior walls of the globes, followed the rotation of the globes and bent towards their posterior aspects. This slightly reduces the actual movement of the optic nerves following the motion of the globes. The rigid movement model used in this study serves as a conservative estimate for the range of motion. It also shows that optic nerves maintain linear shapes following movement. This is consistent with the findings that displacement of the middle points of the optic nerves is always close to half of the displacement values measured for the anterior portions. Therefore, a rigid movement model, which may overestimate the movement slightly, should

still provide a very reasonable and relatively accurate estimation of the range of motion. Finally, the clinical impact of the dosimetric changes found based on the motion-inclusive model warrants more investigation. A prospective study with larger cohort of patients would better elucidate the overall impact on reducing the incidence of RION or improving tumor control, especially in stereotactic radiation therapy with reduced margins of the OARs and/or targets. Future work with accumulation of relevant cases with thinner image slices and longitudinal follow-up will be needed.

CONCLUSION

In this exploratory study, the optic nerves were found to follow a nearly conical shape relatively to the motion of the eyes. The range of motion of the anterior portions of the optic nerves was on the order of centimeters, which exceeds the current considerations in the field of clinical radiation oncology. Special attention may be needed for radiation simulation, treatment planning, and treatment monitoring to avoid excessive dosage to the optic nerves, or to ensure sufficient coverage of the target on the optic nerves, depending on varying clinical scenarios.

DATA AVAILABILITY STATEMENT

The raw data supporting the conclusions of this article will be made available by the authors, without undue reservation.

ETHICS STATEMENT

The studies involving human participants were reviewed and approved by the University of Virginia. The patients/participants provided their written informed consent to participate in this study.

AUTHOR CONTRIBUTIONS

KQ set up the MR protocols, analyzed the data, and wrote the manuscript. KN and AC designed the study, provided patient data, evaluated treatment plan, and revised the manuscript. JS evaluated the MR protocols, supervised the MR studies. JW provided patient data and evaluated the treatment plan. BL prepared **Figures 2–6**, assisted KQ to analyze the data, and revised the manuscript. XF scanned the healthy volunteers on MR scanner and assisted KQ to collect imaging data. TC, YZ, JZ, and XW provided patient data and helped KQ to generate comparison treatment plan. QC analyzed the MRI data and assisted in manuscript writing SP assisted in manuscript writing and data analysis. SK provided patient data and evaluated treatment plan. All authors contributed to the article and approved the submitted version.

REFERENCES

1. Wang W, Yang H, Guo L, Su H, Wei S, Zhang X. Radiation-Induced Optic Neuropathy Following External Beam Radiation Therapy for Nasopharyngeal Carcinoma: A Retrospective Case-Control Study. *Mol Clin Oncol* (2016) 4:868–72. doi: 10.3892/mco.2016.787
2. Danesh-Meyer HV. Radiation-Induced Optic Neuropathy. *J Clin Neurosci* (2008) 15:95–100. doi: 10.1016/j.jocn.2007.09.004
3. Xiang M, Chan C, Wang L, Jani K, Holdsworth SJ, Iv M, et al. Physiological Motion of the Optic Chiasm and its Impact on Stereotactic Radiosurgery Dose. *Br J Radiol* (2019) 92:20190170. doi: 10.1259/bjr.20190170
4. Moodley A, Rae WID, Brijmohan Y, Durand M, Connolly C, Michowicz A, et al. The Impact of Optic Nerve Movement on Optic Nerve Magnetic Resonance Diffusion Parameters. *SA J Radiol* (2014) 2014:18. doi: 10.4102/sajr.v18i1.596
5. Wheeler-Kingshott CA, Trip SA, Symms MR, Parker GJ, Barker GJ, Miller DH. *In Vivo* Diffusion Tensor Imaging of the Human Optic Nerve: Pilot Study in Normal Controls. *Magnetic Resonance Med* (2006) 56:446–51. doi: 10.1002/mrm.20964
6. Marks LB, Yorke ED, Jackson A, Ten Haken RK, Constone LS, Eisbruch A, et al. Use of Normal Tissue Complication Probability Models in the Clinic. *Int J Radiat Oncol Biol Phys* (2010) 76:S10–9. doi: 10.1016/j.ijrobp.2009.07.1754
7. Benedict SH, Yenice KM, Followill D, Galvin JM, Hinson W, Kavanagh B, et al. Stereotactic Body Radiation Therapy: The Report of AAPM Task Group 101. *Med Phys* (2010) 37:4078–101. doi: 10.1118/1.3438081
8. Clarke K, Fogarty GB, Lo S, Izard M, Hong A. Optic Nerve Movement May Need to be Considered When Treating With Stereotactic Radiosurgery. *J Nucl Med Radiat Ther* (2017) 08:321–3. doi: 10.4172/2155-9619.1000321
9. Fassi A, Riboldi M, Forlani CF, Baroni G. Optical Eye Tracking System for Noninvasive and Automatic Monitoring of Eye Position and Movements in Radiotherapy Treatments of Ocular Tumors. *Appl Optics* (2012) 51:2441–50. doi: 10.1364/AO.51.002441
10. Via R, Fassi A, Fattori G, Fontana G, Pella A, Tagaste B, et al. Optical Eye Tracking System for Real-Time Noninvasive Tumor Localization in External Beam Radiotherapy. *Med Phys* (2015) 42:2194–202. doi: 10.1118/1.4915921

Conflict of Interest: The authors declare that the research was conducted in the absence of any commercial or financial relationships that could be construed as a potential conflict of interest.

Publisher's Note: All claims expressed in this article are solely those of the authors and do not necessarily represent those of their affiliated organizations, or those of the publisher, the editors and the reviewers. Any product that may be evaluated in this article, or claim that may be made by its manufacturer, is not guaranteed or endorsed by the publisher.

Copyright © 2022 Qing, Nie, Liu, Feng, Stone, Cui, Zhang, Zhu, Chen, Wang, Zhao, Parikh, Mugler, Kim, Weiner, Yue and Chundury. This is an open-access article distributed under the terms of the Creative Commons Attribution License (CC BY). The use, distribution or reproduction in other forums is permitted, provided the original author(s) and the copyright owner(s) are credited and that the original publication in this journal is cited, in accordance with accepted academic practice. No use, distribution or reproduction is permitted which does not comply with these terms.



Please Place Your Seat in the Full Upright Position: A Technical Framework for Landing Upright Radiation Therapy in the 21st Century

Sarah Hegarty^{1,2}, Nicholas Hardcastle^{2,3,4}, James Korte^{2,5}, Tomas Kron^{2,3,4}, Sarah Everitt^{4,6}, Sulman Rahim⁶, Fiona Hegi-Johnson^{4,7} and Rick Franich^{1,2*}

¹ School of Science, RMIT University, Melbourne, VIC, Australia, ² Department of Physical Sciences, Peter MacCallum Cancer Centre, Melbourne, VIC, Australia, ³ Centre for Medical Radiation Physics, University of Wollongong, Wollongong, NSW, Australia, ⁴ Sir Peter MacCallum Department of Oncology, Faculty of Medicine, Dentistry and Health Science, University of Melbourne, Parkville, VIC, Australia, ⁵ Department of Biomedical Engineering, School of Engineering, University of Melbourne, Melbourne, VIC, Australia, ⁶ Department of Radiation Therapy, Peter MacCallum Cancer Centre, Melbourne, VIC, Australia, ⁷ Department of Radiation Oncology, Peter MacCallum Cancer Centre, Melbourne, VIC, Australia

OPEN ACCESS

Edited by:

Jason W. Sohn,
Allegheny Health Network,
United States

Reviewed by:

Danny Lee,
Allegheny Health Network,
United States

*Correspondence:

Rick Franich
rick.franich@rmit.edu.au

Specialty section:

This article was submitted to
Radiation Oncology,
a section of the journal
Frontiers in Oncology

Received: 24 November 2021

Accepted: 27 January 2022

Published: 03 March 2022

Citation:

Hegarty S, Hardcastle N, Korte J,
Kron T, Everitt S, Rahim S, Hegi-
Johnson F and Franich R (2022)
Please Place Your Seat in the Full
Upright Position: A Technical
Framework for Landing Upright
Radiation Therapy in the 21st Century.
Front. Oncol. 12:821887.
doi: 10.3389/fonc.2022.821887

Delivering radiotherapy to patients in an upright position can allow for increased patient comfort, reduction in normal tissue irradiation, or reduction of machine size and complexity. This paper gives an overview of the requirements for the delivery of contemporary arc and modulated radiation therapy to upright patients. We explore i) patient positioning and immobilization, ii) simulation imaging, iii) treatment planning and iv) online setup and image guidance. Treatment chairs have been designed to reproducibly position seated patients for treatment and can be augmented by several existing immobilisation systems or promising emerging technologies such as soft robotics. There are few solutions for acquiring CT images for upright patients, however, cone beam computed tomography (CBCT) scans of upright patients can be produced using the imaging capabilities of standard Linacs combined with an additional patient rotation device. While these images will require corrections to make them appropriate for treatment planning, several methods indicate the viability of this approach. Treatment planning is largely unchanged apart from translating gantry rotation to patient rotation, allowing for a fixed beam with a patient rotating relative to it. Rotation can be provided by a turntable during treatment delivery. Imaging the patient with the same machinery as used in treatment could be advantageous for online plan adaption. While the current focus is using clinical linacs in existing facilities, developments in this area could also extend to lower-cost and mobile linacs and heavy ion therapy.

Keywords: patient positioning, upright, radiation therapy, lung cancer, immobilization

INTRODUCTION

Radiation therapy is delivered predominantly to patients in the recumbent position on a treatment couch, with a gantry rotating around them to deliver radiation from prescribed angles. Recumbent positioning is intrinsically linked to the acquisition of the required volumetric imaging used for treatment planning. The inherent stability this position provides was particularly important for early computed tomography (CT) scanners, which were quite slow (1).

There are several potential advantages to treating selected patients in an upright position instead of recumbent (2). Some conditions, such as obesity, heart problems, superior vena cava obstruction and phrenic nerve injury, can result in respiratory difficulty when in a supine position resulting in uncomfortable treatment (3, 4). Patients may be unable to complete treatment as a result or have compromised treatment due to poor position stability. Patient position can also influence the position of some tumours and organs at risk (OARs). Treating mediastinal tumours in upright patients resulted in reduced normal lung tissue irradiation due to an increase in lung volume (5–7). An upright position can also reduce the effect of respiratory motion, potentially resulting in reduced normal tissue dose (8). Further, with appropriate immobilization, an upright patient could be comfortably rotated relative to a fixed beam to vary the treatment angle, reducing the need for a rotating gantry (9). Gantry-free treatment is being explored *via* horizontal patient rotation but is complicated by challenges such as angle-dependent patient deformation due to gravity (10, 11). Importantly, the vertical rotation could be done faster than a gantry rotation around the patient (increasing from less than 1 rpm to as much as 3–7 rpm, such as used for Total Skin Electron Treatment) thereby increasing scope for breath-hold and improving image quality (12, 13).

The present work is focused on implementing upright positioning for routine, contemporary photon treatments, including intensity and field-modulated capabilities, using clinical linear accelerators. Aside from the immediate potential benefits outlined above, upright patient positioning may facilitate shrinkage of the machine and shielding and reduction in machine complexity. Such size and complexity reductions open up the potential for portable and low-physical footprint radiation therapy devices. However, other modalities may likely benefit from further addressing the challenges associated with upright radiation therapy. Indeed, some work in this direction already exists in the context of particle beam therapies (14). A dedicated system exists to deliver particle therapy to upright patients *via* a suite of specifically designed equipment (15). While comprehensive, the system is only likely to be implemented in the largest or most specialised centres. The high cost and space requirements of rotating gantries, especially for very heavy ions such as carbon, make upright patient geometry attractive in this setting.

We previously reviewed the historical applications of upright radiation therapy, relevant recent developments and potential benefits (2). While upright radiation therapy has been delivered in various forms, these have typically been limited in complexity and often for palliative intent. The current paper describes the technical requirements and potential solutions for the delivery of radiation therapy to upright patients of the same quality as that achieved in current recumbent treatments. Our current focus relates to state-of-the-art delivery *via* implementation in existing linear accelerator facilities, with a minimum of bespoke additional equipment. This is likely to produce the most immediate clinical benefits and allow for upright patient positioning to become a routine treatment modality option.


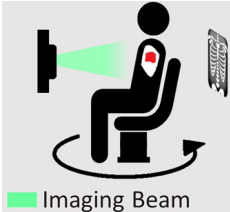

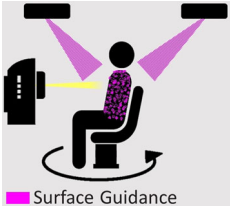
The current framework covers patient positioning and immobilization, simulation imaging, treatment planning and online setup and image guidance (see **Table 1**).

PATIENT POSITIONING AND IMMOBILIZATION

Contemporary radiation therapy is delivered using beams from multiple angles, or continuous arcs around the patient, to improve conformity and reduce dose to critical organs. A fundamental requirement is thus rotation of the radiation beam around the patient, or rotation of a patient relative to a static beam. Transposition of the primary anatomical axis relative to the conventional treatment orientation and the gantry rotation axis will be required. If using a conventional linear accelerator, the patient will therefore need to rotate with respect to the treatment beam to replicate contemporary treatments. Some specifically designed chairs for upright patients have an inbuilt rotating platform suitable for this purpose, but an independent mechanism such as a turntable is also acceptable and could accommodate a range of supports (16). The platform or turntable should be able to rotate continuously or to prescribed angles with a high level of accuracy, and ideally achieve 360° of rotation (17). If the turntable is not permanently in place in the treatment suite, it must be reproducibly positioned each time and calibrated to ensure alignment of its centre of rotation with the imaging and treatment beam isocentre (18). The patient support should feature independent translational adjustment of the patient position relative to the turntable, to facilitate alignment of the target to the rotational and treatment beam isocentres.

When treating a patient in an upright position, a challenge is introduced due to the potential loss of the stability typically provided by the treatment couch for recumbent patients. Patient immobilization devices connected to a turntable, which can rotate the patient relative to the static imaging and treatment beams. The level of support required, such as a seat, stool, or standing frame, will depend on the target location, performance status of the patient, and their ability to remain in the required position for the duration of the procedure. Additional fixation devices, analogous to those currently used in conjunction with the usual couch, can be adapted to be compatible with upright supports mounted on the rotating system (19). Several examples of in-house upright patient positioning have been reported. To treat a thymic carcinoma, a standing patient was secured to a back support with the aid of a belt (20). A similar approach could be used for prostate, rectal or gynaecological patients. A method has been evaluated for treating head and neck cancer (HNC) patients with a forward tilting chair. A thermoplastic mould was wrapped around the back of the head, connecting to a plate with a variable angle. This method was reported to have adequate reproducibility and patient comfort making it a viable option for positioning HNC patients upright (21). Based on an *ad hoc* method of breast immobilisation for upright treatment,

TABLE 1 | Overview of the key requirements that need to be met for clinical upright radiation therapy, and the proposed solutions that are detailed in this paper. This includes patient position and immobilization, treatment planning imaging, treatment planning, and online setup and image guidance.

	Requirements	Proposed solution
Patient positioning and immobilization 	<ul style="list-style-type: none"> • Upright, reproducible, stable, comfortable position • Rotate patient relative to the treatment beam • Angular control with feedback to the delivery system 	<ul style="list-style-type: none"> • Chairs and standing frames • Adapt existing immobilization devices • Augmented by soft robotics • Turntable with interfaced control
Treatment planning imaging 	<ul style="list-style-type: none"> • High-quality 3D and 4D images of an upright patient • Accurate tissue classification/HU for dose calculation • Geometrically accurate 	<ul style="list-style-type: none"> • Upright CT/MRI scanner • Linac onboard CBCT with HU corrections • Deformable registration from recumbent multi-modality imaging
Treatment planning 	<ul style="list-style-type: none"> • TPS accepts upright treatment geometry • Gantry rotation transposed to patient rotation • Implementation of 3DCRT, IMRT, VMAT 	<ul style="list-style-type: none"> • Expand upright geometry availability to photon/electrons • Turntable rotation included as planning and optimization variable
Online setup and image guidance 	<ul style="list-style-type: none"> • In-room patient setup: pose and isocenter alignment • Planar and volumetric imaging for tumour targeting • Continuous patient position monitoring 	<ul style="list-style-type: none"> • Laser/surface guidance systems adapted for an upright position • Upright 2D/3D/4D on-board imaging using kV/MV photons or MRI • Online position monitoring adapted for a continuously moving patient

thermoplastic moulds could be used for breast shape optimisation (22). Due to the potential reduction in respiratory motion for upright patients, the need for motion management such as free-breathing gating or breath-hold for thoracic and upper abdominal tumours may be decreased (8). Recently, systems for upright patient positioning have been developed, including a chair designed to position and rotate patients for HNC treatment using fixed beamline carbon ion therapy (16, 23). Patient stability may be aided by novel solutions, such as soft robotics, as currently used in rehabilitation (24). Several implementations of soft robotics currently being assessed include mask free HNC treatment, upright patient stabilisation and patient stability for horizontal rotation (25–27). The HNC example uses a camera to monitor head position and a pneumatic air bladder system to control position. A similar

approach could be adapted for upright patients. While not commercially available yet, this supports the potential for upright patient positioning to be clinically implemented in the near future.

SIMULATION IMAGING

Simulation images should be a 3D representation of the anatomy in the treatment position. Anatomical changes between supine and upright images may be significant in the thoracic, abdominal, and pelvic regions due to gravity and posture. In some cases, these changes are the motivation for pursuing upright orientation. Image quality must be adequate to

accurately delineate the target volumes and nearby critical organs and be free from geometric distortion. Voxel data must be converted into media information for dose calculation, which typically relies on accurate Hounsfield Units (HU) in the image or an accurate method of mapping material compositions and densities to an acquired image. Standard CT scanners are unable to image an upright patient, making an alternative imaging approach necessary. Dedicated vertical CT scanners exist which can produce the required images (20). However, these are highly specialised, and access to such a system is likely to be limited for most clinics.

A method has been proposed that uses the onboard imaging capabilities of linacs, removing the need for specialist equipment (28). The kV source and detector are fixed and projections are acquired as a seated patient is rotated at the isocentre, producing a cone-beam computed tomography (CBCT) scan. While the original approach used the treatment couch to perform the rotation, it could be substituted for a turntable, permitting a greater variety of patient positioning and an improved imaging speed. 4DCT is also an important part of simulation imaging for tumours subject to respiratory motion (29). Respiratory trace acquisition can be achieved similarly in the upright position using existing respiratory belts or through the use of projection data to derive the respiratory signal (30, 31).

The large radiation angle and detector required in CBCT increases scattered radiation reaching the detector, decreasing image contrast and rendering the HU inaccurate (32). To use CBCT images for treatment planning, improvements in image quality and HU consistency are required. Methods to estimate and correct for the influence of scatter on CBCTs include analytical and Monte Carlo based approaches, and more recently neural network and use of the linear Boltzmann equation (33–39). Other methods for improving CT number accuracy for dose calculations without scatter estimations include creating a synthetic CT *via* a bulk density override, generative adversarial network (GAN) or deformable image registration (DIR) (40–43).

The use of DIR may also be crucial for fusing multiple imaging modalities to deliver accurate radiation therapy to upright patients (44, 45). Intermodality fusion is already a standard part of supine treatment, used to assist with target and critical organ delineation (46). However, image fusion normally occurs between two images acquired with the same patient orientation. The larger anatomical differences between supine imaging modalities (like MR and PET imaging) and upright images may limit the accuracy of directly applying DIR. The upright case may require alternative strategies such as an intermediate step: first implementing the standard supine image fusion with diagnostic images to create required contours. DIR from supine CT to upright CBCT could transfer contours. Research has been undertaken to correct for large anatomical changes and lung changes in DIR, which has the potential to benefit supine-to-upright deformation (47, 48). The issues of image handling, registration and fusion may be the area requiring the most attention to realise routine upright radiotherapy.

TREATMENT PLANNING

The treatment planning process involves the determination of the appropriate beam angles or arc delivery angles, followed by optimisation of the beam apertures and fluences to achieve the planning goals (49). To deliver upright radiotherapy using standard linacs, gantry rotation would be transposed to patient rotation. Mechanical limitations including rotation speed, acceleration and angular range would need to be constrained in forward and inverse planning. A further consideration may be required on speed, acceleration and jerk with respect to patient comfort: this may be used as a constraint/objective in inverse planning of arc treatments. Speed and acceleration tolerances may vary between patients, making this a variable constraint to be considered to ensure patient comfort.

As with supine treatment, the requirements of treatment planning depend on the treatment to be delivered. Simpler treatments, such as 3D conformal radiation therapy (3DCRT) and intensity modulated radiotherapy (IMRT), require multiple beams at different angles around the patient. Typically a multileaf collimator (MLC) is used to shape the beam to the tumour for each angle or modulate the beam intensity (50, 51). Provided the upright patient DICOM simulation images can be imported into the software, current commercial treatment planning systems (TPS) can achieve this through maintenance of a static gantry angle and the use of couch angles to achieve the different beam angles. Treatment planning complexity increases with continuously moving beams such as in dynamic conformal arc therapy (DCAT) and Volumetric Modulated Arc Therapy (VMAT). A feedback loop will be necessary to ensure turntable rotation accuracy, especially for VMAT treatment with variable rotation speed. With minor modifications to optimisation, in which the beam angle is replaced by a turntable/couch angle, both DCAT and VMAT treatments could be planned with little difference compared with supine/prone treatment position.

Non-coplanar treatment to an upright patient with a conventional medical linac may also be feasible. Instead of using only a fixed gantry angle, it could be altered within a small range (likely dependent on immobilization). Further non-coplanar beam angle range could be achieved through the tilt of the patient positioning device. Most current TPS do not accept images in the upright patient geometry, with the exception of some particle therapy systems – the existence of which demonstrates that it is already implementable (52). With vendor cooperation, TPS capabilities could be extended to accept upright images. The ability of TPS to perform related tasks, such as image fusion and dose accumulation, with upright images would also be advantageous.

ONLINE SETUP AND IMAGE GUIDANCE

Patient positioning for treatment as per simulation typically involves set up using the external patient contour followed by

verification using imaging of the target and internal anatomy. Initial patient setup to the machine isocentre is typically achieved using lasers aligned to tattoos on the patient skin, or through surface guidance. In the upright scenario, a 'reference' position/rotation must be defined, which is how the patient will be set up before treatment. This may be the position of the first static treatment beam or the start of the first arc. Lasers and surface tracking may still be applied in the upright position, with optical or thermal surface guidance providing an elegant solution for upright patient positioning (53).

Once the patient is set up in the treatment position, images are acquired to validate anatomy and tumour position before treatment (54). Positional adjustments may then be required, potentially involving manually repositioning the patient or shifting the position of the treatment chair if it allows for 6 degrees of freedom (like current treatment couches). These images can be planar x-ray images or 3D volumetric images. While the image quality does not need to be the same as the simulation image, it still needs to be sufficient to validate patient alignment to ensure that the tumour receives the intended dose (54). Thus, the imaging system on a standard linac can be used to image an upright patient and allows for 2D and/or 3D setup image acquisition before treatment. The acquisition of simulation images using the same system as treatment may facilitate online adaptive radiotherapy, to account for anatomical changes or variations in daily patient positioning (55, 56).

Continuous monitoring of the patient's position during treatment could be achieved by using surface guidance to track the patient's external contour, with reference position updated for each beam (57). This will be more challenging for treatment with continuous rotation (like VMAT), requiring constant updating of the reference image. Positional monitoring could also be achieved *via* images acquired during treatment. If the imaging geometry is such that imaging and treatment can be performed contemporaneously then intra-treatment planar imaging could be used to track internal target anatomy during patient rotation using systems such as beacons or radio-opaque markers (58).

DISCUSSION

Delivering upright radiation therapy to an upright patient is achievable for the most part with current technology. Engagement from vendors would be required to make the treatment planning more clinically acceptable. Vendor cooperation could also aid in the production of simulation images through a formalised acquisition and correction pipeline. While not previously discussed, the shielding requirements for upright radiation therapy must be considered prior to the commencement of treatment. Assuming a fixed horizontal treatment beam for upright radiation therapy, there will only be one primary barrier. Depending on the department, this barrier may not have the required shielding and must be increased, adding an additional requirement for upright radiation therapy. However, concentrating the radiation, and

thus the shielding, in one direction would reduce the total amount of shielding required (59). This reduction, coupled with the potential decrease in cost and size of a fixed beam linac could lead to the potential for portable radiation therapy. It has been proposed to contain the equipment needed for radiation therapy in a truck or shipping container (59).

The framework paper is focused on high-quality MV photon treatment with the same geometric accuracy as recumbent treatment. However, the implementation of such treatment could serve as a gateway to particle therapy. Particle therapies produce advantageous dose distributions resulting in less damage to the normal tissue. However, delivering particle therapy to patients in conventional recumbent positions requires large rotating gantries which come at a considerable cost and technical complexity (60). Particle therapy facilities are frequently constructed with fixed beamlines, even when one or more gantries are included. Advances in patient positioning and rotation in front of a fixed beamline aperture may improve the usefulness of those fixed beams. Treatment of a patient in an upright position may also help to facilitate the use of Synchrotron radiation for emerging techniques such as microbeam radiation therapy (MRT) and FLASH radiotherapy (61, 62). Creating a practical workflow for upright radiation therapy on clinical linacs should help to progress research into upright particle and FLASH radiation therapy aiding their progression towards clinical implementation.

CONCLUSION

While radiation therapy is traditionally delivered to recumbent patients, we have provided a framework to deliver contemporary highly modulated radiation therapy to upright patients. Requirements that must be met for the four aspects of radiation therapy – patient positioning, simulation imaging, treatment planning and setup and image guidance – have been considered. We have identified the most promising developments in each of these areas that could lead to viable solutions, such that implementation in the near future is realistic and feasible. The framework has been written with the intent of routinely delivering upright radiation therapy in current centres with existing facilities and minimal new equipment. However, elements of the framework could be applied to other contexts where upright radiation therapy is preferable. It is hoped that introducing upright radiation therapy could allow patients to be more comfortable during their treatment, receive less normal tissue irradiation or have greater access to treatment.

DATA AVAILABILITY STATEMENT

The original contributions presented in the study are included in the article/supplementary material. Further inquiries can be directed to the corresponding author.

AUTHOR CONTRIBUTIONS

All authors listed have made a substantial, direct, and intellectual contribution to the work, and approved it for publication.

REFERENCES

- Beckmann EC. CT Scanning the Early Days. *Br J Radiol* (2006) 79(937):5–8. doi: 10.1259/bjr/29444122
- Rahim S, Korte J, Hardcastle N, Hegarty S, Kron T, Everitt S. Upright Radiation Therapy-A Historical Reflection and Opportunities for Future Applications. *Front Oncol* (2020) 10:213. doi: 10.3389/fonc.2020.00213
- Kopelman PG. Obesity as a Medical Problem. *Nature* (2000) 404(6778):635. doi: 10.1038/35007508
- Patterson SK. Phrenic Nerve. In: MJ Aminoff, RB Daroff, editors. *Encyclopedia of the Neurological Sciences*. 2 Ed. San Diego: Elsevier Inc (2014). p. 894–6.
- Miller R, Raubitschek A, Harrington F, Van de Geijn Ovadia J, Ovadia J, Glatstein E. An Isocentric Chair for the Simulation and Treatment of Radiation Therapy Patients. *Int J Radiat Oncol Biol Phys* (1991) 21(2):469–73. doi: 10.1016/0360-3016(91)90798-9
- Marcus KC, Svensson G, Rhodes LP, Mauch PM. Mantle Irradiation in the Upright Position: A Technique to Reduce the Volume of Lung Irradiated in Patients With Bulky Mediastinal Hodgkin's Disease. *Int J Radiat Oncol Biol Phys* (1992) 23(2):443–7. doi: 10.1016/0360-3016(92)90766-b
- Yamada Y, Yamada M, Yokoyama Y, Tanabe A, Matsuoka S, Nijima Y, et al. Differences in Lung and Lobe Volumes Between Supine and Standing Positions Scanned With Conventional and Newly Developed 320-Detector-Row Upright CT: Intra-Individual Comparison. *Respiration* (2020) 99:598–605. doi: 10.1159/000507265
- Yang J, Chu D, Dong L, Court LE. Advantages of Simulating Thoracic Cancer Patients in an Upright Position. *Pract Radiat Oncol* (2014) 4(1):e53–8. doi: 10.1016/j.prro.2013.04.005
- Whelan B, Welgampola M, McGarvie L, Makhija K, Turner RM, Holloway L, et al. Patient Reported Outcomes of Slow, Single Arc Rotation: Do We Need Rotating Gantry? *J Med Imaging Radiat Oncol* (2018) 62(4):553–61. doi: 10.1111/1754-9485.12688
- Buckley J, Rai R, Liney GP, Dowling JA, Holloway LC, Metcalfe PE, et al. Anatomical Deformation Due to Horizontal Rotation: Towards Gantry-Free Radiation Therapy. *Phys Med Biol* (2019) 64(17):175014. doi: 10.1088/1361-6560/ab324c
- Buckley JG, Smith AB, Sidhom M, Rai R, Liney GP, Dowling JA, et al. Measurements of Human Tolerance to Horizontal Rotation Within an MRI Scanner: Towards Gantry-Free Radiation Therapy. *J Med Imaging Radiat Oncol* (2021) 65(1):112–9. doi: 10.1111/1754-9485.13130
- Barnes MP, Rowshanfarzad P, Greer PB. VMAT Linear Accelerator Commissioning and Quality Assurance: Dose Control and Gantry Speed Tests. *J Appl Clin Med Phys* (2016) 17(3):246–61. doi: 10.1120/jacmp.v17i3.6067
- Radiation Products Design I. Rotational Total Body Irradiation (TBI) Stand 120 VAC USA: Radiation Products Design, Inc*. Available at: <https://www.rpdinc.com/rotational-total-body-irradiation-tbi-stand-120-vac-1744.html>.
- Yan S, Lu H-M, Flanz J, Adams J, Trofimov A, Bortfeld T. Reassessment of the Necessity of the Proton Gantry: Analysis of Beam Orientations From 4332 Treatments at the Massachusetts General Hospital Proton Center Over the Past 10 Years. *Int J Radiat Oncol Biol Phys* (2016) 95(1):224–33. doi: 10.1016/j.ijrobp.2015.09.033
- Leo Cancer Care* 2020. Available at: <https://www.leocancercare.com/>.
- Sheng Y, Sun J, Wang W, Stuart B, Kong L, Gao J, et al. Performance of a 6D Treatment Chair for Patient Positioning in an Upright Posture for Fixed Ion Beam Lines. *Front Oncol* (2020) 10:122. doi: 10.3389/fonc.2020.00122
- Klein EE, Hanley J, Bayouth J, Yin FF, Simon W, Dresser S, et al. Task Group 142 Report: Quality Assurance of Medical Accelerators a. *Med Phys* (2009) 36 (9Part1):4197–212. doi: 10.1118/1.3190392
- Gao S, Du W, Balter P, Munro P, Jeung A. Evaluation of IsoCal Geometric Calibration System for Varian Linacs Equipped With on-Board Imager and

ACKNOWLEDGMENTS

SH has been supported through the provision of an Australian Government Research Training Program Scholarship.

- Electronic Portal Imaging Device Imaging Systems. *J Appl Clin Med Phys* (2014) 15(3):164–81. doi: 10.1120/jacmp.v15i3.4688
- Q-Fix K Vue 53cm Couch Compatible Treatment Chair: Radiation Products Design, Inc. Available at: <https://www.rpdinc.com/q-fix-k-vue-53cm-couch-compatible-treatment-chair-9314.html>.
- Shah AP, Strauss JB, Kirk MC, Chen SS, Kroc TK, Zusag TW. Upright 3d Treatment Planning Using a Vertical Ct. *Med Dosimetry* (2009) 34(1):82–6. doi: 10.1016/j.meddos.2008.05.004
- McCarroll RE, Beadle BM, Fullen D, Balter PA, Followill DS, Stingo FC, et al. Reproducibility of Patient Setup in the Seated Treatment Position: A Novel Treatment Chair Design. *J Appl Clin Med Phys* (2017) 18(1):223–9. doi: 10.1002/acm2.12024
- Mohiuddin MM, Zhang B, Tkaczuk K, Khakpour N. Upright, Standing Technique for Breast Radiation Treatment in the Morbidly-Obese Patient. *Breast J* (2010) 16(4):448–50. doi: 10.1111/j.1524-4741.2010.00932.x
- Zhang X, Hsi WC, Yang F, Wang Z, Sheng Y, Sun J, et al. Development of an Isocentric Rotating Chair Positioner to Treat Patients of Head and Neck Cancer at Upright Seated Position With Multiple Nonplanar Fields in a Fixed Carbon-Ion Beamline. *Med Phys* (2020) 47:2450–60. doi: 10.1002/mp.14115
- Cianchetti M, Laschi C, Menciassi A, Dario P. Biomedical Applications of Soft Robotics. *Nat Rev Materials* (2018) 3(6):143–53. doi: 10.1038/s41578-018-0022-y
- Ogunmolu O, Gu X, Jiang S, Gans N. A Real-Time Soft Robotic Patient Positioning System for Maskless Head-And-Neck Cancer Radiotherapy: An Initial Investigation. *Med Phys* (2015) 42(6):3266. doi: 10.1118/1.4924100
- Buchner T, Yan S, Li S, Flanz J, Hueso-Gonzalez F, Kietly E, et al. A Soft Robotic Device for Patient Immobilization in Sitting and Reclined Positions for a Compact Proton Therapy System. In: *International Conference for Biomedical Robotics and Biomechanics (BioRob)*. New York, NY, USA: IEEE (2020). p. 981–8.
- Feain I, Coleman L, Wallis H, Sokolov R, O'Brien R, Keall P. Technical Note: The Design and Function of a Horizontal Patient Rotation System for the Purposes of Fixed-Beam Cancer Radiotherapy. *Med Phys (Lancaster)* (2017) 44(6):2490–502. doi: 10.1002/mp.12219
- Fave X, Yang J, Carvalho L, Martin R, Pan T, Balter P, et al. Upright Cone Beam CT Imaging Using the Onboard Imager. *Med Phys* (2014) 41 (6Part1):061906. doi: 10.1118/1.4875682
- Keall PJ, Mageras GS, Balter JM, Emery RS, Forster KM, Jiang SB, et al. The Management of Respiratory Motion in Radiation Oncology Report of AAPM Task Group 76 a. *Med Phys* (2006) 33(10):3874–900. doi: 10.1118/1.2349696
- Glide-Hurst CK, Smith MS, Ajlouni M, Chetty IJ. Evaluation of Two Synchronized External Surrogates for 4D CT Sorting. *J Appl Clin Med Phys* (2013) 14(6):117–32. doi: 10.1120/jacmp.v14i6.4301
- Sonke JJ, Zijp L, Remeijer P, Van Herk M. Respiratory Correlated Cone Beam CT. *Med Phys* (2005) 32(4):1176–86. doi: 10.1118/1.1869074
- Siewersden JH, Jaffray DA. Cone-Beam Computed Tomography With a Flat-Panel Imager: Magnitude and Effects of X-Ray Scatter. *Med Phys* (2001) 28 (2):220–31. doi: 10.1118/1.1339879
- Rührnschopf EP, Klingensbeck K. A General Framework and Review of Scatter Correction Methods in X-Ray Cone-Beam Computerized Tomography. Part 1: Scatter Compensation Approaches. *Med Phys* (2011) 38(7):4296–311. doi: 10.1118/1.3599033
- Rührnschopf EP, Klingensbeck K. A General Framework and Review of Scatter Correction Methods in Cone Beam CT. Part 2: Scatter Estimation Approaches. *Med Phys* (2011) 38(9):5186–99. doi: 10.1118/1.3589140
- Hansen DC, Landry G, Kamp F, Li M, Belka C, Parodi K, et al. ScatterNet: A Convolutional Neural Network for Cone-Beam CT Intensity Correction. *Med Phys* (2018) 45(11):4916–26. doi: 10.1002/mp.13175
- Harms J, Lei Y, Wang T, Zhang R, Zhou J, Tang X, et al. Paired Cycle-GAN-Based Image Correction for Quantitative Cone-Beam Computed Tomography. *Med Phys* (2019) 46(9):3998–4009. doi: 10.1002/mp.13656

37. Maslowski A, Wang A, Sun M, Wareing T, Davis I, Star-Lack J. Acuros CTS: A Fast, Linear Boltzmann Transport Equation Solver for Computed Tomography Scatter – Part I: Core Algorithms and Validation. *Med Phys* (2018) 45(5):1899–913. doi: 10.1002/mp.12850
38. Wang A, Maslowski A, Messmer P, Lehmann M, Strzelecki A, Yu E, et al. Acuros CTS: A Fast, Linear Boltzmann Transport Equation Solver for Computed Tomography Scatter – Part II: System Modeling, Scatter Correction, and Optimization. *Med Phys* (2018) 45(5):1914–25. doi: 10.1002/mp.12849
39. Kurz C, Kamp F, Park YK, Zöllner C, Rit S, Hansen D, et al. Investigating Deformable Image Registration and Scatter Correction for CBCT-Based Dose Calculation in Adaptive IMPT. *Med Phys* (2016) 43(10):5635–46. doi: 10.1118/1.4962933
40. Fotina I, Hopfgartner J, Stock M, Steininger T, Lütgendorf-Caucig C, Georg D. Feasibility of CBCT-Based Dose Calculation: Comparative Analysis of HU Adjustment Techniques. *Radiother Oncol* (2012) 104(2):249–56. doi: 10.1016/j.radonc.2012.06.007
41. Thummerer A, Zaffino P, Meijers A, Marmitt GG, Seco J, Steenbakkers RJ, et al. Comparison of CBCT Based Synthetic CT Methods Suitable for Proton Dose Calculations in Adaptive Proton Therapy. *Phys Med Biol* (2020) 65(9):095002. doi: 10.1088/1361-6560/ab7d54
42. Kazemifar S, Barragán Montero AM, Souris K, Rivas ST, Timmerman R, Park YK, et al. Dosimetric Evaluation of Synthetic CT Generated With GANs for MRI-Only Proton Therapy Treatment Planning of Brain Tumors. *J Appl Clin Med Phys* (2020) 21(5):76–86. doi: 10.1002/acm2.12856
43. Oh S, Kim S. Deformable Image Registration in Radiation Therapy. *Radiat Oncol J* (2017) 35(2):101–11. doi: 10.3857/roj.2017.00325
44. Dowling JA, O'Connor LM. Deformable Image Registration in Radiation Therapy. *J Med Radiat Sci* (2020) 67:257–9. doi: 10.1002/jmrs.446
45. Fortin D, Basran PS, Berrang T, Peterson D, Wai ES. Deformable Versus Rigid Registration of PET/CT Images for Radiation Treatment Planning of Head and Neck and Lung Cancer Patients: A Retrospective Dosimetric Comparison. *Radiat Oncol (London England)* (2014) 9:50. doi: 10.1186/1748-717X-9-50
46. Stuschke M, Pöttgen C. 18f-FDG PET/CT for Target Volume Contouring in Lung Cancer Radiotherapy. *J Nucl Med* (2020) 61(12):178S–9S. doi: 10.2967/jnumed.120.251660
47. Alderliesten T, Sonke J-J, Bosman PAN. Deformable Image Registration by Multi-Objective Optimization Using a Dual-Dynamic Transformation Model to Account for Large Anatomical Differences. Proc. SPIE 8669, Medical Imaging 2013: Image Processing, 866910 (13 March 2013). doi: 10.1117/12.2006783
48. Yang J, Zhang Y, Zhang Z, Zhang L, Balter P, Court L. Technical Note: Density Correction to Improve CT Number Mapping in Thoracic Deformable Image Registration. *Med Phys* (2019) 46(5):2330–6. doi: 10.1002/mp.13502
49. MacDougall N, Nalder C, Morgan A. Radiotherapy Treatment Planning. In: A Sibbain, A Morgan, N MacDougall, editors. *Radiotherapy in Practice Physics for Clinical Oncology. Physics for Clinical Oncology*. Oxford, New York: Oxford University Press (2012).
50. Arbea L, Ramos LI, Martínez-Monge R, Moreno M, Aristu J. Intensity-Modulated Radiation Therapy (IMRT) vs. 3D Conformal Radiotherapy (3DCRT) in Locally Advanced Rectal Cancer (LARC): Dosimetric Comparison and Clinical Implications. *Radiat Oncol* (2010) 5(1):17. doi: 10.1186/1748-717X-5-17
51. Webb S. The Physical Basis of IMRT and Inverse Planning. *Br J Radiol* (2003) 76(910):678–89. doi: 10.1259/bjr/65676879
52. Maes D, Janson M, Regmi R, Egan A, Rosenfeld A, Bloch C, et al. Validation and Practical Implementation of Seated Position Radiotherapy in a Commercial TPS for Proton Therapy. *Physica Med* (2020) 80:175–85. doi: 10.1016/j.ejmp.2020.10.027
53. Bert C, Metheany KG, Doppke K, Chen GT. A Phantom Evaluation of a Stereo-Vision Surface Imaging System for Radiotherapy Patient Setup. *Med Phys* (2005) 32(9):2753–62. doi: 10.1118/1.1984263
54. Boda-Heggemann J, Lohr F, Wenz F, Flentje M, Guckenberger M. kV Cone-Beam CT-Based IGRT. *Strahlentherapie Und Onkologie* (2011) 187(5):284–91. doi: 10.1007/s00066-011-2236-4
55. Brock KK. Adaptive Radiotherapy: Moving Into the Future. *Semin Radiat Oncol* (2019) 29(3):181–4. doi: 10.1016/j.semradonc.2019.02.011
56. Green OL, Henke LE, Hugo GD. Practical Clinical Workflows for Online and Offline Adaptive Radiation Therapy. *Semin Radiat Oncol* (2019) 29(3):219–27. doi: 10.1016/j.semradonc.2019.02.004
57. Zhao B, Maquillan G, Jiang S, Schwartz DL. Minimal Mask Immobilization With Optical Surface Guidance for Head and Neck Radiotherapy. *J Appl Clin Med Phys* (2018) 19(1):17–24. doi: 10.1002/acm2.12211
58. Booth J, Caillet V, Briggs A, Hardcastle N, Angelis G, Jayamanne D, et al. MLC Tracking for Lung SABR Is Feasible, Efficient and Delivers High-Precision Target Dose and Lower Normal Tissue Dose. *Radiother Oncol: J Eur Soc Ther Radiol Oncol* (2021) 155:131–7. doi: 10.1016/j.radonc.2020.10.036
59. Hsieh M-J. *Implementation of Upright Treatments for Lung and Head and Neck Cancers*. Houston, Texas: The University of Texas (2014).
60. Goitein M. Trials and Tribulations in Charged Particle Radiotherapy. *Radiother Oncol* (2010) 95(1):23–31. doi: 10.1016/j.radonc.2009.06.012
61. Ibahim M, Crosbie J, Yang Y, Zaitseva M, Stevenson A, Rogers P, et al. An Evaluation of Dose Equivalence Between Synchrotron Microbeam Radiation Therapy and Conventional Broadbeam Radiation Using Clonogenic and Cell Impedance Assays. *PloS One* (2014) 9(6):e100547–e. doi: 10.1371/journal.pone.0100547
62. Bourhis J, Montay-Gruel P, Jorge PG, Bailat C, Petit B, Ollivier J, et al. Clinical Translation of FLASH Radiotherapy: Why and How? *Radiother Oncol* (2019) 139:11–7. doi: 10.1016/j.radonc.2019.04.008

Conflict of Interest: NH and TK receive collaborative research funding from Varian Medical Systems and Reflexion Medical for unrelated projects.

The remaining authors declare that the research was conducted in the absence of any commercial or financial relationships that could be construed as a potential conflict of interest.

Publisher's Note: All claims expressed in this article are solely those of the authors and do not necessarily represent those of their affiliated organizations, or those of the publisher, the editors and the reviewers. Any product that may be evaluated in this article, or claim that may be made by its manufacturer, is not guaranteed or endorsed by the publisher.

Copyright © 2022 Hegarty, Hardcastle, Korte, Kron, Everitt, Rahim, Hegi-Johnson and Franich. This is an open-access article distributed under the terms of the Creative Commons Attribution License (CC BY). The use, distribution or reproduction in other forums is permitted, provided the original author(s) and the copyright owner(s) are credited and that the original publication in this journal is cited, in accordance with accepted academic practice. No use, distribution or reproduction is permitted which does not comply with these terms.



Clinical Evaluation of an Auto-Segmentation Tool for Spine SBRT Treatment

Yingxuan Chen, Yevgeniy Vinogradskiy, Yan Yu, Wenyin Shi and Haisong Liu*

Department of Radiation Oncology, Sidney Kimmel Medical College, Thomas Jefferson University, Philadelphia, PA, United States

OPEN ACCESS

Edited by:

Nicholas Hardcastle,
Peter MacCallum Cancer Centre,
Australia

Reviewed by:

Jue Jiang,
Memorial Sloan Kettering Cancer
Center, United States
Francesco Ricchetti,
Sacro Cuore Don Calabria Hospital
(IRCCS), Italy

*Correspondence:

Haisong Liu
Haisong.Liu@jefferson.edu

Specialty section:

This article was submitted to
Radiation Oncology,
a section of the journal
Frontiers in Oncology

Received: 23 December 2021

Accepted: 08 February 2022

Published: 14 March 2022

Citation:

Chen Y, Vinogradskiy Y, Yu Y,
Shi W and Liu H (2022) Clinical
Evaluation of an Auto-Segmentation
Tool for Spine SBRT Treatment.
Front. Oncol. 12:842579.
doi: 10.3389/fonc.2022.842579

Purpose: Spine SBRT target delineation is time-consuming due to the complex bone structure. Recently, Elements SmartBrush Spine (ESS) was developed by Brainlab to automatically generate a clinical target volume (CTV) based on gross tumor volume (GTV). The aim of this project is to evaluate the accuracy and efficiency of ESS auto-segmentation.

Methods: Twenty spine SBRT patients with 21 target sites treated at our institution were used for this retrospective comparison study. Planning CT/MRI images and physician-drawn GTVs were inputs for ESS. ESS can automatically segment the vertebra, split the vertebra into 6 sectors, and generate a CTV based on the GTV location, according to the International Spine Radiosurgery Consortium (ISRC) Consensus guidelines. The auto-segmented CTV can be edited by including/excluding sectors of the vertebra, if necessary. The ESS-generated CTV contour was then compared to the clinically used CTV using qualitative and quantitative methods. The CTV contours were compared using visual assessment by the clinicians, relative volume differences (RVD), distance of center of mass (DCM), and three other common contour similarity measurements such as dice similarity coefficient (DICE), Hausdorff distance (HD), and 95% Hausdorff distance (HD95).

Results: Qualitatively, the study showed that ESS can segment vertebra more accurately and consistently than humans at normal curvature conditions. The accuracy of CTV delineation can be improved significantly if the auto-segmentation is used as the first step. Conversely, ESS may mistakenly split or join different vertebrae when large curvatures in anatomy exist. In this study, human interactions were needed in 7 of 21 cases to generate the final CTVs by including/excluding sectors of the vertebra. In 90% of cases, the RVD were within $\pm 15\%$. The RVD, DCM, DICE, HD, and HD95 for the 21 cases were $3\% \pm 12\%$, 1.9 ± 1.5 mm, 0.86 ± 0.06 , 13.34 ± 7.47 mm, and 4.67 ± 2.21 mm, respectively.

Conclusion: ESS can auto-segment a CTV quickly and accurately and has a good agreement with clinically used CTV. Inter-person variation and contouring time can be reduced with ESS. Physician editing is needed for some occasions. Our study supports the idea of using ESS as the first step for spine SBRT target delineation to improve the contouring consistency as well as to reduce the contouring time.

Keywords: spine SBRT, auto-segmentation, target delineation, clinical target volume (CTV), gross tumor volume (GTV)

INTRODUCTION

Bone is a frequent site of metastases and causes significant morbidities including severe pain and spinal cord compression (1–3). Stereotactic body radiotherapy (SBRT) has been increasingly used to provide a treatment option in the multidisciplinary management of metastases located within or adjacent (paraspinal) to vertebrae/spinal cord. In SBRT treatments, high dose will be prescribed in typically one to five fractions. Localization accuracy can be managed at millimeter levels with advances in patient immobilization, target visualization, and image-guidance technology (4–7). Target segmentation accuracy becomes critical for spine SBRT due to the requirement of ablative high dose per fraction to the target volume and minimizing the dose to organ at risks, especially the spinal cord. To standardize the target delineation, consensus guidelines for the target volume were published in 2012 for appropriate target volume definition (8). However, manual contouring is time-consuming and has large inter-observer variance. To improve the efficiency and reduce the inter-observer variance, auto-segmentation tools have been developed mainly in three categories: threshold-based methods (9, 10), atlas-based methods (11, 12), and deep learning methods (13, 14). Some methods require human intervention or the manual setting of parameters. Deep learning methods such as supervised learning might be a solution for fully automated spine auto-segmentation, but large training sets are needed. Moreover, based on the International Spine Radiosurgery Consortium (ISRC) Consensus guidelines (8), different anatomical regions (such as vertebral body, pedicles, spinous process, or transverse processes/lamina) will be included in the clinical target volume (CTV) based on location of gross tumor volume (GTV). Most of the above-mentioned published studies are focused on whole spine segmentation, which might not be available to be applied for clinical spine SBRT treatment yet.

Recently, a dedicated software has been developed for spine SBRT treatment (Elements Spine SRS®, Brainlab AG, Germany) including auto-segmentation, image fusion, and treatment planning.

Previous evaluation studies have shown the advances of Elements Spine SRS in dosimetry (15–17). Moreover, the auto-segmentation tool Elements SmartBrush Spine (ESS) was developed for fast target delineation, which can potentially improve the efficiency of the clinical workflow. Gaj-Levra et al. have demonstrated that the inter-observer difference can be reduced by using ESS (18) by evaluating the GTV contours. The aim of this study is to evaluate the accuracy of the CTV auto-segmentation based on existing GTV contours using ESS for spine SBRT patients.

To evaluate the performance of the auto-segmentation, analysis metrics were developed to evaluate medical image segmentation (19). Among these, Dice similarity coefficients (DICE) and Hausdorff distance (HD) are common metrics to efficiently evaluate the quality of segmentation. In this study, evaluation metrics including volume differences, distance of center of mass, DICE and HD were selected for the spine segmentation evaluation based on the target contour impact on radiation delivery.

MATERIALS AND METHODS

Patients and Treatments

This study was approved by the Institutional Review Board. Eligible patients required metastasis limited to one vertebral level and without severe compression fracture (loss vertebral height more than 50%). A total of 51 spine SBRT cases treated in our institution from 2018 to 2021 were reviewed. Twenty-one of the 51 cases met this inclusion criterion, and the CTV could be successfully segmented and were evaluated in this retrospective comparison study. Details are shown in **Table 1**. The GTV of 21 targets (12 T spine and 9 L spine) were drawn by physicians based on the MR images and were used as input for the CTV auto-segmentation. The CTV was auto-segmented by ESS on CT scans in two steps. In the first step, the affected vertebra including 6 different sectors were auto-segmented using ESS, which is an atlas-based auto-contouring method. This spine segmentation and labeling of spinal structures in the background enables the automatic CTV calculation. Then, the CTV was generated based on the GTV involvement following the rules from the ISRC guidelines (8). After reviewing the initial target contour, a physician reviewed the auto-segmented CTV and edited the CTV by including/excluding different sectors of the vertebra, if needed, using patient-specific clinical judgment, by simple mouse clicking on each sector. After CTV generation, the planning target volume (PTV) was calculated with uniform expansion with 2 mm margin and modified to avoid potential overlap with the cord. Prescription dose and fraction were determined based on the tumor volume, previous radiation treatment, and surrounding organ-at-risk (OAR) dose tolerance limits.

Evaluation Metrics

To evaluate the impact of auto-segmentation for CTV delineation using ESS, the SmartBrush-generated CTVs were compared with the clinically used CTVs using qualitative and quantitative methods. After initial visual assessment and editing by a physician, in-depth quantitative contour comparison metrics were used for comparison, including relative volume difference, distance of center of mass, dice similarity coefficients, structure similarity index measurement, and Hausdorff distance. Both ESS-generated CTVs and clinically used CTVs were exported from Elements as a DICOM file for evaluation. Hausdorff distance was calculated using open source Plastimatch and other evaluation metrics were implemented in MATLAB (The MathWorks, Inc., Natick, MA) using built-in functions. To evaluate the performance statistically, both average and standard deviation (SD) were also calculated for each evaluation metrics.

For the given two different contours A (ESS-generated CTV) and B (clinically used CTV):

Relative volume difference (RVD) is defined as:

$$RVD = \frac{Volume(A) - Volume(B)}{Volume(B)}$$

Distance of center of mass (DCM) is defined as the distance between center of mass of A and B with the unit of mm in this study:

TABLE 1 | Summary of all cases (21 lesions) sorted by clinically used CTV volume.

Case number	Treatment site	CTV volume (cc)	Prescription dose (Gy)	Fractions
1	T8	3.95	20	1
2	T6	12.3	16	2
3	T5	13.7	27	3
4	T4	13.8	16	2
5	T5	15	18	1
6	T11	17.1	16	1
7	T9	17.6	18	1
8	T9	19.3	24	3
9	T5	20.9	24	3
10	T7	27	18	1
11	T12	28.6	24	3
12	L1	39.3	16	1
13	L3	45.4	16	1
14	L3	45.9	16	1
15	L2	46.8	18	1
16	T11	48.2	27	3
17	L4	49.2	18	1
18	T9	50	18	1
19	L3	52.4	20	1
20	L4	54.4	20	1
21	L4	57.4	27	3

$DCM = Dist(\text{Center of } A, \text{Center of } B)$

Dice similarity coefficients (DICE) is defined as:

$$DICE = \frac{2|A \cap B|}{|A| + |B|}$$

DICE is an overlap-based metrics and is widely used for the contour evaluation with a value between 0 to 1. If A and B are exactly the same, then DICE will equal to 1.

Hausdorff distance (HD) is defined as:

$$HD(A, B) = \max\{d(A, B), d(B, A)\}$$

Where $d(A, B) = \sup\{d(a, B) | a \in A\}$, $d(a, B) = \inf\{d(a, b) | b \in B\}$, \sup represents the supremum, \inf represents the infimum. HD is measuring maximum surface distance with the unit of mm in this study. If A and B are exactly the same, then the HD value will equal to 0. As HD is usually sensitive to outliers, 95% Hausdorff distance (HD95) was also calculated. Note that the boundary Hausdorff function in Plastimatch was used to report HD and HD95 in this study.

RESULTS

Figure 1 shows examples of vertebral bodies that were auto-segmented by ESS and CTV was generated automatically based on the GTV involvement following ISRC consensus guidelines. A physician reviewed the auto-segmented CTV and edited it by including/excluding different sectors of the vertebra if needed. In this study, 7 of 21 cases need physician's editing to include/exclude one or more sectors to generate the final CTV. The ESS-generated CTV was labeled as Clinical Target in the software. **Figure 2** shows GTV, ESS-generated CTV, and clinically used CTV of the same patient in 3D and three views (which are axial,

sagittal, and coronal). In addition to the 21 cases, there are 30 of 51 reviewed cases that failed the ESS auto-segmentation due to (a) multiple vertebrae (12 cases), (b) paraspinal soft tissue involved in GTV (15 cases), and (c) large curved anatomy like C spine at neck region or L spine and sacrum junction (3 cases). Both a and b situations are not implemented in the current version of ESS auto-segmentation.

Analysis results are summarized in **Table 2**. Average volume of clinically used CTV was 32.3 cc (range from 3.95 cc to 57.4 cc) while ESS-generated CTV ranged from 5.52 cc to 60.9 cc, with an average volume of 33.17 cc. The average of relative volume difference (RVD), distance of center of mass (DCM), and dice similarity coefficient (DICE), Hausdorff distance (HD), and 95% percentile Hausdorff distance (HD95) for the 21 cases were $3\% \pm 12\%$, 1.9 ± 1.5 mm, 0.86 ± 0.06 , 13.34 ± 7.47 mm, and 4.67 ± 2.21 mm, respectively.

Figure 3 shows DCM for the 21 lesions as a function of clinically used CTV volume. For the treatment planning, the center of the target was usually selected as the treatment isocenter. The DCM was below 2 mm for 16 out of the 21 cases.

Absolute RVD and DICE are shown in **Figure 4**. Both absolute RVD and DICE are volume-based evaluation metrics. Low relative volume is associated with high DICE, which indicate good agreement between ESS-generated CTV and clinically used CTV.

DISCUSSION

Accurate target delineation has significant impact on the quality of the radiation treatment plan. For a spine SBRT approach, correct definition of the treatment volume becomes even more important due to the nature of this treatment with high dose delivery per fraction and the proximity of critical OARs such as the spinal cord. Many studies have already demonstrated that

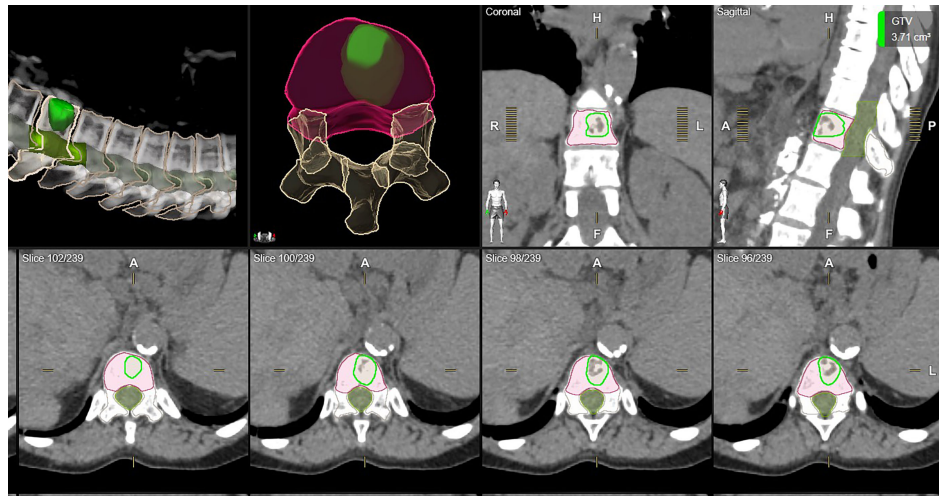


FIGURE 1 | One example of auto-segmented CTV. All vertebrae were segmented and the auto-segmented CTV was automatically generated by ESS following ISRC consensus guidelines. Green: clinically used GTV. Orange: clinically used CTV. Red: ESS-generated CTV, labeled as Clinical Target in Elements.

inter-observer variability can be reduced by using the auto-segmentation tool (18). Our study also supports the findings. Overall, the ESS-generated CTVs have a good agreement with the clinically used CTVs. Different evaluation metrics can display the similarity in different aspects. It is highly recommended to use multiple metrics to evaluate contours in different aspects. For example, DICE is a volume-based evaluation metric that might be less sensitive to evaluate large volume contours. Otherwise, Hausdorff distance measures the surface distance between two contours, which can be used in the contour shape evaluation. For the contour with a small volume, even they have large relative volume differences, and HD and

HD95 might not be large as shown in **Figure 5A**. In contrast, as shown in **Figure 5B**, high DICE cases might also have high HD and HD95 depending on the shape of the contours with outliers of large surface distances.

After reviewing each case, clinically used CTV is more likely to include inter-space between vertebrae more generously if the spine is not parallel to the axial CT slices. ESS splits the vertebra into 6 sectors according to the ISRC consortium guidelines. The accuracy of identifying the vertebra as well as sectors of vertebral body can be improved significantly if the auto-segmentation is used as the first step. Moreover, the users have the flexibility of clicking and selecting to include or exclude different sectors, after

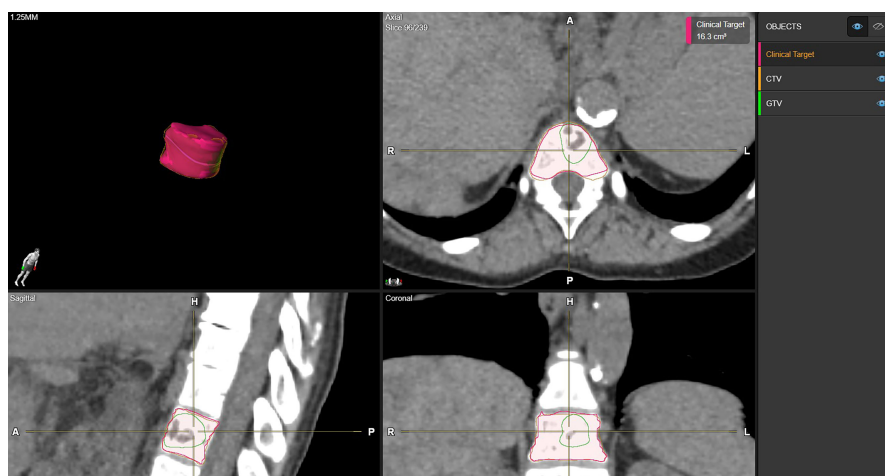


FIGURE 2 | Examples of CTV delineation by manual method and ESS in axial, sagittal, coronal, and 3D views. Green: clinically used GTV. Orange: clinically used CTV. Red: ESS-generated CTV, labeled as Clinical Target in Elements.

TABLE 2 | Summary of comparison between clinically used CTV and auto-segmented CTV regarding volume, DCM, DICE, SSIM, HD, and HD95.

Case number	Clinically used CTV Volume (cc)	SmartBrush-generated CTV Volume (cc)	Absolute Vol Diff (cc)	RVD (%)	DCM (mm)	DICE	HD (mm)	HD95 (mm)
1	3.95	5.52	1.57	42.0%	1.59	0.69	13.55	6.40
2	12.30	14.10	1.80	15.2%	0.73	0.88	6.43	2.77
3	13.70	13.70	0.00	-0.1%	0.66	0.82	9.17	4.18
4	13.80	12.80	-1.00	-7.6%	0.39	0.88	6.25	2.50
5	15.00	14.00	-1.00	-6.7%	1.78	0.87	5.75	2.52
6	17.10	16.30	-0.80	-3.0%	1.06	0.94	2.83	1.27
7	17.60	17.00	-0.60	-1.4%	1.54	0.70	20.80	8.78
8	19.30	17.60	-1.70	-7.8%	2.90	0.89	7.43	2.54
9	20.90	18.80	-2.10	-9.8%	4.17	0.86	7.71	3.75
10	27.00	27.70	0.70	1.9%	1.14	0.84	17.31	4.79
11	28.60	27.00	-1.60	-5.7%	1.59	0.83	21.50	6.94
12	39.30	39.40	0.10	0.9%	0.60	0.94	4.38	2.50
13	45.40	51.70	6.30	13.5%	4.21	0.86	19.52	4.51
14	45.90	47.10	1.20	2.9%	1.63	0.88	23.10	5.60
15	46.80	55.90	9.10	20.4%	0.72	0.86	26.84	9.04
16	48.20	49.07	0.87	1.8%	6.04	0.87	15.84	4.48
17	49.20	47.30	-1.90	-4.1%	0.61	0.87	21.47	6.67
18	50.00	50.50	0.50	1.0%	1.80	0.89	9.81	4.70
19	52.40	56.40	4.00	7.5%	1.50	0.91	6.41	2.65
20	54.40	53.70	-0.70	-1.5%	1.21	0.89	9.02	3.19
21	57.40	60.90	3.50	7.0%	3.65	0.83	24.97	8.24
Average	32.30	33.17	0.87	3.0%	1.90	0.86	13.34	4.67
SD	17.28	18.61	2.83	12.0%	1.50	0.06	7.47	2.21

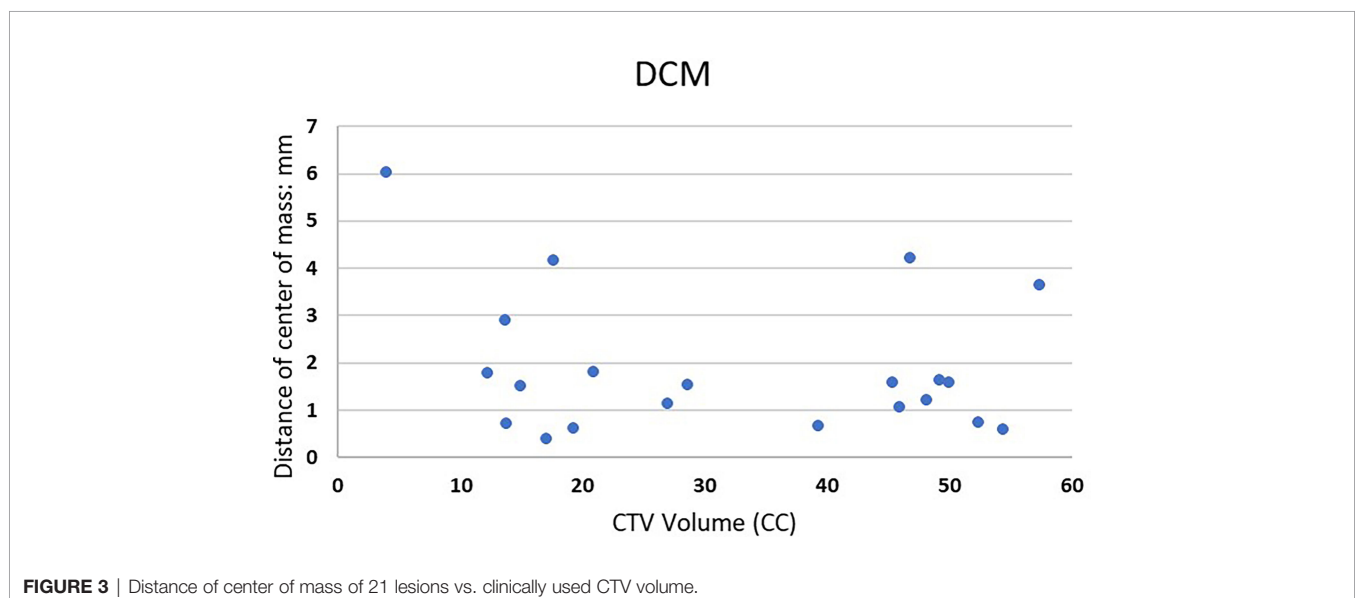
The bold values are Average and SD to distinguish from values of each case.

reviewing the auto-segmented CTV, which will potentially improve the efficiency of the clinical workflow.

For most T or L spine cases, ESS can be an efficient tool to automatically generate CTVs on CT images based on the GTV locations. As discussed in the method session, 21 of the 51 cases met the inclusion criteria and the CTV could be successfully segmented and were evaluated in this study. For the other cases, failed auto-segmentation was due to some limitations for the current version. During the evaluation, we observed that ESS failed to segment a CTV if (a) the GTV involves multiple vertebrae (12 cases) or (b) paraspinal soft tissue was involved

in the treatment target (15 cases). In addition, it might be challenging to segment CTV for C spine (1 case) at the neck region, or the L spine and sacrum junction (2 cases) and spine might be split mistakenly using ESS when large curved anatomy relative to the CT slices exists. Therefore, careful physician review and confirmation is needed.

There are some limitations of this study. Firstly, only 21 cases were in-depth evaluated and the small sample size may introduce some statistical bias. Only CTVs were evaluated in this study. Surrounding OARs contouring accuracy is also important for plan optimization and evaluation. In the future, both CTV and



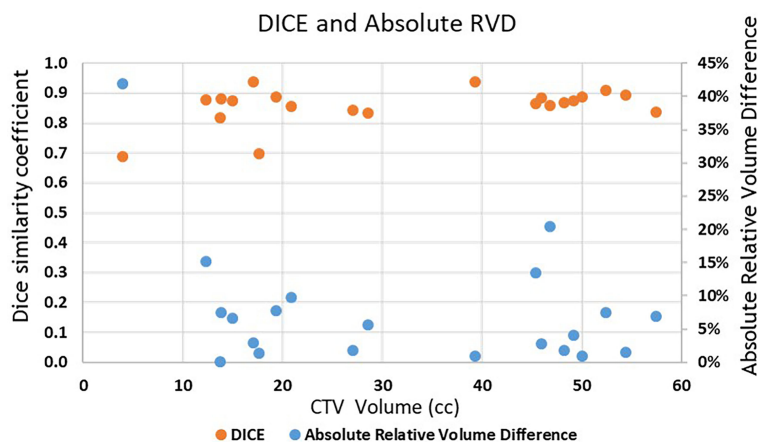


FIGURE 4 | Absolute RVD and DICE of the 21 lesions vs. clinically used CTV volume. Blue dots are Absolute RVD and orange dots are DICE.

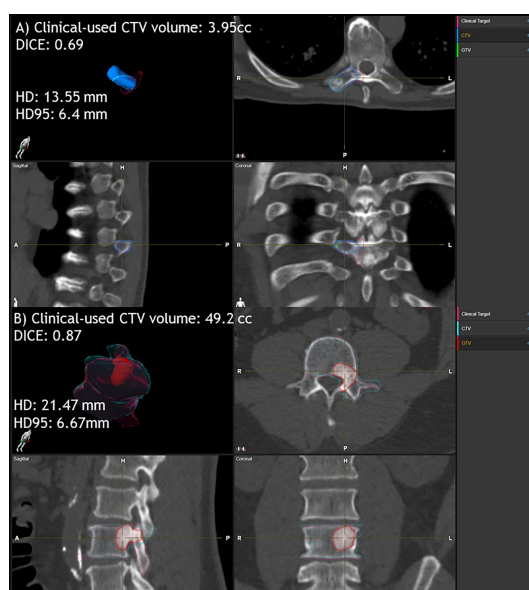


FIGURE 5 | Examples of clinically used CTV and ESS-generated CTV comparison for small and large volumes. Case (A) clinically used CTV volume is 3.95 cc. DICE is 0.69, HD is 13.55 mm and HD95 is 6.4 mm. Case (B) clinically used CTV volume is 49.2 cc. DICE is 0.87, HD is 21.47 mm and HD95 is 6.67 mm. Here, ESS-generated CTV is labeled as Clinical Target.

OAR analysis for larger samples or cross-institutions could be potentially carried out.

CONCLUSION

Elements SmartBrush Spine can auto-segment a CTV quickly and accurately and has good agreement with the clinically used CTV. Inter-person variation can be reduced with ESS. Physician editing is needed for some occasions. Our study supports the idea

of using ESS as the first step for spine SBRT target delineation to improve the contouring consistency as well as to reduce contouring time, which might potentially improve the efficiency and precision of the spine SBRT treatment.

AUTHOR'S NOTE

Part of the study will be presented at the Radiosurgery Society (RSS) Scientific Meeting in 2022.

DATA AVAILABILITY STATEMENT

The raw data supporting the conclusions of this article will be made available by the authors, without undue reservation.

ETHICS STATEMENT

The studies involving human participants were reviewed and approved by Office of Human Research, Institutional Review Board (IRB) of Thomas Jefferson University. Written informed consent for

participation was not required for this study in accordance with the national legislation and the institutional requirements.

AUTHOR CONTRIBUTIONS

YC, HL, and WS contributed to conception and design of the study. HL performed the data collection. YC developed evaluation tools and performed the analysis. YC wrote the first draft of the manuscript. All authors contributed to manuscript revision, read, and approved the submitted version.

REFERENCES

- Macedo F, Ladeira K, Pinho F, Saraiva N, Bonito N, Pinto L, et al. Bone Metastases: An Overview. *Oncol Rev* (2017) 11(1):321. doi: 10.4081/oncol.2017.321
- Cecchini MG, Wetterwald A, Van Der Pluijm G, Thalmann GN. Molecular and Biological Mechanisms of Bone Metastasis. *EAU Update Ser* (2005) 3(4):214–26. doi: 10.1016/j.euus.2005.09.006
- Wong DA, Fornasier VL, MacNab I. Spinal Metastases: The Obvious, the Occult, and the Impostors. *Spine* (1990) 15(1):1–4. doi: 10.1097/00007632-199001000-00001
- Chang Z, Wang Z, Ma J, O'Daniel JC, Kirkpatrick J, Yin F-F. 6D Image Guidance for Spinal Non-Invasive Stereotactic Body Radiation Therapy: Comparison Between ExacTrac X-Ray 6D With Kilo-Voltage Cone-Beam CT. *Radiation Oncol* (2010) 95(1):116–21. doi: 10.1016/j.radonc.2009.12.036
- Foote M, Letourneau D, Hyde D, Massicotte E, Rampersaud R, Fehlings M, et al. Technique for Stereotactic Body Radiotherapy for Spinal Metastases. *J Clin Neurosci* (2011) 18(2):276–9. doi: 10.1016/j.jocn.2010.04.033
- Gerszten PC, Monaco EA, Quader M, Novotny J, Kim JO, Flickinger JC, et al. Setup Accuracy of Spine Radiosurgery Using Cone Beam Computed Tomography Image Guidance in Patients With Spinal Implants. *J Neurosurg: Spine* (2010) 12(4):413–20. doi: 10.3171/2009.10.SPINE09249
- Ho AK, Fu D, Cotrutz C, Hancock SL, Chang SD, Gibbs IC, et al. A Study of the Accuracy of Cyberknife Spinal Radiosurgery Using Skeletal Structure Tracking. *Operative Neurosurg* (2007) 60(suppl_2):ONS-147-ONS-156. doi: 10.1227/01.NEU.0000249248.55923.EC
- Cox BW, Spratt DE, Lovelock M, Bilsky MH, Lis E, Ryu S, et al. International Spine Radiosurgery Consortium Consensus Guidelines for Target Volume Definition in Spinal Stereotactic Radiosurgery. *Int J Radiat Oncol Biol Phys* (2012) 83(5):e597–605. doi: 10.1016/j.ijrobp.2012.03.009
- Kang Y, Engelke K, Kalender WA. A New Accurate and Precise 3-D Segmentation Method for Skeletal Structures in Volumetric CT Data. *IEEE Trans Med Imaging* (2003) 22(5):586–98. doi: 10.1109/TMI.2003.812265
- Mastmeyer A, Engelke K, Fuchs C, Kalender WA. A Hierarchical 3D Segmentation Method and the Definition of Vertebral Body Coordinate Systems for QCT of the Lumbar Spine. *Med Image Anal* (2006) 10(4):560–77. doi: 10.1016/j.media.2006.05.005
- Michopoulou SK, Costaridou L, Panagiotopoulos E, Speller R, Panayiotakis G, Todd-Pokropek A, et al. Atlas-Based Segmentation of Degenerated Lumbar Intervertebral Discs From MR Images of the Spine. *IEEE Trans Biomed Eng* (2009) 56(9):2225–31. doi: 10.1109/TBME.2009.2019765
- Forsberg D. Atlas-Based Registration for Accurate Segmentation of Thoracic and Lumbar Vertebrae in CT Data. In: *Recent Advances in Computational Methods and Clinical Applications for Spine Imaging*. Cham: Springer (2015). p. 49–59. doi: 10.1007/978-3-319-14148-0_5
- Vania M, Mureja D, Lee D. Automatic Spine Segmentation From CT Images Using Convolutional Neural Network via Redundant Generation of Class Labels. *J Comput Des Eng* (2019) 6(2):224–32. doi: 10.1016/j.jcde.2018.05.002
- Kolařík M, Burget R, Uher V, Říha K, Dutta MK. Optimized High Resolution 3D Dense-U-Net Network for Brain and Spine Segmentation. *Appl Sci* (2019) 9(3):404. doi: 10.3390/app9030404
- Saenz DL, Crowner R, Stathakis S, Papanikolaou N. A Dosimetric Analysis of a Spine SBRT Specific Treatment Planning System. *J Appl Clin Med Phys* (2019) 20(1):154–9. doi: 10.1002/acm2.12499
- Giaj-Levra N, Niyazi M, Figlia V, Napoli G, Mazzola R, Nicosia L, et al. Feasibility and Preliminary Clinical Results of Linac-Based Stereotactic Body Radiotherapy for Spinal Metastases Using a Dedicated Contouring and Planning System. *Radiat Oncol* (2019) 14(1):184. doi: 10.1186/s13014-019-1379-9
- Trager M, Landers A, Yu Y, Shi W, Liu H. Evaluation of Elements Spine SRS Plan Quality for SRS and SBRT Treatment of Spine Metastases. *Front Oncol* (2020) 10:346. doi: 10.3389/fonc.2020.00346
- Giaj-Levra N, Figlia V, Cuccia F, Mazzola R, Nicosia L, Ricchetti F, et al. Reduction of Inter-Observer Differences in the Delineation of the Target in Spinal Metastases SBRT Using an Automatic Contouring Dedicated System. *Radiat Oncol* (2021) 16(1):1–6. doi: 10.1186/s13014-021-01924-0
- Taha AA, Hanbury A. Metrics for Evaluating 3D Medical Image Segmentation: Analysis, Selection, and Tool. *BMC Med Imaging* (2015) 15(1):1–28. doi: 10.1186/s12880-015-0068-x

Conflict of Interest: Thomas Jefferson University has a research agreement with Brainlab AG for evaluation of Elements SmartBrush Spine technology, for which HL and WS are the principal investigators. The funder was not involved in the study design, data collection, analysis, and interpretation, the writing of this article, or the decision to submit it for publication. In addition, WS received consulting fee from Varian, Brainlab, Novocure, and Zai lab, and research funding from Brainlab, Novocure, and regeneron. YV received 2 NCI grants (UG3CA247605 and R01CA236857) and a grant from MIM Software. None of these are related to this research work.

The remaining authors declare that the research was conducted in the absence of any commercial or financial relationships that could be construed as a potential conflict of interest.

Publisher's Note: All claims expressed in this article are solely those of the authors and do not necessarily represent those of their affiliated organizations, or those of the publisher, the editors and the reviewers. Any product that may be evaluated in this article, or claim that may be made by its manufacturer, is not guaranteed or endorsed by the publisher.

Copyright © 2022 Chen, Vinogradskiy, Yu, Shi and Liu. This is an open-access article distributed under the terms of the Creative Commons Attribution License (CC BY). The use, distribution or reproduction in other forums is permitted, provided the original author(s) and the copyright owner(s) are credited and that the original publication in this journal is cited, in accordance with accepted academic practice. No use, distribution or reproduction is permitted which does not comply with these terms.



Radiation Oncology: Future Vision for Quality Assurance and Data Management in Clinical Trials and Translational Science

Linda Ding¹, Carla Bradford¹, I-Lin Kuo¹, Yankhua Fan¹, Kenneth Ulin¹, Abdulnasser Khalifeh¹, Suhong Yu¹, Fenghong Liu¹, Jonathan Saleeby¹, Harry Bushe¹, Koren Smith¹, Camelia Bianciu¹, Salvatore LaRosa¹, Fred Prior², Joel Saltz³, Ashish Sharma⁴, Mark Smyczynski¹, Maryann Bishop-Jodoin¹, Fran Laurie¹, Matthew Iandoli¹, Janaki Moni¹, M. Giulia Cicchetti¹ and Thomas J. FitzGerald^{1*}

OPEN ACCESS

Edited by:

Charles A. Kunos,
National Cancer Institute (NIH),
United States

Reviewed by:

Andrei Fodor,
IRCCS San Raffaele Scientific Institute,
Italy
Mark Bernard,
University of Kentucky, United States

*Correspondence:

Thomas J. FitzGerald
T.J.FitzGerald@umassmemorial.org

Specialty section:

This article was submitted to
Radiation Oncology,
a section of the journal
Frontiers in Oncology

Received: 28 April 2022

Accepted: 21 June 2022

Published: 10 August 2022

Citation:

Ding L, Bradford C, Kuo I-L, Fan Y, Ulin K, Khalifeh A, Yu S, Liu F, Saleeby J, Bushe H, Smith K, Bianciu C, LaRosa S, Prior F, Saltz J, Sharma A, Smyczynski M, Bishop-Jodoin M, Laurie F, Iandoli M, Moni J, Cicchetti MG and FitzGerald TJ (2022) Radiation Oncology: Future Vision for Quality Assurance and Data Management in Clinical Trials and Translational Science. *Front. Oncol.* 12:931294. doi: 10.3389/fonc.2022.931294

¹ Department of Radiation Oncology, UMass Chan Medical School, Worcester, MA, United States, ² Department of Biomedical Informatics, University of Arkansas, Little Rock, AR, United States, ³ Department of Biomedical Informatics, Stony Brook University, Stony Brook, NY, United States, ⁴ Department of Biomedical Informatics, Emory University, Atlanta, GA, United States

The future of radiation oncology is exceptionally strong as we are increasingly involved in nearly all oncology disease sites due to extraordinary advances in radiation oncology treatment management platforms and improvements in treatment execution. Due to our technology and consistent accuracy, compressed radiation oncology treatment strategies are becoming more commonplace secondary to our ability to successfully treat tumor targets with increased normal tissue avoidance. In many disease sites including the central nervous system, pulmonary parenchyma, liver, and other areas, our service is redefining the standards of care. Targeting of disease has improved due to advances in tumor imaging and application of integrated imaging datasets into sophisticated planning systems which can optimize volume driven plans created by talented personnel. Treatment times have significantly decreased due to volume driven arc therapy and positioning is secured by real time imaging and optical tracking. Normal tissue exclusion has permitted compressed treatment schedules making treatment more convenient for the patient. These changes require additional study to further optimize care. Because data exchange worldwide have evolved through digital platforms and prisms, images and radiation datasets worldwide can be shared/reviewed on a same day basis using established de-identification and anonymization methods. Data storage post-trial completion can co-exist with digital pathomic and radiomic information in a single database coupled with patient specific outcome information and serve to move our translational science forward with nimble query elements and artificial intelligence to ask better questions of the data we collect and collate. This will be important moving forward to validate our process improvements at an enterprise level and support our science. We have to be thorough and complete in our data acquisition processes, however if we

remain disciplined in our data management plan, our field can grow further and become more successful generating new standards of care from validated datasets.

Keywords: radiation therapy (radiotherapy), clinical trials, cancer treatment, clinical trial imaging, clinical trial data, translational medicine, quality assurance, artificial intelligence

INTRODUCTION

Radiation oncology has undergone fundamental change over the past several decades. The primary turning point in our discipline was the transition from anatomic to volumetric treatment planning pivoting away from previous two-dimensional planning methods. The transition required a seed change in how we identified disease and targeting of tumor volumes in juxtaposition to normal tissue which we could now evaluate in three and four dimensions. We became closer to our imaging colleagues but asked different questions of the images we review in collaboration. While imaging colleagues told us that a mass was present, radiation oncologists needed to know the size and peripheral location including the boundaries of involvement. We also needed to adapt our plans to our understanding of the natural history of disease and predictable routes of tumor spread including additional tissues at risk for disease. We need to balance our plans with our growing knowledge of normal tissue constraints and how systemic therapy modulates these constraints. We had to and continue to adapt our therapy to growing concerns of normal tissue pre-existing co-morbidity as society ages and need for radiation therapy in older populations becomes the sole option for treatment. Today there are innumerable medical coefficients to the management of each patient and the modern radiation oncologist must be fluent and knowledgeable in each detail of medical care.

Our technology has matured at a rapid rate, at times outpacing our ability to fully harness its strength and apply modern technology in a strategic manner to daily care. Historically, once the radiation oncologist left the simulator, most of the physician work was completed with less nuance and detail applied to treatment planning. We simply did not have tools to optimize our craft beyond fluoroscopy and two-dimensional treatment platforms. Today, the simulation appointment is designed to construct immobilization devices and provide four-dimensional imaging with fusion of diagnostic images as needed for target definition. The work of the radiation oncologist today only begins when the patient leaves the simulator. This has a profound impact on department workflow as the work of the physics planning team can only begin once the volumes to treat and constraints to follow are made available as part of the directive of care. If the patient requires rapid initiation of therapy and the contours are not completed in a timely manner, the physics planning team does not have the time to both optimize planning and perform quality assurance of the plan including the appropriate checks of the chart for patient care. Tools and strategy for daily image guidance are now an integrated component of patient care. Historically, we assumed it was self-evident that treatments were reproduced daily validated by a weekly mega electron volt (MeV) image. Today, directive for

image guidance using volumetric and kilovoltage (kV) imaging coupled with optical tracking tools are standard of care. Magnetic resonance (MR) integrated tools monitor biological parameters of care and artificial intelligence tools are applied to predict outcome from radiomics and pathomics in multiple disease areas with protocols designed to both augment and titrate care based on evolving patient specific biomarkers.

The changes in both work scope and workflow in our discipline have been profound and continue to grow. Although the infrastructure of our skill set has roots with our first mentors, training in radiation oncology bears more limited resemblance to training programs of the past. The skill set required for the modern radiation oncologist is now broad, detailed, and requires comprehensive knowledge of medicine, surgery, radiology, and pathomics. Radiation oncology interacts on a near daily basis with every medical subspecialty, surgical subspecialty, radiology, pathology, and disease-based program within a cancer center. Radiation oncologists need to maintain the skill set of a surgeon for brachytherapy and simultaneously remain fluent in the pharmacokinetics of integrated systemic therapy for multi-disciplinary management. We must maintain expertise in imaging and applied pathology for biomarker assessment of developing treatment plans which may require dose titration or augmentation/dose painting. Radiopharmacy has the potential to mature into a powerful tool for both diagnosis and patient treatment. Modern care is challenging requiring constant communication between providers to ensure consistent messaging to patients and families.

We need to understand the strengths and limitations of our colleagues in oncology related disciplines and fill gaps in service and communication when appropriate. Every patient brings an opportunity for clinical research in tumor control and normal tissue outcome analysis, and we need to work harder at imbedding this activity into our daily work as part of our patient care management. We need to educate the next generation of providers and colleagues in primary care disciplines to recognize the fingerprints of therapy on normal tissue structure and function and optimize care as best as possible to prevent symptomatic normal tissue sequelae including the impact imposed on tissue by combined modality therapy. Medical education has begun to recognize the importance of oncology in medical practice establishing courses in oncology and oncology related patient care at several timepoints during each year of medical school. This will serve to provide common language between disciplines and promote improved understanding of oncology related matters.

Coupled with improvements in our discipline comes the responsibility of increasing our visibility in direct patient care and leadership in multi-disciplinary management. Radiation oncologists have historically and superficially been perceived through the prism of proceduralists and less involved with the longitudinal care of the

cancer patient, often managed by colleagues in medical oncology. Today is a different day. Hepatocellular oncology, thoracic oncology, and central nervous system disease management invites multiple complex procedural based therapies including radiopharmacy directed care with radiation oncologists often assuming primary management for the coordination of care between medical and interventional radiology colleagues. Because of primary management of sub-total whole brain therapy, gastrointestinal presentations and pulmonary nodules of both primary and metastatic origin, radiation oncologists are following patients with equipoise previously associated with medical oncology in multiple disease areas. Interpretation of follow up therapy images in computed tomography (CT), positron emission tomography (PET), and magnetic resonance (MR) imaging require radiation oncology review to validate image interpretation relative to the radiation therapy treatment field. Often therapy leaves predictable changes on images which can be misinterpreted as disease. Accordingly, response assessment is often best accomplished in a multi-disciplinary setting including the fields of radiation therapy. This requires fingertip availability of radiation therapy treatment objects for review by colleagues outside of our discipline. Aside from improving patient care, this would also serve to educate our colleagues concerning process improvements in our discipline and educate trainees in other disciplines (1–5).

In this area, radiation oncologists are poised to assume more visible and influential leadership roles in disease-based disciplines. Our treatment has become more valuable to patient care due to improvements in tumor control and titration of sequelae of management. Because we are integrated with all liquid and solid disease systems with increasing patient care responsibility, we are maturing as thought leaders in oncology programs. This is both a strength and a potential weakness as we need to first mature and accept the responsibility as leaders and make certain our science and written manuscripts reflect the maturation of our discipline. Our clinical -translational science is improving and our basic science is drawing more attention and support at a national level. Our next objective is to move these functions to an enterprise level and establish integrated processes to move our science forward with validation. Process improvements in data acquisition and data management need to become part of our daily work.

RESPONSIBILITY OF CLINICAL TRIALS AND TRANSLATIONAL MEDICINE

Radiation oncologists have participated in clinical trials sponsored by the National Clinical Trials Network's (NCTN) former cooperative groups for more than 50 years. We have managed clinical trials as a primary discipline and participated in trials when the study required radiation therapy but not necessarily as the primary study question. Quality assurance in clinical trials initially centered in generating consistency in computational analytics. Prior to planning systems becoming more commercialized, field dose calculations were performed onsite with two-dimensional algorithms calculated at field isocenter or at depth. Phantoms were constructed by colleagues at the Radiological Physics Center

(RPC, now IROC Houston) for protocols to generate consistency in computation and therapy execution across institutions. Fluoroscopic simulation images and images taken under megavoltage were submitted for quality assurance initially without diagnostic images to validate how the targets were chosen. Therapy fields were designed by anatomical considerations and were not necessarily driven by image guidance.

With the advent and development of three-dimensional planning systems, the paradigm shifted, and quality assurance moved beyond computational analytics generated through phantoms as a sole source identifying a plan as study compliant. Although consistency in computational algorithms remains important; harmonization through vendor technology facilitated consistent and reproducible approach to computations validating dose to volume. Equally relevant was the introduction of imaging directly into treatment planning and the skill set of the radiation oncologist pivoted towards a balance between imaging and computational analytical treatment planning algorithms. Diagnostic imaging colleagues often place focus on the presence or absence of a structure. Radiation oncologists needed to know the peripheral boundaries and three-dimensional shape of the target corresponding to normal tissue abutting the target. Radiation oncologists now had to think in terms of volumes and the relationship of target volumes to structure. Normal tissues likewise had volumetric measures and radiation oncologists now had to think and apply therapy with consideration to dose and volume both to disease and normal tissue. The dose volume histogram became an invaluable two-dimensional reconstruction of volumetric therapy and care plans could be compared through this prism. Therapy plans and full radiation oncology datasets could be shared, and protocols matured rapidly in the cooperative groups using volumetric language. These tools gave us voice and an opportunity for sharing information with providers and colleagues with common ground. More importantly, our discipline could speak in a more unified voice in a quantitative language germane to radiation oncology. Protocols matured with constraints to tumor targeting and normal tissue and provided us the opportunity to share information as colleagues in a digital format and intercompare outcome analysis with a common denominator. However, we understand our discipline does not function in isolation. Patient care and translational science require multiple disciplines to work in synergy and complement the strengths and weaknesses of other disciplines. We need to make certain colleagues in other direct and indirect patient care disciplines understand our technology and more importantly, the application of our technology to patient care and the meaning of radiation dose to volume. These processes affect all disease sites with opportunities for improvement in our science and patient care (1–21).

THE NEED FOR PROCESS IMPROVEMENTS IN OUR CLINICAL TRANSLATIONAL SCIENCE

Clinical trials are mechanisms designed to improve patient care. Although clinical trials can be designed to ask direct questions in

radiation therapy, often radiation oncologists participate applying radiation therapy in a uniform format in protocols evaluating chemotherapy and targeted therapy with radiation therapy. This is of equal importance to trials evaluating radiation therapy endpoints. Radiation therapy may not be the primary study question, however if not applied in a uniform manner, study questions may not be answered in the manner intended by the study design. The HeadSTART trial evaluated the role of the hypoxic cell sensitizer Tirapazamine in the management of patients with locally advanced head and neck carcinoma. There were multiple favorable phase 2 data supporting the use of the agent in management. The phase 3 trial was one of the first trials using volumetric planning in the management of patients with head and neck cancer. Because the trial was one of the first trials involving worldwide participation, the trial was managed with interventional review in near real time, but not pre-therapy real time as managed today with digital data exchange. Data including diagnostic imaging required to validate the choice of target volumes were submitted with radiation therapy treatment objects and was reviewed within the first three days of treatment. On review, radiation therapy quality had a direct impact on the results of the study and undermined the goal of the study. There were interesting caveats as patients of investigators who made adjustment on plans after the initiation of therapy had decreased survival compared to patients whose plans were approved on quality review *de novo*. These patients had survival similar to patients who were scored initially as study deviations but on retrospective review had volume deviations considered less clinically meaningful as the fields did not transgress gross tumor seen on imaging. This study demonstrated that the quality of radiation therapy mattered and despite our improved technology, we did not apply our technology in a uniform matter during an important study. Accordingly, the deviations overrode the primary study question and the utility of Tirapazamine as a hypoxic cell sensitizer could not be established. This demonstrated that we as a discipline had

work to do to in supporting our colleagues in clinical trials, otherwise the benefits of our technology would remain less visible to oncology colleagues (10).

A similar problem arose in Hodgkin lymphoma studies which revealed a survival benefit to patients treated with radiation therapy in a protocol compliant manner when the study did not demonstrate a benefit to radiation therapy as part of the primary evaluation due to the number of study deviations (**Figure 1**). Accordingly, we could not demonstrate our value in this disease. American College of Surgeons Oncology Group (now Alliance for Clinical Trials in Oncology) Z0011 breast cancer clinical trial was designed to assess the utility of surgical and radiation therapy titration of therapy to the axilla, however the lack of interventional review precluded uniform application of radiation therapy, thus did not answer the primary study point relative to radiation therapy. Today, axillary radiation therapy remains understudied and often misunderstood despite our multiple efforts to address these questions in clinical trials. This creates confusion among medical and surgical colleagues and became an opportunity lost to optimize care for these patients. Non-small cell lung carcinoma clinical trial formerly Radiation Therapy Oncology Group (RTOG) 0617 was designed as a two-tier randomization between low and high dose radiation therapy with systemic therapy for patients treated with definitive chemoradiotherapy. The trial did not show a benefit to higher dose radiation therapy and investigators moving forward assumed lower dose therapy was a standard of care. Less well known is the local control rate in the high dose arm was 12% less during the first three years of the study, possibly suggesting that tumor may/may not have been fully contoured as part of the gross tumor volume. Unfortunately, diagnostic imaging validating the contour of gross tumor was not collected, therefore the reason for the unanticipated result could not be evaluated. Therefore, an opportunity lost to ask an important question. If full diagnostic imaging datasets were reviewed as part of the study process, would trial outcome have been different? The trial has had and continues to have influence in the thoracic community

Deviation Adjustment

Survival According to Treatment* (POG 8725)

Treatment	5 Year Relapse Free Survival (%)
Arm 1: Chemotherapy Alone	85
Arm 2: Chemotherapy + RT:	
Appropriate volume	96
Major & Minor Deviations	86

* Only patients who were in complete remission at the end of chemotherapy

FIGURE 1 | Non-protocol compliant radiation therapy had equal survival to patients treated with chemotherapy alone. Patients with protocol compliant radiation therapy had improved survival which was statistically significant (22).

as the results suggested that “less is better” when in fact there was no explanation for why the higher dose arm had worse local control in the initial management of the trial. We can only speculate that targeting of disease may have been incomplete due in part to concern of toxicity by investigators who may have unintentionally under contoured disease to spare parenchyma from toxicity. Today, in clinical trials evaluating the role of immunotherapy in lung cancer management assume that 60 Gray (Gy) to gross tumor is the standard of care. Although several other trials have suggested that higher dose may be optimal for local control, it remains challenging to convince others, including peers and insurance providers, that the trial may have had imperfections which influenced outcome. Therefore, despite our effort and good intentions, our trials have, at times, brought unintended downstream consequence to clinical management due to self-directed imperfections in data acquisition and data management drawing conclusions on studies that may or may not be accurate. Moving forward, we can only prove our point by collecting all data including outcome imaging and identify issues associated with local control and what can be done to both mitigate this point and not compromise normal tissue metrics. Constraints are influenced both by volume and intended dose and we need to study this in greater depth to become confident in our standards. These examples bring us to an understanding that as our discipline matures, we must accept greater responsibility for trial management and the narrative associated with the trial results if we are to be believed and recognized as thought leaders. We need to commit to normal tissue constraints in our trials and make effort to treat patients on trials abiding by normal tissue constraints to make accurate assessments of normal tissue tolerance. All too often, we let other disciplines control the narrative about radiation therapy. We need to mature as leaders with presence at interdisciplinary events where we can speak with respect but also speak from a leadership position. We need to not unintentionally contradict each other without understanding the context associated with the information. We must let the facts drive the narrative. Our presence at interdisciplinary national and international meetings will be increasingly important moving forward as we continue to treat a larger percentage of the oncology population. Our technology has matured, and we need to mature with our technology and represent the strengths of our discipline balanced with the inclusion of the strengths of colleagues. Our translational and basic science needs to continue to improve and this will improve our clinical trials. The National Cancer Institute recently established the core of a radiation oncology biology integrated network (ROBIN). This will promote the strengths of our science and provide visibility for our role in basic science and clinical trials. ROBIN will provide infrastructure to move our science into clinical trials. We need to integrate our science with current biomarkers, pathomics, and radiomics at an enterprise level as these vehicles become points of validation for our work and will serve to 1) identify patients of increased/decreased risk for recurrence, 2) interpret outcomes relative to science, and 3) improve clinical pathways for future patients and translational studies. A new initiative is being developed to house patient care data in a uniform format to develop programs in artificial intelligence in both our clinics and translational science laboratories. We understand that artificial intelligence will only be

successful if built on strong datasets with complete information, otherwise we will be committed to continue to make the mistakes of the past limiting our credibility with colleagues from other disciplines (22–37).

NEXT STEPS

For our discipline to promote and apply our science in a meaningful manner to clinical trials, we will need to adapt our data management process. This will include all elements of information currently used to manage patients including outcome data with imaging to validate our performance and identify gaps for process improvements. The National Clinical Trials Network (NCTN) has tissue banks, clinical data, and outcome information associated with biomarkers housed in various platforms often within separate statistical centers. The Imaging and Radiation Oncology Core (IROC) supports the NCTN with imaging and radiation oncology data acquisition and management including real time review of objects to support the clinical objectives of study and the quality of treatment delivered during the clinical trial. These are important components to the infrastructure required to perform sound and modern translational science; however, each continues to function in relative isolation to each other with no natural pathway to generate interactions between the centers housing pathology, imaging, radiation therapy objects, and clinical outcome data. In addition, there are administrative layers which require approval to move data/information to investigators. Many within disease and discipline committees of the NCTN members point to the separation of data and redundant and duplicative effort required to retrieve data as a barrier to translational science involving secondary and unanticipated events associated with clinical trials. Accordingly, it remains challenging for investigators to bring all components necessary for research concerning secondary trial objectives not necessarily recognized at the time of trial development. Often, secondary questions, including review of quality assurance data, can only be optimally done at closure of the study and after the study has collected enough outcome information, including imaging, to assess questions concerning tumor control and toxicity (22, 34, 36, 37).

The Cancer Imaging Archive (TCIA) houses information on completed trials including clinical information, pathomics, imaging, and radiation therapy objects. TCIA has tools to permit research integrating all elements of data used for patient care and clinical trials. Investigators can apply established and novel tools for analysis including applications for the development of artificial intelligence to repurpose the data and ask questions not previously recognized during the conduct of the trial. The archive is rich and complete. The archives house all relevant information that can be rapidly retrieved for evaluation. Moving forward, TCIA will place enhanced emphasis on acquisition of radiation oncology objects including imaging used for target definition and outcome imaging for evaluation. With radiation therapy

technology including theranostics rapidly moving forward, we need to accept the responsibility of making certain we collect and analyze all information to validate outcome and learn to appropriately apply our tools for patient care. If we do not collect all the relevant pathomic and radiomic information, we risk replicating our mistakes of the past and reach invalid conclusions as we have done far too often in previous trials as discussed. If we are to gain the most information from each trial, the trial must be conducted in a comprehensive manner with data transparency and sound acquisition processes to generate outcome analysis that can be trusted (38, 39).

Artificial intelligence models require validated and complete databases to develop strong algorithms which can serve as predictive indices for outcome. We will need artificial intelligence programs in all facets of our clinical, planning and research effort moving forward. The more complete the datasets used to build the models for artificial intelligence development, the more useful the models will be in clinical and academic practice. The challenge is to make this information available as quickly as possible to investigators. Although the data should naturally flow to an informatics platform that can be queried by investigators in near real time, the challenge remains that each group has the responsibility of data management and data protection, therefore data transfer to different programs requires approvals and integration of data flow processes between the centers of data acquisition for the information to be used and re-purposed in a meaningful manner. The databases have to be structured with a self-renewal process as images acquired more than a decade ago may or may not be relevant to a modern question as imaging platforms mature and diversify. Housing the information in the informatics library is important and the information must be curated to maintain relevance.

The TCIA infrastructure has been established at several institutions to serve as an institutional data management service as few platforms can store varied data and function at an enterprise level for review of information. This can serve as a platform to move data into the national archive. Radiation oncologists interact with all surgical, medical, imaging, pathology, and basic science colleagues daily. Our discipline needs to use our central position as caregivers as a strength and become leaders in data acquisition and management. It is only through this process can we provide opportunities for meaningful continuous self-improvement as our discipline is maturing a rapid pace. Having tools such as this housed within

institutions gives investigators opportunities to review internal data and compare outcomes to information housed in the archive. Through this process we adjust and improve our skill and publish manuscripts with meaning and relevance. We can compare clinical drug x-ray interaction relative to normal tissue and functional metrics in similar clinical trials identified from the archive. Through these processes we can mature as a discipline, improve our metrics for normal tissue tolerance, and improve our definitions of risk categories and assign titrated or augmented therapies to patients within similar disease categories. The challenge is moving modern information with up-to-date imaging and pathomics to both IROC and TCIA platforms rapidly and in an enterprise manner. The biology data will include information obtained from modern pathomics including genomic sequencing and mutation analysis. The more we can streamline our processes, the more quickly we can build robust platforms to support our science. We need to build our departmental infrastructure to support data transfer in uniform formats to be repurposed for use in the next iteration of clinical science (38–50).

CONCLUSION

Radiation oncology is no longer a lateral or secondary component in cancer management. We are important to current oncology management and are maturing as thought leaders in disease-based disciplines. Oncology patients will receive radiation oncology service today more than any other discipline in cancer management. We interact with patients from all disease sites and play a more prominent central role in the coordination of care for cancer patients. We are a primary resource for follow up in many disease sites treated with advanced technology radiation therapy. The visibility we now possess comes with the responsibility of closing gaps in both our clinical care and translational science with equal attention to follow up care and management.

AUTHOR CONTRIBUTIONS

First author, LD. Senior author, TF. All authors contributed to the article and approved the submitted version.

REFERENCES

- Withers HR, Taylor JM, Maciejewski B. Treatment Volume and Tissue Tolerance. *Int J Radiat Oncol Biol Phys* (1988) 14:751–9. doi: 10.1016/0360-3016(88)90098-3
- Emami B, Lyman J, Brown A, Coia L, Goitein M, Munzenrider JE, et al. Tolerance of Normal Tissue to Therapeutic Irradiation. *Int J Radiat Oncol Biol Phys* (1991) 21:109–22. doi: 10.1016/0360-3016(91)90171-y
- Niemierko A. A Unified Model of Tissue Response to Radiation. *Med Phys* (1999) 26:1100.
- Bentzen SM, Constine LS, Deasy JO, Eisbruch A, Jackson A, Marks LB, et al. Quantitative Analyses of Normal Tissue Effects in the Clinic (QUANTEC): An Introduction to the Scientific Issues. *Int J Radiat Oncol Biol Phys* (2010) 76:S3–9. doi: 10.1016/j.ijrobp.2009.09.040
- Marks LB, Yorke ED, Jackson A, Ten Haken RK, Constine LS, Eisbruch A, et al. Use of Normal Tissue Complication Probability Models in the Clinic. *Int J Radiat Oncol Biol Phys* (2010) 76:S10–9. doi: 10.1016/j.ijrobp.2009.07.1754
- Kalaparakal JA, Gopalakrishnan M, Walterhouse DO, Rigsby CK, Rademaker A, Helenowski I, et al. Cardiac-Sparing Whole Lung IMRT in Patients With Pediatric Tumors and Lung Metastasis: Final Report of a Prospective Multicenter Clinical Trial. *Int J Radiat Oncol Biol Phys* (2019) 103:28–37. doi: 10.1016/j.ijrobp.2018.08.034
- Mendenhall NP, Fitzgerald TJ. Conventional Radiation Therapy Compared With Stereotactic Conformal Therapy-A Rare and Laudable Randomized Trial. *JAMA Oncol* (2017) 3:1376–77. doi: 10.1001/jamaoncol.2017.1552

8. Ding Z, Zhang H, Lv XF, Xie F, Liu L, Qiu S, et al. Radiation-Induced Brain Structural and Functional Abnormalities in Presymptomatic Phase and Outcome Prediction. *Hum Brain Mapp* (2018) 39:407–27. doi: 10.1002/hbm.23852
9. Lin J, Lv X, Niu M, Liu L, Chen J, Xie F, et al. Radiation-Induced Abnormal Cortical Thickness in Patients With Nasopharyngeal Carcinoma After Radiotherapy. *NeuroImage Clin* (2017) 14:610–21. doi: 10.1016/j.nicl.2017.02.025
10. Yusuf SW, Venkatesulu BP, Mahadevan LS, Krishnan S. Radiation Induced Cardiovascular Disease: A Clinical Perspective. *Front Cardiovasc Med* (2017) 4:66. doi: 10.3389/FCVM.2017.00066
11. Darby SC, Ewertz M, McGale P, Bennet AM, Blom-Goldman U, Brønnum D, et al. Risk of Ischemic Heart Disease in Women After Radiotherapy for Breast Cancer. *N Engl J Med* (2013) 368:987–98. doi: 10.1056/NEJMoa1209825
12. Kwa SL, Lebesque JV, Theuvs JC, Marks LB, Munley MT, Bentel G, et al. Radiation Pneumonitis as a Function of Mean Lung Dose: An Analysis of Pooled Data of 540 Patients. *Int J Radiat Oncol Biol Phys* (1998) 42:1–9. doi: 10.1016/s0360-3016(98)00196-5
13. Graham MV. Predicting Radiation Response. *Int J Radiat Oncol Biol Phys* (1997) 39:561–2. doi: 10.1016/s0360-3016(97)00353-2
14. Graham MV, Purdy JA, Emami B, Harms W, Bosch W, Lockett MA, et al. Clinical Dose-Volume Histogram Analysis for Pneumonitis After 3D Treatment for non-Small Cell Lung Cancer (NSCLC). *Int J Radiat Oncol Biol Phys* (1999) 45:323–9. doi: 10.1016/s0360-3016(99)00183-2
15. Hanania AN, Mainwaring W, Ghebre YT, Hanania NA, Ludwig M. Radiation-Induced Lung Injury: Assessment and Management. *Chest* (2019) 156:150–62. doi: 10.1016/j.chest.2019.03.033
16. Käsmann L, Dietrich A, Staab-Weijnitz CA, Manapov F, Behr J, Rimmer A, et al. Radiation-Induced Lung Toxicity - Cellular and Molecular Mechanisms of Pathogenesis, Management, and Literature Review. *Radiat Oncol* (2020) 15:214. doi: 10.1186/s13014-020-01654-9
17. Dawson LA, McGinn CJ, Normolle D, Ten Haken RK, Walker S, Ensminger W, et al. Escalated Focal Liver Radiation and Concurrent Hepatic Artery Fluorodeoxyuridine for Unresectable Intrahepatic Malignancies. *J Clin Oncol* (2000) 18:2210–8. doi: 10.1200/JCO.2000.18.11.2210
18. Dawson LA, Ten Haken RK, Lawrence TS. Partial Irradiation of the Liver. *Semin Radiat Oncol* (2001) 11:240–6. doi: 10.1053/srao.2001.23485
19. Baradaran-Ghahfarokhi M. Radiation-Induced Kidney Injury. *J Renal Inj Prev* (2012) 1:49–50. doi: 10.12861/jrip.2012.17
20. Lukez A, O'Loughlin L, Bodla M, Baima J, Moni J. Positioning of Port Films for Radiation: Variability is Present. *Med Oncol* (2018) 35:77. doi: 10.1007/s12032-018-1138-z
21. Oh D, Huh SJ. Insufficiency Fracture After Radiation Therapy. *Radiat Oncol J* (2014) 32:213–20. doi: 10.3857/roj.2014.32.4.213
22. FitzGerald TJ. What We Have Learned: The Impact of Quality From a Clinical Trials Perspective. *Semin Radiat Oncol* (2012) 22:18–28. doi: 10.1016/j.semradi.2011.09.004
23. Peters LJ, O'Sullivan B, Giral J, FitzGerald TJ, Trotti A, Bernier J, et al. Critical Impact of Radiotherapy Protocol Compliance and Quality in the Treatment of Advanced Head and Neck Cancer: Results From TROG 02.02. *J Clin Oncol* (2010) 28:2996–3001. doi: 10.1200/JCO.2009.27.4498
24. Friedman DL, Chen L, Wolden S, Buxton A, McCarten K, FitzGerald TJ, et al. Dose-Intensive Response-Based Chemotherapy and Radiation Therapy for Children and Adolescents With Newly Diagnosed Intermediate-Risk Hodgkin Lymphoma: A Report From the Children's Oncology Group Study Ahod0031. *J Clin Oncol* (2014) 32:3651–8. doi: 10.1200/JCO.2013.52.5410
25. Henderson IC, Berry DA, Demetri GD, Cirincione CT, Goldstein LJ, Martino S, et al. Improved Outcomes From Adding Sequential Paclitaxel But Not From Escalating Doxorubicin Dose in an Adjuvant Chemotherapy Regimen for Patients With Node-Positive Primary Breast Cancer. *J Clin Oncol* (2003) 21:976–83. doi: 10.1200/JCO.2003.02.063
26. Citron ML, Berry DA, Cirincione C, Hudis C, Winer EP, Gradishar WJ, et al. Randomized Trial of Dose-Dense Versus Conventionally Scheduled and Sequential Versus Concurrent Combination Chemotherapy as Postoperative Adjuvant Treatment of Node-Positive Primary Breast Cancer: First Report of Intergroup Trial C9741/Cancer and Leukemia Group B Trial 9741. *J Clin Oncol* (2003) 21:1431–9. doi: 10.1200/JCO.2003.09.081
27. Sartor CI, Peterson BL, Woolf S, Fitzgerald TJ, Laurie F, Turrisi AJ, et al. Effect of Addition of Adjuvant Paclitaxel on Radiotherapy Delivery and Locoregional Control of Node-Positive Breast Cancer: Cancer and Leukemia Group B 9344. *J Clin Oncol* (2005) 23:30–40. doi: 10.1200/JCO.2005.12.044
28. Giuliano AE, Ballman KV, McCall L, Beitsch PD, Brennan MB, Kelemen PR, et al. Effect of Axillary Dissection vs No Axillary Dissection on 10-Year Overall Survival Among Women With Invasive Breast Cancer and Sentinel Node Metastasis: The ACOSOG Z0011 (Alliance) Randomized Clinical Trial. *JAMA* (2017) 318:918–26. doi: 10.1001/jama.2017.11470
29. Jaggi R, Chadha M, Moni J, Ballman K, Laurie F, Buchholz TA, et al. Radiation Field Design in the ACOSOG Z0011 (Alliance) Trial. *J Clin Oncol* (2014) 32:3600–6. doi: 10.1200/JCO.2014.56.5838
30. Wang X, Wang W, Li JB, Huo ZW, Xu M, Qiu PF, et al. Definition of Internal Mammary Node Target Volume Based on the Position of the Internal Mammary Sentinel Lymph Nodes Presented on SPECT/CT Fusion Images. *Front Oncol* (2020) 9:1553. doi: 10.3389/fonc.2019.01553
31. Reznik J, Cicchetti MG, Degaspe B, Fitzgerald TJ. Analysis of Axillary Coverage During Tangential Radiation Therapy to the Breast. *Int J Radiat Oncol Biol Phys* (2005) 61:163–8. doi: 10.1016/j.ijrobp.2004.04.065
32. Borm KJ, Voppichler J, Düsberg M, Oechsner M, Vag T, Weber W, et al. FDG/PET-CT-Based Lymph Node Atlas in Breast Cancer Patients. *Int J Radiat Oncol Biol Phys* (2019) 103:574–82. doi: 10.1016/j.ijrobp.2018.107.2025
33. Gentile MS, Usman AA, Neuschler EI, Sathiaselan V, Hayes JP, Small WJr. Contouring Guidelines for the Axillary Lymph Nodes for the Delivery of Radiation Therapy in Breast Cancer: Evaluation of the RTOG Breast Cancer Atlas. *Int J Radiat Oncol Biol Phys* (2015) 93:257–65. doi: 10.1016/j.ijrobp.2015.07.002
34. FitzGerald TJ, Bishop-Jodoin M, Followill DS, Galvin J, Knopp MV, Michalski JM, et al. Imaging and Data Acquisition in Clinical Trials for Radiation Therapy. *Int J Radiat Oncol Biol Phys* (2016) 94:404–11. doi: 10.1016/j.ijrobp.2015.10.028
35. Salama JK, Stinchcombe TE, Gu L, Wang X, Morano K, Bogart JA, et al. Pulmonary Toxicity in Stage III non-Small Cell Lung Cancer Patients Treated With High-Dose (74 Gy) 3-Dimensional Conformal Thoracic Radiotherapy and Concurrent Chemotherapy Following Induction Chemotherapy: A Secondary Analysis of Cancer and Leukemia Group B (CALGB) Trial 30105. *Int J Radiat Oncol Biol Phys* (2011) 81:e269–74. doi: 10.1016/j.ijrobp.2011.01.056
36. FitzGerald TJ, Bishop-Jodoin M, Bosch WR, Curran WJ, Followill DS, Galvin JM, et al. Future Vision for the Quality Assurance of Oncology Clinical Trials. *Front Oncol* (2013) 3:31. doi: 10.3389/fonc.2013.00031
37. FitzGerald TJ. A New Model for Imaging and Radiation Therapy Quality Assurance in the National Clinical Trials Network of the National Cancer Institute. *Int J Radiat Oncol Biol Phys* (2014) 88:272–3. doi: 10.1016/j.ijrobp.2013.09.030
38. Saltz J, Sharma A, Iyer G, Bremer E, Wang F, Jasnowski A, et al. A Containerized Software System for Generation, Management, and Exploration of Features From Whole Slide Tissue Images. *Cancer Res* (2017) 77:e79–82. doi: 10.1158/0008-5472.CAN-17-0316
39. Prior F, Almeida J, Kathiravelu P, Kurc T, Smith K, Fitzgerald TJ, et al. Open Access Image Repositories: High-Quality Data to Enable Machine Learning Research. *Clin Radiol* (2020) 75:7–12. doi: 10.1016/j.crad.2019.04.002
40. FitzGerald TJ, Bishop-Jodoin M, Laurie F, Hanusik R, Iandoli M, Karolczuk K, et al. "Acquisition and Management of Data for Translational Science in Oncology". In: S Sundaresan, editor. *Translational Research in Cancer*. London, England: IntechOpen (2019). doi: 10.5772/intechopen.89700
41. Mayo CS, Moran JM, Xiao Y, Bosch W, Matuszak MM, Marks LB, et al. AAPM Task Group 263: Tackling Standardization of Nomenclature for Radiation Therapy. *Int J Radiat Oncol Biol Phys* (2015) 93:SE383–4. doi: 10.1016/j.ijrobp.2015.07.1525
42. Uehara K, Sasayama T, Miyawaki D, Nishimura H, Yoshida K, Okamoto Y, et al. Patterns of Failure After Multimodal Treatments for High-Grade Glioma: Effectiveness of MIB-1 Labeling Index. *Radiat Oncol* (2012) 7:104. doi: 10.1186/1748-717X-7-104

43. Lao J, Chen Y, Li ZC, Li Q, Zhang J, Liu J, et al. A Deep Learning-Based Radiomics Model for Prediction of Survival in Glioblastoma Multiforme. *Sci Rep* (2017) 7:10353. doi: 10.1038/s41598-017-10649-8
44. Zhou M, Chaudhury B, Hall LO, Goldof DB, Gillies RJ, Gatenby RA. Identifying Spatial Imaging Biomarkers of Glioblastoma Multiforme for Survival Group Prediction. *J Magn Reson Imaging* (2017) 46:115–23. doi: 10.1002/jmri.25497
45. Xi YB, Guo F, Xu ZL, Li C, Wei W, Tian P, et al. Radiomics Signature: A Potential Biomarker for the Prediction of MGMT Promoter Methylation in Glioblastoma. *J Magn Reson Imaging* (2018) 47:1380–87. doi: 10.1002/jmri.25860
46. Eckel-Passow JE, Decker PA, Kosel ML, Kollmeyer TM, Molinaro AM, Rice T, et al. Using Germline Variants to Estimate Glioma and Subtype Risks. *Neuro Oncol* (2019) 21:451–61. doi: 10.1093/neuonc/noz009
47. Followill D, Knopp M, Galvin J, FitzGerald T, Michalski J, Rosen M, et al. The Imaging and Radiation Oncology Core (IROC) Group: A Proposed New Clinical Trial Quality Assurance Organization. *Med Phys* (2013) 40:507. doi: 10.1118/1.4815652
48. Fairchild A, Straube W, Laurie F, Followill D. Does Quality of Radiation Therapy Predict Outcomes of Multicenter Cooperative Group Trials? A Literature Review. *Int J Radiat Oncol Biol Phys* (2013) 87:246–60. doi: 10.1016/j.ijrobp.2013.03.036
49. FitzGerald TJ, Bishop-Jodoin M, Laurie F, O'Meara E, Davis C, Bogart J, et al. The Importance of Imaging in Radiation Oncology for National Clinical Trials Network Protocols. *Int J Radiat Oncol Biol Phys* (2018) 102:775–82. doi: 10.1016/j.ijrobp.2018.08.039
50. FitzGerald TJ, Rosen MA, Bishop-Jodoin M. The Influence of Imaging in the Modern Practice of Radiation Oncology. *Int J Radiat Oncol Biol Phys* (2018) 102:680–2. doi: 10.1016/j.ijrobp.2018.08.028

Conflict of Interest: Dr Ulin, Ms Smith, Ms Bishop-Jodoin, Ms Laurie, Mr Iandoli, Dr Moni, Dr Cicchetti, Dr FitzGerald report grants from the National Cancer Institute.

The remaining authors declare the absence of any commercial or financial relationships that could be construed as a potential conflict of interest.

Publisher's Note: All claims expressed in this article are solely those of the authors and do not necessarily represent those of their affiliated organizations, or those of the publisher, the editors and the reviewers. Any product that may be evaluated in this article, or claim that may be made by its manufacturer, is not guaranteed or endorsed by the publisher.

Copyright © 2022 Ding, Bradford, Kuo, Fan, Ulin, Khalifeh, Yu, Liu, Saleeby, Bushe, Smith, Bianciu, LaRosa, Prior, Saltz, Sharma, Smyczynski, Bishop-Jodoin, Laurie, Iandoli, Moni, Cicchetti and FitzGerald. This is an open-access article distributed under the terms of the Creative Commons Attribution License (CC BY). The use, distribution or reproduction in other forums is permitted, provided the original author(s) and the copyright owner(s) are credited and that the original publication in this journal is cited, in accordance with accepted academic practice. No use, distribution or reproduction is permitted which does not comply with these terms.

Advantages of publishing in Frontiers



OPEN ACCESS

Articles are free to read
for greatest visibility
and readership



FAST PUBLICATION

Around 90 days
from submission
to decision



HIGH QUALITY PEER-REVIEW

Rigorous, collaborative,
and constructive
peer-review



TRANSPARENT PEER-REVIEW

Editors and reviewers
acknowledged by name
on published articles

Frontiers

Avenue du Tribunal-Fédéral 34
1005 Lausanne | Switzerland

Visit us: www.frontiersin.org

Contact us: frontiersin.org/about/contact



REPRODUCIBILITY OF RESEARCH

Support open data
and methods to enhance
research reproducibility



DIGITAL PUBLISHING

Articles designed
for optimal readership
across devices



FOLLOW US

@frontiersin



IMPACT METRICS

Advanced article metrics
track visibility across
digital media



EXTENSIVE PROMOTION

Marketing
and promotion
of impactful research



LOOP RESEARCH NETWORK

Our network
increases your
article's readership